Syntheses of Seiricuprolide and Pestalotioprolide B

Pitipat Sanphetchaloemchok

A Thesis Submitted in Partial Fulfillment of the Requirements for the
Degree of Master of Science in Chemistry (International Program)
Prince of Songkla University
2023

Syntheses of Seiricuprolide and Pestalotioprolide B

Pitipat Sanphetchaloemchok

A Thesis Submitted in Partial Fulfillment of the Requirements for the Degree of Master of Science in Chemistry (International Program)

Prince of Songkla University

2023

Thesis Title   Syntheses of Seiricuprolide and Pestalotioprolide B

Author   Mr. Pitipat   Sanphetchaloemchok

Major Program Chemistry (International Program)

Major Advisor

....
K. Tadpetch

(Assoc. Prof. Dr. Kwanruthai Tadpetch)

Examining Committee:

....Chairperson
Darunee Soorukram

(Assoc. Prof. Dr. Darunee Soorukram)

....Committee
K. Tadpetch

(Assoc. Prof. Dr. Kwanruthai Tadpetch)

....Committee
Jutanut Kaeo

(Assoc. Prof. Dr. Juthanat Kaeobamrung)

....Committee
Chittreeya Tansakul

(Asst. Prof. Dr. Chittreeya Tansakul)

     The Graduate School, Prince of Songkla University, has approved this thesis as partial fulfillment of the requirements for the Master of Science Degree in Chemistry (International program).

....

(Asst. Prof. Dr. Thakerng Wongsirichot)

Acting Dean of Graduate School

This is to certify that the work here submitted is the result of the candidate's own investigations. Due acknowledgement has been made of any assistance received.

....Signature

(Assoc. Prof. Dr. Kwanruthai Tadpetch)

Major Advisor

....Signature

(Mr. Pitipat Sanphetchaloemchok)

Candidate

I hereby certify that this work has not been accepted in substance for any degree, and is not being currently submitted in candidature for any degree.

....Signature

(Mr. Pitipat Sanphetchaloemchok)

Candidate

ชื่อวิทยานิพนธ์	การสังเคราะห์ seiricuprolide และ pestalotioprolide B
ผู้เขียน	นายปิติพัฒน์ สรรเพชรเฉลิมโชค
สาขาวิชา	เคมี (หลักสูตรนานาชาติ)
ปีการศึกษา	2565

บทคัดย่อ

seiricuprolide (**1**) และ pestalotioprolide B (**2**) เป็นสารกลุ่ม macrolide ไม่อิ่มตัววง 14 เหลี่ยมที่มีหมู่ chiral epoxide ซึ่งพบได้น้อยในธรรมชาติ seiricuprolide (**1**) ถูกแยกเป็นครั้งแรกจากเชื้อรา *Seiridium cupressi* และแสดงฤทธิ์ที่เป็นพิษต่อพืชโดยงานวิจัยของ Sparapano และคณะในปี ค.ศ. 1998 สาร **1** มีโครงสร้างหลักเป็นวงแลคโทน 14 เหลี่ยมที่มีหมู่ (*E*)-α,β-unsaturated ester ที่ตำแหน่ง 2–3 รวมถึงหมู่ β-epoxide ที่ตำแหน่ง 5–6 และพันธะคู่แบบ *Z* ที่ตำแหน่ง 8–9 และมีไครัลคาร์บอนที่ตำแหน่ง 4 7 และ 13 pestalotioprolide B (**2**) ซึ่งเป็นอนุพันธ์ของสาร **1** ที่มีพันธะคู่แบบ *E* ที่ตำแหน่ง 8–9 ถูกค้นพบเป็นครั้งแรกในรูปอนุพันธ์อะซิเตทจากเชื้อรา *Pestalotiopsis* sp. PSU-MA119 โดยงานวิจัยของ Rukachaisirikul และคณะในปี ค.ศ. 2012 ถึงแม้ต่อมาในปี ค.ศ. 2016 สาร **1** และ **2** ถูกรายงานว่าไม่มีฤทธิ์ในการยับยั้งเซลล์มะเร็งเต้านมชนิด L5178Y และเซลล์มะเร็งรังไข่ชนิด A2780 โดยงานวิจัยของ Liu และ Proksch และคณะ แต่เนื่องด้วยโครงสร้างที่ใหม่และยังไม่เคยมีรายงานการสังเคราะห์ของสารทั้งสองมาก่อน ทำให้กลุ่มวิจัยของเราดำเนินการสังเคราะห์สาร **1** และ **2** เพื่อเพิ่มปริมาณสารในการทดสอบฤทธิ์การยับยั้งเซลล์มะเร็งชนิดอื่นๆรวมถึงฤทธิ์ทางชีวภาพอื่นๆ ในการสังเคราะห์สาร **1** และ **2** เริ่มต้นจากการใช้ปฏิกิริยา ring-closing metathesis และ Yamaguchi esterification เป็นปฏิกิริยาหลักในการสร้างวงแลคโทนของสาร **1** และ **2** แต่พบว่าหมู่ epoxide ของ diene **8** ไม่สามารถทนทานต่อปฏิกิริยา ring-closing metathesis ในขั้นตอนสุดท้ายได้ จึงนำไปสู่การแก้ไขเส้นทางการสังเคราะห์ของสาร **1** และ **2** ซึ่งเส้นทางการสังเคราะห์ใหม่มีปฏิกิริยาหลักที่สำคัญคือ Shiina macrolactonization ของ seco acid **14** และ **15** เพื่อสร้างวงแลคโทนสำหรับหมู่ (*E*)-α,β-unsaturated ester ที่ตำแหน่ง 2–3 ของสาร **14** และ **15** สร้างได้จากปฏิกิริยา Wittig olefination ส่วนพันธะคู่แบบ *Z* หรือ *E* ที่ตำแหน่ง 8–9 ของสาร **14** และ **15** สร้างได้จาก

ปฏิกิริยา Lindlar หรือ Red-Al reduction ของ propargylic alcohol **13S** ถึงแม้ปฏิกิริยา acetylide addition ระหว่าง alkyne **12** และ epoxy aldehyde **11** ให้ propargylic alcohol **13S** ที่ต้องการเป็นผลิตภัณฑ์รอง แต่อย่างไรก็ตามสารผลิตภัณฑ์หลัก **13R** ที่ไม่ต้องการสามารถเปลี่ยนไปเป็น **13S** ได้ใน 2 ขั้นตอนโดยปฏิกิริยา Mitsunobu inversion สำหรับการสร้างหมู่ β-epoxide เริ่มจากการใช้ปฏิกิริยา *m*-CPBA epoxidation ของ *Z*-allylic alcohol **4** ที่มีหมู่ (*S*)-silyloxy ที่ตำแหน่งแอลฟา โดยวิธีนี้ได้รายงานไว้โดยกลุ่มวิจัยของ Baltas และคณะ แต่พบว่าวิธีการสังเคราะห์นี้ให้ α-epoxide ที่ไม่ต้องการเป็นผลิตภัณฑ์หลัก ดังนั้นจึงเปลี่ยนสารตั้งต้นของปฏิกิริยา epoxidation ไปเป็น *Z*-allylic alcohol **10** ซึ่งเตรียมได้จาก alcohol **9** ใน 3 ขั้นตอน ซึ่งพบว่าปฏิกิริยา *m*-CPBA epoxidation ของ *Z*-allylic alcohol **10** เป็นวิธีที่มีประสิทธิภาพในการสร้างหมู่ β-epoxide ของสาร **11** ที่มีความจำเพาะทางสเตอริโอเคมีสูงและพบว่าหมู่ β-epoxide ที่สร้างขึ้นมานั้นมีความทนทานเนื่องจากสาร **11** สามารถทำปฏิกิริยาต่อจนขั้นสุดท้ายโดยไม่พบการสลายหมู่ β-epoxide สำหรับการสังเคราะห์สาร **1** และ **2** เสร็จสมบูรณ์ได้ในทั้งหมด 19 ขั้นตอนและ 17 ขั้นตอนของเส้นทางที่ยาวที่สุดแบบเส้นตรง ซึ่งมีร้อยละผลิตภัณฑ์โดยรวมเป็น 1.9 และ 1.6 โดยเริ่มจาก chiral allylic alcohol **9** ซึ่งเตรียมได้จาก D-mannitol ใน 4 ขั้นตอน จากนั้นได้นำสารสังเคราะห์ **1** และ **2** ไปทดสอบฤทธิ์ความเป็นพิษต่อเซลล์มะเร็งลำไส้ชนิด HCT116 รวมไปถึงทดสอบฤทธิ์ในการยับยั้งการหลั่งคลอไรด์ที่ใช้ cystic fibrosis transmembrane regulator (CFTR) เป็นสื่อกลางในเซลล์เยื่อบุในลำไส้ (T84) ของมนุษย์ เปรียบเทียบกับอนุพันธ์ของสาร **1** และ **2** ที่ได้รายงานไว้ก่อนหน้านี้ พบว่าสาร **1** และ **2** ไม่แสดงฤทธิ์ทางชีวภาพที่ได้ทดสอบดังกล่าวและจากการการศึกษาความสัมพันธ์ระหว่างโครงสร้างและฤทธิ์ของสารเบื้องต้นพบว่าหมู่ β-epoxide ตำแหน่ง 5–6 ของสาร **1** และ **2** มีผลในการยับยั้งการออกฤทธิ์ความเป็นพิษต่อเซลล์มะเร็งลำไส้ชนิด HCT116 และฤทธิ์ในการยับยั้งการหลั่งคลอไรด์ใน CFTR

selective epoxidation mediated by m-CPBA
2 steps

epichlorohydrin (**3**)
8 steps

4

5

Wittig olefination
6 steps

ring-closing metathesis ✕

Yamaguchi esterification
2 steps

+

seiricuprolide (**1**): *Z*-alkene at C8-C9
pestalotioprolide B (**2**): *E*-alkene at C8-C9

8

7

6

12 + 11

OH-directed epoxidation mediated by m-CPBA

10

3 steps

9

4 steps

D-mannitol

acetylide addition

- Lindlar or Red-Al reduction
- Wittig olefination
7 steps

Shiina macrolactonization
2 steps

14: *Z*-alkene at C8-C9
15: *E*-alkene at C8-C9
R = TBDPS

seiricuprolide (**1**): *Z*-alkene at C8-C9
pestalotioprolide B (**2**): *E*-alkene at C8-C9

13S: (7*S*)-stereogenic center
13R: (7*R*)-stereogenic center

Mitsunobu inversion
2 steps

Thesis Title   Syntheses of Sericuprolide and Pestalotioprolide B

Author   Mr. Pitipat   Sanphetchaloemchok

Major Program   Chemistry (International Program)

Academic Year   2022

ABSTRACT

Seiricuprolide (**1**) and pestalotioprolide B (**2**) belong to a rare 14-membered α,β-unsaturated macrolides bearing a chiral epoxide functionality. Seiricuprolide (**1**) was originally isolated from a fungus *Seiridium cupressi* and was discovered to display phytotoxic activity by Sparapano et al. in 1988. Macrolide **1** is a 14-membered unsaturated lactone core with (E)-α,β-unsaturated ester at C2–C3 position, β-epoxide at C5–C6 position and Z-alkene at C8–C9 position as well as three alcohol stereogenic centers at the 4, 7 and 13 positions. The C8–C9 E-alkene analogue of **1**, pestalotioprolide B (**2**), was first discovered as a diacetate derivative from the mangrove-derived endophytic fungus *Pestalotiopsis* sp. PSU-MA119 by Rukachaisirikul et al. in 2012. Although macrolides **1** and **2** were later reported to have no cytotoxicity against the L5178Y murine lymphoma and the A2780 human ovarian cancer cell lines by Liu and Proksch et al., their novel structure and unprecedented chemical syntheses led us to set out the syntheses of **1** and **2** in order to provide material for further evaluation of their cytotoxic activities against other cancer cell lines as well as other biological activities. The ring-closing metathesis (RCM) and Yamaguchi esterification were initially chosen as the key strategies for forming the macrocyclic core of **1** and **2**. However, the epoxide moiety of RCM precursor diene **8** proved to be incompatible with the final ring-closing metathesis which prompted us to revise the synthetic route for **1** and **2**. The revised synthetic route involved Shiina macrolactonization of seco acids **14** and **15** to construct the macrocyclic skeletons of **1** and **2**. The C2–C3 (E)-α,β-unsaturated ester of **14** and **15** was generated via Wittig olefination. The Z- or E-double bond at C8–C9 of **14** or **15** was constructed from Lindlar or Red-Al reduction of chiral propargylic alcohol **13***S*. Although the addition of alkyne **12** to epoxy aldehyde **11** afforded the desired **13***S* as a minor product, the

undesired major **13*R*** could be converted to **13*S*** in 2 steps via Mitsunobu inversion. The installation of β-epoxide moiety of **11** was first undertaken via *m*-CPBA epoxidation of *Z*-allylic alcohol **4** which contains (*S*)-α-silyloxy stereogenic center following a protocol by Baltas et al. but this methodology apparently led to the α-epoxide product as a major product. The substrate for epoxidation was then changed to *Z*-allylic alcohol **10** which can be easily prepared from known alcohol **9** in 3 steps. OH-Directed epoxidation of *Z*-allylic alcohol **10** mediated by *m*-CPBA was highlighted as an efficient tool for installing β-epoxide of **11** in high stereoselectivity (dr = 16:1). The β-epoxide moiety proved to be robust since degradation of epoxide was not observed in any steps upon carrying epoxy aldehyde **11** to the final target. Overall, the total syntheses of **1** and **2** have been accomplished in 17 longest linear and 19 total steps and 1.9% and 1.6% overall yields starting from chiral allylic alcohol **9** derived from commercially available D-mannitol in 4 steps. Synthetic macrolides **1** and **2** were evaluated for their cytotoxic activity against the HCT116 colon cancer cells as well as their inhibitory effect on cystic fibrosis transmembrane regulator (CFTR) in human intestinal epithelial (T84) cells compared to their previously reported analogues. These two synthetic macrolides were discovered to possess no reactivity of both biological activities tested. Preliminary structure–activity relationship suggested that the C5–C6 β-epoxide moiety of both **1** and **2** suppressed the cytotoxic activity against the HCT116 colon cancer cells as well as their CFTR inhibitory effect.

epichlorohydrin (**3**)

8 steps

4

selective epoxidation mediated by *m*-CPBA

2 steps

5

Wittig olefination

6 steps

ring-closing metathesis

Yamaguchi esterification

2 steps

8

7

6

seiricuprolide (**1**): *Z*-alkene at C8-C9
pestalotioprolide B (**2**): *E*-alkene at C8-C9

12

11

OH-directed epoxidation mediated by *m*-CPBA

4 steps

10

3 steps

9

4 steps

D-mannitol

acetylide addition

- Lindlar or Red-Al reduction
- Wittig olefination

7 steps

Shiina macrolactonization

2 steps

13S: (7*S*)-stereogenic center
13R: (7*R*)-stereogenic center

Mitsunobu inversion
2 steps

14: *Z*-alkene at C8-C9
15: *E*-alkene at C8-C9

R = TBDPS

seiricuprolide (**1**): *Z*-alkene at C8-C9
pestalotioprolide B (**2**): *E*-alkene at C8-C9

ACKNOWLEDGEMENT

CONTENTS

CONTENTS (Continued)

LIST OF TABLES

LIST OF FIGURES

LIST OF FIGURES (Continued)

LIST OF FIGURES (Continued)

LIST OF FIGURES (Continued)

LIST OF FIGURES (Continued)

LIST OF FIGURES (Continued)

LIST OF SCHEMES

LIST OF SCHEMES (Continued)

LIST OF ABBREVIATIONS AND SYMBOLS

[α]	=	specific rotation
Acetone-d_6	=	hexadeuteroacetone
AcOH	=	Acetic acid
br	=	broad (spectral)
brsm	=	Based on decovered starting material
Bz		benzoyl
°C	=	degree Celsius
c	=	concentration
cat	=	catalytic
CHP		cumene hydroperoxide
cm^{-1}	=	wavenumbers
$CDCl_3$	=	deuterochloroform
δ	=	Chemical shift in parts per million
		downfield from tetramethylsilane
d	=	doublet (spectral)
DDQ	=	2,3-dichloro-5,6-dicyano-1,4-benzoquinone
DEAD	=	Diethyl azodicarboxylate
DET	=	Diethyl tartrate
DIPT	=	Diisopropyl tartrate
DMAP	=	4-dimethylaminopyridine
DMP	=	Dess–Martin periodinane
DMF	=	dimethylformamide
DMSO	=	dimethylsulfoxide
equiv	=	equivalent
ESI	=	Electrospray ionization

LIST OF ABBREVIATIONS AND SYMBOLS (Continued)

FT	=	Fourier transform
g	=	Gram(s)
h		Hour(s)
HRMS	=	High-performance liquid chromatography
Hz	=	hertz
IBX	=	2-iodoxybenzoic acid
IR	=	infrared
J	=	Coupling constant (spectral)
L	=	Liter(s)
μ	=	micro
m	=	Multiplet (spectral)
M	=	molar
m-CPBA		3-chloroperbenzoic acid
min	=	Minute(s)
MNBA	=	2-methyl-6-nitrobenzoic anhydride
mol	=	mole
MTPA	=	Methoxy trifluoromethyl phenyl acetate
m/z	=	Mass-to-charge ratio
NMR	=	Nuclear magnetic resonance
PMB	=	p-methoxybenzyl
ppm	=	parts per million
PPTS	=	pyridinium p-toluenesulfonate
q	=	quartet
R_f	=	Retention factor
rt	=	Room temperature

LIST OF ABBREVIATIONS AND SYMBOLS (Continued)

s	=	singlet
SAE	=	Sharpless Asymmetric Epoxidation
t	=	triplet
TBS	=	*tert*-butyldimethylsilyl
TBDPS	=	*tert*-butyldiphenylsilyl
TBAF	=	tetrabutylammonium fluoride
TBHP	=	*tert*-butyl hydroperoxide
THF	=	tetrahydrofuran
TLC	=	Thin-layer chromatography

LIST OF PUBLICATION

Sanphetchaloemchok, P.; Saikachain, N.; Khumliang, R.; Muanprasat, C.; Tadpetch, K. 2023. Total Synthesis and Biological Evaluation of Seiricuprolide and Pestalotioprolide B. Eur. J. Org. Chem. 26. e202300034.

COPYRIGHT PERMISSION NOTICE

CHAPTER 1

INTRODUCTION

CHAPTER 1

INTRODUCTION

1.1 Introduction

14-Membered macrolides are a significant class of polyketide metabolites that show diverse biological profiles particularly antibacterial activity (Chu *et al*., 1995, Zhanel *et al*., 2001 and Park *et al*., 2019). The structure of this class of macrolides possesses 14-membered macrolactone functionalized by various groups. This class of macrolides can be divided into two groups based on the presence of sugar moiety. The remarkable examples of 14-membered macrolides containing sugar moiety, which are widely utilized in human antibiotic medicine, are erythromycin (**1**) and its derivatives (**Figure 1**) (McGuire *et al*., 1952, Kanfer *et al*., 1998 and Galvidis *et al*., 2015). Another important subclass of bioactive 14-membered macrolides are those bearing an (*E*)-α,β-unsaturated ester subunit as depicted in **Figure 1**. Sch 725674 (**2**), isolated from *Aspergillus* sp. by Yang and co-workers in 2005, exhibited promising antifungal activity against *Saccharomyces cevrevisiae* (PM503) and *Candida albicans* (C43) with MICs of 8 and 32 μg/mL, respectively. 7-*O*-Methylnigrosporolide (**3**) and pestalotioprolide E (**4**) were found from the mangrove-derived endophytic fungus *Pestalotiopsis microspora* in 2016 by Liu and co-workers. Macrolides **3** and **4** displayed potent cytotoxic activity against the L5178Y murine lymphoma cells with an IC_{50} value of 0.7 μM and significant cytotoxic activity against the A2780 human ovarian cancer cells with an IC_{50} value of 1.2 μM, respectively. Another example that displayed a broad range of biological activities is mutolide (**5**), originally discovered from culture broth of fungus strain derived from UV mutagenesis of the fungus *Sphaeropsidales* sp. by Bode and co-workers in 2000. The Bode group also reported that compound **5** exhibited weak antibacterial activity against *B. subtillis* and *E. coli*. In 2015, macrolide **5** was

reisolated from the coprophilous fungus *Lepidosphaeria* sp. (PM0651419) and its promising anti-inflamatory activity was also disclosed in this work (Shah *et al.*, 2015). Isolation of **5** from the endophytic fungus *Aplosprella javeedii* was later reported by Gao and co-workers in 2020. Moreover, the isolated **5** was discovered to exhibit significant cytotoxic activity against the L5178Y mouse lymphoma, the Jurkat J16 human leukemia and the Ramos lymphoma cell lines with IC_{50} values of 0.4, 5.8 and 4.4 μM, respectively.

Figure 1 Structures of erythromycin (**1**) and selected examples of 14-membered membered macrolides bearing an (*E*)-α,β-unsaturated ester subunit (**2**-**5**)

erythromycin (**1**)　　　　　　Sch 725674 (**2**)

7-*O*-methylnigrosporolide (**3**)　　pestalotioprolide E (**4**)　　mutolide (**5**)
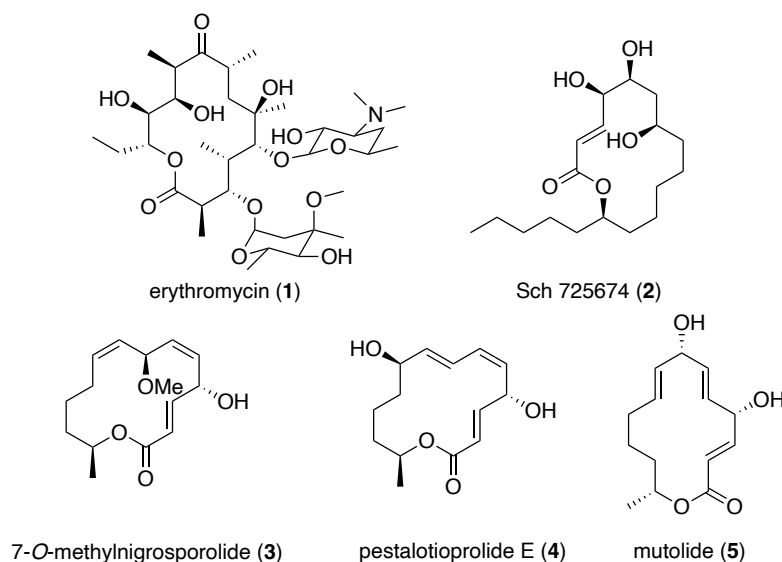
An interesting subgroup of 14-unsaturated macrolides are those containing chiral epoxide that also display diverse and promising biological activities. This subgroup of macrolides can be broadly classified into two groups based on the presence of a β-resorcylic acid subunit. The biologically active examples of β-resorcylic acid lactones (RALs) containing chiral epoxide motif are illustrated in **Figure 2**. Radicicol (**6**) was first isolated from *Monocillium nordinii* along with its dechlorinated analogue, monocillin I (**7**). Both RALs were found to show a variety of antifungal activities by Ayer et al. in 1980. RAL **6** was later disclosed to display other biological activities including antimalarial, anti-inflammatory and antiviral activities (Mejia *et al.*, 2014, Zhao *et al.*, 2013 and Isaacs *et al.* 2003), whereas RAL **7** was found to inhibit the proliferation of various human cancer cell lines (Turbyville et al., 2006, McLellan *et al.*, 2007 and Paranagama et al., 2007). In 2009, Shinonaga and co-workers reported

the isolation of pochonins K (**8**) and O (**9**) along with **6** and **7** from a culture broth of the fungus *Pochonia Chlamydosporia* TF-0480. Furthermore, RALs **6-9** were evaluated for their inhibitory activity against wingless-type mouse memory tumor virus integration site family, member 5A (WNT-5A) expression by the Shinonaga group. It was found that RALs **6** and **7** showed potent inhibitory activity against the WNT-5A expression with IC_{50} values of 0.19 and 1.93 µM, whereas RALs **8** and **9** exhibited moderate inhibitory activity with IC_{50} values of 8.57 and 9.39 µM. Notably, the *trans*-epoxide moiety at C4–C5 of **6-9** was suggested to be one of necessary functional groups for this activity. Hypothemycin (**10**), another 14-membered RAL with C10–C11 *trans*-epoxide motif, was originally obtained from a fungus *Hypomyces tricothecoides* by Nair *et al.* in 1980. In 2002, Isaka *et al.* reisolated RAL **10** from the fungus *Aigialus parvus* BCC 5311 and discovered that **10** displayed strong antimalarial activity against *Plasmodium falciparum* K1 with an IC_{50} value of 2.2 µg/mL. Furthermore, the isolations of bioactive analogues of **10** were later reported. 5'-*O*-Methylhypothemycin (**11**), isolated from the fruiting body of *Helvella acetabulum*, was found to act as a potent and specific inhibitor of a mitogen-activated protein kinase (MEK), a popular target of anticancer drugs, with an IC_{50} value of 4 µM by Zhao and co-workers in 1999. In 2006, 4-*O*-demethylhypothemycin (**12**) was isolated from the fungal strain *Hypomyces subiculosus* DSM 11931. RAL **12** was disclosed to show potent cytotoxic activity against the COL829 and the HT29 human colon cancer cell lines with IC_{50} values of 0.1 and 0.2 µM, respectively (Wee *et al.*, 2006).

Figure 2 Structures of selected examples of 14-membered RALs containing a chiral epoxide moiety

R = Cl, radicicol (**6**)
R = H, monocillin I (**7**)

pochonin K (**8**)

pochonin O (**9**)

R_1 = Me, R_2 = H, hypothemycin (**10**)
R_1 = Me, R_2 = Me, 5'-*O*-methylhypothemycin (**11**)
R_1 = H, R_2 = H, 4-*O*-demethylhypothemycin (**12**)
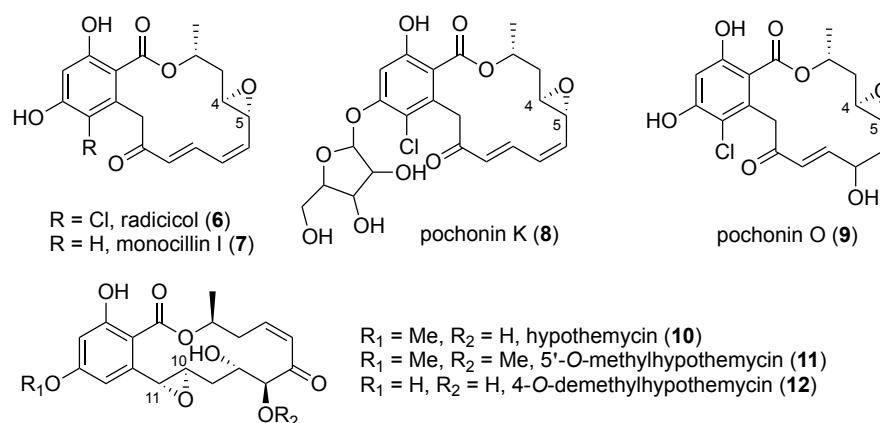
Another group of 14-membered unsaturated macrolides bearing chiral epoxide moiety features those lacking the β-resorcylic acid moiety. This group of macrolides is rare in nature and only a few examples have been reported as shown in **Figure 3**. Seiricuprolide (**13**) was first isolated from a fungus *Seiridium cupressi* by Ballio *et al*. in 1988. Macrolide **13** was reported to display phytotoxic activity by the isolation group. Pestalotioprolide B (**14**) was first discovered as a diacetate derivative (**15**) from the mangrove-derived endophytic fungus *Pestalotiopsis* sp. PSU-MA119 by Rukachaisirikul *et al*. in 2012. The isolation of macrolides **13** and **14** was reported again from the mangrove-derived endophytic fungus *Pestalotiopsis microspora* by the Liu and Proksch group in 2016. Structurally, seiricuprolide (**13**) possesses a 14-membered unsaturated lactone core with (*E*)-α,β-unsaturated ester at C2–C3, β-epoxide at C5–C6 and internal *Z*-alkene at C8–C9 as well as three alcohol stereogenic centers at the 4, 7 and 13 positions. Pestalotioprolide B (**14**) differs from **13** by the configuration of the internal alkene at C8–C9 which is an *E*-double bond. The absolute configurations of the five chiral centers of crystalline **13** were first determined by Bartolucci *et al*. in 1991, to be 4*R*, 5*S*, 6*R*, 7*S* and 13*S* by single-crystal X-ray diffraction analysis. The Liu group later reported the absolute configurations of **14** to be analogous to those of **13** via X-ray crystallographic analysis. The Liu group also disclosed the evaluation of cytotoxic activity against the L5178Y and A2780 cell lines for macrolides **13** and **14** using MTT assay. Unfortunately, they were inactive against these two cell lines. Since macrolides **13** and **14** were tested against only two cancer cell lines and there has been no report on the syntheses of these two compounds, we are interested in synthesizing seiricuprolide (**13**) and pestalotioprolide B (**14**) in order to further evaluate their cytotoxic activities against other cancer cell lines.

Figure 3 Structures of 14-membered unsaturated macrolides containing a chiral epoxide moiety

seiricuprolide (**13**)   pestalotioprolide B (**14**)   **15**   43
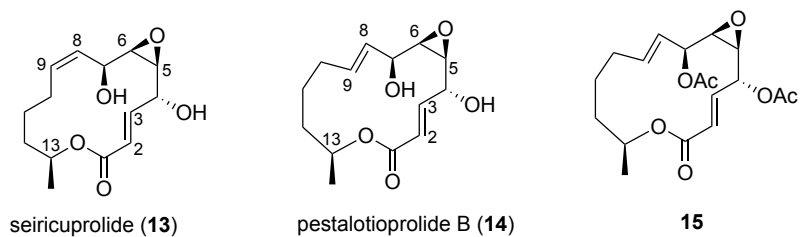
Currently, there has been no report on syntheses of seiricuprolide (**13**) and pestalotioprolide B (**14**). However, a few reports on syntheses of other 14-unsaturated macrolides having the core structure similar to **13** and **14** are precedented. According to the previous reports on syntheses of other 14-unsaturated macrolides containing (*E*)-α,β-unsaturated esters at C2–C3 and *Z*-alkenes at C8–C9, it was found that the synthetic strategies of macrocyclic formation mainly relied on Shiina macrolactonization and Yamaguchi esterification. Moreover, Lindlar's reduction and ring-closing metathesis were disclosed as strategies for generation of *Z*-alkene at C8–C9 (Tadpetch *et al.*, 2015 and Baikadi *et al.*, 2019). In addition, the formation of (*E*)-α,β-unsaturated esters at C2–C3 of previously reported 14-unsaturated macrolides possessing this functionality was achieved via Wittig olefination, ring-closing metathesis (RCM) and intramolecular Horner-Wadsworth-Emmons (HWE) (Tadpetch *et al.*, 2015, Paul *et al.*, 2018 and Baikadi *et al.*, 2019).

Figure 4 Key bond formations of previously reported examples of 14-membered unsaturated macrolides containing (*E*)-α,β-unsaturated esters at C2–C3 and *Z*-alkenes at C8–C9
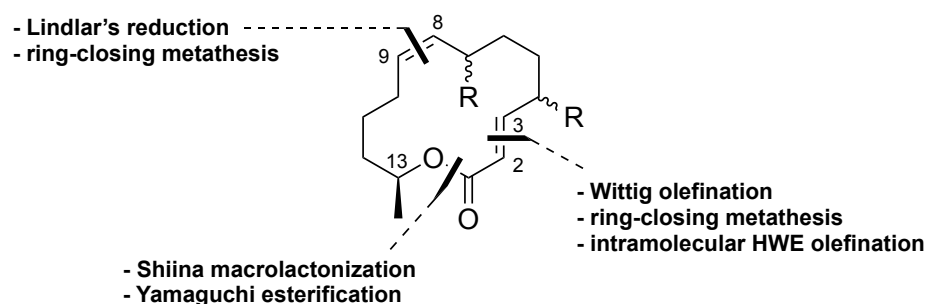
To date, there has been no report on synthesis of 14-unsaturated macrolide natural products possessing chiral epoxide motif at C5–C6, however, only 2 examples of syntheses of 14-unsaturated macrolides containing (*E*)-α,β-unsaturated ester at C2–C3 and *Z*-double bond at C8–C9 have been reported. This section will focus on details of these two reported examples. Firstly, Tadpetch and co-workers disclosed the synthesis of the proposed structure of pestalotioprolide A (**16**) in 2015 as depicted in **Scheme 1**. They utilized the Wittig olefination to generate (*E*)-α,β-unsaturated ester at

C2–C3. In addition, Yamaguchi esterification and ring-closing metathesis were employed as key strategies to construct the macrocyclic core of **16.** The synthesis started with preparation of known chiral epoxide **18** from D-(+)-gluconic acid δ-lactone (**17**) in 4 steps. Epoxide **18** was converted to chiral allylic alcohol **19** by regioselective ring opening using sulfonium ylide in excellent yield. Allylic alcohol **19** was then transformed to primary alcohol **20** in 5 steps via standard protection-deprotection reactions. Alcohol **20** was treated with PhI(OAc)$_2$ in the presence of catalytic TEMPO to give the corresponding aldehyde **21**. Wittig olefination of aldehyde **21** using stabilized phosphonium ylide Ph$_3$P=CHCO$_2$Et furnished (*E*)-α,β-unsaturated ester **22** as a single stereoisomer in 90% yield. The (*E*)-geometry was confirmed by the ^{1}H–^{1}H coupling constant of 15.6 Hz between H2 and H3. Subjection of **22** to basic hydrolysis resulted in the key intermediate carboxylic acid **23**. Coupling of carboxylic acid **23** with (*S*)-6-hepten-2-ol (**23**) via Yamaguchi esterification afforded diene ester **25** in 87% yield. Both silyl protecting groups of diene **25** were then removed to avoid steric hindrance of terminal diene to facilitate the ensuing RCM by using tetrabutylammonium fluoride (TBAF) to give **26**. Diol **26** was treated with Grubbs's first-generation catalyst (50 mol %) in refluxing dichloromethane to furnish the macrocycle in 35% yield based on recovered starting diene and formed the requisite *Z*-olefin at C8–C9 of **27** which was confirmed with the ^{1}H–^{1}H coupling constant of 10.5 Hz between H8 and H9. It should be noted that, based upon their optimization, ring-closing metathesis of **26** using 10 mol % of the more reactive Grubbs's second-generation catalyst led to reverse stereoselectivity which afforded (*E*)-isomer **28** as a major product in low combined yield. Lastly, removal of the acetonide protecting group of **27** utilizing HCl delivered the proposed structure of pestalotioprolide A (**16**) in 70% yield.

Scheme 1 Synthesis of the proposed structure of pestalotioprolide A (**16**) by Tadpetch *et al.*
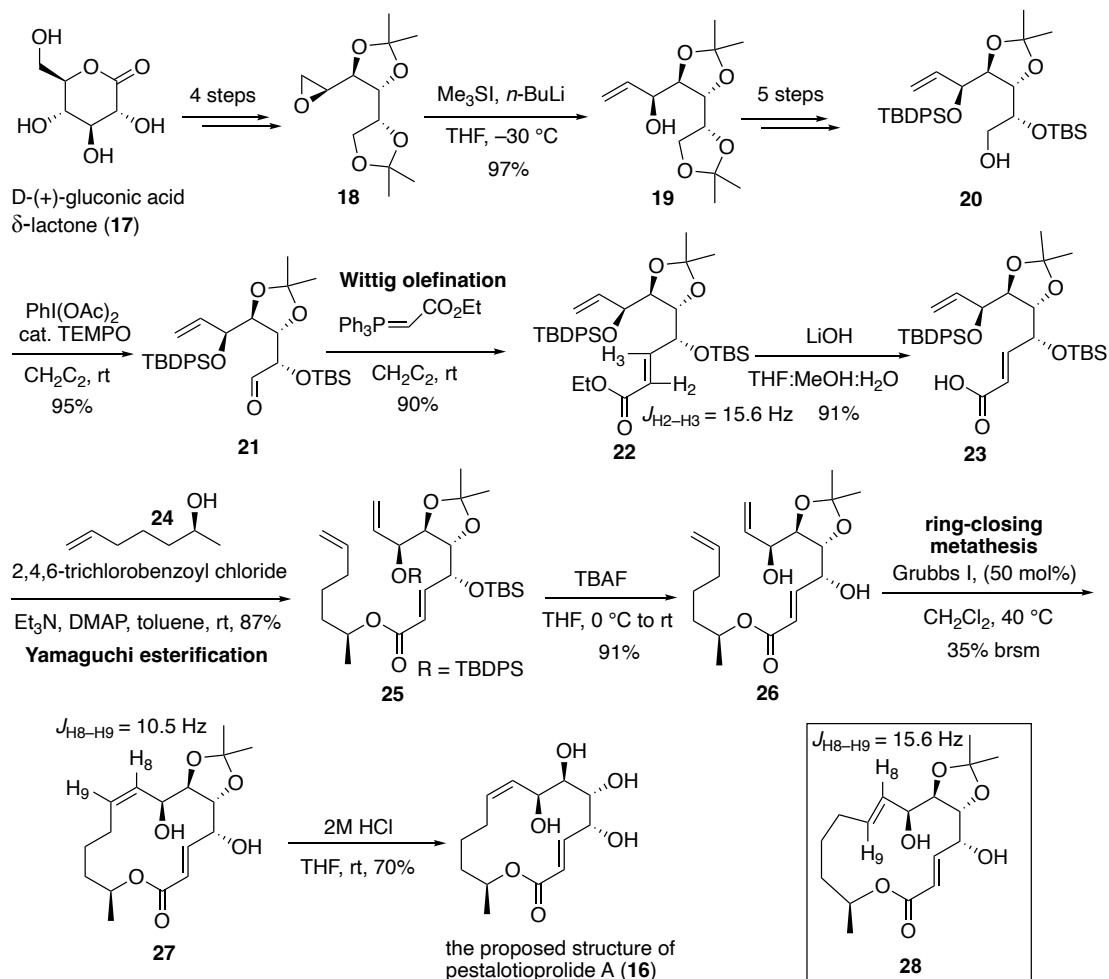
In 2019, the synthesis of advanced intermediate of 7-*O*-methylnigrosporolide (**3**), another 14-membered macrolactone containing (*E*)-α,β-unsaturated ester at C2–C3 and *Z*-double bond at C8–C9, was reported by Baikadi and co-workers (**Scheme 2**). The key reactions of their synthesis included HWE olefination to generate (*E*)-α,β-unsaturated ester at C2–C3, asymmetric carbonyl reduction to install the alcohol stereogenic center at C7-position, Lindlar reduction for formation of C8–C9 *Z*-alkene and construction of the macrocyclic ring via Shiina macrolactonization. The synthesis began with preparation of racemic propargylic alcohol **32** via acetylide addition between known alkyne **31** and (*Z*)-α,β-unsaturated aldehyde **30**, in which aldehyde **30** was derived from commercially available D-mannitol (**29**) in 4 steps. Alcohol **32** was then oxidized with 2-iodoxybenzoic acid

(IBX) to afford the corresponding ynone **33**. After that, **33** was selectively reduced using (*R*)-Corey-Bakshi-Shibata (CBS) reagent (**34**) to generate chiral alcohol **35** in 86% yield with good diastereoselectivity (*dr* = 90:10). The absolute configuration of the newly generated chiral center of propargylic alcohol **35** was confirmed by Mosher ester analysis. Propargylic alcohol **35** was then further converted to primary alcohol **36** in 5 steps via protection-deprotection reactions. The methoxymethyl (MOM) ether was chosen to be a protecting group of secondary alcohol at C4 position of **36**. Alcohol **36** was transformed to (*E*)-α,β-unsaturated ester **38** in 2 steps by treatment with Dess-Martin periodinane (DMP), followed by HWE olefination of the corresponding enal with triethylphosphonoacetate (**37**) and sodium hydride. The (*E*)-geometry of C2–C3 olefin was confirmed with the ^{1}H–^{1}H coupling constant of 15.6 Hz between H2 and H3. The seco acid **39** was then prepared by hydrolysis of ester **38** with LiOH and deprotection of silyl ether with HF·Py in 2 high-yielding steps. The key macrocyclization was accomplished via Shiina macrolactonization using 2-methyl-6-nitrobenzoic anhydride (**40**) and 4-dimethylaminopyridine (DMAP) in toluene to yield macrocycle **41** in 80% yield. Lindlar reduction of **41** with Pd/BaSO$_4$ in EtOAc/pyridine/1-octene was utilized to generate *Z*-olefin at C8–C9 of **42** as a single stereoisomer in 88% yield, which was confirmed with the ^{1}H–^{1}H coupling constant of 11.4 Hz between H8 and H9. However, in the final step they failed to remove the MOM protecting group at C4-position of **42** under various acidic conditions and these conditions only led to decomposition of the starting material.

Scheme 2 Attempted synthesis of 7-*O*-methylnigrosporolide (**3**) by Baikadi *et al*.
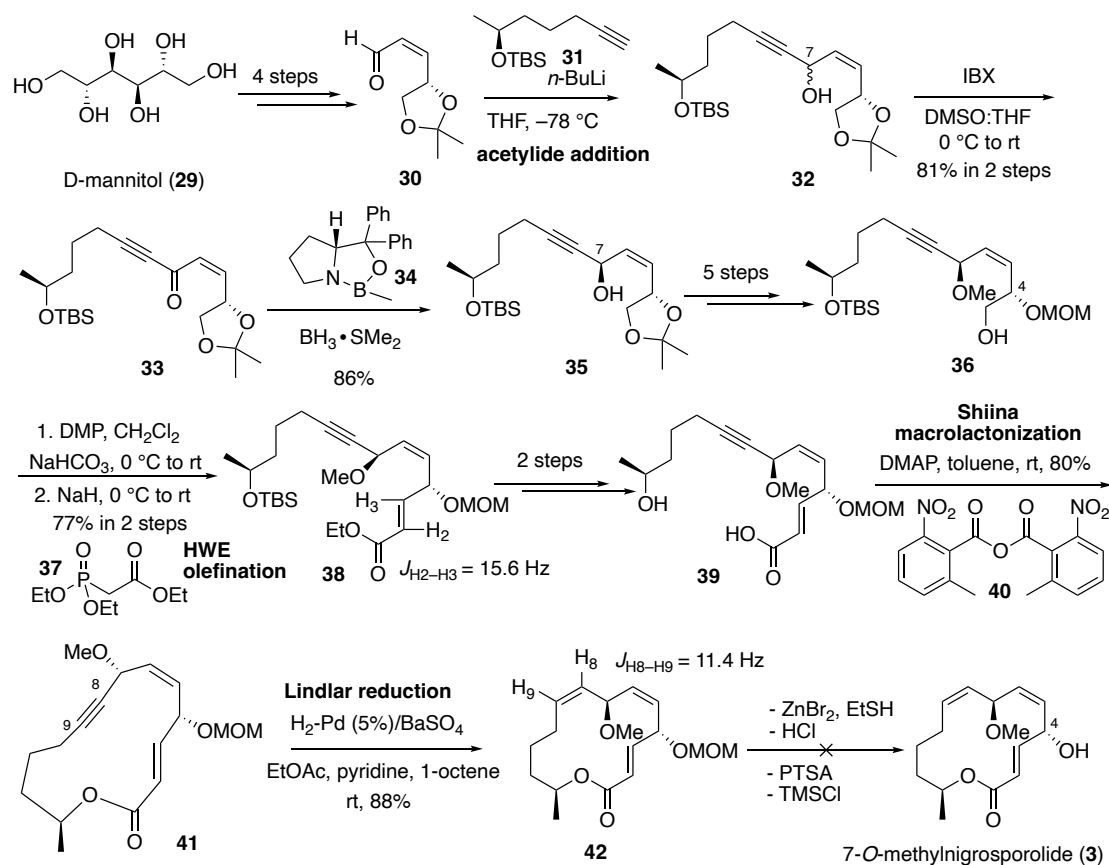
According to the two reports mentioned above, Wittig olefination is apparently an efficient strategy for generation of (*E*)-α,β-unsaturated ester at C2–C3 with high selectivity and excellent yield. Moreover, Yamaguchi esterification and Shiina macrolactonization are reliable strategies for generating C–O ester linkage with impressive yields. Therefore, we envisioned that these three strategies would be applicable in the syntheses of macrolides **13** and **14**. In addition, based on Tadpetch's report, the ring closing metathesis of diene intermediate **26** could lead to selective formation of *Z*- or *E*- double bonds at C8–C9 of **27** or **28** by using different Grubbs catalysts. Since structures of macrocycles **27** and **28** are nearly identical to our targeted macrolides **13** and **14**, we then anticipated that diene intermediate **26** could be employed as a precursor for constructing *Z*- and *E*- double bonds of **13** and **14** via selective ring-closing metathesis. Nonetheless, the more challenging part of syntheses of **13** and **14** is the installation of the *cis*-β-epoxide since epoxides are sensitive functional groups and

late stage installation of epoxides would ideally be preferable. Furthermore, there has been no report on synthesis of other 14-membered unsaturated natural products containing *cis*-β-epoxide. This section will focus on literature precedents on synthesis of previously reported 14-, 15- and 17-membered macrolactone natural products containing a chiral epoxide. It was found that installations of chiral epoxide of such natural products could be performed in both early and late stages of the syntheses. The first part will focus on the syntheses of macrolactones bearing chiral epoxide motif, in which the chiral epoxides were installed in the early stage via Sharpless asymmetric epoxidation (SAE). Generally, the SAE is a useful method for preparing chiral epoxy alcohols from allylic alcohol substrates and *tert*-butyl hydroperoxide (TBHP) is commonly utilized as an oxidizing agent in the presence of chiral tartrate ligand. The chirality of newly formed epoxide of the SAE product is usually predicted following Sharpless's mnemonic as depicted in **Figure 5**. The interaction of an oxidizing agent and the face of olefin is controlled by chiral tartrate ligand. The use of (–)-diethyl or (–)-diisopropyl tartrate preferentially leads to epoxidation on the top face of olefin to provide β-epoxide, while the use of (+)-diethyl or (+)-diisopropyl tartrate preferentially occurs on the bottom face of olefin to obtain α-epoxide (Goswami et al., 1980).

Figure 5 Mnemonic for prediction of facial selectivity of Sharpless asymmetric epoxidation by Goswami *et al*.
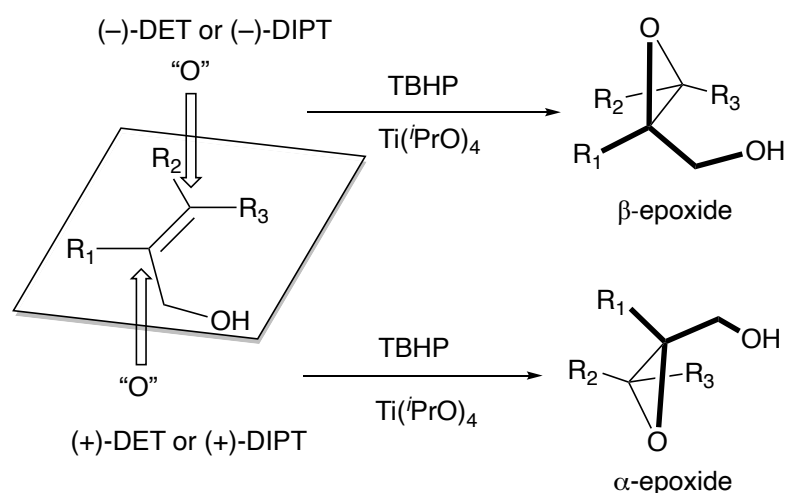
The first example is the convergent synthesis of two 14-membered RALs embedding *trans*-epoxide, radicicol (**6**) and monocillin I (**7**), reported by the Garbaccio group in 1998 as illustrated in **Scheme 3**. They utilized SAE to form *trans*-epoxide at C4–C5 position. In addition, Mitsunobu esterification and ring-closing metathesis were employed as key strategies to construct their macrocyclic cores. The synthesis began with preparation of SAE precursor **44** in 4 steps from (*S*)-methyl 3-hydroxybutanoate (**43**) via key HWE olefination. *E*-Allylic alcohol **44** was therefore subjected to SAE using TBHP and titanium isopropoxide in the presence of (+)-diethyl tartrate to yield the corresponding chiral epoxy alcohol **45** in 90% yield and 95% ee. Epoxy alcohol **45** was then converted to alcohol **46** in 3 steps. Coupling of alcohol **46** and carboxylic acid counterpart **47** was then affected by Mitsunobu esterification to give ester **48** in 75% yield. To prepare the ring-closing metathesis precursor **50**, ester **48** was then coupled with **49** via dithiane alkylation, followed by TBS protection. Diene **50** was then subjected to ring-closing metathesis to furnish macrolactone **51** in 60% yield. The global deprotection of silyl and dithiane protecting groups was performed in 3 steps to afford monocillin I (**7**) in 60% over 3 steps. In addition, radicicol (**6**) was obtained from regioselective aromatic chlorination of **7** using sulfuryl chloride. It is important to note that degradation of C4–C5 epoxide functional group, which was installed in the early stage, was not observed from any transformations in this synthetic route.

Scheme 3 Syntheses of radicicol (**6**) and monocillin I (**7**) by Garbaccio *et al.*
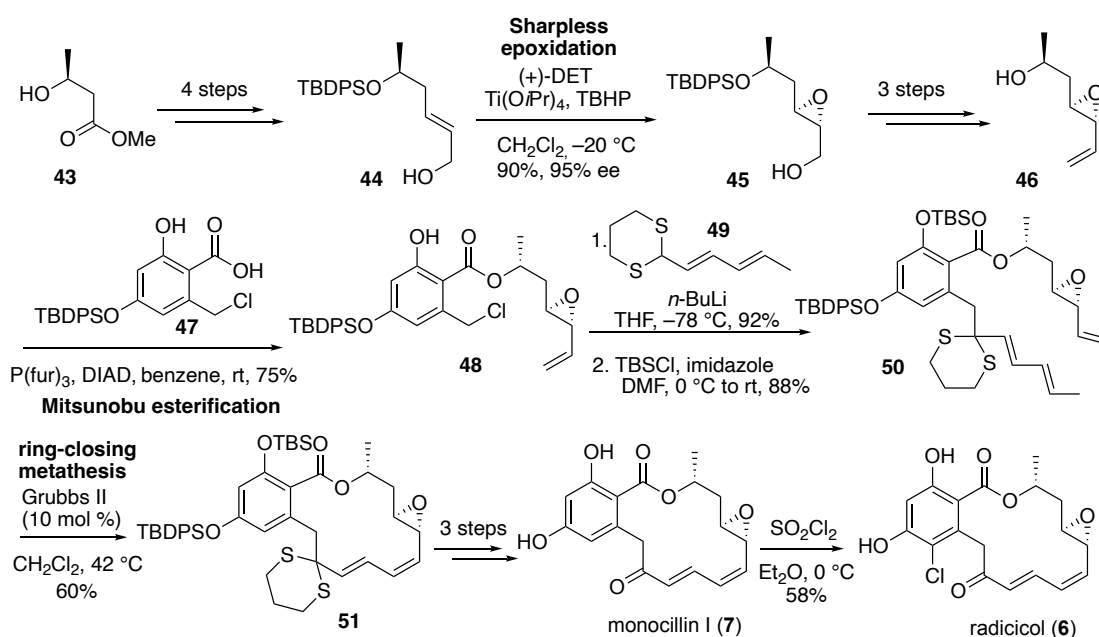
Another example of synthesis of 14-membered macrolactone bearing *trans*-epoxide, amphinolide V (**52**), in which early stage installation of epoxidation was also affected by SAE to form C8–C9 *trans* epoxide (**Scheme 4**). The key reactions for forming their macrocyclic backbone included ring-closing alkyne metathesis and intermolecular enyne metathesis. The synthesis started with coupling of alcohol **54** and 4-hexynoic acid (**53**) via standard esterification to provide ester **55** in excellent yield. To prepare SAE precursor **56**, the terminus tetrahydropyranyl (THP) protecting group of **55** was removed using PPTS to deliver *E*-allylic alcohol **56**. Sharpless epoxidation of **56** was then performed by using TBHP and titanium isopropoxide in the presence of (+)-diethyl tartrate to furnish the corresponding epoxy alcohol **57** in 83% yield and a diastereomeric ratio of 98:2. Epoxy alcohol **57** was further subjected to 2-step transformation to obtain key diyne intemedate **59** via DMP oxidation, followed by treatment with bis(alkynyl)zinc reagent **58** which provided separable alcohol diastereomers in 64% combined yield and good diastereoselectivity. The silylation of major diastereomer **59** was performed to prepare substrate for ring-closing alkyne metathesis in the next step. The ring-closing alkyne metathesis of the resulting diyne was then affected by employing a catalyst generated in situ from molybdenum complex **60** in dichloromethane to form the strained 14-membered cycloalkyne **61** in 84% yield without reacting to other olefin functional groups. The alkyne functionality of **61**was next elaborated to vicinal methylene branches of **62** by subjection of **61** to enyne metathesis by reacting with ethylene gas (1.8 atm) using Grubbs's second-generation catalyst. Lastly, macrolactone **62** was further transformed in 4 steps to complete the synthesis of amphidinolide V (**52**), which did not lead to any degradations of requisite C8–C9 epoxide (Fürstner *et al*., 2009).

Scheme 4 Syntheses of amphidinolide V (**52**) by Fürstner *et al*.
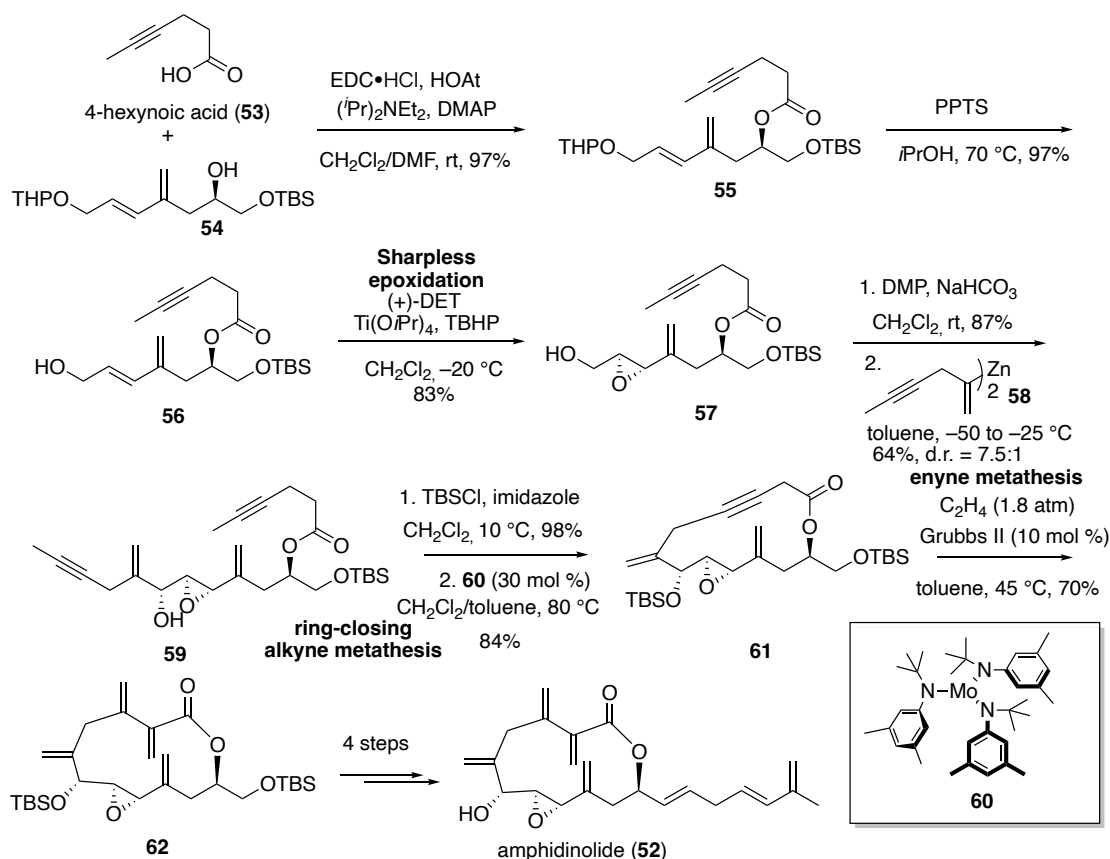
The last example is the synthesis of macrocyclic core of iriomoteolide 3a (**63**), 15-membered macrolactone containing *trans*-epoxide, which was reported by Reddy and co-workers in 2009 (**Scheme 5**). This work also utilized SAE to generate C11–C12 *trans* epoxide of advanced intermediate **71** in early stage of the synthesis. In addition, Yamaguchi esterification and ring-closing metathesis were used as key strategies for constructing its macrocyclic core. Firstly, *E*-allylic alcohol **65** was prepared from lactone **64** in 6 steps. *E*-allylic alcohol **65** was then subjected to SAE by using TBHP and titanium isopropoxide in the presence of (+)-diisopropyl tartrate to deliver epoxy alcohol **66** in 88%. It should be noted that the exact values of diastereomeric ratio of SAE was not provided, however, Reddy and co-workers only claimed that these conditions led to good stereoselectivity to provide **66**. After that, epoxy alcohol **66** was elaborated to alcohol **67** in 4 steps. Yamaguchi esterification of alcohol **67** and carboxylic acid **68** was later performed to furnish RCM precursor **69** in

93% yield. Diene **69** was then subjected to ring-closing metathesis using 15 mol % of Grubbs's second-generation catalyst to afford the separable *E*- and *Z*-isomers (8:2) of RCM products in 71% combined yield. The *E*-isomer **70** was exposed to desilylation to deliver the macrocyclic core **71** in 89% yield. Although C11–C12 epoxide moiety of **66** was installed in the early stage of synthesis, the intermediate **66** could be carried through multistep without affecting the requisite epoxide moiety (Reddy *et al*., 2009).

Scheme 5 Syntheses of macrocyclic core of iriomoteolide 3a (**63**) by Reddy *et al*.
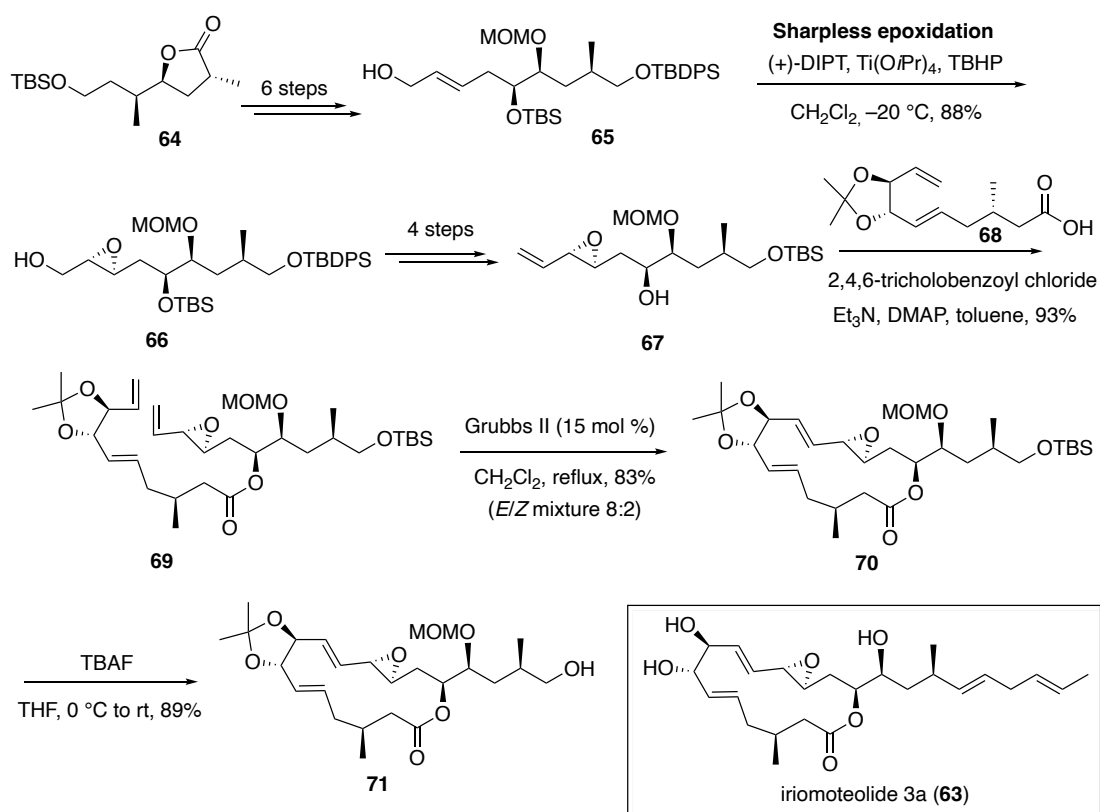
Our attention will next focus on examples of syntheses of macrolactones bearing chiral epoxide which was installed in the late stage of the syntheses. The first example is the synthesis of a 14-membered RAL consisting of *trans*-epoxide motif, hypothemycin (**10**), which was reported by Sellès and co-workers (**Scheme 6**). Their methodology for forming chiral epoxide of **10** was totally different from the previously described epoxidation in syntheses of **6** and **7**. In this work, epoxidation was performed in the final stage of synthesis and *m*-CPBA epoxidation was utilized for constructing

C10–C11 *trans*-epoxide. The synthesis commenced with Suzuki coupling of **72** and **73** to provide alkene **74** in 76% yield. Ester **74** was then converted to seco acid **75** in 3 steps. Macrolactonization of **75** was performed via Mitsunobu reaction to afford macrolactone **76** in 67% yield. The next task was the installation of chiral epoxide functional group, in which macrolactone **76** was then subjected to 3-step transformation to smoothly afford **77** as a precursor of *m*-CPBA epoxidation. Lastly, *m*-CPBA epoxidation of **77** was performed to yield C10–C11 α-epoxide of the desired hypothemycin (**10**) in 17% yield along with unreacted starting **77** (30%) and no other epoxide products were observed. The absolute configuration of the newly formed epoxide was identified by comparison of ^{1}H NMR and ^{13}C NMR spectra with those of previously reported natural product. However, the rationale of the stereoselectivity of epoxidation of **77**, which was presumably substrate-controlled, was not provided in this work.

Scheme 6 Syntheses of hypothemycin (**10**) by Sellès *et al*.
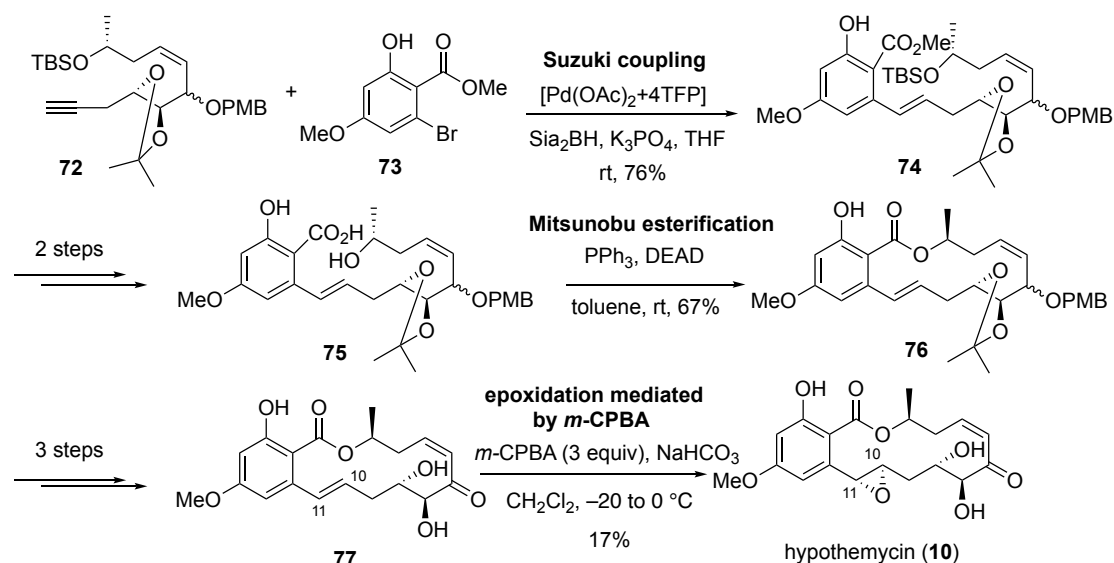
Another crucial example is synthesis of ivorenolide B (**78**), 17-membered macrolide bearing *cis*-epoxide which was reported by Wang and co-workers in 2014 (**Scheme 7**). The formation of *cis*-epoxide of ivorenolide B (**78**) was performed in the late stage of its synthesis and substrate-controlled epoxidation mediated by *m*-CPBA was utilized as an efficient tool to provide high yield and excellent selectivity. Initially, diene **81** was prepared via Cadiot-Chodkiewicz coupling of **79** and **80** in the presence

of Cu(I). Diene **81** was then subjected to ring-closing metathesis using Grubbs's first-generation catalyst to obtain separable *Z*- and *E*-products in the ratio of 1:1.5 and 90% combined yield. The next task was installation of chiral epoxide moiety. Epoxidation of the minor *Z*- product **82** was therefore affected using *m*-CPBA to afford the desired epoxide **83** as a sole product. They proposed that the *m*-CPBA approached the double bond of **82** from sterically less hindered olefin face to provide the desired α-epoxide **83**. Finally, TBDPS protecting group was removed to complete the synthesis of ivorenolide B (**78**).

Scheme 7 Synthesis of ivorenolide B (**78**) by Wang *et al*.
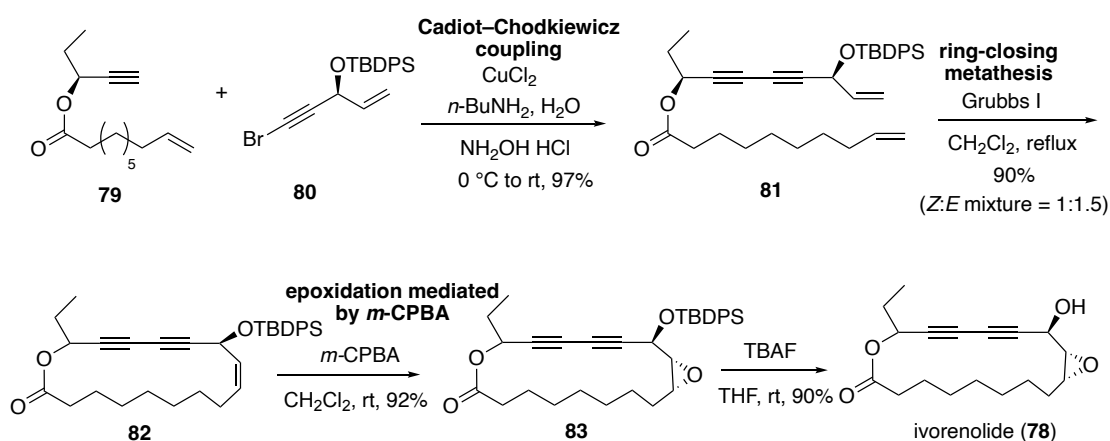
According to the previously reported syntheses of macrolactones embedding chiral epoxide moiety mentioned above, it is obvious that the epoxide formation could be performed in both early and late stages of the synthesis. Sharpless asymmetric epoxidation proved to be an efficient method to form *trans*-epoxide moiety from *E*-allylic alcohol substrates with high yield and good selectivity. Epoxidation of *Z*-allylic alcohol mediated by *m*-CPBA was an alternative strategy that provided good stereoselectivity, however, the stereoselectivity outcome would be substrate-controlled. Nevertheless, most examples were formations of *trans*-epoxides, whereas our targeted natural products contain a *cis*-epoxide. To gain an insight on *cis*-epoxide formation, the next section will focus on literature precedents on general methods for *cis*-epoxide formation which might be applicable for syntheses of **13** and **14**. The general methods reported for forming *cis* epoxides rely on epoxide formation from 1,2-*trans* diol and *Z*-

allylic alcohol. The first method is the generation of *cis*-epoxide from 1,2-*trans* diol which was reported by Migawa *et al.* in 2013. Migawa and co-workers reported the synthesis of constrained D-altriol nucleic acid **84**, in which epoxide **88** was utilized as a key intermediate. The preparation of epoxide **88** commenced with the conversion of 1,2-diol **85** to monotosylate **87** in 2 steps via tosylation by treatment with tosyl chloride and pyridine to provide bis-tosylate **86**, followed by selective methanolysis. Alcohol **87** was later exposed to sodium hydride to afford *cis*-epoxide **88** in excellent yield (**Scheme 8**). Since the rationale for selective methanolysis was not mentioned in this work, the regioselective removal of the tosyl moiety might be substrate-dependent. Although the regioselectivity for monotosylate removal was unclear and this methodology required three steps for epoxide formation, this method can presumably be an alternative guideline to screen the preparation of the desired β-epoxide of **13** and **14** from 1,2-diol substrate in the late stage of synthesis.

Scheme 8 Generation of *cis*-epoxide **88** from 1,2-*trans* diol **85** by Migawa *et al.*
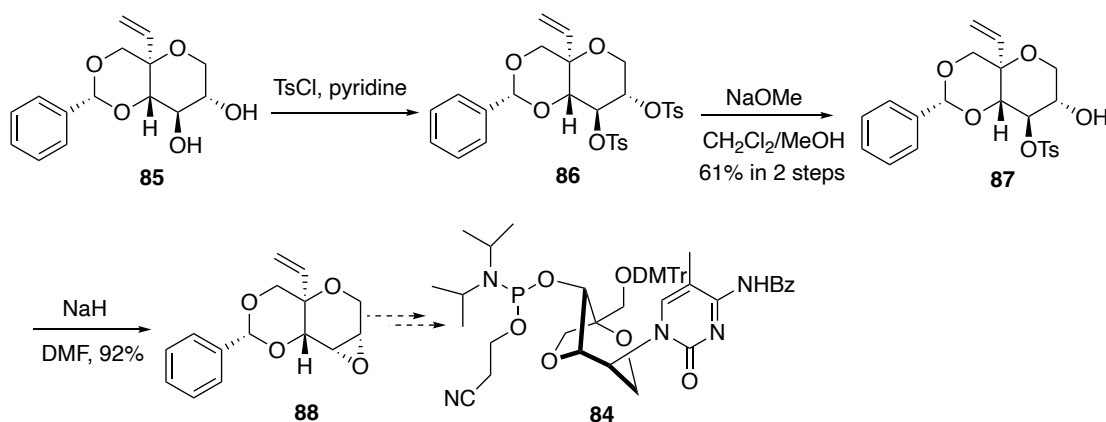
The next approach is the installation of *cis*-epoxide from *Z*-allylic alcohol. Although Sharpless asymmetric epoxidation is well known as a very efficient method to install chiral epoxide from *E*-allylic alcohols, *Z*-allylic alcohols are generally poor and inactive substrates for SAE (Matsumoto et al., 2012). However, a few examples on SAE of *Z*-allylic alcohol substrates utilizing (–)-diethyl tartrate that provided β-epoxides as major product with good selectivity, have been reported (**Scheme 9**). In 2016, Thirupathi and co-workers reported the SAE of intermediate **89** for construction of C17 stereogenic center of herboxidiene (**91**). *Z*-Allylic alcohol **89** was treated with

TBHP and titanium isopropoxide in the presence of (–)-diethyl tartrate to deliver the β-epoxide of **90** in 87% yield and a diastereomeric ratio of 10:1 as determined by HPLC analysis. In the same year, Bodugam and co-workers also disclosed the Sharpless asymmetric epoxidation of intermediate **92** which promoted the generation of C4 stereogenic center of Sch 725674 (**2**). Employment of *Z*-allylic alcohol **92** with cumene hydroperoxide (CHP) and titanium isopropoxide in the presence of (–)-diethyl tartrate selectively provided β-epoxide of **93** as a major product in 80% based on recovered of starting **92** along with minor antipode in 9% yield.

Scheme 9 A) Sharpless epoxidation of *Z*-allylic alcohol **89** by Thirupathi *et al*; B) Sharpless epoxidation of *Z*-allylic alcohol **92** by Bodugam *et al*
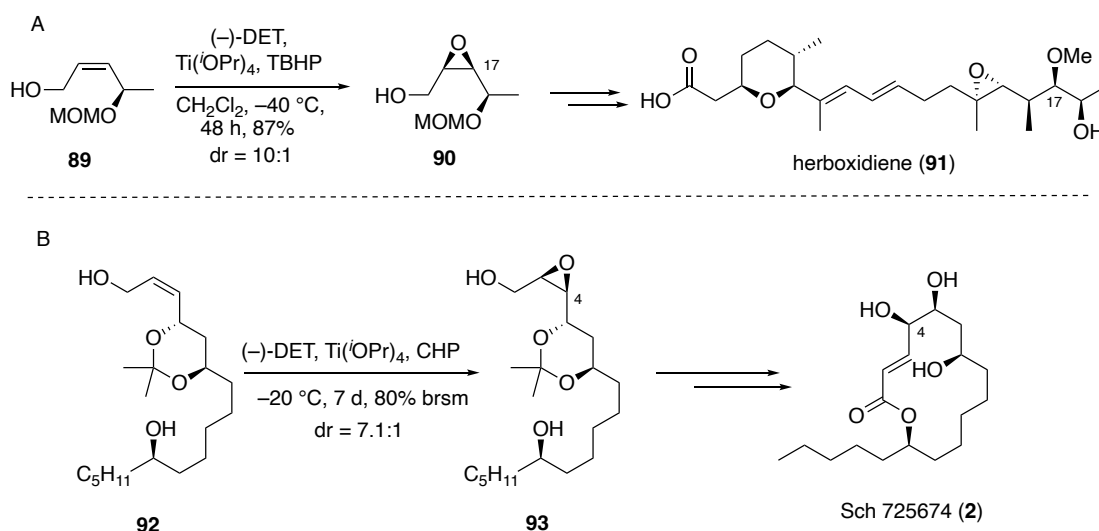
Another crucial example is selective *m*-CPBA epoxidation of *Z*-allylic alcohol bearing adjacent (*S*)-silyloxy stereogenic centers by Baltas *et al*. in 2013 as shown in **Scheme 10**. Baltas and co-workers reported the preparation of epoxy alcohols intermediates **93a** and **94a** which were utilized as precursors for the synthesis of octulsonic acids. To prepare β-epoxy alcohols **93a** and **94a**, epoxidations of *Z*-allylic alcohols **93** and **94** was performed using *m*-CPBA in the presence of $NaHCO_3$ to provide 2:1 and 6:1 *erythro*/*threo* of epoxy alcohol products **93a:93b** and **94a:94b**, in which the major *erythro* products **93a** and **94a** contain a β-epoxide moiety. In addition, this work disclosed the particular trend in the vicinal coupling constants between

methine protons of the chiral epoxides α to silyloxy stereogenic centers and the methine protons of the silyloxy stereogenic centers ($J_{3/4}$). The $J_{3/4}$ of *threo* products were generally observed to possess higher values compared to those of the *erythro* counterparts. This information could be utilized as a guideline to verify the absolute configurations of chiral epoxides bearing adjacent silyloxy stereogenic centers. Nonetheless, the rationale of the stereoselectivity of epoxidation of this substrate was not discussed. Since epoxidation of this particular substrates delivered the *erythro* series as major products in good selectivity, we envisioned that this method would be also applicable in β-epoxide formations of **13** and **14**.

Scheme 10 Selective epoxidation of *Z*-allylic alcohols **93** and **94** by Baltas *et al*.
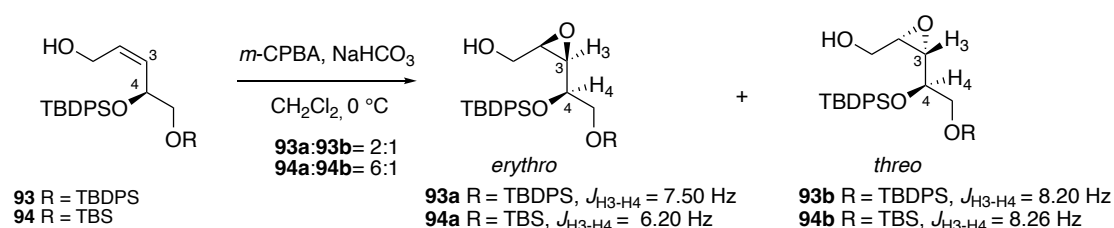
Based on the literature precedents, we envisioned that the β-epoxide of **13** and **14** could be installed in both early and late stages of the synthesis. The proposed synthesis of our targeted natural products was set out in two schemes. The first proposed syntheses of **13** and **14**, which was planned to install the β-epoxide motif from 1,2-*trans* diol intermediate in the late stage of the synthesis, is depicted in **Scheme 11**. The construction of 14-membered macrocycles of **95** and **96** would be achieved by ring-closing metathesis of Tadpetch's intermediate **26**, which was prepared via key Yamaguchi esterification and Wittig olefination. The *Z*- or *E*-olefin at C8–C9 of **95** and **96** would be derived from the selective ring-closing metathesis. In order to elaborate the acetonide protecting group to β-epoxide, protection of both free hydroxyl groups of **95** and **96** would be required before removal of the acetonide protecting group was performed to provide diol of **97** and **98**. The 1,2-*trans* diols **97** and **98** would be transformed to the corresponding tosylates **99** and **100** by selective monotosylation of C5-hydroxyl group or by subsequently converting diol to bis tosylate and selectively

hydrolysis of C6-tosylate. It should be noted that selective monotosylation or selective hydrolysis of bis tosylate as mentioned could be challenging because the most stable conformation of 14-membered macrolide is not known and steric hindrance around the two hydroxyl groups are not different. The β-epoxides of **13** and **14** would then be accomplished by displacement of tosylate of **99** and **100** mediated by a base. Inspired by Baltas's epoxidation, another proposed synthesis of **13** and **14** was designed to install the β-epoxide functional groups from starting *Z*-allylic alcohol bearing adjacent (*S*)-silyloxy stereogenic center substrate and this epoxidation step was planned to perform in the early stage of the synthesis. However, carrying epoxide intermediate through multistep synthesis could be also challenging since the requisite use of acidic conditions might lead to degradation of the sensitive epoxide functional group. The β-epoxide of proposed key intermediate **102** would be prepared from *Z*-allylic alcohol **101** via *m*-CPBA epoxidation. The synthesis of the remaining parts of **13** and **14** were proposed to utilize the same key strategies previously mentioned including ring-closing metathesis, Yamaguchi esterification and Wittig olefination (**Scheme 12**).

Scheme 11 Proposed syntheses of seiricuprolide (**13**) and pestalotioprolide B (**14**) (route I) via late stage installation of epoxide from 1,2-diol
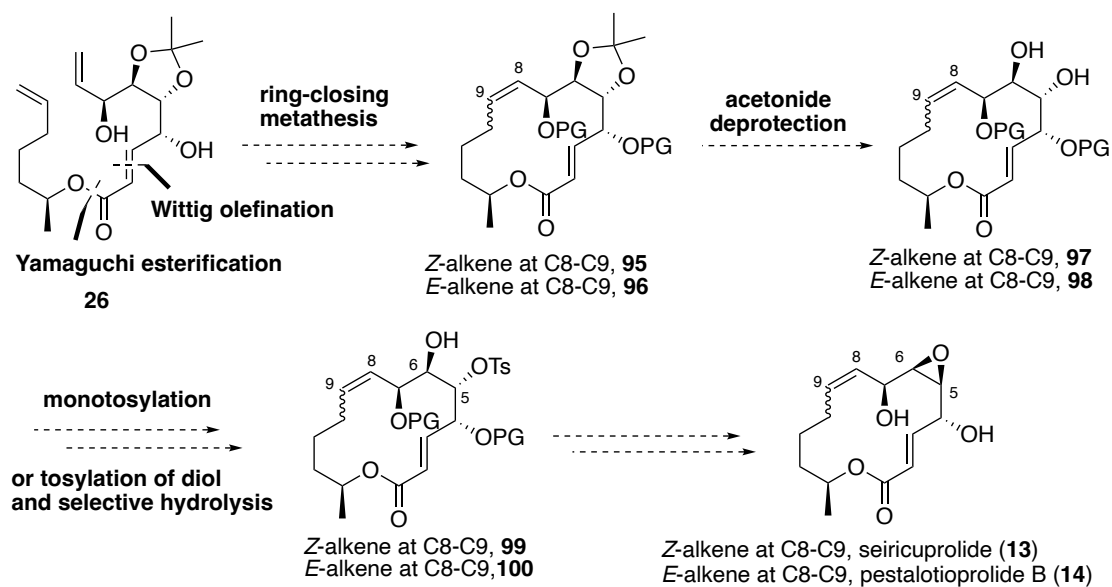
Scheme 12 Proposed syntheses of seiricuprolide (**13**) and pestalotioprolide B (**14**)
(route II) via early stage epoxidation of *Z*-allylic alcohol mediated by
m-CPBA
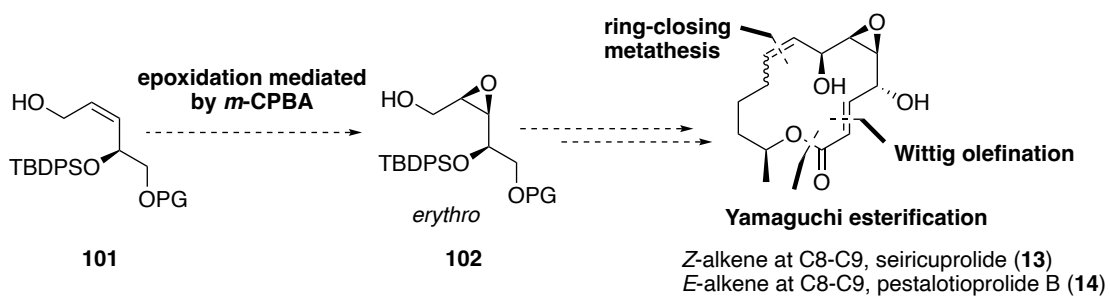
1.2 Objectives

1. To synthesize seiricuprolide (**13**) and pestalotioprolide (**14**)
2. To provide materials for further evaluation of biological activities

CHAPTER 2

ATTEMPTED SYNTHESES OF
SEIRICUPROLIDE
AND PESTALOTIOPROLIDE B

CHAPTER 2

ATTEMPTED SYNTHESES OF SEIRICUPROLIDE AND PESTALOTIOPROLIDE B

2.1 Results and Discussion

Synthesis of seiricuprolide (**13**) and pestalotioprolide B (**14**) was first attempted using the proposed synthetic procedure (route I) which was planned to install the epoxide functionality of **13** and **14** in the late stage of the synthesis as previously described in **Scheme 11**. The synthesis commenced with the preparation of RCM precursor **26** in 15 steps starting from D-(+)-gluconic acid δ-lactone (**17**) utilizing Yamaguchi esterification and Wittig olefination as key steps, in which the details of all transformations were mentioned in **Scheme 1** (Tadpetch *et al*., 2015). The next task was formation of *Z*- and *E*-olefins at C8–C9 position of **13** and **14** as well as their macrocyclic cores via ring-closing metathesis (**Scheme 13**). Ring-closing metathesis of **26** was then undertaken using 5 mol % of the second generation Grubbs catalyst in refluxing dichloromethane at high dilution (0.8 mM). Notably, these conditions afforded separable stereoisomers **27** and **28** in 17% and 52% along with dimeric compound **102** in 11% yield. The *Z*- and *E*-geometries of **27** and **28** were confirmed with the ^{1}H–^{1}H coupling constants between H8 and H9 of 10.6 and 15.6 Hz, respectively. Since macrolactone **28** was obtained as a major product, we decided to carry **28** to screen conditions for constructing C5–C6 β-epoxide.

Scheme 13 Synthesis of macrolactones **27** and **28**
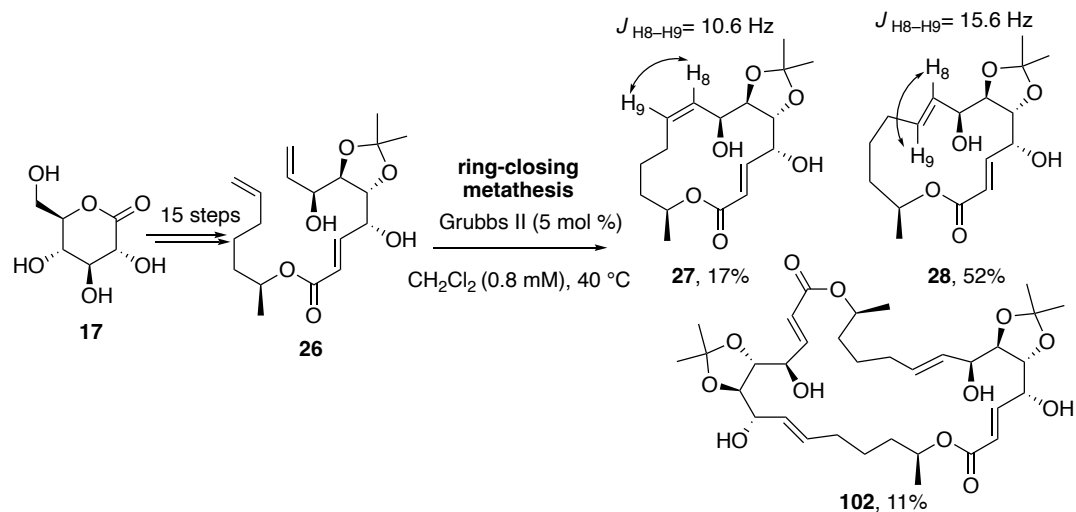
The next task was protection of free alcohols at C4- and C7-positions of **28**, followed by removal of acetonide protecting group. Since acetonide protecting group is generally removed under acidic conditions, the protecting group for the two free alcohols of **28** should not be acid sensitive. We decided to choose the benzoyl (Bz) group as protecting groups at C4- and C7-positions of **28** since the Bz group generally can be deprotected under basic conditions. In addition, previous reports on removal of acetonide between two vicinal benzoates are widely precedented under acidic conditions (McKenzie *et al*., 2018, Kim *et al*., 2007, Yu *et al*., 2001 Cid *et al*., 2009 and Vinaykumar *et al*., 2017). Diol **28** was therefore treated with 5 equivalents of benzoyl chloride and triethylamine to obtain benzoate ester **103** in 74% yield. We then screened various acidic conditions in order to remove the acetonide protecting group of **103** as shown in **Table 1**. We began investigation of deprotection of acetonide under mild conditions. In 2012, Palframan and co-workers reported a methodology for deprotection of acetonide adjacent to benzoate using iodine as soft acid in MeOH at room temperature, in which the benzoyl group was compatible with the reaction conditions. Unfortunately, no desired diol product **104** was observed when **103** was subjected to the conditions and the starting material was recovered (entry 1). We next turned our attention to screen reaction conditions utilizing typical acids such as HCl in THF or MeOH (entries 2 and 3), *p*TSA in MeOH:CH$_2$Cl$_2$ (entry 4) and 90%

trifluoroacetic acid (TFA) in CH_2Cl_2 (entry 5) (Sun *et al*., 2021, Yu *et al*., 2001 and Kim *et al*., 2007). However, the desired diol product was again not observed from any of these conditions. Further optimization was then performed using harsher conditions, **103** was treated with   80% AcOH in the absence of solvent at 60 °C (McKenzie *et al*., 2018) (entry 6). Disappointingly, no desired product was observed. In an attempt to use stronger acid, deprotection of acetonide of **103** was therefore performed using 12 equivalents of 90% TFA without any solvent at 0 °C (Cid *et al*., 2009 and Vinaykumar *et al*., 2017). After maintaining the reaction at this temperature for 2 h, there was no noticeable change upon monitoring by TLC. Thus, the reaction temperature was raised to room temperature (entry 7). Unexpectedly, several spots on TLC plate were noticed after maintaining the reaction temperature at room temperature for 1 h. Since the reaction conditions in entry 7 was screened in only 30 milligrams scale, we could not purify and identify all observed products. However, this result suggested that room temperature was not suitable for acetonide deprotection using neat TFA. The next optimization was performed by increasing the amount of 90% TFA to 100 equivalents while maintaining the reaction temperature at 0 °C (entry 8). Surprisingly, these conditions provided the desired product **104** in 9% yield (30% yield based on recovered **103**). In an attempt to improve the product yield, the amount of 90% TFA was further increased to 200 equivalents under the same conditions (entry 9). Gratifyingly, the yield of **104** was observed to increase to 43% yield (56% yield based on recovered **103**). Nonetheless, when **103** was treated with greater amount of 90% TFA (250 equiv) at 0 °C (entry 10), the yield of **104** decreased to 36% yield (41% yield based on recovered **103**) and other unidentified products were observed. After that, we tried to use milder reagent, trifluoroacetic anhydride (TFAA) in aqueous solution, with anticipation that reaction might be cleaner. Therefore, **103** was treated with 90% TFAA at 0 °C. After warming the reaction to room temperature and maintaining reaction at this temperature for 19 h, it was found that the reaction was inert and the diol **104** was observed in trace amount. Thus, the use of 200 equivalents of 90% TFA at 0 °C would be the optimal conditions for deprotection of acetonide group of **103**. Nonetheless, it was found that these conditions were irreproducible and the observed product yields were inconsistent and decreased to 10-20%. Since the desired diol **104** could not be produced in large

quantity for screening the next epoxide formation, we decided to change the synthetic route for synthesis of **13** and **14**.

Table 1 Optimization of removal of acetonide protecting group of **103**
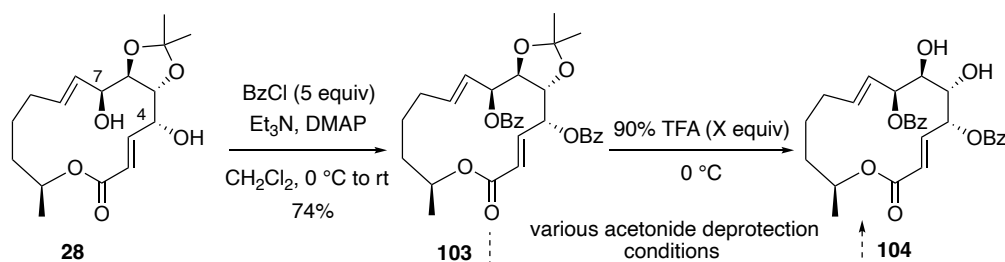
entry	conditions	time (h)	results
1	iodine, MeOH, rt	18	no reaction
2	1M HCl, THF, 0 °C to 40 °C	3.5	no reaction
3	4M HCl, MeOH, rt	4.5	no reaction
4	pTSA (12 equiv), MeOH: CH$_2$Cl$_2$, rt	5	no reaction
5	90% TFA (12 equiv), CH$_2$Cl$_2$, 0 °C to rt	5	no reaction
6	80% AcOH, 60 °C	4	no reaction
7	90% TFA (12 equiv), 0 °C to rt	3	unidentified products
8	90% TFA (100 equiv), 0 °C	1.5	**104**, 9% (30% brsm)
9	90% TFA (200 equiv), 0 °C	1.5	**104**, 43% (56% brsm)
10	90% TFA (250 equiv), 0 °C	1	**104**, 36% (41% brsm)
11	90% TFAA (100 equiv), 0 °C to rt	22	trace of **104**

We then turned our attention to the proposed synthetic route II which was planned to install the β-epoxide in the early stage of the synthesis according to Baltas's protocol. However, this synthetic route still utilized the same key strategies for forming macrocyclic skeletons of **13** and **14** as the proposed synthetic route I as shown in **Scheme 14**. Retrosynthetically, the macrocyclic cores of **13** and **14** would be constructed by ring-closing metathesis of diene **105**. Diene **105** would be prepared via

Yamaguchi esterification of (*S*)-hept-6-en-2-ol (**24**) and carboxylic acid **106**. The terminal alkene of **106** would be installed by vinylation of epoxy aldehyde **107**. It was anticipated that the adjacent chiral epoxide of aldehyde **107** would direct the stereoselectivity of vinylation step. Chiral epoxy aldehyde **107** would be prepared from substrate-controlled and selective epoxidation of known *Z*-allylic alcohol bearing (*S*)-silyloxy stereogenic center **108** which is nearly identical to Baltas's substrate. *Z*-allylic alcohol **108** would be synthesized from (±)-epichlorohydrin (**109**) via a protocol previously reported by our research group (Thiraporn *et al*., 2022a).

Scheme 14 Retrosynthetic analysis of seiricuprolide (**13**) and pestalotioprolide B (**14**)
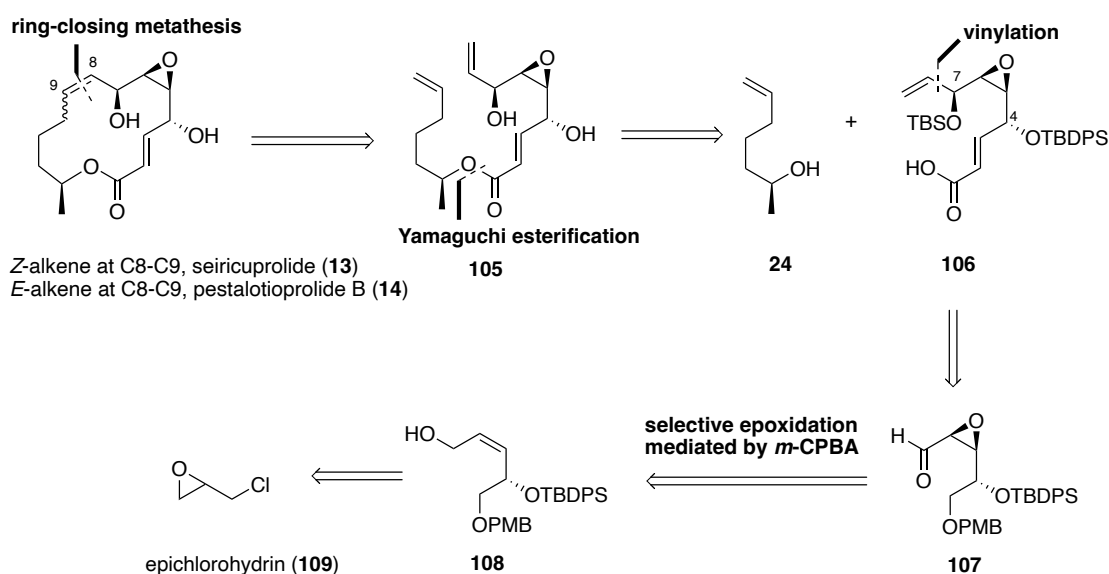
The synthesis of **13** and **14** began with preparation of known *Z*-allylic alcohol **108** from (±)-epichlorohydrin (**109**) in 8 steps via key Jacobsen hydrolytic kinetic resolution (HKR) and Still-Gennari olefination that allowed for multi-gram scale synthesis (Thiraporn *et al*., 2022) (**Scheme 15**). Twenty grams of (±)-epichlorohydrin (**109**) was initially subjected to 2-step transformation via substitution reaction using PMBOH to yield racemic epoxide **110**, followed by Jacobsen HKR using (*R,R*)-Co Salen·OAc catalyst to afford 12 grams of (*S*)-chiral epoxide **110S** (44%) along with diol **111** in 48% yield. The chiral epoxide **110S** was further converted to

silyl ether **112** in 2 steps via epoxide ring opening using sulfonium ylide, followed by protection of the secondary alcohol of the resulting allylic alcohol with *tert*-butyldiphenylsilyl (TBDPS) group. The alkene **112** was subsequently elaborated to aldehyde **113** in 2 steps via dihydroxylation, followed by oxidative cleavage. Aldehyde **113** was next exposed to Still-Gennari olefination to give (*Z*)-α,β-unsaturated ester **115** in 79% yield. The *Z*-geometry was confirmed with the ^{1}H–^{1}H coupling constant of 12.0 Hz. After that, the (*Z*)-α,β-unsaturated ester **115** was treated with DIBAL-H to provide the desired *Z*-allylic alcohol **108** as epoxidation substrate according to Baltas's protocol in a 6-gram scale.

Scheme 15 Synthesis of Z-allylic alcohol **108** by Thiraporn *et al*.
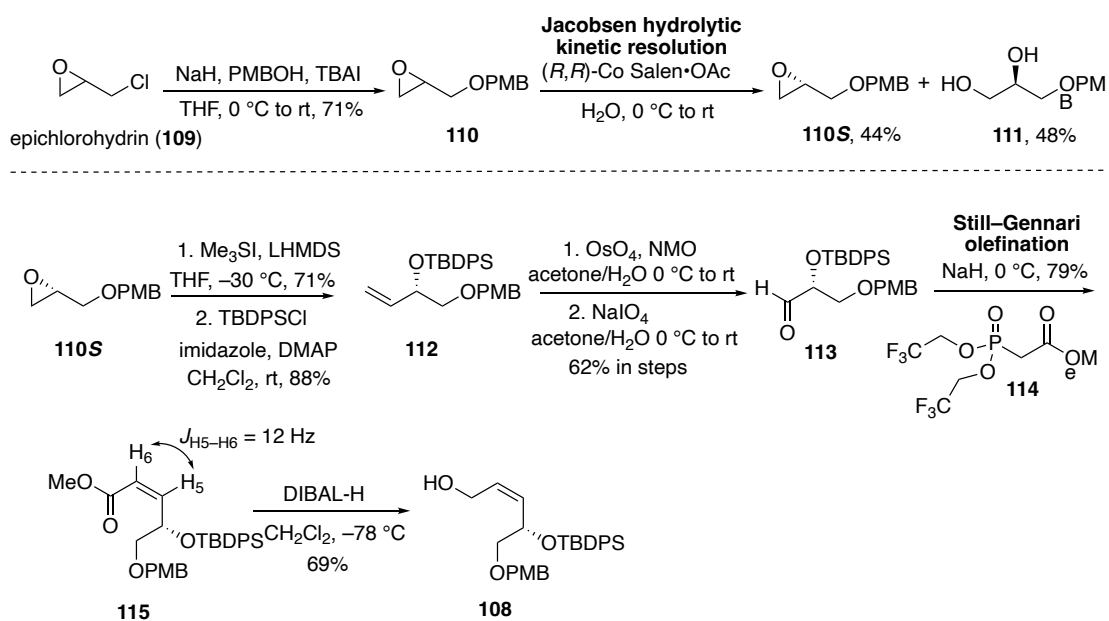
Having accomplished the synthesis of **108** in multi-gram scale, *Z*-allylic alcohol **108** was therefore subjected to Baltas's protocol (*m*-CPBA in the presence of NaHCO$_3$ at 0 °C) to provide the separable epoxy alcohol diastereomers **116a** (18%, R_f = 0.57 in 2% EtOAc/CH$_2$Cl$_2$) and **116b** (50%, R_f = 0.38 in 2% EtOAc/CH$_2$Cl$_2$) in 68% combined yield (dr = 1:2.7) as depicted in **Scheme 16**. Unfortunately, the absolute configuration of newly formed epoxides could not be determined by comparison of $J_{3/4}$ vicinal coupling constants due to unclear multiplicity of H3 and H4 signals of the major product **116b**. However, we observed the $J_{3/4}$ vicinal coupling constant in the minor

product **116a** to be 8.40 Hz, which was comparable to the values observed for *threo* products in Baltas's report. Although the absolute configuration of **116a** and **116b** were not known at this stage, we decided to elaborate epoxy alcohols **116a** and **116b** to the final targets with anticipation that the absolute configurations of **116a** and **116b** would be verified in the final stage by comparison of spectroscopic data to those of previously reported natural products **13** and **14**. Since epoxy alcohol **116b** was obtained in larger quantity than its diastereomer **116a**, we initially decided to carry epoxy alcohol **116b** to the remaining steps for evaluating the robustness of epoxide moiety.

Scheme 16 Synthesis of epoxy alcohol **116a** and **116b**
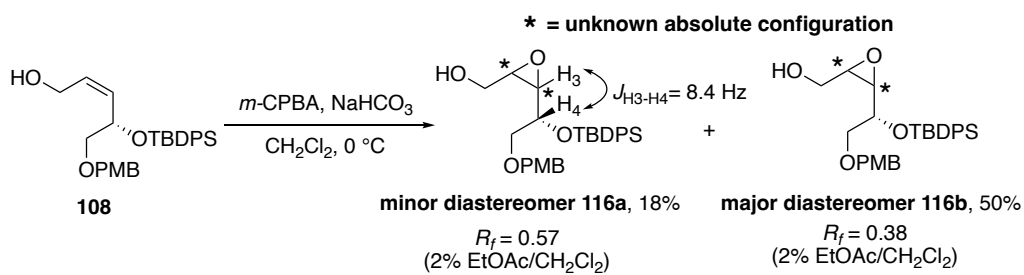
Epoxy alcohol **116b** was then subjected to oxidation mediated by IBX to afford epoxy aldehyde **117** in 78% yield. Our next task was generation of (7*S*)-stereogenic center of targeted **13** and **14** by vinylation of chiral epoxy aldehyde **117**. Vinylation of **117** was performed by treatment with vinylmagnesium bromide to provide separable diastereomeric propargylic alcohols **118*S*** and **118*R*** in 35% and 39% yields without affecting the epoxide moiety. The (7*S*)- and (7*R*)-stereogenic centers of **118*S*** and **118*R*** were confirmed by Mosher's ester analysis (**Scheme 17**).

Scheme 17 Synthesis of allylic alcohols **118*S*** and **118*R***
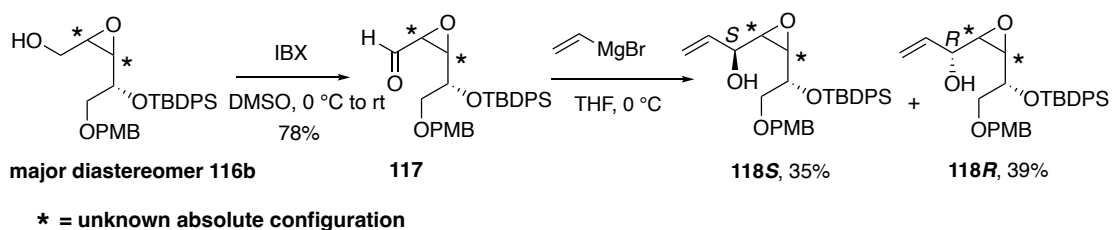
With the desired allylic alcohol **118*S*** in hand, we next continued to elaborate **118*S*** to the diene precursor for ring-closing metathesis. Initially, protection of allylic alcohol **118*S*** was required and TBS group was chosen as a protecting group at this position due to its ease of removal since we planned to remove both silyl protecting group at C4- and C7-alcohols before ring-closing metathesis to reduce steric hindrance of terminal diene of RCM precursor. Allylic alcohol **118*S*** was then treated with TBSCl and imidazole to give silyl ether **119** in 84% yield. Subsequent deprotection of PMB moiety of **119** with DDQ, followed by oxidation of the resulting primary alcohol mediated by Dess-Martin periodinane (DMP) to afford the corresponding aldehyde **120** in 95% yield. To install the requisite 2-carbon α,β-unsaturated ester subunit, aldehyde **120** was subjected Wittig olefination using $Ph_3P=CHCO_2Et$ to provide (*E*)-α,β-unsaturated ester **121** in 94% yield. Notably, (*E*)-α,β-unsaturated ester **121** was obtained as a single stereoisomer and the (*E*)-geometry was confirmed with the $^1H–^1H$ coupling constant of 15.7 Hz between H2 and H3. Ethyl ester of **121** was next hydrolyzed with $LiOH \cdot H_2O$ and subsequent acidic workup to give carboxylic acid **122** in 78%, in which the epoxide moiety remained untouched. After that, coupling of carboxylic acid **122** with (*S*)-hept-6-en-2-ol (**24**) (Tadpech *et al.*, 2015) via Yamaguchi esterification smoothly provided diene ester **123** in 71%. Both silyl protecting groups of diene **123** were then removed to avoid steric hindrance of terminal diene to facilitate RCM in the next step by using tetrabutylammonium fluoride (TBAF) to smoothly give diol **124** in 89% yield (**Scheme 18**). The final yet challenging step was the ring-closing metathesis to assemble the macrocycle and to selectively form C8–C9 olefin (**Table 2**). Initially, diene **124** was treated with Grubbs's second generation catalyst (5 mol %) in refluxing dichloromethane (0.8 mM) (entry 1). Disappointingly, these conditions only led to decomposition of starting material suggesting that the epoxide moiety of **124** was apparently incompatible with these conditions. Based on the results from synthetic route I, ring-closing metathesis of diene **26** which contains the acetonide group in this emplacement was not problematic when performed under the same conditions. Lowering the catalyst loading to 2 mol % and higher dilution of CH_2Cl_2 solvent (0.5 mM) at room temperature also resulted in the decomposition of diene **124** (entry 2). Further optimizations were then performed by changing the solvent to toluene (0.5 mM) (entry 3) or the catalyst to Grubbs's first generation (entry 4). Unfortunately, these

conditions only led to the same results. Thus, it is obvious that the epoxide moiety of **124** was not suitable for ring-closing metathesis reaction. Due to unsuccessful final ring-closing metathesis described, the synthetic scheme for **13** and **14** needs to be revised and will be discussed in the next chapter.

Scheme 18 Synthesis of ring-closing metathesis precursor **124**

∗ = unknown absolute configuration
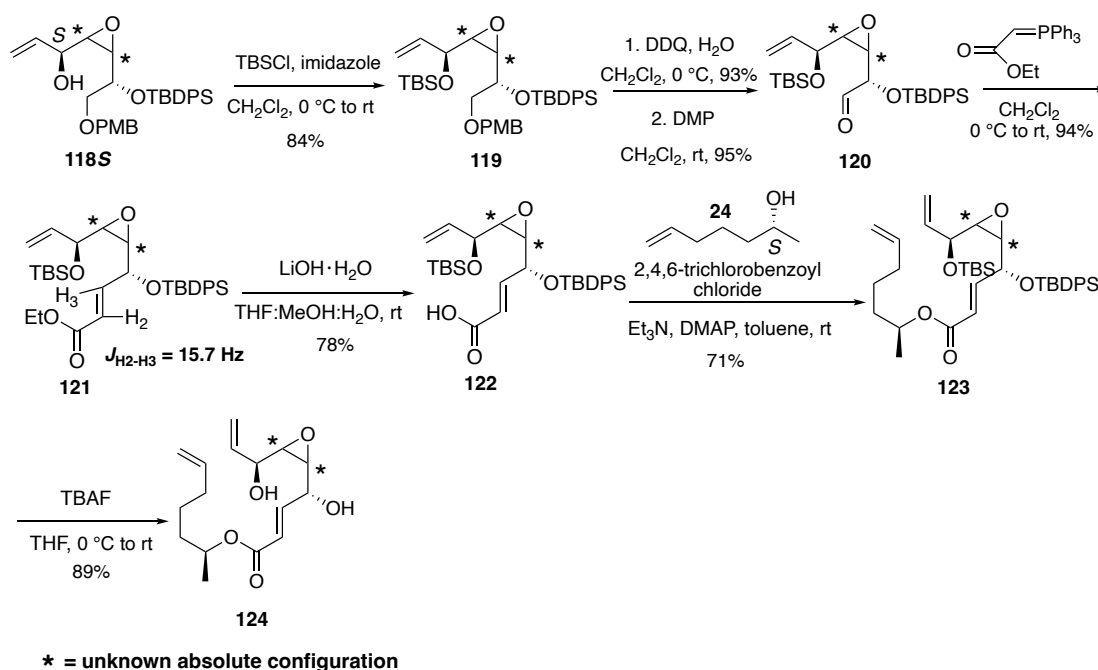
Table 2 Attempted synthesis of **13** and **14** via ring-closing-metathesis of **124**
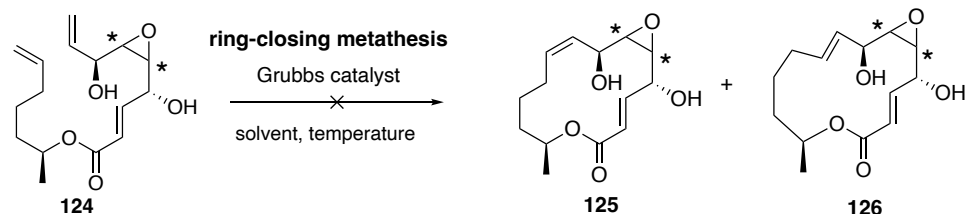
* = unknown absolute configuration

entry	catalyst	solvent	temperature	results
1	Grubbs II (5 mol %)	CH$_2$Cl$_2$ (0.8 mM)	43 °C	decomposition of diene **124**
2	Grubbs II (2 mol %)	CH$_2$Cl$_2$ (0.5 mM)	rt	
3	Grubbs II (2 mol %)	toluene (0.5 mM)	rt	
4	Grubbs I (10 mol %)	toluene (0.5 mM)	rt to 60 °C	

2.2 Conclusion

Syntheses of seiricuprolide (**13**) and pestalotioprolide B (**14**) following our proposed synthetic routes I and II were unsuccessful. In the case of screening of synthetic route I, ring-closing metathesis of diene **26** was achieved to furnish 14-membered skeletons of **13** and **14**, in which acetonide protecting group at C5–C6 position of **26** proved to be compatible with these reaction conditions. However, further removal of the acetonide protecting group was problematic because the optimal conditions (200 equivalents of 90% TFA at 0 °C) was irreproducible. In addition, the observed product yields of the resulting diol from all reaction conditions attempted were low. Owing to paucity of the diol intermediate, the subsequent epoxide formation could not be screened. Another synthetic route, which differs from synthetic route I by switching the step of epoxide formation to the early stage of the synthesis, was also screened. The preparation of epoxidation precursor, *Z*-allylic alcohol **108**, was achieved in 8 steps starting from commercially available epichlorohydrin (**109**) via Jacobsen hydrolytic kinetic resolution and Still-Gennari olefination. However, *m*-CPBA epoxidation of **108** led to separable epoxy alcohols **116a** and **116b** in only a modest

diastereoselective ratio. Since absolute configurations of generated epoxides **116a** and **116b** could not be verified at this stage, the major epoxy alcohol **116b** was then chosen as intermediate for screening remaining reactions. It was discovered that epoxide moiety of **116b** is quite robust because **116b** could be elaborated to ring-closing metathesis precursor **124** in 8 steps, in which the degradation of the epoxide moiety was not observed from any steps. However, upon attempts to assemble the macrocycle by using various ring-closing metathesis conditions in the last step, we failed to obtain macrocycle product since all conditions only led to decomposition of starting diene **124** and the epoxide moiety at C5–C6 position of **124** was likely incompatible with ring-closing metathesis reaction. Therefore, the revision of the synthetic route will be discussed in the next chapter.

CHAPTER 3

COMPLETION OF SYNTHESES
OF SEIRICUPROLIDE AND
PESTALOTIOPROLIDE B

CHAPTER 3

COMPLETION OF SYNTHESES OF SEIRICUPROLIDE AND PESTALOTIOPROLIDE B

3.1 Results and Discussion

According to the unsuccessful ring-closing metathesis in the final step of synthetic route II described in the previous chapter, we then need to revise the synthetic route for synthesizing seiricuprolide (**13**) and pestalotioprolide B (**14**). The new synthetic route was inspired by a previous accomplishment of syntheses of 14-membered macrolide analogues of **13** and **14**, nigrosporolide (**127**) and (4*S*,7*S*,13*S*)-4,7-dihydroxy-13-tetradeca-2,5,8-trienolide (**128**) (**Figure 6**), reported by our research group (Thiraporn *et al*., 2022b). The key synthetic features for syntheses of **127** and **128** involved Shiina macrolactonization and acetylide addition to form the macrocyclic core, Wittig olefination and selective reduction of propargylic alcohol to construct internal *E* or *Z*-olefins. Since macrolides **127** and **128** are essentially C5–C6 β-epoxy analogues of **13** and **14**, respectively, we anticipated that key bond formation strategies previously employed in syntheses of **127** and **128** would be applicable for syntheses of **13** and **14**. Nevertheless, the challenging part of syntheses of **13** and **14** was a stereoselective installation of the β-epoxide moiety. Ideally, our targeted macrolides **13** and **14** might be directly prepared via selective epoxidation **127** and **128**. However, this strategy posed a challenge due to the presence of two olefins in the molecules of **127** and **128** in addition to facial selectivity of the epoxidation step. Thus, the installation of the chiral epoxide moiety would be performed in the early stage to avoid such challenges. The new retrosynthetic analysis of **13** and **14** is outlined in **Scheme 19**. To assemble the macrocycles of **13** and **14**, Shiina macrolactonization of seco acids **129** and **130** would be employed in place of ring-closing metathesis which was unsuccessful in the previous route. Wittig olefination would still be utilized to generate

the C2–C3 (*E*)-α,β-unsaturated ester moiety of both **129** and **130**. The *Z*- or *E*-double bond at   C8–C9 (of **129** or **130**, respectively) would be derived from selective reduction of chiral propargylic alcohol **131**, which would in turn be elaborated from acetylide addition of known alkyne **132** prepared from (*S*)-propylene oxide (**133**) to chiral epoxy aldehyde **107**. It was again anticipated that the adjacent chiral epoxide of aldehyde **107** would direct the stereoselectivity of this acetylide addition step (Li *et al*., 2009). It should be noted that chiral epoxy aldehyde **107** was prepared from *Z*-allylic alcohol **108** via the Baltas's protocol in the previous synthetic route (Method I) discussed in **Chapter 2** and these conditions provided epoxy alcohol products **116a** and **116b** in a modest diastereomeric ratio (**116a**:**116b** = 1:2.7). Moreover, the absolute configurations of epoxide moiety of **116a** and **116b** could not be verified at the stage of epoxide formation as described in **Scheme 16**. Due to such problems, we then turned our attention to screen other methodologies for installing the β-epoxide moiety. SAE of **108** using (–)-diethyl tartrate as a chiral ligand (Method II) was initially chosen for constructing β-epoxide of **107**, with hope that the stereoselectivity of this reaction might improve and the absolute configuration of major product might be unambiguously predicted by analogy following Sharpless's mnemonic shown in **Figure 5** (**Chapter 1**) (Mohapatra *et al*., 2016 and Hassan *et al*., 2016). Alternatively, we envisioned that β-epoxide of **107** could be obtained via chiral OH-directed *m*-CPBA epoxidation of **134** (Method III) (Minami *et al*., 1995), in which modified *Z*-allylic alcohol **134** would be easily derived from *Z*-allylic alcohol **108**.

Figure 6 Structures of nigrosporolide (**127**) and (4*S*,7*S*,13*S*)-4,7-dihydroxy-13-tetradeca-2,5,8-trienolide (**128**)

nigrosporolide (**127**)

(4*S*,7*S*,13*S*)-4,7-dihydroxy-13-tretadeca-2,5,8-trienolide (**128**)
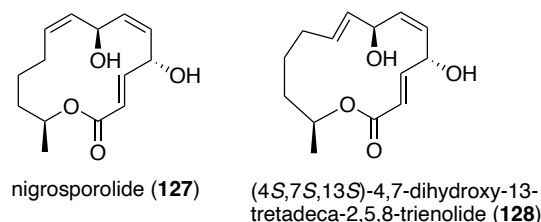
Scheme 19 Retrosynthetic analysis of seiricuprolide (**13**) and pestalotioprolide B (**14**)

seiricuprolide (**13**): *Z*-alkene at C8-C9
pestalotioprolide B (**14**): *E*-alkene at C8-C9

129: *Z*-alkene at C8-C9
130: *E*-alkene at C8-C9

(*S*)-propylene oxide (**133**)

epichlorohydrin (**109**)
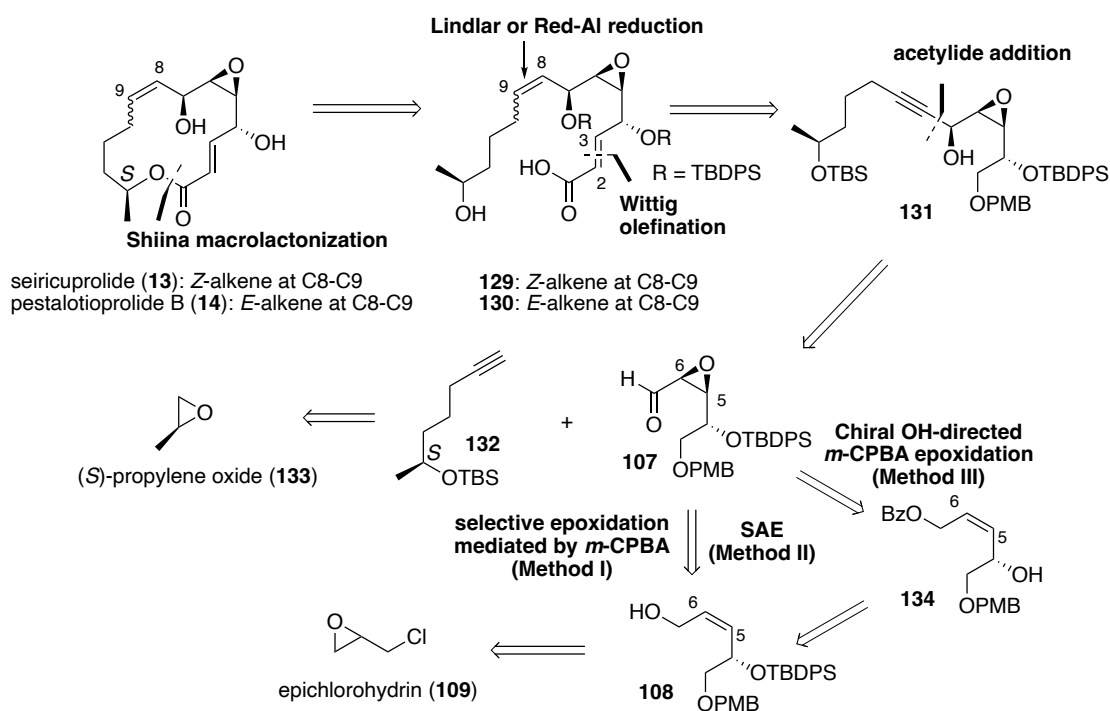
The first task was focused on screening for selective epoxidation following Methods II and III (**Scheme 20**). We initially attempted to utilize SAE of *Z*-allylic alcohol **108** by employment of *tert*-butyl hydroperoxide or cumene hydroperoxide in the presence of (–)-diethyl tartrate and titanium isopropoxide in CH$_2$Cl$_2$ at –40 °C (Method II) (Thirupathi *et al.*, 2016 and Bodugam *et al.*, 2016). Disappointingly, after maintaining both reactions at this temperature for 6-7 days, there was no noticeable change upon monitoring by TLC and only unreacted starting material was recovered. Since SAE of *Z*-allylic alcohol **108** in the presence of (–)-diethyl tartrate was unsuccessful in our hands, we proposed that the bulky TBDPS protecting group of the adjacent chiral alcohol moiety of **108** might obstruct the approach of (–)-diethyl tartrate to the olefin. In addition, literature precedents on SAE of *Z*-allylic alcohol bearing a TBDPS protecting group at α-chiral center in the presence of (–)-diethyl tartrate are scarce. To the best of our knowledge, there has been only one report on SAE of such a substrate which was achieved by using (+)-diisopropyl tartrate as a chiral ligand, in which the reaction reached only 56% completion after 5 h (Kumar *et al.*, 2018). Since *Z*-allylic alcohol **108** was inert to SAE conditions using (–)-diethyl tartrate in our hands and further screening on SAE in the presence of (–)-diisopropyl tartrate ligand was not

performed due to the lack of chemical supply at the time, our attention focused then on chiral OH-directed epoxidation (Method III). We then decided to transform *Z*-allylic alcohol **108** to chiral allylic alcohol **134** as anticipation that the α-hydroxy chiral center of substrate **134** would direct the stereoselectivity of epoxidation. Primary alcohol of **108** was then protected with a benzoyl group due to its orthogonality to other protecting groups to yield benzoate **135** in 88% yield, followed by TBDPS deprotection using TBAF to deliver alcohol **134**. The *m*-CPBA epoxidation of chiral allylic alcohol **134** was then performed to provide inseparable diastereomeric epoxy alcohols **136** in 78% combined yield. The inseparable mixture was then elaborated to epoxy alcohols **116a** and **116b** in order to determine the stereoselectivity outcome compared to Method I. Interestingly, ensuing 2-step transformations, including TBDPS protection and methanolysis, proceeded smoothly to give separable epoxy alcohols **116a** and **116b** in excellent diastereomeric ratio of 16:1, in which the ^{1}H and ^{13}C NMR spectroscopic data as well as retention factor values (0.57 and 0.38 in 2% EtOAc/CH$_2$Cl$_2$) of **116a** and **116b** from this protocol are identical to those of epoxy alcohol products obtained from *m*-CPBA epoxidation of *Z*-allylic alcohol **108** in Method I (**Chapter 2**).

Scheme 20 Methods II and III for installing epoxide moiety of **116a** and **116b**
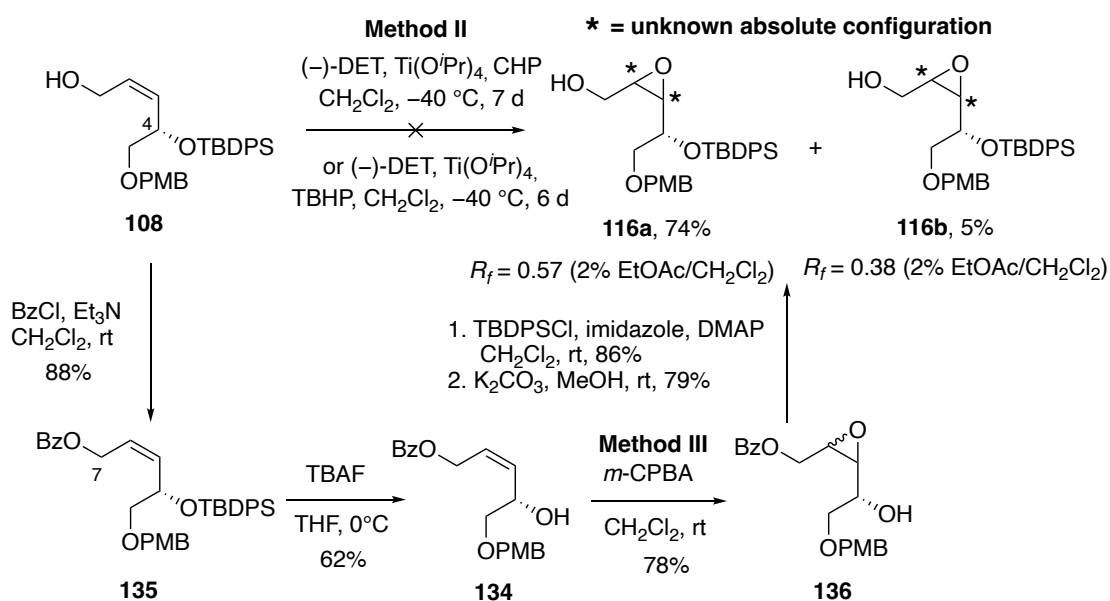
According to contrastively observed results from Methods I and III, we therefore proposed the conformational models to rationalize the stereoselectivity observed in each chiral substrate based on Sharpless model as shown in **Scheme 21** (Rossiter *et al*., 1979, Narula *et al*., 1983, Adam *et al*., 1999, Freccero *et al*., 2000 and Bressin *et al*., 2020). In the case of chiral allylic alcohol substrate **134** (Method III), the major product, β-epoxide **136 *erythro***, would result from *m*-CPBA epoxidation directed by the adjacent chiral hydroxyl group via the lower-energy transition state **TS1** due to minimization of 1,3-allylic strain (Hoffmann *et al*., 1989) whereas the other transition state **TS2** leading to α-epoxide **136 *threo*** would suffer from 1,3-allylic strain. On the other hand, *m*-CPBA epoxidation of allylic alcohol substrate **108** bearing adjacent (*S*)-silyloxy stereogenic center provided a reversed diastereoselectivity. Since the allylic hydroxyl group of **108** contains no chiral entity to differentiate the facial selectivity of epoxidation via hydrogen bonding, we proposed that the observed stereoselectivity in the epoxidation of **108** would derive from the minimization of 1,3-allylic strain controlled by the bulky adjacent silyloxy stereogenic center as shown in transition states **TS3** and **TS4**. **TS4** would be preferred due to the minimized 1,3-allylic strain compared to **TS3** rendering the epoxidation to occur on the alkene face opposite to the bulky OTBDPS group and delivered α-epoxide **116b *threo*** as a major product. Based on our proposed conformations, the absolute configurations of epoxide moiety of **116a** and **116b** were proposed to be β- (*erythro*) and α- (*threo*) epoxides, respectively. To verify our proposed rationale, we decided to elaborate epoxy alcohols **116a** and **116b** to Baltas's epoxy alcohol intermediates (**94a** and **94b**) in 4 steps via standard protection-deprotection (**Scheme 22A**). Epoxy alcohol **116b** (a major product from Method I, a minor product from Method III and the proposed *threo* isomer) was initially converted to epoxy alcohol **140**. To our surprise, the ^{1}H and ^{13}C NMR data of **140** matched those reported by the Baltas group for *'erythro'* intermediate **94a** which was their major product (**Table 3**). In addition, we further converted epoxy alcohol **116a** (a minor product from Method I, a major product from Method III and the proposed *erythro* isomer) to epoxy alcohol **144** (**Scheme 22B**) and found that the ^{1}H and ^{13}C NMR data of **144** were identical to those reported for the minor '*threo*' intermediate **94b** by the Baltas group (**Table 4**). It is obvious that our proposed absolute configuration of epoxide moiety of **116a** and **116b** was contradictory to the previously reported results

by the Baltas group. Even though the absolute configuration of each epoxy alcohol still could not be unambiguously confirmed at this stage, we were certain, based on these results, that the α-epoxide *threo* product would predominate from *m*-CPBA epoxidation of *Z*-allylic alcohol containing (*S*)-α-silyloxy stereogenic center such as **108**. Thus, we decided to proceed with epoxy alcohol **116a**, a major diastereomer from Method III, due to its availability in larger quantity and the excellent *erythro* diastereoselectivity rationalized above.

Scheme 21 Proposed rationale for observed diastereoselectivities in the epoxidation of *Z*-allylic alcohols **108** (Method I) and **134** (Method III)
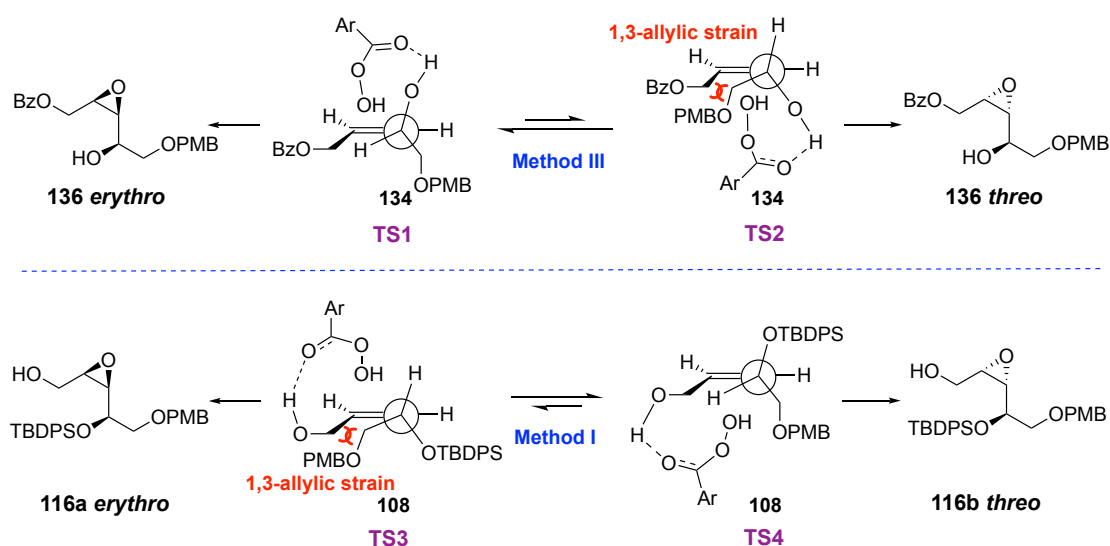
Scheme 22 A) Conversion of epoxy alcohol **116b** *thero* to Baltas's epoxy alcohol **140**.

B) Conversion of epoxy alcohol **116a** *erythro* to Baltas's epoxy alcohol **144**.
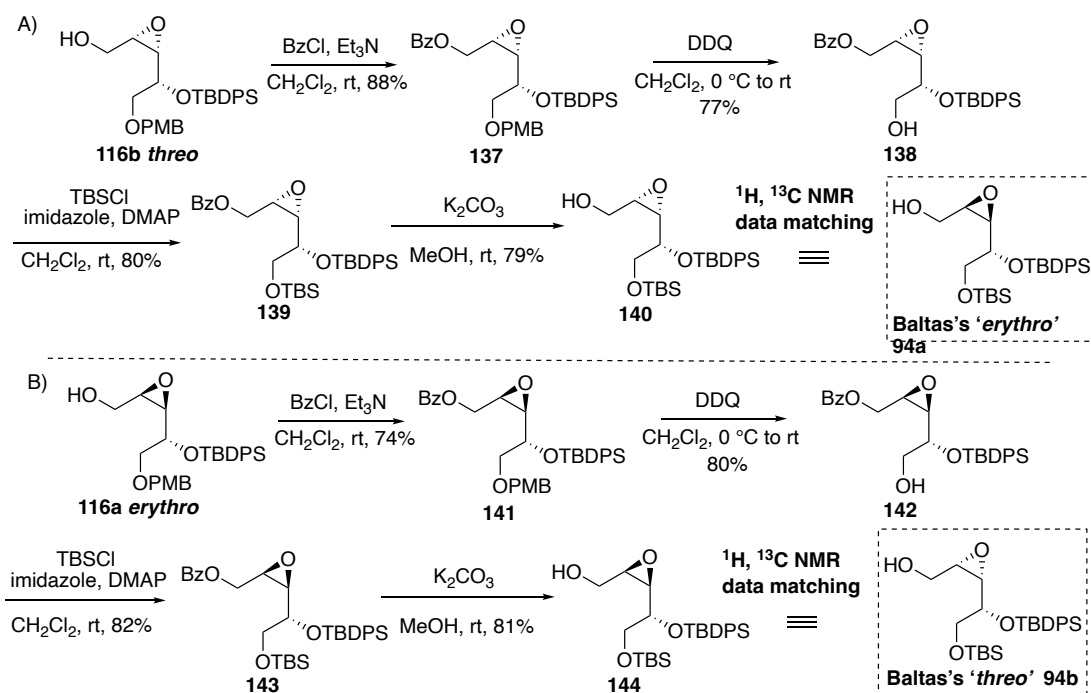
With the proposed β-epoxy alcohol **116a** in hand, we then proceeded to assemble the key fragments as shown in **Scheme 23A**. β-Epoxy alcohol **116a** was then subjected to oxidation mediated by IBX to yield the requisite epoxy aldehyde **107** in 81% yield. Another key fragment, known alkyne **132**, was prepared from (*S*)-propylene oxide (**133**) in 5 steps using our previously reported protocol via the key Bestmann−Ohira homologation (Thiraporn *et al*., 2022a). The next task was coupling of chiral epoxy aldehyde **107** with known alkyne **132** via acetylide addition. Epoxy aldehyde **107** was exposed to a premixed solution of alkyne **132** and *n*-butyl lithium at −78 °C in THF. After warming to 0 °C for 2 hours, separable propargylic alcohols **131*S*** and **131*R*** were obtained in respective 21% and 56% yields upon purification by column chromatography. Notably, the degradation of epoxide moiety was not observed from these reaction conditions. The absolute configuration of the newly formed alcohol stereogenic center of each diastereomer was assigned by Mosher's ester analysis.

Table 3 Comparison of ^{1}H and ^{13}C NMR data for epoxy alcohols **Baltas's *'erythro'*** **94a** and **140**.

Position	^{1}H NMR (δ and J in Hz)		^{13}C NMR (δ)	
	94a (400 MHz) in CDCl$_3$	**140** (300 MHz) in CDCl$_3$	**194a** (100 MHz) in CDCl$_3$	**140** (75 MHz) in CDCl$_3$
1	3.27–3.18, m/ 3.38–3.28, m	3.25–3.18, m/ 3.32, dd (12.27, 3.96)	60.77	60.65
2	3.03, dt (6.90, 4.18)	3.03, dt (6.90, 4.05)	57.19	57.17
3	3.15, dd (6.20, 4.18)	3.16, dd (5.85, 4.05)	57.44	57.27
4	3.66–3.64, m	3.74–3.64, m	71.11	71.00
5			66.23	66.11
Cq of *t*Bu (TBS)	-	-	18.64	18.52
CH$_3$ of *t*Bu (TBS)	1.07	1.08	27.00	26.89
CH$_3$ of TBS	–0.04/–0.06	0.08/0.05	–5.35 –5.23	–5.45 –5.35
Cq of *t*Bu (TBDPS)	-	-	19.50	19.38
CH$_3$ of *t*Bu (TBDPS)	0.92	0.92	26.15	26.04
Cq of Phe (TBDPS)	-	-	133.46 133.70	133.35 133.56
CH of Phe TBDPS	7.42–7.34, m/ 7.71–7.67, m	7.48–7.36, m/7.79– 7.71, m	127.91 127.94 130.12 130.21 136.10 136.14	127.78 127.82 130.00 130.09 135.98 136.01
OH	1.60–1.50, m	1.86, brs	-	-

Table 4 Comparison of ^{1}H and ^{13}C NMR data for epoxy alcohols **Baltas's *'threo'* 94b** and **144**.

Position	^{1}H NMR (δ and *J* in Hz)		^{13}C NMR (δ)	
	94b (400 MHz) in CDCl₃	**144** (300 MHz) in CDCl₃	**94b** (100 MHz) in CDCl₃	**144** (75 MHz) in CDCl₃
1	3.27–3.18, m/ 3.71–3.49, m	3.28–3.17, m/ 3.78–3.49, m	61.09	61.01
2	3.27–3.18, m	3.28–3.17, m	56.81	56.17
3	3.11, dd (8.26, 4.13)	3.10, dd (7.86, 3.75)	59.97	59.89
4	3.71–3.49, m	3.78–3.49, m	72.03	72.02
5			65.55	65.47
Cq of *t*Bu (TBS)	-	-	18.64	18.65
CH₃ of *t*Bu (TBS)	1.12	1.09	26.17	26.07
CH₃ of TBS	−0.02/−0.00	−0.05/−0.02	−5.49 −5.38	−5.58 −5.48
Cq of *t*Bu (TBDPS)	-	-	19.50	19.46
CH₃ of *t*Bu (TBDPS)	0.83	0.80	27.12	27.04
Cq of Phe (TBDPS)	-	-	133.31 134.02	133.27 133.97
CH of Phe TBDPS	7.42–7.34, m/ 7.71–7.67, m	7.46–7.34, m/ 7.78–7.66, m	127.74 127.87 129.85 136.02 136.09	127.64 127.76 129.96 136.00 136.15
OH	2.71–2.68, m	2.74, brs	-	-

Although the β-epoxide moiety of **107** did not lead to the desired (*S*)-propargylic alcohol **131*S*** as a major product as anticipated, the undesired (*R*)-propargylic alcohol **131*R*** could be smoothly transformed to **131*S*** in 2 steps with satisfying yield (78% in 2 steps) via Mitsunobu inversion with acetic acid, followed by methanolysis (Li *et al.*, 2009). In addition, the reaction conditions for coupling of **107** and **132** in asymmetric fashion using Trost's asymmetric Zn-mediated alkynylation was also screened (**Scheme 23B**). However, these reaction conditions were unsuccessful in our hands, in which substrates **107** and **132** were presumably inert to such conditions (Trost *et al.*, 2006 and 2012).

Scheme 23 A) Coupling of the key fragments **107** and **132** via acetylide addition. B) Attempted coupling of the key fragments **107** and **132** via Trost's asymmetric alkyne addition.
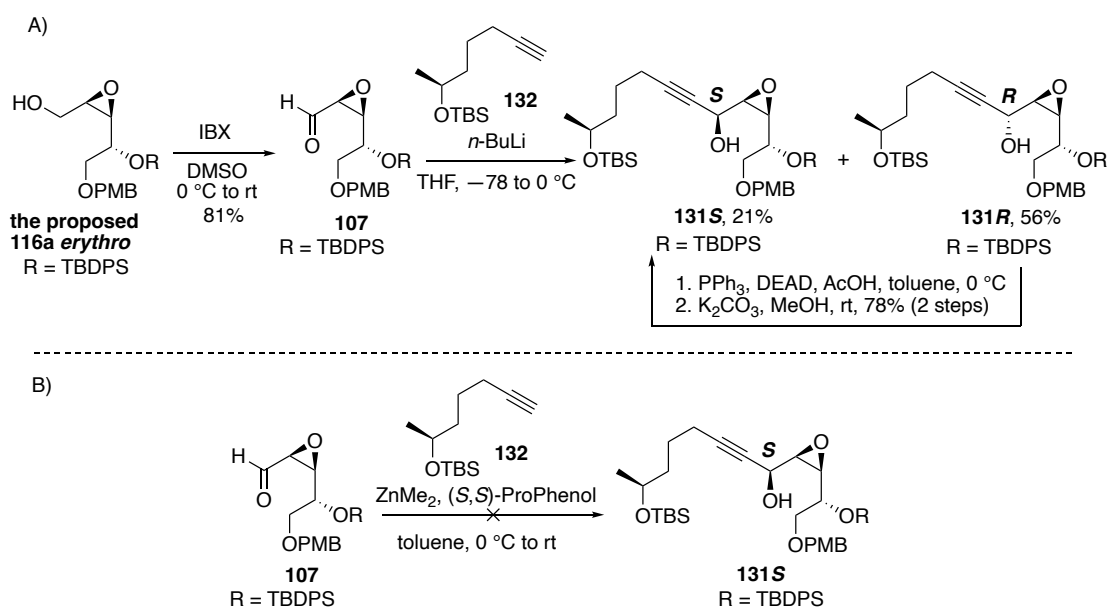
After chiral propargylic alcohol **131*S*** was successfully synthesized, our next task was to complete the synthesis of seiricuprolide (**13**) using our previously established sequence for its closely related analogue (Thiraporn *et al.*, 2022b) (**Scheme 24**). The synthesis commenced with preparation of C8–C9 *Z*-alkene subunit of **13**, *Z*-selective reduction of propargylic alcohol **131*S*** was therefore undertaken via Lindlar hydrogenation in ethyl acetate to furnish *Z*-allylic alcohol **145** in 89% yield. The *Z*-geometry of **145** was confirmed by a coupling constant of 10.8 Hz between H8 and

H9. Subsequent protection of allylic alcohol of **145** with TBDPSCl, followed by removal of a PMB protecting group of the resulting silyl ether using DDQ afforded primary alcohol **146** in high yield. The next task was to install the C2–C3 (*E*)-α,β-unsaturated ester subunit of **13** which was carried out in 2 steps. Oxidation of **146** mediated by Dess–Martin periodinane, followed by Wittig olefination with Ph₃P=CHCO₂Et furnished (*E*)-α,β-unsaturated ester **147** as a single isomer in excellent 85% yield over 2 steps. The *E*-geometry of **147** was confirmed by a coupling constant of 15.5 Hz between H2 and H3. Upon completion of installing all 14 carbons of **13**, our remaining task was to construct the macrocyclic core via Shiina macrolactonization. To prepare macrolactonization precursor **130**, ester **147** was then subjected to selective deprotection of TBS protecting group using 4 equivalents of weakly acidic pyridinium *p*-toluenesulfonate (PPTS) to give alcohol **148** in 84% yield. Gratifyingly, the β-epoxide remained untouched and deprotection of TBDPS protecting groups was not observed. Ensuing ester hydrolysis and acidic workup also smoothly furnished seco acid **130** in 77% yield without affecting the epoxide moiety. Shiina macrolactonization was performed by slowly adding a solution of seco acid **130** in toluene to a premixed solution of 2-methyl-6-nitrobenzoic anhydride (MNBA) and DMAP in toluene at high dilution (2 mM) at room temperature over 8 h to provide macrolactone **149** in 65% yield. Final global deprotection of **149** was achieved using our established conditions using 10 equivalents of TBAF in the presence of 4 mol % of acetic acid in THF at 60 °C to provide seiricuprolide (**13**) in 49% yield as a white solid along with 12% of monoprotected analogue **150**. The ¹H and ¹³C NMR spectroscopic data of synthetic **13** were identical to those reported for natural **13** (**Table 5**) (Ballio *et al*., 1988). Moreover, the observed range of melting point of synthetic **13** (126.5–127.9 °C) was comparable to that of natural product **13** (128–130 °C) (Ballio *et al*., 1988). The specific rotation ([α]$_D^{25}$) of synthetic **13** of +48.12 (*c* 2.70, MeOH) was in good agreement with the reported value for natural product **13** ([α]$_D^{20}$ = +40, *c* 2.7, MeOH) by the Liu group, which unambiguously confirmed the absolute configuration of β-epoxide intermediate **116a** and verified our rationale for the diastereoselectivity of *m*-CPBA epoxidation. It is clear that the installation of chiral epoxide moiety can be performed in the early stage and β-epoxide **116a** proved to be a very robust substrate for the total synthesis.

Scheme 24 Completion of synthesis of seiricuprolide (**13**)
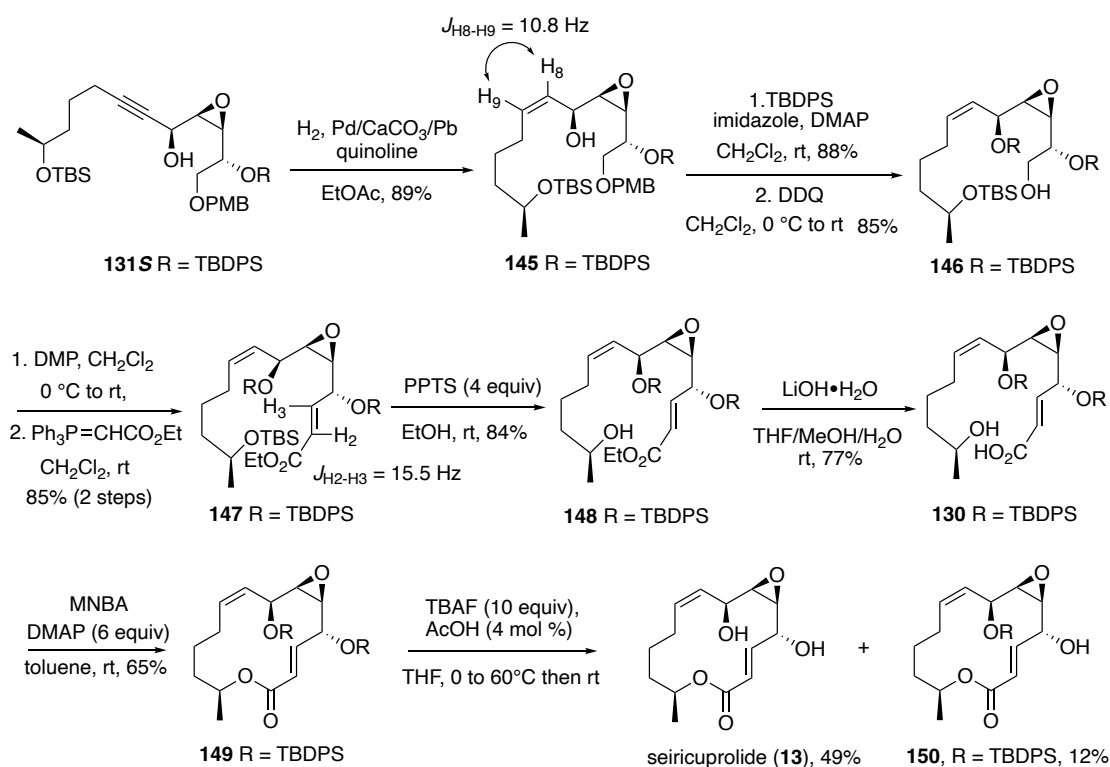
After our rationale for the diastereoselectivity of *m*-CPBA epoxidation was verified through the synthesis of sericuprolide (**13**) mentioned above, it could reaffirm that OH-directed *m*-CPBA epoxidation of modified *Z*-allylic alcohol **134** (Method III) was an excellent method for constructing the desired β-epoxide motif. However, our synthetic sequence for **134** is lengthy (10 linear steps from epichlorohydrin in 3.6% overall yield) and requires the use of some relatively expensive reagents such as osmium tetroxide, *n*-butyllithium and Still–Gennari reagent, leading us to develop a more concise synthetic route of **134** that also allowed for multigram scale synthesis (**Scheme 25**). We therefore set out the preparation of *Z*-allylic alcohol **134** from known allylic alcohol **151** in 3 steps. Allylic alcohol **151** was easily prepared in 10-gram scale from D-mannitol in 4 steps via the key Wittig olefination following a procedure reported by Baltas *et al*. and Chu *et al*. Allylic alcohol **151** was further transformed to diol **153** in 2 steps by benzoylation to give benzoate ester **152** in 89% yield, followed by acetonide deprotection by treatment with 2M HCl in acetonitrile.

Table 5 Comparison of ^{1}H and ^{13}C NMR data for natural and synthetic seiricuprolide (**13**).

Position	^{1}H NMR (δ and J in Hz)		^{13}C NMR (δ)	
	Natural (500 MHz) in CDCl$_3$	Synthetic (500 MHz) in CDCl$_3$	Natural (125 MHz) in CDCl$_3$	Synthetic (125 MHz) in CDCl$_3$
1	-	-	166.0	166.1
2	6.14, dd (15.4, 1.5)	6.15, dd (15.5, 0.5)	123.8	123.7
3	6.84, dd (15.4, 6.1)	6.85, dd (15.5, 6.5)	142.9	143.0
4	4.32, ddd (6.3, 6.1, 1.5)	4.36–4.29, m	71.9	71.9
5	3.23, dd (6.3, 4.4)	3.28–3.24, m	62.6	62.6
6	3.01, dd (8.5, 3.3)	3.03, dd (8.5, 4.5)	58.9	59.0
7	4.23, dd (8.5, 8.5)	4.27–4.20, m	64.4	64.4
8	5.37, ddd (11.0, 8.5, 2.6)	5.39, ddd (11.5, 9.5, 1.5)	127.4	127.4
9	5.54, ddd (11.0, 9.6, 3.3)	5.57, ddd (11.5, 9.5, 1.0)	135.5	135.6
10	2.43, m/ 2.07, m	2.51–2.39, m/ 2.14–2.04, m	28.8	29.0
11	1.78, m/ 1.23, m	1.85–1.75, m/ 1.27–1.21, m	25.1	25.2
12	1.86, ddd (13.6, 10.6, 7.4)/ 1.44, ddd (13.6, 7.4, 7.4)	1.94–1.85, m/1.46, ddd (14.5, 9.0, 1.5)	33.5	33.6
13	4.91, ddq (8.8, 7.4, 3.3, 2.5)	5.00–4.91, m	73.1	73.3
14	1.26, d (6.6)	1.29, d (6.5)	19.8	20.1
4-OH	-	2.55, brs	-	-
7-OH	-	2.16, brs	-	-

The next task was to regioselectively protect of the primary alcohol of diol **153** with a PMB group and the optimizations of this step are shown in **Table 6**. Initially, the use of typical conditions for PMB protection (PMBCl and NaH in the presence of TBAI in anhydrous DMF at 0 °C) was screened (entry 1). Disappointingly, these conditions only produced undesired diol **154** in 62% yield, in which the degradation of benzoyl protecting moiety presumably caused by basic hydrolysis. In addition, hydroxyl proton at C4-position was apparently the most acidic proton of starting **153** since only C4-hydroxyl group was protected with a PMB group of diol **154** under these conditions. From these results, we turned our attention to the use of a more reactive reagent in the absence of a strong base with hope that the regioselective PMB protection of C3-hydroxyl group might occur, diol **153** was then treated with *p*-methoxybenzyl trichloroacetamidate (PMBTCA) in the presence of PPTS in dichloromethane at 0 °C (entry 2) (Ikeuchi *et al.*, 2019). Unfortunately, these conditions provided a mixture of the desired PMB ethers **134** and its regioisomer **155** in a poor regioisomeric ratio of 1:1.3 (84% combined yield) upon maintaining the reaction temperature at 0 °C for 1 h. Further optimization was performed by lowering reaction temperature to –78 °C (entry 3) or slowly adding starting **153** at 0 °C (entry 4). Disappointingly, the results from both conditions were similar to entry 2. Since the regioselective PMB protection of diol **153** was difficult to control, we decided to convert diol **153** to stannylene acetal by using dibutyltin oxide, followed by employment of PMBCl in the presence of TBAB to provide the desired **134** in 71% yield along with 24% of undesired regioisomer **155** (entry 5) (Gucchait *et al.*, 2021). As a result, these conditions were chosen as optimized PMB protection conditions. Overall, the revised synthetic route for *Z*-allylic alcohol **134** starting from commercially available D-mannitol was shortened by 3 steps and overall yield increased to 10.3%.

Scheme 25 Synthesis of diol **153** from known allylic alcohol **151**
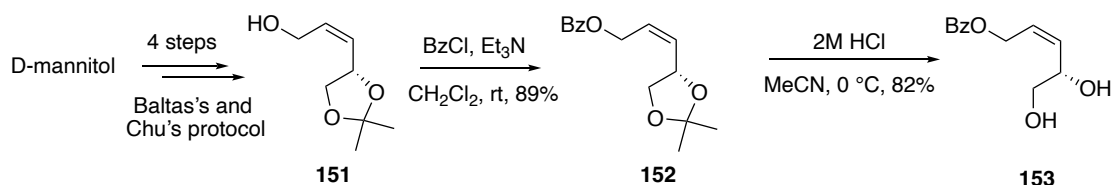
Table 6 Optimization of regioselective PMB protection of diol **153**
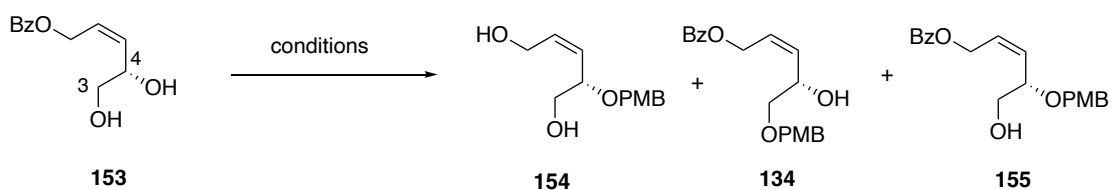
entry	reagents	solvent	temp	time (h)	results
1	PMBCl, NaH, TBAI	DMF	0 °C	2	**154** (62%)
2	PMBTCA, PPTS	DCM	0 °C	1	**134:155** = 1:1.3* 84% combined yield
3	PMBTCA, PPTS	DCM	–78 °C	1	**134:155** = 1:1.2* 84% combined yield
4	PMBTCA, PPTS (slowly adding **153**)	DCM	0 °C	12	**134:155** = 1:1.3* 84% combined yield
5	Bu$_2$SnO in MeOH at 80 °C then PMBCl, TBAB in DMF at 65 °C			5	**134** (71%) and **155** (24%)

* Determined by the integration ratio of ^{1}H NMR data

Our attention focused then on completion of synthesis of pestalotioprolide B (**14**). The synthesis began with optimization of *E*-selective reduction of propargylic alcohol **131S** mediated by sodium(2-methoxyethoxy)aluminium hydride (Red-Al) as a reducing agent (**Table 7**). Propargylic alcohol **131S** was initially treated with 1.2 or 3.0 equivalents of Red-Al in THF from 0 °C to room temperature (entries 1 and 2) (Li *et al*., 2009). Disappointingly, these conditions gave no desired product and the starting material was recovered. Increasing Red-Al to 5 equivalents under the same conditions provided an inseparable mixture of the desired **156** and overreduced product **157** in 53% combined yield and a ratio of 1:2.1 as determined by ^{1}H NMR spectroscopy (entry 3). Further optimization was then performed by changing the solvent to toluene (entry 4) or ether (entry 5) under the same conditions as entry 3. Unfortunately, only the starting material **131S** was observed from both conditions. These results suggested that THF should be the appropriate solvent for Red-Al-mediated reduction of **131S**. Formation of overreduced product **157** observed in entry 3 thus prompted us to perform this reaction at lower temperature. After slowly warming the reaction mixture from –30 °C to 0 °C for 6.5 h (Albert *et al*., 2007 and Meta *et al*., 2004), no undesired overreduced product **157** was obtained under these conditions and only an inseparable mixture (1:1) of the desired **156** and unreacted starting material **131S** in a combined 79% was observed (entry 6). Further optimization was then performed by slightly increasing the reaction temperature to 4 °C. Gratifyingly, after maintaining the reaction at this temperature for 5 h, starting **131S** was completely consumed and the desired *E*-allylic alcohol **156** was observed in 74% yield without the overreduced counterpart. The *E*-geometry of **156** was confirmed by a coupling constant of 15.5 Hz between H8 and H9.

Table 7 Optimization of *E*-selective reduction of propargylic alcohol **131S** mediated by Red-Al
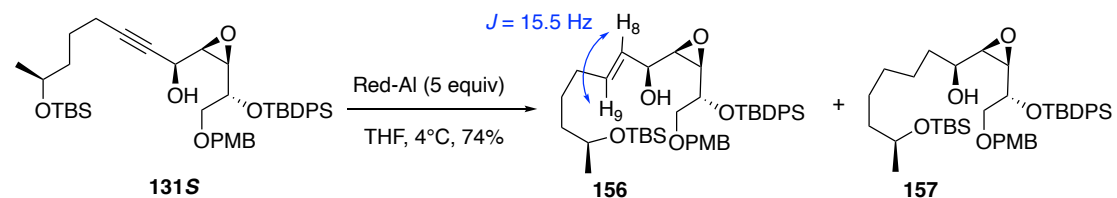
entry	Red-Al (equiv)	solvent	temp	time (h)	results
1	1.2	THF	0 °C to rt	6	no reaction
2	3.0	THF	0 °C to rt	20	no reaction
3	5.0	THF	0 °C to rt	4.5	**156:157** = 1:2.1* (53% combined yield)
4	5.0	toluene	0 °C to rt	5	no reaction
5	5.0	ether	0 °C to rt	5	no reaction
6	5.0	THF	−30 °C to 0 °C	6.5	**156** (40%)* and **131S** (39%)*
7	5.0	THF	4 °C	5	**156** (74% yield)

* Determined by the integration ratio of ^{1}H NMR data

With the requisite intermediate **156** in hand, the remaining installation of (*E*)-α,β-unsaturated ester as well as the construction of macrocyclic core of **14** were accomplished by transformation of **156** to macrolactone **161** in 7 steps via the same synthetic sequence established in the synthesis of **13**. The global deprotection of **161** was also performed under the same conditions employed for **13** to deliver pestalotioprolide B (**14**) in slightly higher yield (56%) as a white solid (**Scheme 26**). The ^{1}H and ^{13}C NMR data of synthetic **14** were excellent agreement with those reported for natural **14** by the Liu group (**Table 8**). Similarly, the observed range of melting point of synthetic **14** (109.6–111.3 °C) was nearly identical to the value reported by the Liu group (111–115 °C). Moreover, the observed specific rotation of synthetic **14**, $[\alpha]_D^{25} = +75.96$ (*c* 1.00, CHCl$_3$), was also essentially identical to that of natural product **14**, ($[\alpha]_D^{20} = +72$, *c* 1.0, CHCl$_3$). These results once again verified the absolute

configuration of β-epoxide intermediate **116a**, thereby rendering its diastereomer **116b** an α-epoxide antipode.

Scheme 26 Completion of synthesis of Pestalotioprolide B (**14**)

pestalotioprolide B (**14**)
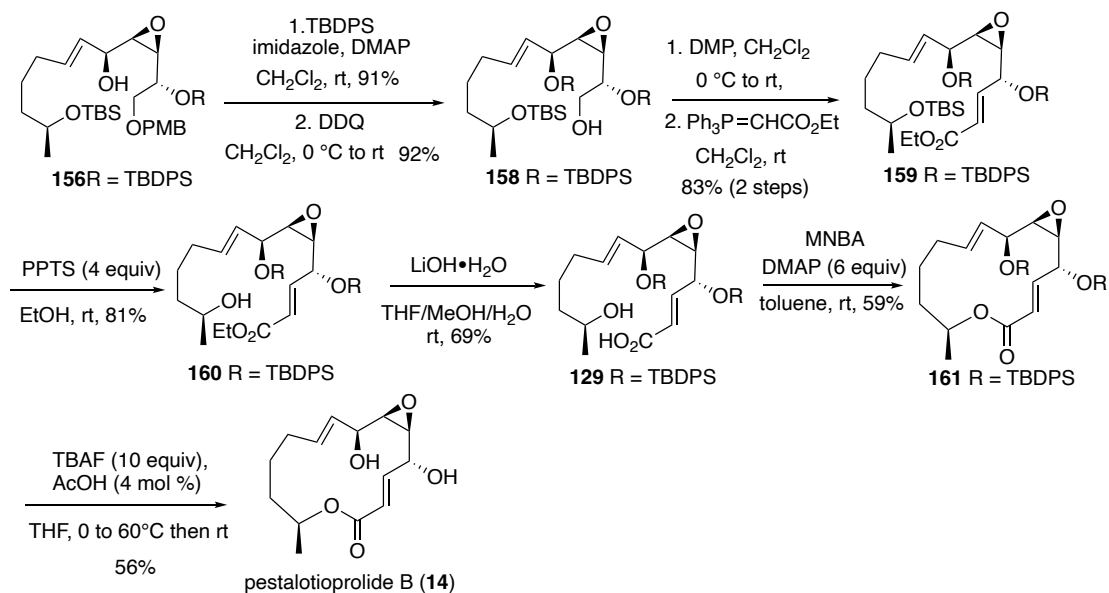
Table 8 Comparison of ^{1}H and ^{13}C NMR data for natural and synthetic pestalotioprolide B (**14**).

Position	^{1}H NMR (δ and J in Hz)		^{13}C NMR (δ)	
	Natural (600 MHz) in acetone-d_6	Synthetic (500 MHz) in acetone-d_6	Natural (150 MHz) in acetone-d_6	Synthetic (125 MHz) in acetone-d_6
1	-	-	166.1	166.1
2	5.99, dd (15.5, 2.0)	5.99, dd (15.5, 1.8)	120.9	120.8
3	7.11, dd (15.5, 4.0)	7.11, dd (15.5, 3.6)	148.2	148.2
4	4.32, m	4.35–4.28, m	71.4	71.4
5	2.92, dd (5.6, 4.6)	2.93–2.89, m	61.8	61.7
6	2.94, dd (8.9, 4.6)	2.94, dd (8.9, 4.5)	59.3	59.2
7	3.94, ddd (8.9, 7.7, 3.9)	3.97–3.91, m	71.7	71.7
8	5.55, dd (15.6, 7.7)	5.55, dd (15.5, 7.8)	130.9	130.9
9	5.96, m	6.30–5.90, m	135.2	135.2
10	2.12, m/ 2.01, m	2.16–2.08, m/ 2.03–1.93, m	33.7	33.7
11	1.86, m/ 1.13, m	1.89–1.75, m/ 1.16–1.09, m	25.4	25.3
12	1.80, m/ 1.56, m	1.89–1.75, m/ 1.60–1.50, m	35.1	35.1
13	4.66, m	4.69–4.62, m	72.3	72.3
14	1.22, d (6.2)	1.21, d (6.2)	20.3	20.3
4-OH	4.99, d (4.4)	5.01, brs	-	-
7-OH	4.17, d (3.9)	4.21, brs	-	-

Having successful syntheses of seiricuprolide (**13**) and pestalotioprolide B (**14**), our next focus was to evaluate biological activity of synthetic **13** and **14**. Recently, our research group has reported the *in vitro* cytotoxic activity of 14-membered analogues of **13** and **14**, nigrosprolide (**127**), (4*S*,7*S*,13*S*)-4,7-dihydroxy-13-tetra-2,5,8-trienolide (**128**) and mutolide (**5**), against three human cancer cell lines including HCT116 colorectal carcinoma, MCF-7 breast adenocarcinoma and Calu-3 lung adenocarcinoma using the MTT assay (Thiraporn *et al*., 2022b). Synthetic mutolide (**5**) apparently was significantly active against the HCT116 colon cancer cells ($IC_{50} = 12$ μM) and was inactive against the other two cell lines ($IC_{50} > 50$ μM), whereas macrolactone analogues **127** and **128** showed no cytotoxic effects on all three cancer cell lines tested. The HCT116 cancer cell was then chosen for screening of cytotoxic activity of compounds **13** and **14** using MTT assay which was performed by the laboratory of Prof. Dr. Chatchai Muanprasat of Chakri Naruebadin Medical Institute, Faculty of Medcine Ramathibodi Hospital, Mahidol University (**Figure 7**). In addition, synthetic **13** and **14** were evaluated for their cytotoxicity against non-cancerous (Vero) cells determined by MTT assay (**Figure 8**). Viability of both cells treated with compounds **13** and **14** at 0, 10, 20, 50 and 100 μM at 24, 48 and 72 h of incubation were then performed. It was discovered that both compounds showed no cytotoxic effects on the HCT116 colon cancer cells even at 100 μM and prolonged incubation time of 72 h. Similar results were observed for seiricuprolide (**13**) on Vero cells viability, whereas pestalotioprolide B (**14**) slightly inhibited the viability of Vero cells when **14** was treated at high concentration and was incubated in prolonged time. The latter observation suggested that macrolide **14** was more cytotoxic to Vero cells to other related analogues **13**, **127**, **128** and **5**. Based on the cytotoxic activity results, it can be roughly concluded that the β-epoxide moiety at C5–C6 of this group of macrolides suppressed the cytotoxicity against HCT116 cancer cells. This preliminary structure–activity relationship is in accordance with Liu's report that the β-epoxide group of natural products **13** and **14** decreased cytotoxic activities against the L5178Y mouse lymphoma cells compared to natural products **126** and **127** which possess the *Z*-olefin at this emplacement.

Figure 7 Viability of HCT116 cells treated with synthetic compounds **13** and **14** after 24 h, 48 h and 72 h of incubations at indicated concentrations determined by the MTT assay. * indicated the *p*-value of < 0.05 (1 way ANOVA compared with concentration 0 μM).
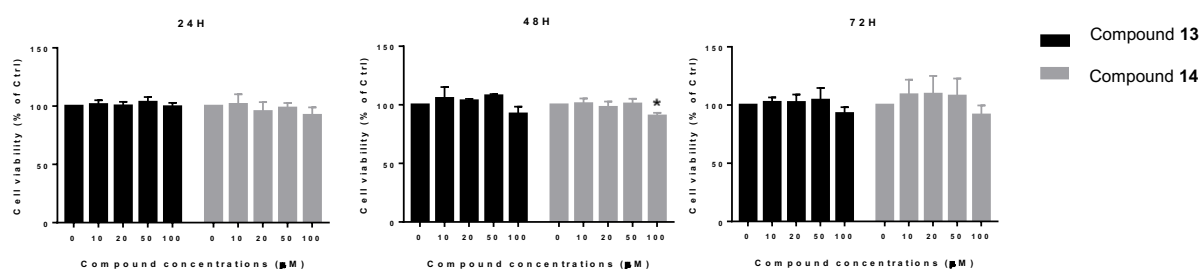
Figure 8 Viability of Vero cells treated with synthetic compounds **13** and **14** after 24 h, 48h and 72h of incubations at indicated concentrations determined by the MTT assay. *, **, *** and **** indicated the *p*-values of < 0.05, < 0.01, < 0.0005, <0.0001, respectively (1 way ANOVA compared with concentration 0 μM)
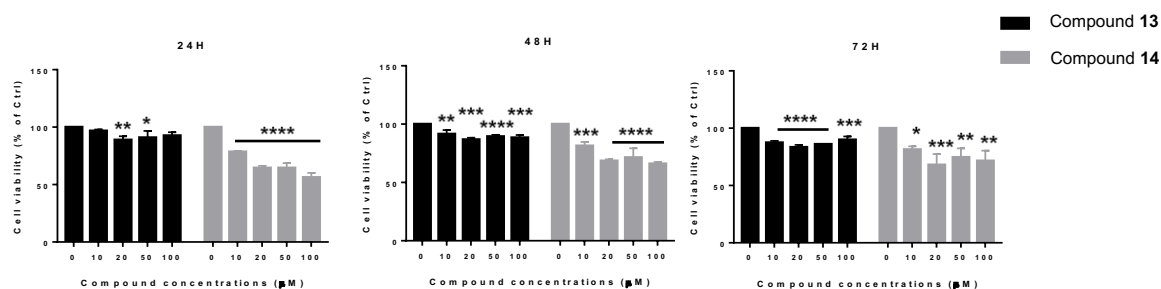
Synthetic seiricuprolide (**13**) and pestalotioprolide B (**14**) were further subjected to evaluation on inhibitory activity of cystic fibrosis transmembrane regulator (CFTR)-mediated chloride secretion in human intestinal epithelial (T84) cells using short-circuit analysis (I_{sc}) which was also tested by the laboratory of Prof. Dr. Chatchai Muanprasat of Chakri Naruebadin Medical Institute, Faculty of Medcine Ramathibodi Hospital, Mahidol University. Our group has also recently disclosed the CFTR inhibitory activity of synthetic macrolides **127**, **128** and **5**, in which mutolide (**5**) showed stronger inhibition (~70% inhibition) compared to analogues **127** (40%

inhibition) and **128** (30% inhibition) at the same concentration (5 μM) (Thiraporn *et al.*, 2022b). Disappointingly, synthetic macrolides **13** and **14** showed no effects on CFTR-mediated chloride secretion in T84 cells stimulated by forskolin (a cAMP donor) at both 5 and 10 μM compared to a positive control, CFTR(inh)-172 (**Figure 9**). Clearly, the β-epoxide moiety of macrolides **13** and **14** suppressed the CFTR inhibitory activity compared to compounds **127** and **128**, which are their C5–C6 *Z*-olefin counterparts.

Figure 9 Evaluation of effects of synthetic compounds **13** and **14** (5 and 10 μM) on CFTR-mediated chloride secretion in T84 cells. Forskolin (20 μM) was used to stimulate the CFTR-mediated chloride secretion. CFTR(inh)-172 (20 μM) was used as a positive control. Representative tracings of 3 experiments as shown.
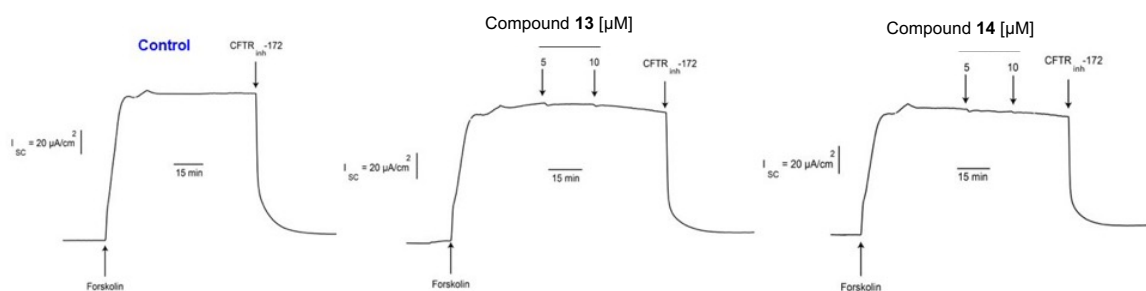
3.2 Conclusion

In conclusion, we have accomplished the first and convergent total synthesis of seiricuprolide (**13**) and pestalotioprolide B (**14**) in a longest linear sequence of 17 steps and a total of 19 steps in 1.9 and 1.6% overall yields starting from known alkyne **132** and chiral *Z*-allylic alcohol **151**, in which **151** was derived from D-mannitol, an inexpensive and commercially available chiral building block. Our key bond formations involved in Shiina macrolactonization and acetylide addition to construct 14-membered skeleton, Wittig olefination to generate the (*E*)-α,β-unsaturated ester subunit and selective reduction of propargylic alcohol to form *Z*- or *E*-olefin at C8–C9 for **13** and **14**. Highly stereoselective substrate-controlled *m*-CPBA epoxidation was

highlighted as an efficient method for installing the C5–C6 β-epoxide at the early stage of the synthesis, which reaffirmed the remarkable robustness of this β-epoxide moiety of both natural products. Our work also verified that *m*-CPBA epoxidation of *Z*-allylic alcohol substrate containing (*S*)-α-silyloxy stereogenic center according to Baltas's protocol would selectively form the α-epoxide *threo* product which led to the revision of the absolute configurations of Baltas's originally proposed chiral epoxy alcohol intermediates. Synthetic macrolides **13** and **14** were evaluated for their cytotoxic activity against the HCT116 colon cancer cell line as well as their inhibitory effect on CFTR in human intestinal epithelial (T84) cells compared to their previously reported analogues. These two synthetic macrolides were discovered to possess no reactivity of both biological activities tested. Preliminary structure–activity relationship suggested that the C5–C6 β-epoxide moiety of both **13** and **14** suppressed the cytotoxic activity against the HCT116 colon cancer cells as well as their CFTR inhibitory effect.

CHAPTER 4

EXPERIMENTAL

CHAPTER 4

EXPERIMENTAL

4.1 General Information

Unless otherwise stated, all reactions were performed under a nitrogen or argon atmosphere in oven- or flamed-dried glassware. Solvents were used as received from suppliers or distilled before use using standard procedures. All other reagents were obtained from commercial sources and used without further purification. Column chromatography was carried out on silica gel 60 (0.063–0.200 mm, Merck). Thin-layer chromatography (TLC) was carried out on silica gel 60 F_{254} plates (Merck). ^{1}H, ^{13}C and 2D NMR spectroscopic data were recorded on 300 or 500 MHz Bruker FT NMR Ultra Shield spectrometers. Chemical shifts (δ) in the ^{1}H and ^{13}C NMR spectra are reported in ppm relative to internal tetramethylsilane. The data are presented as follows: chemical shift, multiplicity (s = singlet, d = doublet, t = triplet, q = quartet, m = multiplet, , br = broad), coupling constant(s) in hertz (Hz), and integration. Infrared (IR) spectra were recorded with a Perkin-Elmer 783 FTS165 FT-IR spectrometer. High-resolution mass spectra were obtained on a Ultra-Performance Liquid Chromatography-High Resolution Mass Spectrometer (Agilent LC-QTOF 6500 system), Mae Fah Luang University or a High-Performance Liquid Chromatograph–Mass Spectrometer (Shimadzu LCMS-IT-TOF Model LC-20ADXR), Thammasat University. Melting points were measured using an Electrothermal IA9200 melting point apparatus and are uncorrected. The optical rotations were recorded on a JASCO P-2000 polarimeter.

4.2 Experimentals and Characterization data

4.2.1 General procedure for IBX oxidation

To a solution of epoxy alcohol derivative (1.0 equiv) in DMSO (0.5 M) at room temperature was added 2-iodoxybenzoic acid (IBX, 3.0 equiv). After being stirred at room temperature until the starting epoxy alcohol was completely consumed, the reaction was cooled to 0 °C and then quenched with H_2O. The resulting mixture was then filtered through a pad of Celite and washed with EtOAc. The organic layer of the colorless filtrate was separated and the aqueous layer was extracted with EtOAc (x2). The combined organic layers were washed with brine, dried over anhydrous Na_2SO_4 and concentrated *in vacuo*. The crude residue was purified by column chromatography to give the corresponding epoxy aldehyde derivative.

4.2.2 General procedure for TBS protection

To a solution of alcohol derivative (1.0 equiv) in anhydrous CH_2Cl_2 (0.2 M) at room temperature was added 4-dimethylaminopyridine (DMAP, 0.3 equiv), imidazole (2.0 equiv) and *tert*-butyl(chloro)dimethylsilane (TBSCl, 1.5 equiv). After being stirred at room temperature until the starting alcohol derivative was completely consumed, the reaction was quenched with H_2O. The organic layer was separated and the aqueous layer was extracted with CH_2Cl_2 (x2). The combined organic phases were washed with brine, dried over anhydrous Na_2SO_4 and concentrated *in vacuo*. The crude residue was purified by column chromatography to give the corresponding TBS ether derivative.

4.2.3 General procedure for PMB deprotection

To a solution of PMB ether derivative (1.0 equiv) in CH_2Cl_2:H_2O (3:1, 0.06 M) at 0 °C was added 2,3-dichloro-5,6-dicyano-1,4-benzoquinone (DDQ, 1.5 equiv). The reaction mixture was stirred from 0 °C to room temperature until the starting alcohol derivative was completely consumed. The reaction was then quenched with saturated aqueous $NaHCO_3$. The organic layer was separated and the aqueous layer was extracted with CH_2Cl_2 (x3). The combined organic phases were washed with brine, dried over anhydrous Na_2SO_4 and concentrated *in vacuo*. The crude residue was purified by column chromatography to give the corresponding alcohol derivative.

4.2.4 General procedure for DMP oxidation

To a solution of alcohol derivative (1.0 equiv) in anhydrous CH_2Cl_2 (0.02 M) at room temperature was added Dess–Martin periodinane (DMP, 2.0 equiv), After being stirred at room temperature until the starting alcohol was completely consumed, the reaction was quenched with saturated aqueous $NaHCO_3$. The organic layer was separated and the aqueous layer was extracted with CH_2Cl_2 (x2). The combined organic phases were washed with brine, dried over anhydrous Na_2SO_4 and concentrated *in vacuo*. The crude residue was purified by column chromatography to give the corresponding aldehyde derivative.

4.2.5 General procedure for Wittig olefination

To a solution of aldehyde derivative (1.0 equiv) in anhydrous CH_2Cl_2 (0.08 M) at room temperature was added (carbethoxymethylene)triphenylphosphorane (2.2 equiv). The reaction mixture was stirred at room temperature overnight. The reaction mixture was then concentrated *in vacuo*. The crude residue was purified by column chromatography to give the corresponding *E*-α,β-unsaturated ester derivative.

4.2.6 General procedure for ester hydrolysis

To a solution of ester derivative (1.0 equiv) in THF:MeOH:H_2O (8:1:1, 0.03 M) at room temperature was added LiOH (5.0 equiv). After being stirred at room temperature overnight, the reaction was neutralized with 4M HCl. The organic layer was separated and the aqueous layer was extracted with EtOAc (x5). The combined organic phases were washed with brine, dried over anhydrous Na_2SO_4 and concentrated *in vacuo*. The crude residue was purified by column chromatography to give the corresponding carboxylic acid derivative.

4.2.7 General procedure for TBDPS protection

To a solution of alcohol derivative (1.0 equiv) in anhydrous CH_2Cl_2 (0.2 M) at room temperature was added 4-dimethylaminopyridine (DMAP, 0.2 equiv), imidazole (3.0 equiv) and *tert*-butyl(chloro)diphenylsilane (TBDPSCl, 2.0 equiv). After being stirred at room temperature overnight, the reaction was quenched with H_2O. The organic layer was separated and the aqueous layer was extracted with CH_2Cl_2 (x2). The combined organic phases were washed with brine, dried over anhydrous Na_2SO_4 and concentrated *in vacuo*. The crude residue was purified by column chromatography to give the corresponding TBDPS ether derivative.

4.2.8 General procedure for benzoate ester protection

To a solution of alcohol derivative (1.0 equiv) in anhydrous CH_2Cl_2 (0.26 M) at room temperature was added triethylamine (Et_3N, 2.0 equiv) and benzoyl chloride (BzCl, 1.05 equiv). After being stirred at room temperature overnight, the reaction was quenched with saturated aqueous NH_4Cl. The organic layer was separated and the aqueous layer was extracted with CH_2Cl_2 (x2). The combined organic phases were washed with brine, dried over anhydrous Na_2SO_4 and concentrated *in vacuo*. The crude residue was purified by column chromatography to give the corresponding benzoate ester derivative.

4.2.9 General procedure for methanolysis

To a solution of ester derivative (1.0 equiv) in methanol (0.17 M) at room temperature was added potassium carbonate (1.5 equiv). After being stirred at room temperature until the starting benzoate ester derivative was completely consumed, the reaction was quenched with H_2O. The organic layer was separated and the aqueous layer was with EtOAc (x3). The combined organic phases were washed with brine, dried over anhydrous Na_2SO_4 and concentrated *in vacuo*. The crude residue was purified by column chromatography to give the corresponding alcohol derivative.

4.2.10 General procedure for TBS deprotection

To a solution of TBS ether derivative (1.0 equiv) in EtOH (0.05 M) at room temperature was added pyridinium *p*-toluenesulfonate (PPTS, 4.0 equiv). After being stirred at room temperature overnight, the reaction was quenched with H_2O. The organic layer was separated and the aqueous layer was with EtOAc (x4). The combined organic phases were washed with brine, dried over anhydrous Na_2SO_4 and concentrated *in vacuo*. The crude residue was purified by column chromatography to give the corresponding alcohol derivative.

4.2.11 General procedure for Shiina macrolactonization

To a solution of 2-methyl-6-nitrobenzoic anhydride (MNBA, 0.7 equiv) in anhydrous toluene (0.0021 M) was added 4-dimethylaminopyridine (DMAP, 6.0 equiv). After being stirred for 15 min, the reaction was slowly added a solution of seco acid (1.0 equiv) in anhydrous toluene (0.012 M) by syringe pump at room temperature for 8 h. The reaction mixture was then concentrated *in vacuo*. The crude residue was purified by column chromatography to give the corresponding macrolactone derivative.

4.2.12 General procedure for global TBDPS deprotection

To a solution of TBDPS ether derivative (1.0 equiv) in anhydrous THF (0.04 M) at 0 °C was added dropwise acetic acid (0.04 equiv) and tetrabutylammonium fluoride (TBAF, 1.0 M solution in THF, 10.0 equiv). The reaction mixture was stirred from 0 °C to 60 °C overnight. The reaction was then quenched with saturated aqueous NaHCO$_3$ and H$_2$O. The organic layer was separated and the aqueous layer was extracted with EtOAc (x5). The combined organic phases were washed with brine, dried over anhydrous Na$_2$SO$_4$ and concentrated *in vacuo*. The crude residue was purified by column chromatography to give the corresponding alcohol derivative.
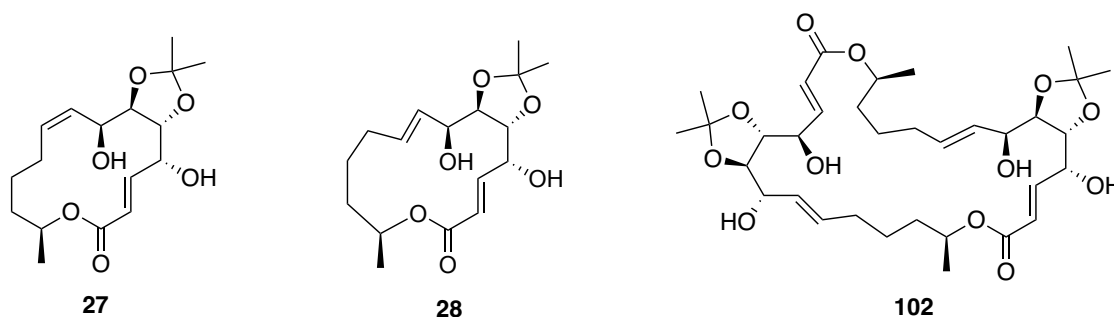
Macrolactones 27, 28 and 102: A solution of known diene **26** (101.1 mg, 0.29 mmol, 1.0 equiv) in anhydrous CH$_2$Cl$_2$ (357 mL, 0.8 mM) at room temperature was purged with argon over 5 min before Grubbs second generation catalyst (12.1 mg, 14.3 μmol, 5 mol %) was added in one portion at room temperature. The reaction mixture was then heated at 40 °C. After maintaining reaction temperature at 40 °C for 2 h, the reaction was cooled to room temperature and concentrated *in vacuo*. The resulting crude was purified by column chromatography (20−80% EtOAc/hexanes) to give macrolactones **27** (15.8 mg, 17%), **28** (47.9 mg, 52%) and **102** (20.5 mg, 11%).

Macrolactone 27: R_f = 0.60 (60% EtOAc/hexanes); [^1]H NMR (300 MHz, CDCl$_3$) δ 6.79 (dd, J = 15.6, 2.5 Hz, 1H), 6.25 (dd, J = 15.6, 2.5 Hz, 1H), 5.59 (dt, J = 10.6, 7.8 Hz, 1H), 5.53–5.41 (m, 1H), 5.18–5.04 (m, 1H), 4.84–4.71 (m, 1H), 4.34–4.23 (m, 2H), 3.79 (d, J = 8.5 Hz, 1H), 2.85 (brs, 1H), 2.09–1.94 (m, 2H), 1.94–1.78 (m, 1H), 1.48 (s, 3H), 1.45 (s, 3H), 1.30 (d, J = 6.2 Hz, 3H); [^13]C NMR (75 MHz, CDCl$_3$) δ 165.2, 141.4, 132.7, 129.9, 122.8, 110.9, 78.2, 78.0, 71.4, 67.4, 65.3, 33.9, 28.8, 27.3, 27.2, 24.9, 20.1. The spectral data of **27** matched those previously described (Tadpetch et al., 2015).

Macrolactone 28: R_f = 0.40 (60% EtOAc/hexanes); ^{1}H NMR (300 MHz, CDCl$_3$) δ 6.60 (dd, J = 15.7, 2.3 Hz, 1H), 6.25 (dd, J = 15.7, 2.3 Hz, 1H), 5.75 (dt, J = 15.6, 7.8 Hz, 1H), 5.09–4.92 (m, 2H), 4.71–4.63 (m, 1H), 4.05–3.96 (m, 2H), 3.92 (dd, J = 9.3, 5.9 Hz, 1H), 2.63 (d, J = 8.5 Hz, 1H), 2.19–2.02 (m, 1H), 1.98–1.80 (m, 1H), 1.75–1.60 (m, 4H) 1.51 (s, 3H), 1.45 (s, 3H), 1.32 (d, J = 6.6 Hz, 3H); ^{13}C NMR (75 MHz, CDCl$_3$) δ 165.6, 144.5, 136.2, 128.6, 122.2, 110.2, 80.9, 78.7, 76.6, 69.8, 69.7, 34.0, 29.9, 27.6, 27.5, 23.6, 21.1.

Macrolactone 102: R_f = 0.13 (60% EtOAc/hexanes); ^{1}H NMR (300 MHz, CDCl$_3$) δ 6.89 (dd, J = 15.7, 3.9 Hz, 1H), 6.16 (dd, J = 15.7, 3.9 Hz, 1H), 5.60 (dt, J = 15.7, 6.3 Hz, 1H), 5.49 (dd, J = 15.7, 6.0 Hz, 1H), 5.06–4.88 (m, 1H), 4.57–4.44 (m, 1H), 4.05 (dd, J = 6.9, 4.8 Hz, 1H), 3.96–3.89 (m, 2H), 3.38 (brs, 1H), 3.13 (brs, 1H), 2.20–1.87 (m, 2H), 1.73–1.51 (m, 2H), 1.43 (s, 9H), 1.24 (d, J = 6.2 Hz, 3H); ^{13}C NMR (75 MHz, CDCl$_3$) δ 165.7, 144.3, 134.0, 129.1, 122.5, 110.0, 79.8, 78.6, 72.1, 71.3, 69.9, 35.6, 31.9, 27.4, 25.3, 20.4.
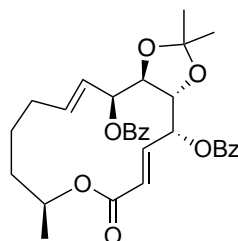
103

Benzoate ester 103: To a solution of diol **28** (100.1 mg, 0.31 mmol, 1.0 equiv) in anhydrous CH$_2$Cl$_2$ (11 mL, 0.03 M) at 0 °C was added triethylamine (300 μL, 2.14 mmol, 7.0 equiv), benzoyl chloride (180 μL, 1.53 mmol, 1.05 equiv) and DMAP (62.4 mg, 0.51 mmol, 0.6 equiv), respectively. After being stirred at room temperature overnight, the reaction was quenched with saturated aqueous NH$_4$Cl. The organic layer was separated and the aqueous layer was extracted with CH$_2$Cl$_2$ (2×10 mL). The combined organic phases were washed with brine, dried over anhydrous Na$_2$SO$_4$ and concentrated *in vacuo*. The crude residue was purified by column chromatography (10−20% EtOAc/hexanes) to give benzoate ester **103** (122.6 mg, 74%) as a light yellow oil: R_f = 0.61 (20% EtOAc/hexanes); ^{1}H NMR (300 MHz, CDCl$_3$) δ 8.22–8.00 (m, 4H), 7.69–7.36 (m, 6H), 6.81 (dd, J = 15.7, 3.2 Hz, 1H), 6.20–6.15 (m, 1H), 6.02 (dt, J = 15.7, 6.3 Hz, 1H), 5.96 (dd, J = 15.7, 6.0 Hz, 1H), 5.65 (t, J = 9.4, 3.2 Hz, 1H), 5.19

(dd, J = 15.3, 8.8 Hz, 1H), 5.12–4.97 (m, 1H), 4.53 (dd, J = 9.8, 1.7 Hz, 1H), 4.36 (dd, J = 5.3, 1.7 Hz, 1H), 2.20–2.04 (m, 1H), 1.98–1.77 (m, 1H), 1.76–1.61 (m, 3H), 1.60–1.47 (m, 1H), 1.43 (s, 9H), 1.32 (d, J = 6.1 Hz, 3H), 1.24 (s, 3H); ^{13}C NMR (75 MHz, CDCl$_3$) δ 165.7, 165.3, 165.2, 142.7, 138.5, 133.7, 133.1, 130.4, 130.0, 129.9, 128.8, 128.4, 125.3, 122.3, 111.5, 79.6, 77.5, 77.3, 71.8, 69.9, 33.8, 29.9, 27.5, 23.3, 21.0.
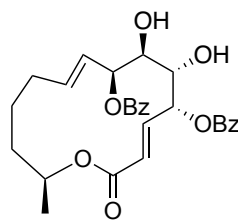
104

Diol 104: To a round-bottom flask containing acetonide **103** (40.2 mg, 0.07 mmol, 1.0 equiv) at 0 °C was added 90% trifluoroacetic acid (1.32 mL, 17.2 mmol, 200 equiv). After being stirred at 0 °C for 1.5 h, the reaction was quenched with saturated aqueous NaHCO$_3$. The organic layer was separated and the aqueous layer was extracted with EtOAc (4×5 mL). The combined organic phases were washed with brine, dried over anhydrous Na$_2$SO$_4$ and concentrated *in vacuo*. The crude residue was purified by column chromatography (15−25% EtOAc/hexanes) to give diol **104** (14.9 mg, 43%) along with unreacted **103** (12.2 mg, 30%).

Diol 104: White solid; R_f = 0.54 (30% EtOAc/hexanes); ^{1}H NMR (300 MHz, CDCl$_3$) δ 8.21–7.96 (m, 4H), 7.66–7.55 (m, 2H), 7.51–7.39 (m, 4H), 6.83 (dd, J = 15.7, 3.2 Hz, 1H), 6.03 (dt, J = 15.7, 6.3 Hz, 1H), 5.98 (dd, J = 15.7, 6.0 Hz, 1H), 5.69 (dd, J = 9.4, 3.2 Hz, 1H), 5.40 (dd, J = 15.3, 8.8 Hz, 1H), 5.32–5.18 (m, 1H), 4.09 (d, J = 9.8 Hz, 1H), 4.01–3.85 (m, 1H), 2.28–2.08 (m, 1H), 2.08–1.83 (m, 2H), 1.83–1.44 (m, 6H), 1.28 (d, J = 6.5 Hz, 2H), 1.25 (s, 3H); ^{13}C NMR (75 MHz, CDCl$_3$) δ 166.3, 165.3, 143.0, 137.0, 133.7, 133.5, 130.1, 130.0, 129.9, 129.8, 129.3, 128.7, 128.6, 126.0, 123.5, 74.5, 70.6, 70.1, 70.0, 33.0, 31.0, 29.8, 22.9, 18.5.
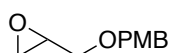
110

2-(((4-Methoxybenzyl)oxy)methyl)oxirane (110): To a stirred suspension of sodium hydride (NaH, 60% dispersion in mineral oil, 10.37 g, 259.4 mmol, 1.2 equiv) in THF

(117 mL, 1.85 M) at 0 °C was added a solution of 4-methoxybenzyl alcohol (PMBOH 32.8 g, 237.6 mmol, 1.1 equiv) in THF (80 mL, 2.7 M). The reaction was then stirred from 0 °C to room temperature for 1.5 h. After that, tetrabutylammonium iodide (TBAI, 638.8 mg, 1.7 mmol, 8 mol %) and a solution of epichlorohydrin (**109**) (20.21 g, 216.2 mmol, 1.0 equiv) in THF (40 mL, 4.45 M) were added at 0 °C. The reaction mixture was stirred from 0 °C to room temperature overnight before being quenched with saturated aqueous NH_4Cl (80 mL). The organic layer was separated and the aqueous layer was extracted with EtOAc (3×70 mL). The combined organic layers were washed with brine, dried over anhydrous Na_2SO_4 and concentrated *in vacuo*. The crude residue was purified column chromatography (10–20% EtOAc/hexanes) to yield **110** as a light yellow oil (29.71 g, 71%): R_f = 0.20 (10% EtOAc/hexanes); ^{1}H NMR (300 MHz, CDCl$_3$) δ 7.27 (d, *J* = 8.4 Hz, 2H), 6.88 (d, *J* = 8.7 Hz, 2H), 4.51 (dd, *J* = 18.9, 11.4 Hz, 2H), 3.80 (s, 3H), 3.72 (dd, *J* = 11.4, 3.3 Hz, 1H), 3.41 (dd, *J* = 11.4, 5.7 Hz, 1H), 3.20–3.14 (m, 1H), 2.79 (t, *J* = 4.5 Hz, 1H), 2.60 (dd, *J* = 5.1, 2.7 Hz, 1H). ^{1}H NMR data of **110** matched those previously described (Thiraporn et al., 2022).
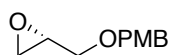
110*S*

(***S***)- 2-(((4-Methoxybenzyl)oxy)methyl)oxirane (110*S*): To a 100-mL round-bottom flask was added (*R,R*)-cobalt(II)salen (330.4 mg, 0.5 mmol, 5 mol %) and toluene (2.3 mL) at room temperature. The mixture was added acetic acid (135 μL, 2.18 mmol, 20 mol %) and stirred open air at room temperature for 1 h. The resulting dark brown solution was then concentrated under reduced pressure to afford a brown solid before racemic epoxide **110** (22.43 g, 109.4 mmol) was added in one portion. The reaction mixture was then cooled to 0 °C and H_2O (1.3 mL, 0.6 equiv) was added dropwise. The mixture was stirred from 0 °C to room temperature overnight before being concentrated under reduced pressure and purified by column chromatography (10–30% EtOAc/hexanes) to provide chiral epoxide **110*S*** as a yellow oil (9.64 g, 45%): R_f = 0.20 (10% EtOAc/hexanes); $[\alpha]_D^{25}$ = –2.90 (*c* 1.00, CHCl$_3$); ^{1}H NMR (300 MHz, CDCl$_3$) δ 7.25 (d, *J* = 8.7 Hz, 2H), 6.86 (d, *J* = 8.7 Hz, 2H), 4.48 (dd, *J* = 18.3, 11.4 Hz, 2H), 3.76 (s, 3H), 3.70 (dd, *J* = 11.4, 3.0 Hz, 1H), 3.37 (dd, *J* = 11.4, 6.0 Hz, 1H), 3.16–3.11 (m,

1H), 2.75 (t, J = 4.5 Hz, 1H), 2.56 (dd, J = 5.1, 2.7 Hz, 1H). Specific rotation and ^{1}H NMR data of **110S** matched those previously described (Thiraporn et al., 2022).
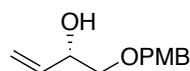
162

(S)-1-((4-Methoxybenzyl)oxy)but-3-en-2-ol (162): To a stirred suspension of trimethylsulfonium iodide (11.82 g, 57.9 mmol, 1.5 equiv) in anhydrous THF (128 mL, 0.3 M) at 0 °C was added dropwise lithium bis(trimetylsilyl)amide (LHMDS, *ca*. 1.3 M solution in THF, 74 mL, 96.5 mmol, 2.5 equiv). After being stirred at 0 °C for 1 h, the light yellow cloudy solution was added a solution of chiral epoxide **110S** (7.52 g, 38.6 mmol, 1.0 equiv) at 0 °C. The mixture was then stirred from 0 °C to room temperature for 1 h, then quenched with saturated aqueous NH$_4$Cl (80 mL). The organic layer was separated and the aqueous layer was extracted with EtOAc (3×80 mL). The combined organic layers were washed with brine, dried over anhydrous Na$_2$SO$_4$ and concentrated *in vacuo*. The crude residue was purified column chromatography (10–30% EtOAc/hexanes) to yield allylic alcohol **162** as a light yellow oil (5.37 g, 71%): R_f = 0.24 (20% EtOAc /hexanes); ^{1}H NMR (300 MHz, CDCl$_3$) δ 7.26 (d, J = 8.4 Hz, 2H), 6.88 (d, J = 8.7 Hz, 2H), 5.82 (ddd, J = 16.8, 10.5, 5.7 Hz, 1H), 5.35 (d, J = 17.4 Hz, 1H), 5.18 (d, J = 10.8 Hz, 1H), 4.50 (s, 2H), 4.33 (brs, 1H), 3.80 (s, 3H), 3.51 (dd, J = 9.6, 3.3 Hz, 1H), 3.37–3.31 (m, 1H). ^{1}H NMR data of **162** matched those previously described (Thiraporn et al., 2022).
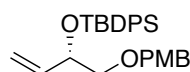
112

(S)-*tert*-Butyl((4-Methoxybenzyl)oxy)but-3-en-2-yl)oxy)diphenylsilane (112): To a stirred solution of allylic alcohol **162** (6.98 g, 33.5 mmol, 1.0 equiv) in anhydrous CH$_2$Cl$_2$ (112 mL, 0.3 M) at 0 °C was added DMAP (1.22 g, 10.0 mmol, 30 mol %), imidazole (4.56 g, 67.0 mmol, 2.0 equiv) and *tert*-butyldiphenylchlorosilane (10.3 mL, 40.2 mmol, 1.2 equiv), respectively. The reaction mixture was stirred from 0 °C to room temperature overnight before being quenched with H$_2$O (70 mL). The organic layer was separated and the aqueous layer was extracted with CH$_2$Cl$_2$ (3 × 50 mL). The combined

organic layers were washed with brine, dried over anhydrous Na_2SO_4, and concentrated *in vacuo*. The crude residue was purified by column chromatography (100% hexanes– 2% EtOAc/hexanes) to yield TBDPS ether **112** as a colorless oil (20.75 g, 88%): $R_f =$ 0.73 (20% EtOAc/hexanes); ^{1}H NMR (300 MHz, $CDCl_3$) δ 7.69–7.62 (m, 6H), 7.10 (d, $J = 8.4$ Hz, 2H), 6.80 (d, $J = 8.4$ Hz, 2H), 5.87 (ddd, $J = 17.1$, 10.5, 5.7 Hz, 1H), 5.16 (dt, $J = 17.1$, 1.5 Hz, 1H), 5.06 (dt, $J = 10.5$, 1.5 Hz, 1H), 4.33–4.30 (m, 3H), 3.79 (s, 3H), 3.36 (qd, $J = 10.5$, 1.5 Hz, 1H), 1.06 (s, 9H). ^{1}H NMR data of **112** matched those previously described (Thiraporn et al., 2022).

113
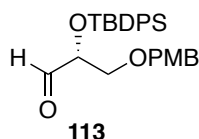
(*R*)-2-((*tert*-Butyldiphenylsilyl)oxy)-3-((4-methoxybenzyl)oxy)propanal (113): To a stirred solution of allylic alcohol **112** (10.21 g, 22.4 mmol, 1.0 equiv) in acetone/H_2O (4:1, 223 mL, 0.1 M) at 0 °C was added *N*-methylmorpholine *N*-oxide (NMO, 50 wt% in H_2O, 9.4 mL, 44.7 mmol, 2.0 equiv), followed by osmium tetroxide (OsO_4, 4 wt% in H_2O, 1.42 mL, 0.22 mmol, 1 mol %). The reaction mixture was stirred from 0 °C to room temperature overnight. The mixture was then concentrated under reduced pressure, diluted with H_2O (50 mL) and EtOAc (50 mL). The aqueous phase was separated and further extracted with EtOAc (3×50 mL). The combined organic layers were washed with brine, dried over anhydrous Na_2SO_4, and concentrated *in vacuo*. The crude residue was purified by column chromatography (10–70% EtOAc/hexanes) to yield the diol intermediate as a colorless oil (9.04 g, 84%): $R_f = 0.30$ (40% EtOAc/hexanes). The diol intermediate was immediately carried to the next step.

To a stirred solution of diol intermediate (9.04 g, 18.8 mmol, 1.0 equiv) in acetone/H_2O (5:1, 75 mL, 0.25 M) at 0 °C was added sodium periodate ($NaIO_4$, 8.17 g, 37.6 mmol, 2.0 equiv). After being stirred from 0 °C to room temperature for 2.5 h, the reaction mixture was concentrated under reduced pressure and diluted with H_2O (40 mL). The aqueous phase was separated and further extracted with EtOAc (3×40 mL). The combined organic layers were washed with brine, dried over anhydrous Na_2SO_4, and concentrated *in vacuo*. The crude residue was purified by column chromatography (7% EtOAc/hexanes) to yield aldehyde **113** as a colorless oil (6.14 g, 73%): $R_f = 0.26$

(10% EtOAc/hexanes); ^{1}H NMR (300 MHz, CDCl$_3$) δ 9.65 (s, 1H), 7.67–7.31 (m, 6H), 7.15 (d, J = 8.1 Hz, 2H), 6.84 (d, J = 8.4 Hz, 2H), 4.37 (s, 2H), 4.16–4.13 (m, 1H), 3.79 (s, 3H), 3.64 (dd, J = 10.2, 4.8 Hz, 1H), 3.56 (dd, J = 10.2, 4.2 Hz), 1.11 (s, 9H). ^{1}H NMR data of **113** matched those previously described (Thiraporn et al., 2022).
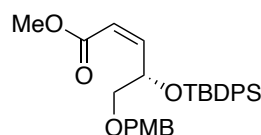
115

(_S_,_Z_)-Methyl-4-((_tert_-Butyldiphylsilyl)oxy)-5-((4-methoxybenzoyl)oxy)pent-2-enoate (115): To a solution of methyl _P_,_P_-bis(2,2,2-trifluoroethyl)phosphonoacetate (**114**) (4.96 g, 13.8 mmol, 1.2 equiv) in anhydrous THF (100 mL, 0.14 M) at 0 °C was added sodium hydride (60% dispersion in mineral oil, 652.7 mg, 16.3 mmol, 1.2 equiv). After stirring at 0 °C for 1 h, a solution of aldehyde **113** (5.14 g, 11.4 mmol, 1.0 equiv) in anhydrous THF (50 mL, 0.28 M) was slowly added. The reaction mixture was stirred at 0 °C for 10 min before being quenched with saturated aqueous NH$_4$Cl (50 mL). The organic layer was separated and the aqueous layer was extracted with EtOAc (3×60 mL). The combined organic layers were washed with brine, dried over anhydrous Na$_2$SO$_4$, and concentrated _in vacuo_. The crude residue was purified by column chromatography (5–10% EtOAc/hexanes) to yield _Z_-ester **115** as a colorless oil (5.20 g, 79%): R_f = 0.33 (10% EtOAc/hexanes); ^{1}H NMR (300 MHz, CDCl$_3$) δ 7.70–7.61 (m, 4H), 7.41–7.27 (m, 6H), 7.19 (d, _J_ = 8.4 Hz, 2H), 6.22 (dd, _J_ = 11.7, 7.8 Hz, 1H), 5.58 (dd, _J_ = 11.7, 0.9 Hz, 1H), 5.54–5.51 (m, 1H), 4.42 (s, 2H), 3.77 (s, 3H), 3.57 (dd, _J_ = 10.5, 5.4 Hz, 1H), 3.49–3.45 (m, 4H), 1.08 (s, 9H). ^{1}H NMR data of **115** matched those previously described (Thiraporn et al., 2022).
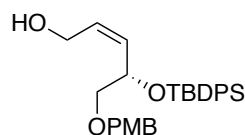
108

(_S_,_Z_)-4-((_tert_-Butyldiphylsilyl)oxy)-5-((4-methoxybenzoyl)oxy)pent-2-en-1-ol (108): To a solution of ester **115** (6.19 g, 12.3 mmol, 1.0 equiv) in anhydrous CH$_2$Cl$_2$ (120 mL, 0.1 M) at –78 °C was slowly added DIBAL-H (1.0 M in THF, 28 mL, 28.3 mmol, 2.3 equiv). The reaction was then stirred at –78 °C for 30 min before being

quenched with saturated aqueous potassium sodium tartrate (100 mL). The mixture was further stirred at room temperature for 1 h. After that, the organic layer was separated and the aqueous layer was extracted with CH_2Cl_2 (3×70 mL). The combined organic layers were washed with brine, dried over anhydrous Na_2SO_4 and concentrated *in vacuo*. The crude residue was purified by column chromatography (20–30% EtOAc/hexanes) to yield alcohol **115** as a colorless oil (3.8 g, 69%): $R_f = 0.33$ (10% EtOAc/hexanes); ^{1}H NMR (300 MHz, CDCl_3) δ 7.64 (t, $J = 7.5$ Hz, 4H), 7.41–7.31 (m, 6H), 7.14 (d, $J = 8.1$ Hz, 2H), 6.82 (d, $J = 8.4$ Hz, 2H), 3.51 (dd, $J = 9.0, 5.1$ Hz, 1H), 3.33–3.27 (m, 1H), 1.04 (s, 9H). ^{1}H NMR data of **108** matched those previously described (Thiraporn et al., 2022).

116a   **116b**

Epoxy alcohols 116a and 116b (Method I): To a suspension of 3-chloroperbenzoic acid (70–75%, 768.9 mg, 3.12 mmol, 2.0 equiv) in anhydrous CH_2Cl_2 (32 mL, 0.5 M) at 0 °C was added $NaHCO_3$ (131.0 mg, 1.56 mmol). The resultant white cloudy suspension was stirred at 0 °C for 15 min before a solution of *Z*-allylic alcohol **108** (740.3 mg, 1.56 mmol, 1.0 equiv) in anhydrous CH_2Cl_2 (23 mL, 0.068 M) was slowly added. The colorless mixture was stirred at 0 °C for 3 h. The yellow cloudy mixture was quenched with saturated aqueous $NaHCO_3$ (35 mL). The aqueous layer was extracted with CH_2Cl_2 (3×50 mL). The combined organic layers were washed with brine, dried over anhydrous Na_2SO_4, and concentrated *in vacuo*. The crude residue was purified by column chromatography (1−10% EtOAc/CH_2Cl_2) to give epoxy alcohols **116a** and **116b**.

Epoxy alcohol 116a: Colorless oil (137.7 mg, 18%): $R_f = 0.57$ (2% EtOAc/CH_2Cl_2); $[\alpha]_D^{25} = -36.08$ (*c* 1.00, CHCl_3); ^{1}H NMR (300 MHz, CDCl_3) δ 7.68 (t, $J = 7.2$ Hz, 4H), 7.51–7.30 (m, 6H), 7.11 (d, $J = 8.7$ Hz, 2H), 6.83 (d, $J = 8.7$ Hz, 2H), 4.27 (s, 2H), 3.78 (s, 3H), 3.74–3.62 (m, 2H), 3.48 (t, $J = 9.3$ Hz, 1H), 3.36 (dd, $J = 9.0, 4.5$ Hz, 1H), 3.15 (dt, $J = 8.4, 4.3$ Hz, 1H), 3.07 (dd, $J = 8.4, 4.3$ Hz, 1H), 3.02 (dd, $J = 11.7, 8.5$ Hz, 1H), 2.89 (brs, 1H), 1.07 (s, 9H); ^{13}C NMR (75 MHz, CDCl_3) δ 159.7, 136.1, 135.9, 133.9,

133.1, 129.9, 129.8, 128.7, 127.7, 127.6, 144.1, 73.5, 71.1, 70.4, 60.6, 59.9, 55.7, 55.3, 27.0, 19.4; IR (thin film): 3447, 2932, 1514, 1249, 1111, 703 cm⁻¹; HRMS (ESI) *m/z* calcd for $C_{29}H_{36}NaO_5Si$ (M+Na)⁺ 515.2230, found 515.2215.

Epoxy alcohol 116b: Colorless oil (382.6 mg, 50%): R_f = 0.38 (2% EtOAc/CH₂Cl₂); $[\alpha]_D^{25}$ = −17.57 (*c* 1.00, CHCl₃); ¹H NMR (300 MHz, CDCl₃) δ 7.69 (d, *J* = 6.9 Hz, 4H), 7.47–7.30 (m, 6H), 7.18 (d, *J* = 8.4 Hz, 2H), 6.85 (d, *J* = 8.4 Hz, 2H), 4.38 (s, 2H), 3.81 (s, 3H), 3.53–3.42 (m, 3H), 3.20 (dd, *J* = 12.0, 6.3 Hz, 1H), 3.15–3.04 (m, 2H), 1.04 (s, 9H); ¹³C NMR (75 MHz, CDCl₃) δ 159.2, 139.5, 133.4, 133.2, 130.0, 129.9, 129.5, 127.8, 127.7, 113.8, 73.1, 72.5, 69.7, 60.5, 57.1, 57.0, 55.3, 26.9, 19.3; IR (thin film): 3423, 2932, 2857, 1514, 1248, 1112 cm⁻¹; HRMS (ESI) *m/z* calcd for $C_{29}H_{36}NaO_5Si$ (M+Na)⁺ 515.2230, found 515.2229.

117
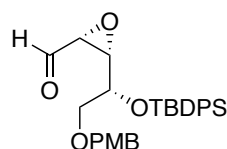
Epoxy aldehyde 117: Epoxy aldehyde **117** was prepared from epoxy alcohol **116b** (1.79 g, 3.65 mmol, 1.0 equiv) using a general procedure for IBX oxidation. The crude residue was purified by column chromatography (10–15% EtOAc/hexanes) to yield epoxy aldehyde **117** as a colorless oil (1.41 g, 78%): R_f = 0.64 (5% EtOAc/hexanes); ¹H NMR (300 MHz, CDCl₃) δ 9.32 (d, *J* = 4.6 Hz, 1H), δ 7.67–7.61 (m, 4H), 7.43–7.25 (m, 6H), 7.06 (d, *J* = 7.8 Hz, 2H), 6.82 (d, *J* = 7.5 Hz, 2H), 4.29–4.03 (m, 4H), 3.79 (s, 3H), 3.47–3.30 (m, 4H), 1.06 (s, 9H); ¹³C NMR (75 MHz, CDCl₃) δ 198.1, 159.2, 135.9, 133.4, 132.4, 130.1, 129.3, 127.8, 113.7, 72.9, 71.6, 68.5, 60.4, 57.6, 55.3, 29.7, 26.9, 19.2. The epoxy aldehyde **117** was immediately carried to the next step.
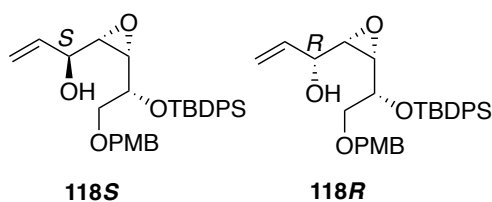
118*S*   **118*R***

Allylic alcohols 118*S* **and 118***R*: To a solution of epoxy aldehyde **117** (1.13 g, 2.31 mmol, 1.0 equiv) in anhydrous THF (6 mL, 0.4 M) at 0 °C was added vinylmagnesium chloride (1.0 M in THF, 2.77 mL, 2.77 mmol, 1.2 equiv). The reaction was then stirred at 0 °C for 10 min before being quenched with saturated aqueous NH$_4$Cl (5 mL). The organic layer was separated and the aqueous layer was extracted with CH$_2$Cl$_2$ (3×5 mL). The combined organic layers were washed with brine, dried over anhydrous Na$_2$SO$_4$ and concentrated *in vacuo*. The crude residue was purified by column chromatography (1−10% EtOAc/CH$_2$Cl$_2$) to give allylic alcohols **118***S* (419.3 mg, 35%) and **118***R* (467.2 mg, 39%). The absolute configuration was determined by Mosher's method using the corresponding (*S*)-MTPA and (*R*)-MTPA esters.

Allylic alcohol 118*S*: Colorless oil; R_f = 0.62 (20% EtOAc/hexanes); $[\alpha]_D^{25}$ = –8.56 (*c* 1.00, CHCl$_3$); ^{1}H NMR (300 MHz, CDCl$_3$) δ 7.81–7.61 (m, 4H), 7.52–7.32 (m, 6H), 7.16 (d, *J* = 8.6 Hz, 1H), 6.83 (d, *J* = 8.6 Hz, 1H), 5.97 (ddd, *J* = 16.4, 10.6, 5.7 Hz, 1H), 5.32 (dt, *J* = 16.4, 1.5 Hz, 1H), 5.19 (dd, *J* = 10.6, 1.2 Hz, 1H), 4.51–4.42 (m, 1H), 4.39 (d, *J* = 11.6 Hz, 1H), 4.32 (d, *J* = 11.6 Hz, 1H), 4.25–4.15 (m, 1H), 3.77 (s, 3H), 3.47–3.32 (m, 3H), 3.02–2.85 (m, 2H), 1.06 (s, 3H); ^{13}C NMR (75 MHz, CDCl$_3$) δ 159.5, 137.9, 136.2, 135.9, 133.8, 132.8, 130.1, 129.9, 129.8, 129.3, 127.8, 127.7, 116.2, 113.9, 73.2, 71.3, 69.8, 69.5, 59.2, 57.3, 55.3, 26.9, 19.4.
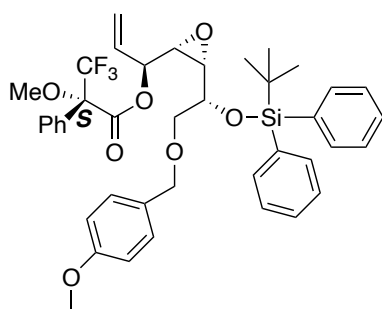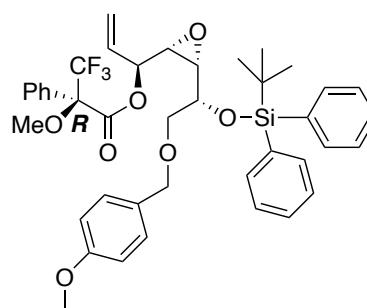
(*S*)-MTPA ester of 118*S*   **(*R*)-MTPA ester of 118***S*

(*S*)-MTPA ester of allylic alcohol 118*S*: ^{1}H NMR (300 MHz, CDCl$_3$) δ 7.76–7.62 (m, 4H), 7.53–7.44 (m, 2H), 7.44–7.32 (m, 9H), 7.01 (d, *J* = 8.6 Hz, 1H), 6.79 (d, *J* = 8.6 Hz, 1H), 5.64 (ddd, *J* = 16.4, 10.6, 5.7 Hz, 1H), 5.15 (d, *J* = 9.6 Hz, 1H), 4.99 (d, *J* = 16.2 Hz, 1H), 4.19 (d, *J* = 11.6 Hz, 1H), 4.13 (d, *J* = 11.6 Hz, 1H), 4.04 (dd, *J* = 10.5, 5.3 Hz, 1H), 3.80 (s, 3H), 3.49 (s, 3H), 3.39 (t, *J* = 4.4 Hz, 1H), 3.21 (dd, *J* = 5.8, 3.4 Hz, 1H), 3.11 (dd, *J* = 5.3, 3.4 Hz, 1H), 1.06 (s, 9H).

(*R*)-MTPA ester of allylic alcohol 118*S*: ^{1}H NMR (300 MHz, CDCl$_3$) δ 7.76–7.62 (m, 4H), 7.53–7.447 (m, 2H), 7.47–7.29 (m, 9H), 7.00 (d, *J* = 8.6 Hz, 1H), 6.79 (d, *J* = 8.6 Hz, 1H), 5.76 (ddd, *J* = 16.4, 10.6, 5.7 Hz, 1H), 5.62 (t, *J* = 5.7 Hz, 1H), 5.20 (d, *J* = 10.5 Hz, 1H), 5.08 (d, *J* = 10.5 Hz, 1H), 4.12 (d, *J* = 11.6 Hz, 1H), 4.06 (d, *J* = 11.6 Hz, 1H), 4.03 (dd, *J* = 10.5, 5.3 Hz, 1H), 3.79 (s, 3H), 3.49 (s, 3H), 3.28 (d, *J* = 5.0 Hz, 1H), 3.16 (dd, *J* = 5.8, 3.4 Hz, 1H), 3.04 (dd, *J* = 5.3, 3.4 Hz, 1H), 1.06 (s, 9H).

Table 9 Δδ (δ$_S$– δ$_R$) data for (*S*)- and (*R*)-MTPA esters of allylic alcohol **118*S***

position	δ$_{S\text{-ester}}$ (ppm)	δ$_{R\text{-ester}}$ (ppm)	Δδ (δ$_S$– δ$_R$) (ppm)
6	4.19	4.12	+0.07
	4.13	4.06	+0.07
9	3.21	3.16	+0.05
10	3.11	3.04	+0.07
12	5.64	5.76	-0.12
13	4.99	5.08	-0.09
	5.15	5.20	-0.05

Allylic alcohol 118*R*: Colorless oil; R_f = 0.48 (60% EtOAc/hexanes); [α]$_D^{24}$ = +22.16 (*c* 1.00, CHCl$_3$); ^{1}H NMR (300 MHz, CDCl$_3$) δ 7.73–7.62 (m, 4H), 7.46–7.27 (m, 6H), 7.09 (d, *J* = 8.6 Hz, 1H), 6.82 (d, *J* = 8.6 Hz, 1H), 5.66 (ddd, *J* = 16.4, 10.7, 4.9 Hz, 1H), 5.21 (dt, *J* = 17.3, 1.3 Hz, 1H), 5.05 (dd, *J* = 10.6, 1.0 Hz, 1H), 4.28 (d, *J* = 11.5 Hz, 1H), 4.24 (d, *J* = 11.5 Hz, 1H), 3.95 (dt, *J* = 6.7, 4.6 Hz, 1H), 3.84–3.76 (m, 1H), 3.77 (s, 3H), 3.55–3.40 (m, 2H), 3.25 (dd, *J* = 6.9, 3.9 Hz, 1H), 2.88 (dd, *J* = 6.9, 4.1 Hz, 1H), 2.22 (brs, 1H), 1.04 (s, 3H); ^{13}C NMR (75 MHz, CDCl$_3$) δ 159.2, 136.3, 136.1, 135.9, 133.7, 133.3, 130.3, 129.9, 129.8, 129.3, 127.7, 127.6, 72.9, 72.6, 69.4, 69.3, 59.9, 58.4, 55.3, 27.1, 27.0, 19.4.

(S)-MTPA ester of 118R   **(R)-MTPA ester of 118R**

(S)-MTPA ester of allylic alcohol 118R: ^{1}H NMR (300 MHz, CDCl$_3$) δ 7.75–7.64 (m, 4H), 7.45–7.36 (m, 11H), 7.06 (d, J = 8.5 Hz, 1H), 6.81 (d, J = 8.5 Hz, 1H), 5.74 (ddd, J = 17.1, 10.8, 6.0 Hz, 1H), 5.51–5.46 (m, 1H), 5.29 (d, J = 17.1 Hz, 1H), 5.16 (d, J = 10.6 Hz, 1H), 4.21 (d, J = 11.8 Hz, 1H), 4.16 (d, J = 11.8 Hz, 1H), 4.05 (dd, J = 10.3, 5.2 Hz, 1H), 3.90 (t, J = 4.7 Hz, 1H), 3.80 (s, 3H), 3.52 (s, 3H), 3.47–3.36 (m, 2H), 3.26 (dd, J = 5.6, 4.2 Hz, 1H),   3.11 (dd, J = 8.5, 4.1 Hz, 1H), 1.06 (s, 9H).

(R)-MTPA ester of allylic alcohol 118R: ^{1}H NMR (300 MHz, CDCl$_3$) δ 7.71–7.66 (m, 4H), 7.44–7.36 (m, 11H), 7.07 (d, J = 8.6 Hz, 1H), 6.81 (d, J = 8.6 Hz, 1H), 5.65 (ddd, J = 17.1, 10.8, 5.7 Hz, 1H), 5.52 (dd, J = 8.7, 5.7 Hz, 1H), 5.17–5.13 (m, 1H), 5.08 (d, J = 10.8 Hz, 1H), 4.21 (d, J = 11.8 Hz, 1H), 4.17 (d, J = 11.8 Hz, 1H), 4.08 (dd, J = 9.9, 4.8 Hz, 1H), 3.94 (s, 3H), 3.80 (s, 3H), 3.48–3.35 (m, 2H), 3.30 (dd, J = 5.7, 4.2 Hz, 1H), 3.14 (dd, J = 8.7, 4.2 Hz, 1H), 1.05 (s, 9H).
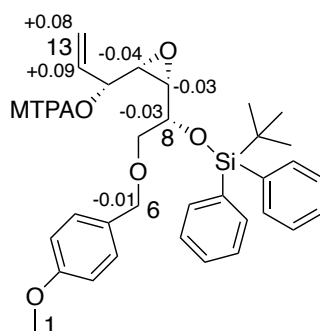
Table 10 Δδ ($δ_S$– $δ_R$) data for (S)- and (R)-MTPA esters of allylic alcohol **118R**

position	$δ_{S\text{-ester}}$ (ppm)	$δ_{R\text{-ester}}$ (ppm)	Δδ ($δ_S$– $δ_R$) (ppm)
6	4.16	4.17	-0.01
8	4.05	4.08	-0.03
9	3.11	3.14	-0.03
10	3.26	3.30	-0.04
12	5.16	5.08	+0.08
13	5.74	5.65	+0.09

119
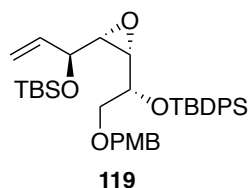
Silyl ether 119: Silyl ether **119** was prepared from alcohol **118***S* (411.1 mg, 0.79 mmol) using the general procedure for TBS protection. The crude residue was purified by column chromatography (5% EtOAc/hexanes) to give silyl ether **119** (501.5 mg, 84%) as a colorless oil: R_f = 0.54 (10% EtOAc/hexanes); $[\alpha]_D^{22}$ = –17.12 (*c* 1.00, CHCl$_3$); ^{1}H NMR (300 MHz, CDCl$_3$) δ 7.78 (dd, *J* = 6.7, 1.2 Hz, 4H), δ 7.49–7.45 (m, 2H), 7.42–7.37 (m, 4H), 7.13 (d, *J* = 8.5 Hz, 2H), 6.87 (d, *J* = 8.5 Hz, 2H), 5.77–5.65 (m, 1H), 5.00 (d, *J* = 10.3 Hz, 1H), 4.90 (d, *J* = 17.2 Hz, 1H), 4.34–4.29 (m, 4H), 3.85 (s, 9H), 3.57–3.56 (m, 2H), 3.22 (dd, *J* = 6.5, 3.9 Hz, 1H), 3.21–3.01 (m, 1H), 1.13 (s, 9H), 0.88 (s, 9H), 0.02 (s, 3H), 0.00 (s, 3H); ^{13}C NMR (75 MHz, CDCl$_3$) δ 159.1, 137.9, 136.2, 136.0, 134.4, 133.7, 130.6, 129.7, 129.6, 129.4, 127.6, 127.5, 166.7, 113.6, 72.9, 72.8, 71.1, 69.2, 59.5, 57.7, 55.3, 27.1, 25.9, 19.5, 18.2, –4.1, –4.5.

163
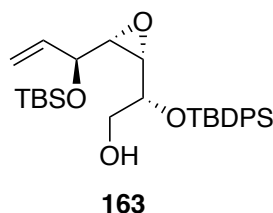
Alcohol 163: Alcohol **163** was prepared from PMB ether **119** (328.2 mg, 0.52 mmol) using a general procedure for PMB deprotection. The crude residue was purified by column chromatography (50% CH$_2$Cl$_2$/EtOAc) to yield alcohol **163** as a light yellow oil (245.8 mg, 93%): R_f = 0.42 (10% EtOAc/hexanes); $[\alpha]_D^{24}$ = –43.80 (*c* 1.00, CHCl$_3$); ^{1}H NMR (300 MHz, CDCl$_3$) δ 7.77–7.72 (m, 4H), 7.47–7.43 (m, 6H), 5.62–5.50 (m, 1H), 4.95 (d, *J* = 10.3 Hz, 2H), 4.87 (d, *J* = 17.2 Hz, 1H), 4.26–4.19 (m, 2H), 3.70 (d, *J* = 4.3 Hz, 2H), 3.19 (dd, *J* = 6.3, 3.9 Hz, 1H), 2.97–2.94 (m, 1H), 2.05 (brs, 1H), 1.12 (s, 9H), 0.83 (s, 9H), 0.03 (s, 3H), 0.05 (s, 3H); ^{13}C NMR (75 MHz, CDCl$_3$) δ 137.5, 136.0, 135.7, 133.7, 133.3, 130.1, 128.0, 127.9, 117.0, 71.4, 69.3, 65.5, 59.3, 58.4, 27.0, 25.9, 19.4, 18.2, –4.2, –4.5.

121
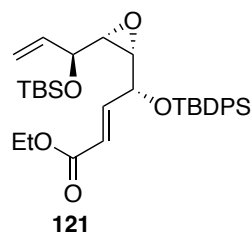
Ester 121: Alcohol **163** (138.1 mg, 0.27 mmol) was first transformed to aldehyde intermediate **120** using a general procedure for DMP oxidation. The crude residue was purified by column chromatography (7% EtOAc/hexanes) to yield aldehyde **120** as a colorless oil (130.6 mg, 95%): R_f = 0.61 (10% EtOAc/hexanes) as a colorless oil, which was immediately converted to ester **121** using a general procedure for Wittig olefination. The crude residue was purified by column chromatography (2% EtOAc/hexanes) to yield ester **120** as a colorless oil (255.4 mg, 93%): R_f = 0.38 (5% EtOAc/hexanes); $[\alpha]_D^{22}$ = −1.68 (*c* 1.00, CHCl$_3$); ^{1}H NMR (300 MHz, CDCl$_3$) δ 7.72–7.62 (m, 4H), 7.46–7.34 (m, 6H), 6.83 (dd, *J* = 15.7, 6.8 Hz, 1H), 5.69 (d, *J* = 15.7 Hz, 1H), 5.48–5.41 (m, 1H), 5.24 (dd, *J* = 17.0, 1.1 Hz, 1H), 4.96 (dd, *J* = 10.4, 1.7 Hz, 1H), 4.82–4.24 (m, 1H), 4.16 (q, *J* = 7.1 Hz, 2H), 3.79–3.76 (m, 1H), 3.12 (dd, *J* = 5.8, 4.1 Hz, 1H), 2.85 (dd, *J* = 7.9, 4.0 Hz, 1H), 1.27 (t, *J* = 7.1 Hz, 3H), 1.08 (s, 9H), 0.86 (s, 9H), 0.05 (s, 3H), 0.05 (s, 3H), −0.06 (s, 3H); ^{13}C NMR (75 MHz, CDCl$_3$) δ 165.8, 145.7, 136.1, 136.0, 133.0, 132.7, 130.3, 130.1, 127.9, 122.9, 115.7, 71.6, 70.5, 61.1, 60.5, 59.2, 27.1, 25.9, 19.4, 18.4, 14.3, −4.5, −4.8.

122
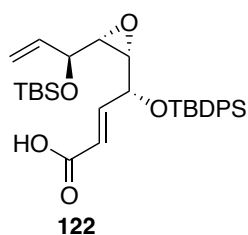
Carboxylic acid 122: Carboxylic acid **122** was prepared from ester **29** (290.8 mg, 0.49 mmol) using a general procedure for ester hydrolysis. The crude residue was purified by column chromatography (30% EtOAc/hexanes−100% EtOAc) to give carboxylic acid **122** as a colorless oil (214.5 mg, 78%): R_f = 0.44 (30% EtOAc/hexanes); $[\alpha]_D^{22}$ = −5.98 (*c* 1.00, CHCl$_3$); ^{1}H NMR (300 MHz, CDCl$_3$) δ 7.75–7.65 (m, 4H), 7.47–7.37 (m, 6H), 7.06 (dd, *J* = 15.7, 5.3 Hz, 1H), 5.96 (d, *J* = 15.7 Hz, 1H), 5.56–5.44 (m, 1H), 4.87 (d, *J* = 10.3 Hz, 1H), 4.81 (d, *J* = 4.6 Hz, 1H), 4.81–4.77 (m, 1H), 4.23 (dd, *J* = 7.1, 3.8 Hz, 1H), 3.08 (dd, *J* = 5.7, 3.8 Hz, 1H), 2.94–2.91 (m, 1H), 1.10 (s, 9H), 0.81

(s, 9H), –0.05 (s, 6H); ^{13}C NMR (75 MHz, CDCl$_3$) δ 171.5, 149.6, 137.5, 136.0, 135.9, 133.3, 132.9, 130.2, 130.1, 127.9, 121.1, 117.1, 71.3, 68.8, 59.8, 59.1, 27.0, 25.9, 19.5, 18.2, –4.2, –4.4.

123
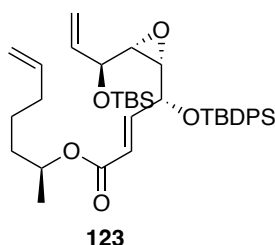
Ester 123: To a solution of carboxylic acid **122** (85.3 mg, 0.15 mmol, 1.0 equiv) in anhydrous toluene (960 μL, 0.16 M) at room temperature was added triethylamine (65 μL, 0.46 mmol, 3.0 equiv) and 2,4,6-trichlorobenzoyl chloride (36 μL, 0.23 mmol, 1.5 equiv). The reaction mixture was then stirred at room temperature for 1.5 h. After that, a solution of (*S*)-hept-6-en-2-ol (**24**) (18 mg, 0.15 mmol, 1.0 equiv) in anhydrous toluene (730 μL, 0.21 M) and DMAP (23.4 mg, 0.18 mmol, 1.2 equiv) were added and the reaction mixture was further stirred for 10 min. The resulting white cloudy solution was then quenched with saturated NaHCO$_3$ (2 mL). The aqueous layer was extracted with EtOAc (3×3 mL). The combined organic layers were washed with brine, dried over anhydrous Na$_2$SO$_4$, and concentrated *in vacuo*. The crude residue was purified by column chromatography (2% EtOAc/hexanes) to give ester **123** (67.7 mg, 71%) as a light yellow oil: R_f = 0.76 (10% EtOAc/hexanes); ^{1}H NMR (300 MHz, CDCl$_3$) δ 7.73– 7.63 (m, 4H), 7.45–7.36 (m, 6H), 6.87 (dd, J = 15.8, 5.8 Hz, 1H), 5.84–5.72 (m, 2H), 5.61–5.49 (m, 1H), 4.72–4.69 (m, 1H), 4.24–4.20 (m, 1H), 3.07–3.04 (m, 1H), 2.92– 2.89 (m, 1H), 2.10–2.03 (m, 2H), 1.65–1.39 (m, 4H), 1.26–1.21 (m, 1H), 1.07 (s, 9H), 1.07 (s, 9H), 0.80 (s, 9H), –0.05 (s, 6H); ^{13}C NMR (75 MHz, CDCl$_3$) δ 165.7, 146.1, 138.6, 137.7, 136.0, 133.4, 133.1, 130.1, 127.8, 122.7, 116.9, 114.9, 71.1, 70.9, 69.2, 59.9, 59.2, 35.5, 33.6, 27.0, 25.9, 24.7, 20.1, 19.5, 18.2, –4.2, –4.4.
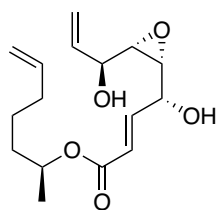
124

Diol 124: To a solution of silyl ether **123** (50.1 mg, 0.07 mmol, 1.0 equiv) in anhydrous THF (1 mL, 0.07 M) at 0 °C was added TBAF (1.0 M solution in THF, 465 µL, 6.0 equiv). The stirred reaction was then heated to 60 °C. After maintaining reaction temperature at 60 °C for 8 h, the reaction was cooled to room temperature, and quenched with saturated aqueous NH$_4$Cl (1 mL). The organic layer was separated and the aqueous layer was extracted with EtOAc (4×3 mL). The combined organic phases were washed with brine, dried over anhydrous Na$_2$SO$_4$ and concentrated *in vacuo*. The crude residue was purified by column chromatography (30% EtOAc/hexanes) to give diol **124** as colorless oil: R_f = 0.56 (40% EtOAc/hexanes); ^{1}H NMR (300 MHz, CDCl$_3$) δ 7.02 (dd, J = 15.8, 4.5 Hz, 1H), 6.15 (dd, J = 15.8, 1.6 Hz, 1H), 6.07–5.96 (m, 1H), 5.81–5.69 (m, 1H), 5.41 (d, J = 17.3 Hz, 1H), 5.29 (d, J = 10.5 Hz, 1H), 5.02–4.92 (m, 2H), 4.30–4.25 (m, 1H), 4.13–4.09 (m, 1H), 3.06–3.00 (m, 2H), 2.08–2.01 (m, 2H), 1.66–1.50 (m, 2H), 1.48–1.34 (m, 2H), 1.23 (d, J = 6.2 Hz, 3H); ^{13}C NMR (75 MHz, CDCl$_3$) δ 166.2, 145.7, 138.5, 137.0, 122.5, 117.4, 114.9, 71.6, 71.0, 69.2, 58.4, 58.0, 35.4, 33.5, 24.7, 20.0.
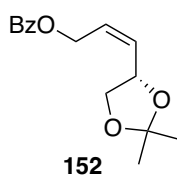
152

(*S,Z*)-3-(2,2-Dimethyl-1,3-dioxolan-4-yl)allyl benzoate (152): Benzoate ester **152** was prepared from the known allylic alcohol **151** (5.87 g, 37.1 mmol) using the general procedure for benzoate ester protection. The crude residue was purified by column chromatography (10−20% EtOAc/hexanes) to yield benzoate ester **152** as a colorless oil (8.66 g, 89%): R_f = 0.57 (20% EtOAc/hexanes); $[\alpha]_D^{26}$ = −18.19 (*c* 1.00, CHCl$_3$); ^{1}H NMR (300 MHz, CDCl$_3$) δ 8.06–7.99 (m, 2H), 7.54 (t, J = 7.5 Hz, 1H), 7.47–7.37 (m, 2H), 5.86 (dt, J = 10.2, 6.9 Hz, 1H), 5.75–5.65 (m, 1H), 4.99–4.84 (m, 3H), 4.13 (dd, J = 8.1, 6.2 Hz, 1H), 3.65–3.52 (m, 1H), 1.43 (s, 1H), 1.39 (s, 1H); ^{13}C NMR (75

MHz, CDCl$_3$) δ 166.3, 133.1, 132.4, 130.1, 129.7, 128.5, 127.4, 109.7, 72.0, 69.5, 60.6, 26.7, 25.9; IR (thin film): 2986, 2930, 1721, 1452, 1271, 1061 cm^{-1}; HRMS (ESI) *m/z* calcd for C$_{15}$H$_{18}$NaO$_4$ (M+Na)$^+$ 285.1103, found 285.1059.
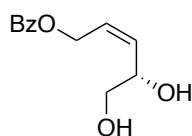
153

(***S*,*Z***)-4,5-Dihydroxypent-2-en-1-yl benzoate (153)**: To a solution of acetonide **152** (8.60 g, 32.8 mmol, 1.0 equiv) in acetonitrile:H$_2$O (5:1, 480 mL, 0.068 M) at 0 °C was slowly added 2M HCl (40 mL). After stirring from 0 °C to room temperature for 3 h, the reaction mixture was quenched with saturated aqueous NaHCO$_3$ (80 mL). The aqueous phase was extracted with EtOAc (4×100 mL). The combined organic layers were washed with brine, dried over anhydrous Na$_2$SO$_4$, and concentrated *in vacuo*. The crude residue was purified by column chromatography (50–80% EtOAc/hexanes) to give diol **153** as a colorless oil (5.97 g, 82%): R_f = 0.21 (50% EtOAc/hexanes); [α]$_D^{27}$ = +27.32 (*c* 1.00, CHCl$_3$); ^{1}H NMR (300 MHz, CDCl$_3$) δ 8.06–7.95 (m, 2H), 7.52 (t, *J* = 7.5 Hz, 1H), 7.45–7.34 (m, 2H), 5.81–5.63 (m, 2H), 5.03 (dd, *J* = 12.9, 6.9 Hz, 1H), 4.85 (dd, *J* = 12.9, 6.0 Hz, 1H), 4.69 (dt, *J* = 10.8, 3.9 Hz, 1H), 4.17 (brs, 1H), 3.82 (brs, 1H), 3.71–3.47 (m, 2H); ^{13}C NMR (75 MHz, CDCl$_3$) δ 166.8, 133.2, 133.1, 129.9, 129.7, 128.5, 126.9, 68.8, 66.2, 61.1; IR (thin film): 3385, 2931, 1718, 1451, 1274, 1070 cm^{-1}; HRMS (ESI) *m/z* calcd for C$_{12}$H$_{14}$NaO$_4$ (M+Na)$^+$ 245.0709, found 245.0761.
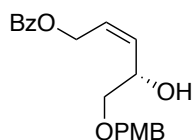
134

(***S*,*Z***)-4-Hydroxy-5-((4-methoxybenzyl)oxy)pent-2-en-1-yl benzoate (134)**: To a solution of diol **153** (5.01 g, 22.5 mmol, 1.0 equiv) in methanol (132 mL, 0.17 M) at room temperature was added dibutyltin oxide (6.73 g, 27.1 mmol, 1.2 equiv). The reaction mixture was then heated to 80 °C and stirred for 3 h before being cooled to room temperature. After that, the solvent was evaporated and co-evaporated with

toluene (3×100 mL) under reduced pressure. The resulting crude residue was redissolved in anhydrous DMF (56 mL, 0.4 M) at room temperature and *p*-methoxybenzyl chloride (3.3 mL, 24.8 mmol, 1.1 equiv) and tetrabutylammonium bromide (TBAB, 5.81 g, 17.9 mmol, 0.8 equiv) were added. The mixture was then heated to 65 °C and stirred for 2 h before being cooled to room temperature. The solvent was evaporated by co-evaporation with toluene (200 mL) under reduced pressure. The crude was diluted with EtOAc (100 mL) and washed with 2M HCl (2×30 mL) and H_2O (50 mL), dried over anhydrous Na_2SO_4 and concentrated *in vacuo*. The crude residue was purified by column chromatography (10–30% EtOAc/hexanes) to give PMB ether **134** as a light yellow oil (5.48 g, 71%): R_f = 0.21 (20% EtOAc/hexanes); $[\alpha]_D^{25}$ = +13.88 (*c* 1.00, $CHCl_3$); ^1H NMR (300 MHz, $CDCl_3$) δ 8.09–7.99 (m, 2H), 7.55 (t, *J* = 7.5 Hz, 1H), 7.49–7.37 (m, 2H), 7.25 (d, *J* = 8.7 Hz, 2H), 6.87 (d, *J* = 8.7 Hz, 2H), 5.79 (dt, *J* = 11.1, 7.2 Hz, 1H), 5.74–5.63 (m, 1H), 4.99 (dd, *J* = 12.9, 6.9 Hz, 1H), 4.87 (dd, *J* = 12.9, 6.3 Hz, 1H), 4.75 (dt, *J* = 11.4, 3.9 Hz, 1H), 4.50 (s, 2H), 3.78 (s, 2H), 3.52–3.38 (m, 2H); ^{13}C NMR (75 MHz, $CDCl_3$) δ 166.5, 159.5, 133.1 , 130.2, 130.0, 129.7, 129.5, 128.4, 127.1, 114.0, 73.5, 73.2, 67.2, 61.1, 55.3; IR (thin film): 3422, 2859, 1717, 1272, 1109, 710 cm^{-1}; HRMS (ESI) *m/z* calcd for $C_{20}H_{22}NaO_5$ (M+Na)$^+$ 365.1365, found 365.1307.
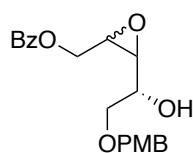
136

Epoxy alcohol 136 (Method III): To a solution of *Z*-allylic alcohol **134** (4.27 g, 12.5 mmol, 1.0 equiv) in CH_2Cl_2 (156 mL, 0.08 M) at room temperature was added 3-chloroperbenzoic acid (70–75%, 5.54 g, 22.5 mmol, 1.8 equiv) and the mixture was stirred at room temperature overnight. The white cloudy solution was then quenched with saturated aqueous $NaHCO_3$ (80 mL). The aqueous layer was extracted with CH_2Cl_2 (3×70 mL). The combined organic layers were washed with brine, dried over anhydrous Na_2SO_4, and concentrated *in vacuo*. The crude residue was purified by column chromatography (10−20% EtOAc/hexanes) to yield inseparable diastereomeric mixture of epoxide **136** as a colorless oil (3.48 g, 78%): R_f = 0.10 (20% EtOAc/hexanes); $[\alpha]_D^{25}$ = +17.22 (*c* 1.00, $CHCl_3$); ^1H NMR (300 MHz, $CDCl_3$) δ 8.06

(d, J = 7.2 Hz, 2H), 7.60–7.55 (m, 1H), 7.49–7.39 (m, 1H), 7.25 (d, J = 8.7 Hz, 2H), 6.87 (d, J = 8.7 Hz, 2H), 4.61 (dd, J = 12.6, 3.6 Hz, 1H), 4.50 (s, 2H), 4.38 (dd, J = 12.6, 7.2 Hz, 1H), 3.88–3.76 (m, 1H), 3.79 (s, 3H), 3.57 (d, J = 5.4 Hz, 2H), 3.41 (dt, J = 7.5, 4.2 Hz, 1H), 3.16 (dd, J = 6.6, 4.2 Hz, 1H); ^{13}C NMR (75 MHz, CDCl$_3$) δ 166.4, 159.5, 133.3, 129.9, 129.8, 129.5, 128.5, 114.1, 73.4, 71.2, 68.9, 63.4, 57.7, 55.4, 54.4; IR (thin film): 3447, 2932, 2857, 1722, 1513, 1110 cm^{-1}; HRMS (ESI) m/z calcd for C$_{20}$H$_{22}$KO$_6$ (M+K)$^+$ 397.1053, found 397.1053. This mixture was further elaborated to epoxy alcohols **116a** and **116b** by a 2-step transformation.

164
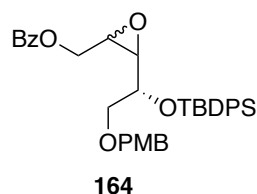
Silyl ether 164: Silyl ether **164** was prepared from epoxy alcohol **136** (2.74 g, 7.65 mmol, 1.0 equiv) using a general procedure for TBDPS protection. The crude residue was purified by column chromatography (100% hexanes–5% EtOAc/hexanes) to yield inseparable diastereomeric mixture of silyl ether **164** as a light yellow oil (3.92 g, 86%): R_f = 0.33 (5% EtOAc/hexanes); $[\alpha]_D^{25}$ = +11.46 (c 1.00, CHCl$_3$); ^{1}H NMR (300 MHz, CDCl$_3$) δ 8.01 (d, J = 7.2 Hz, 2H), 7.81–7.63 (m, 4H), 7.59–7.49 (m, 1H), 7.48–7.29 (m, 8H), 7.11 (d, J = 8.4 Hz, 2H), 6.82 (d, J = 8.4 Hz, 2H), 4.41 (dd, J = 12.3, 2.7 Hz, 1H), 4.27 (s, 2H), 3.89–3.73 (m, 1H), 3.76 (s, 3H), 3.69 (dt, J = 9.9, 5.1 Hz, 1H), 3.49–3.32 (m, 3H), 3.27 (dd, J = 8.19, 4.5 Hz, 1H), 1.09 (s, 9H) ; ^{13}C NMR (75 MHz, CDCl$_3$) δ 166.3, 159.3, 136.1, 136.0, 133.9, 133.2, 133.1, 129.9, 129.8, 129.7, 129.3, 128.4, 127.7, 127.6, 113.9, 73.1, 71.5, 71.3, 64.2, 59.1, 55.3, 54.5, 27.0, 19.5; IR (thin film): 2932, 2857, 1722, 1270, 1110, 708 cm^{-1}; HRMS (ESI) m/z calcd for C$_{36}$H$_{41}$O$_6$Si (M+H)$^+$ 597.2672, found 597.2675. Silyl ether **164** (4.97 g, 8.33 mmol, 1.0 equiv) was then transformed to epoxy alcohols **116a** and **116b** using the general procedure for methanolysis. The crude residue was purified by column chromatography (1−10% EtOAc/CH$_2$Cl$_2$) to give separable epoxy alcohols **116a** (3.04 g, 74%): R_f = 0.57 (2% EtOAc/ CH$_2$Cl$_2$) and **116b** (205.1 mg, 5%): R_f = 0.38 (2% EtOAc/ CH$_2$Cl$_2$) as colorless oils.
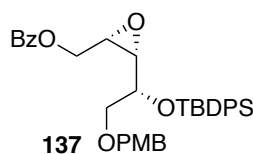
((2S,3S)-3-((R)-1-((tert-Butyldiphenylsilyl)oxy)-2-((4-methoxybenzyl)oxy)ethyl) oxiran-2-yl)methyl benzoate (137). Benzoate ester **137** was prepared from epoxy alcohol **116b** (387.6 mg, 0.79 mmol) using a general procedure for benzoate ester protection. The crude residue was purified by column chromatography (2–5% EtOAc/hexanes) to give benzoate ester **137** as a colorless oil (394.4 mg, 84%): R_f = 0.63 (5% EtOAc/hexanes); $[\alpha]_D^{24}$ = −29.38 (c 1.00, CHCl$_3$); ^{1}H NMR (300 MHz, CDCl$_3$) δ 7.98 (d, J = 7.7 Hz, 2H), 7.70 (d, J = 6.8 Hz, 4H), 7.53 (t, J = 7.2 Hz, 2H), 7.48−7.29 (m, 8H), 7.16 (d, J = 8.3 Hz, 2H), 6.84 (d, J = 8.3 Hz, 2H), 4.36 (s, 2H), 4.22−4.10 (m, 1H), 3.94−3.69 (m, 2H), 3.79 (s, 3H), 3.62−3.51 (m, 2H), 3.34−3.20 (m, 2H), 1.06 (s, 9H); ^{13}C NMR (75 MHz, CDCl$_3$) δ 166.2, 159.2, 136.1, 136.0, 133.4, 133.1, 130.3, 130.1, 129.9, 129.8, 129.4, 128.4, 127.9, 127.7, 113.8, 73.1, 72.7, 69.8, 63.3, 56.6, 55.4, 54.4, 27.0, 19.4; IR (thin film): 2932, 1723, 1513, 1270, 1111, 708 cm^{-1}; HRMS (ESI) m/z calcd for C$_{36}$H$_{40}$NaO$_6$Si (M+Na)$^+$ 619.2492, found 619.2481.
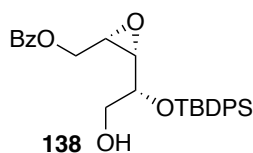
((2S,3S)-3-((R)-1-((tert-Butyldiphenylsilyl)oxy)-2-((4-methoxybenzyl)oxy)ethyl) oxiran-2-yl)methyl benzoate (138). Alcohol **138** was prepared from PMB ether **137** (340.2 mg, 0.57 mmol) using a general procedure for PMB deprotection. The crude residue was purified by column chromatography (10–20% EtOAc/hexanes) to give alcohol **138** (209.2 mg, 77%) as a colorless oil: R_f = 0.53 (20% EtOAc/hexanes); $[\alpha]_D^{24}$ = −23.26 (c 1.00, CHCl$_3$); ^{1}H NMR (300 MHz, CDCl$_3$) δ 8.01−7.91 (m, 2H), 7.79−7.64 (m, 4H), 7.58−7.51 (m, 1H), 7.51−7.35 (m, 8H), 3.92 (dd, J = 12.4, 2.9 Hz, 1H), 3.81−3.74 (m, 2H), 3.73−3.60 (m, 2H), 3.26 (dd, J = 7.6, 4.2 Hz, 1H), 3.18 (dt, J = 9.9, 4.2 Hz, 1H), 1.09 (s, 9H); ^{13}C NMR (75 MHz, CDCl$_3$) δ 166.2, 135.9, 135.7, 132.2, 132.8, 130.4, 129.8, 129.7, 128.5, 128.2, 128.1, 70.1, 65.5, 63.0, 56.7, 54.4, 27.0, 19.4;

IR (thin film): 3448, 2931, 1722, 1271, 1111, 704 cm^{-1}; HRMS (ESI) m/z calcd for C$_{28}$H$_{32}$NaO$_5$Si (M+Na)$^+$ 499.1917, found 499.1919.
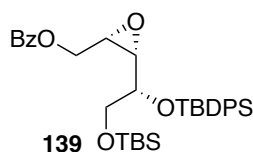
139 OTBS

((2S,3S)-3-((R)-2,2,8,8,9,9-Hexamethyl-3,3-diphenyl-4,7-dioxa-3,8-disiladecan-5-yl)oxiran-2-yl)methyl benzoate (139). Silyl ether **139** was prepared from alcohol **138** (210.9 mg, 0.44 mmol) using a general procedure for TBS protection. The crude residue was purified by column chromatography (2–5% EtOAc/hexanes) to give silyl ether **139** as a colorless oil (209.1 mg, 80%): R_f= 0.80 (5% EtOAc/hexanes); [α]$_D^{25}$ = −19.08 (c 1.00, CHCl$_3$); ^{1}H NMR (300 MHz, CDCl$_3$) δ 8.06−7.99 (m, 2H), 7.83−7.74 (m, 4H), 7.61−7.53 (m, 1H), 7.51−7.36 (m, 8H), 4.16 (dd, J = 12.5, 2.5 Hz, 1H), 3.89 (dd, J = 12.5, 7.6 Hz, 1H), 3.77−3.68 (m, 1H), 3.73 (s, 3H), 3.33−3.20 (m, 2H), 1.10 (s, 9H), 0.92 (s, 9H), 0.06 (s, 3H), 0.03 (s, 3H); ^{13}C NMR (75 MHz, CDCl$_3$) δ 166.2, 136.1, 133.5, 133.4, 133.1, 130.1, 130.0, 129.8, 128.4, 127.9, 127.8, 70.9, 65.9, 63.5, 56.6, 54.5, 27.0, 26.0, 19.4, 18.5, −5.3, −5.4; IR (thin film): 2930, 1724, 1270, 1111, 708 cm^{-1}; HRMS (ESI) m/z calcd for C$_{34}$H$_{46}$NaO$_5$Si$_2$ (M+Na)$^+$ 613.2781, found 613.2762.

140 OTBS
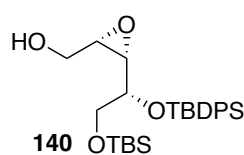
((2S,3S)-3-((R)-2,2,8,8,9,9-Hexamethyl-3,3-diphenyl-4,7-dioxa-3,8-disiladecan-5-yl)oxiran-2-yl)methanol (140). Epoxy alcohol **140** was prepared from benzoate ester **139** (167.0 mg, 0.28 mmol) using a general procedure for methanolysis. The crude residue was purified by column chromatography (10–20% EtOAc/hexanes) to give epoxy alcohol **140** (108.8 mg, 79%) as a colorless oil: R_f= 0.67 (20% EtOAc/hexanes); [α]$_D^{25}$ = −25.33 (c 1.08, CHCl$_3$); ^{1}H NMR (300 MHz, CDCl$_3$) δ 7.71–7.67 (m, 4H), 7.42–7.34 (m, 6H), 3.66–3.64 (m, 3H), 3.32 (dd, J = 12.3, 4.0 Hz, 1H), 3.25–3.18 (m, 1H), 3.16 (dd, J = 5.9, 4.0 Hz, 1H), 3.03 (dt, J = 6.9, 4.0 Hz, 1H), 1.86 (brs, 1H) 1.08 (s, 9H), 0.92 (s, 9H), 0.08 (s, 3H), 0.05 (s, 3H); ^{13}C NMR (75 MHz, CDCl$_3$) δ 136.0,

135.9, 133.6, 133.3, 130.1, 130.0, 127.8, 127.7, 71.0, 66.1, 60.6, 57.3, 57.2, 26.9, 26.0, 19.4, 18.5, −5.35, −5.45; IR (thin film): 3421, 2930, 2857, 1270, 1104, 774 cm^{-1}; HRMS (ESI) m/z calcd for C$_{27}$H$_{42}$NaO$_4$Si$_2$ (M+Na)$^+$ 509.2519, found 509.2523.
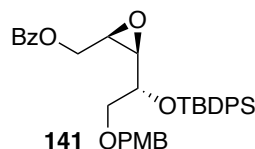
((2R,3R)-3-((R)-1-((*tert*-Butyldiphenylsilyl)oxy)-2-((4-methoxybenzyl)oxy)ethyl) oxiran-2-yl)methyl benzoate (141). Benzoate ester **141** was prepared from epoxy alcohol **116a** (250.1 mg, 0.51 mmol) using a general procedure for benzoate ester protection. The crude residue was purified by column chromatography (2–5% EtOAc/hexanes) to give benzoate ester **141** as a colorless oil (224.2 mg, 74%): R_f= 0.60 (5% EtOAc/hexanes); [α]$_D^{25}$ = −1.38 (*c* 1.00, CHCl$_3$); ^{1}H NMR (300 MHz, CDCl$_3$) δ 8.22 (d, *J* = 7.7 Hz, 2H), 7.98−7.88 (m, 4H), 7.74 (t, *J* = 7.2 Hz, 2H), 7.67−7.49 (m, 8H), 7.32 (d, *J* = 8.3 Hz, 2H), 7.02 (d, *J* = 8.3 Hz, 2H), 4.64 (dd, *J* = 12.4, 2.2 Hz, 1H), 4.48 (s, 2H), 4.04 (dd, *J* = 12.4, 7.8 Hz, 1H), 3.97 (s, 3H), 3.95−3.85 (m, 1H), 3.75−3.53 (m, 3H), 3.49 (dd, *J* = 8.2, 4.5 Hz, 1H), 1.31 (s, 9H); ^{13}C NMR (75 MHz, CDCl$_3$) δ 166.2, 159.2, 136.1, 135.9, 133.8, 133.1, 129.9, 129.8, 129.7, 129.3, 128.4, 127.7, 127.6, 113.8, 73.0, 71.4, 71.3, 64.1, 59.1, 55.3, 54.5, 27.0, 19.5; IR (thin film): 2932, 1718, 1508, 1270, 1110, 772 cm^{-1}; HRMS (ESI) m/z calcd for C$_{36}$H$_{40}$NaO$_6$Si (M+Na)$^+$ 619.2492, found 619.2472.
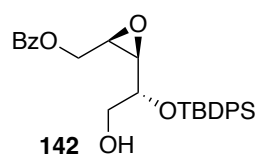
((2R,3R)-3-((R)-1-((*tert*-Butyldiphenylsilyl)oxy)-2-hydroxyethyl)oxiran-2-yl) methyl benzoate (142). Alcohol **142** was prepared from PMB ether **S5** (164.4 mg, 0.28 mmol) using a general procedure for PMB deprotection. The crude residue was purified by column chromatography (10–20% EtOAc/hexanes) to give alcohol **141** (105.0 mg, 80%) as a colorless oil: R_f= 0.50 (20% EtOAc/hexanes); [α]$_D^{25}$ = −3.02 (*c* 1.00, CHCl$_3$); ^{1}H NMR (300 MHz, CDCl$_3$) δ 8.05−7.94 (m, 2H), 7.79−7.65 (m, 4H), 7.60−7.49 (m, 1H), 7.47−7.29 (m, 8H), 4.28 (dd, *J* = 12.1, 3.5 Hz, 1H), 3.93 (dd, *J* = 12.1, 6.7 Hz,

1H), 3.69−3.53 (m, 3H), 3.40−3.26 (m, 2H), 1.11 (s, 9H); ^{13}C NMR (75 MHz, CDCl$_3$) δ 166.3, 136.1, 135.9, 133.5, 133.4, 132.9, 130.1, 130.0, 129.8, 129.5, 128.5, 127.9, 127.7, 72.8, 64.6, 63.4, 58.2, 54.2, 27.0, 19.5; IR (thin film): 3613, 1717, 1270, 1111, 772 cm^{-1}; HRMS (ESI) m/z calcd for C$_{34}$H$_{46}$NaO$_5$Si$_2$ (M+Na)$^+$ 499.1917, found 499.1928.
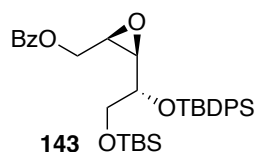
((2R,3R)-3-((R)-2,2,8,8,9,9-Hexamethyl-3,3-diphenyl-4,7-dioxa-3,8-disiladecan-5-yl)oxiran-2-yl)methyl benzoate (143). Silyl ether **143** was prepared from alcohol **142** (120.3 mg, 0.25 mmol) using a general procedure for TBS protection. The crude residue was purified by column chromatography (2–5% EtOAc/hexanes) to give silyl ether **143** (122.3 mg, 82%) as a colorless oil: R_f = 0.83 (5% EtOAc/hexanes); [α]$_D^{25}$ = +7.94 (c 1.00, CHCl$_3$); ^{1}H NMR (300 MHz, CDCl$_3$) δ 8.15−8.03 (m, 2H), 7.92−7.68 (m, 4H), 7.62−7.53 (m, 1H), 7.53−7.34 (m, 8H), 4.59 (dd, J = 12.5, 2.1 Hz, 1H), 3.78 (dd, J = 12.5, 8.3 Hz, 1H), 3.68−3.47 (m, 3H), 3.46−3.36 (m, 1H), 3.32−3.25 (m, 1H), 1.13 (s, 9H), 0.84 (s, 9H), −0.03 (s, 3H), −0.04 (s, 3H); ^{13}C NMR (75 MHz, CDCl$_3$) δ 166.3, 136.1, 136.0, 134.0, 133.3, 133.2, 129.9, 129.8, 128.5, 127.7, 127.6, 72.9, 65.1, 64.5, 59.2, 54.7, 27.1, 26.1, 19.5, 18.5, −5.4, −5.5; IR (thin film): 2932, 2857, 1724, 1513, 1270, 1109, 709 cm^{-1}; HRMS (ESI) m/z calcd for C$_{34}$H$_{46}$NaO$_5$Si$_2$ (M+Na)$^+$ 613.2781, found 613.2772.
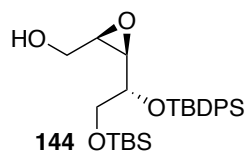
((2R,3R)-3-((R)-2,2,8,8,9,9-Hexamethyl-3,3-diphenyl-4,7-dioxa-3,8-disiladecan-5-yl)oxiran-2-yl)methanol (144). Epoxy alcohol **144** was prepared from benzoate ester **143** (60.2 mg, 0.10 mmol) using a general procedure for methanolysis. The crude residue was purified by column chromatography (10–20% EtOAc/hexanes) to give epoxy alcohol **144** (40.2 mg, 80%) as a colorless oil: R_f = 0.80 (20% EtOAc/hexanes); [α]$_D^{25}$ = −17.66 (c 2.31, CHCl$_3$); ^{1}H NMR (300 MHz, CDCl$_3$) δ 7.71–7.67 (m, 4H), 7.42–7.34 (m, 6H), 3.71–3.49 (m, 4H), 3.28–3.17 (m, 2H), 3.10 (dd, J = 7.9, 3.8 Hz,

1H), 2.74 (brs, 1H), 1.09 (s, 9H), 0.80 (s, 9H), –0.02, –0.05; ^{13}C NMR (75 MHz, CDCl$_3$) δ 136.2, 136.0, 134.0, 133.3, 130.0, 127.8, 127.6, 72.0, 65.5, 61.0, 59.9, 56.1, 27.0, 26.0, 19.5, 18.6, –5.49, –5.58; IR (thin film): 3447, 2931, 2857, 1723, 1258, 1104, 775 cm^{-1}; HRMS (ESI) *m/z* calcd for C$_{27}$H$_{42}$NaO$_4$Si$_2$ (M+Na)$^+$ 509.2519, found 509.2526.

107
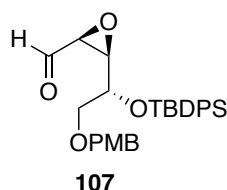
(2*S*,3*R*)-3-((*R*)-1-((*tert*-Butyldiphenylsilyl)oxy)-2-((4-methoxybenzyl)oxy) ethyl)oxirane-2-carbaldehyde (107): Epoxy aldehyde **107** was prepared from epoxy alcohol **116a** (2.71 g, 5.50 mmol) using a general procedure for IBX oxidation. The crude residue was purified by column chromatography (5−10% EtOAc/hexanes) to yield epoxy aldehyde **107** (2.41 g, 81%): R_f = 0.47 (20% EtOAc/hexanes); [α]$_D^{24}$ = –67.58 (*c* 1.00, CHCl$_3$); ^{1}H NMR (300 MHz, CDCl$_3$) δ 8.90 (d, *J* = 5.7 Hz, 1H), 7.76– 7.66 (m, 4H), 7.49–7.34 (m, 3H), 7.06 (d, *J* = 8.4 Hz, 1H), 6.83 (d, *J* = 8.4 Hz, 1H), 4.22 (d, *J* = 11.8 Hz, 1H), 4.17 (d, *J* = 11.8 Hz, 1H), 3.98–3.80 (m, 1H), 3.81 (s, 3H), 3.47–3.41 (m, 1H), 3.41–3.32 (m, 2H), 3.28 (dd, *J* = 9.6, 4.5 Hz, 1H), 1.10 (s, 9H) ; ^{13}C NMR (75 MHz, CDCl$_3$) δ 196.8, 159.4, 136.1, 136.0, 133.6, 132.9, 130.1, 130.0, 129.8, 127.7, 129.4, 127.8, 113.9, 72.9, 70.6, 70.5, 61.5, 58.2, 55.4, 27.0, 19.5; IR (thin film): 2932, 2857, 1722, 1513, 1248, 1111 cm^{-1}; HRMS (ESI) *m/z* calcd for C$_{29}$H$_{34}$NaO$_5$Si (M+Na)$^+$ 513.2073, found 513.2069.
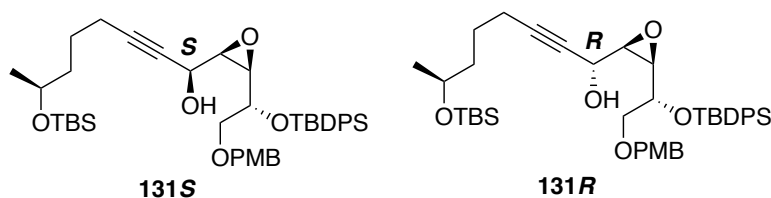
131*S*   **131*R***

Propargylic alcohols 131*S* and 131*R*: To a solution of (*S*)-*tert*-butyl(hept-6-yn-2-yloxy)dimethylsilane (**132,** 2.10 g, 9.27 mmol, 2.0 equiv) (prepared from (*S*)-propylene oxide in 5 steps using a protocol previously described by Thiraporn et al in 2022) in anhydrous THF (20 mL, 0.23 M) at –78 °C was added *n*-butyllithium (*ca*. 1.6 M

solution in hexanes, 12 mL, 9.27 mmol, 2.0 equiv) dropwise. The mixture was then stirred at –78 °C for 1 h before a solution of epoxy aldehyde **107** (2.27g, 4.64 mmol, 1.0 equiv) in anhydrous THF (9 mL, 0.5 M) at –78 °C was added. The reaction mixture was further stirred from –78 °C to 0 °C for 1.5 h. The white cloudy mixture was quenched with saturated aqueous NH_4Cl (10 mL). The aqueous layer was extracted with EtOAc (2 × 10 mL). The combined organic layers were washed with brine, dried over anhydrous Na_2SO_4, and concentrated *in vacuo*. The crude residue was purified by column chromatography (10−20% EtOAc/hexanes) to give the separable propargylic alcohols **131***S* and **131***R*. The absolute configuration was determined by Mosher's method using the corresponding (*S*)-MTPA and (*R*)-MTPA esters.

Propargylic alcohol 131*S*: Colorless oil (0.69 g, 21%): R_f = 0.50 (20% EtOAc/hexanes); $[\alpha]_D^{24}$ = –23.56 (*c* 1.00, $CHCl_3$); ^{1}H NMR (300 MHz, $CDCl_3$) δ 7.75−7.62 (m, 4H), 7.47−7.28 (m, 6H), 7.13 (d, *J* = 8.6 Hz, 1H), 6.83 (d, *J* = 8.6 Hz, 1H), 4.38−4.25 (m, 2H), 4.08−3.99 (m, 1H), 3.96 (dt, *J* = 8.2, 6.0 Hz, 1H), 3.79 (s, 3H), 3.76−3.69 (m, 1H), 3.51−3.36 (m, 2H), 3.25 (dd, *J* = 8.2, 4.3 Hz, 1H), 3.17 (dd, *J* = 6.2, 4.3 Hz, 1H), 2.31 (d, *J* = 3.9 Hz, 1H), 2.10−1.92 (m, 2H), 1.56−1.32 (m, 4H), 1.07 (s, 12H), 0.86 (s, 9H), 0.02 (s, 3H), 0.01 (s, 3H); ^{13}C NMR (75 MHz, $CDCl_3$) δ 159.4, 136.3, 136.1, 134.2, 133.5, 130.0, 129.9, 129.8, 129.4, 127.63, 127.60, 113.9, 87.8, 73.1, 71.7, 71.0, 68.3, 61.1, 60.2, 59.7, 55.4, 38.9, 27.1, 26.0, 24.8, 23.9, 19.5, 18.9, 18.2, −4.2, −4.6; IR (thin film): 3427, 2932, 2857, 1727, 1248, 1111 cm^{-1}; HRMS (ESI) *m/z* calcd for $C_{42}H_{60}NaO_6Si_2$ (M+Na)$^+$ 739.3826, found 739.3837.
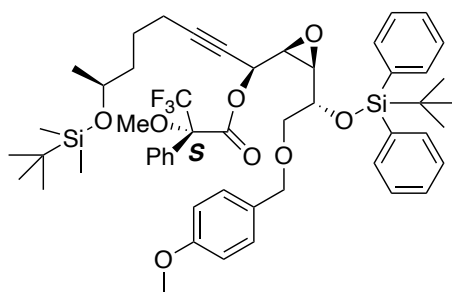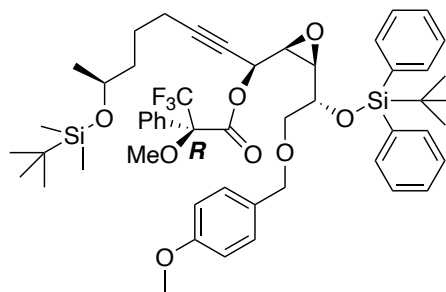
(*S*)-MTPA ester of 113*S***   **(*R*)-MTPA ester of 113***S*

(*S*)-MTPA ester of propargylic alcohol 131*S*: ^{1}H NMR (300 MHz, $CDCl_3$) δ 7.76−7.64 (m, 4H), 7.46−7.36 (m, 6H), 7.37−7.28 (m, 5H), 7.14 (d, *J* = 8.6 Hz, 2H),

6.84 (d, J = 8.6 Hz, 2H), 4.98 (d, J = 8.8 Hz, 1H), 4.35 (s, 2H), 3.81 (s, 3H), 3.78−3.68 (m, 2H), 3.59 (s, 3H), 3.44 (d, J = 4.7 Hz, 2H), 3.38 (dd, J = 8.2, 4.3 Hz, 1H), 3.33 (dd, J = 8.8, 4.3 Hz, 1H), 2.05 (t, J = 5.6Hz, 1H), 1.45−1.32 (m, 4H), 1.09 (s, 12H), 0.87 (s, 9H), 0.02 (s, 3H), 0.01 (s, 3H).

 (***R***)-**MTPA ester of propargylic alcohol 131*S***: ^{1}H NMR (300 MHz, CDCl₃) δ 7.76−7.65 (m, 4H), 7.46−7.32 (m, 11H), 7.13 (d, J = 8.6 Hz, 2H), 6.83 (d, J = 8.6 Hz, 2H), 5.11 (d, J = 8.7 Hz, 1H), 4.33 (s, 2H), 3.80 (s, 3H), 3.86−3.77 (m, 1H), 3.77−3.69 (m, 1H), 3.58 (s, 3H), 3.47−3.40 (m, 2H), 3.35 (dd, J = 8.1, 4.4 Hz, 1H), 3.29 (dd, J = 8.7, 4.4 Hz, 1H), 2.08 (t, J = 6.6 Hz, 1H), 1.49−1.33 (m, 6H), 1.10 (s, 12H), 0.86 (s, 9H), 0.03 (s, 3H), 0.01 (s, 3H).
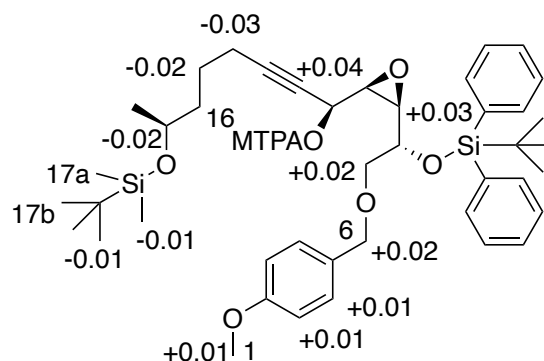
Table 11 Δδ (δ_S– δ_R) data for (*S*)- and (*R*)-MTPA esters of propargylic alcohol **131*S***

position	$\delta_{S\text{-ester}}$ (ppm)	$\delta_{R\text{-ester}}$ (ppm)	Δδ (δ_S– δ_R) (ppm)
1	3.81	3.80	+0.01
3	7.14	7.13	+0.01
4	6.84	6.83	+0.01
6	4.35	4.33	+0.02
7	3.44	3.42	+0.02
9	3.38	3.35	+0.03
10	3.33	3.29	+0.04
14	2.05	2.08	-0.03
15	1.38	1.40	-0.02
17	3.73	3.75	-0.02
17a	1.09	1.10	-0.01
17b	0.02	0.03	-0.01

Propargylic alcohol 131*R*: Colorless oil (1.85 g, 56%): R_f = 0.57 (20% EtOAc/hexanes); $[\alpha]_D^{24}$ = +35.41 (*c* 1.00, CHCl₃); ^{1}H NMR (300 MHz, CDCl₃) δ 7.73–

7.59 (m, 4H), 7.48–7.29 (m, 6H), 7.10 (d, J = 7.3 Hz, 1H), 6.83 (d, J = 7.3 Hz, 1H), 4.33–4.18 (m, 2H), 3.80 (s, 3H), 3.84–3.74 (m, 1H), 3.70–3.55 (m, 2H), 3.47 (t, J = 9.2 Hz, 1H), 3.34 (dd, J = 8.9, 4.2 Hz, 1H), 3.16, (dd, J = 8.6, 4.1 Hz, 1H), 3.08 (dd, J = 8.6, 4.1 Hz, 1H), 2.30–2.11 (m, 2H), 1.67–1.46 (m, 4H), 1.14 (d, J = 6.1 Hz, 1H), 1.08 (s, 9H), 0.90 (s, 9H), 0.06 (s, 6H); ^{13}C NMR (125 MHz, CDCl$_3$) δ 159.8, 136.2, 136.1, 136.0, 133.7, 132.9, 130.1, 130.0, 128.2, 127.8, 127.7, 114.2, 86.6, 73.5, 70.8, 70.2, 68.4, 61.3, 60.3, 59.3, 55.4, 38.9, 27.0, 26.1, 26.0, 24.9, 24.0, 19.4, 19.1, 18.3, −4.3, −4.6; IR (thin film): 3421, 2931, 2857, 1515, 1252, 1111 cm^{-1}; HRMS (ESI) m/z calcd for C$_{42}$H$_{60}$NaO$_6$Si$_2$ (M+H)$^+$ 717.4007, found 717.4006.
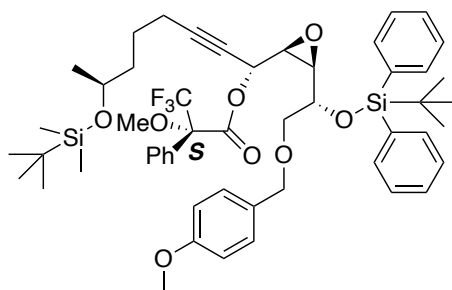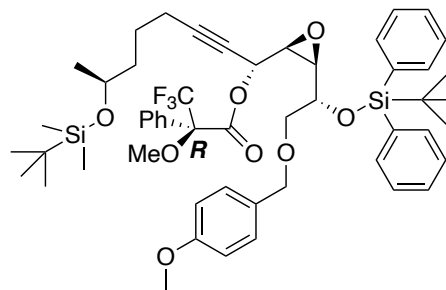
(S)-MTPA ester of 113R   **(R)-MTPA ester of 113R**

(S)-MTPA ester of propargylic alcohol 131R: ^{1}H NMR (300 MHz, CDCl$_3$) δ 7.74−7.62 (m, 4H), 7.44−7.41 (m, 5H), 7.40−7.24 (m, 6H), 7.12 (d, J = 8.6 Hz, 2H), 6.84 (d, J = 8.6 Hz, 2H), 5.07 (d, J = 5.9 Hz, 1H), 4.24−4.12 (m, 2H), 3.81 (s, 3H), 3.78−3.72 (m, 2H), 3.51 (s, 3H), 3.30 (dd, J = 8.3, 4.0 Hz, 1H), 3.24−3.12 (m, 2H), 3.07 (dd, J = 10.1, 4.0 Hz, 1H), 2.15−1.98 (m, 2H), 1.48−1.38 (m, 4H), 1.10 (d, J = 5.9 Hz, 1H), 1.08 (s, 9H), 0.89 (s, 9H), 0.05 (s, 3H), 0.04 (s, 3H).

(R)-MTPA ester of propargylic alcohol 131R: ^{1}H NMR (300 MHz, CDCl$_3$) δ 7.74−7.65 (m, 4H), 7.46−7.40 (m, 5H), 7.39−7.31 (m, 6H), 7.10 (d, J = 8.6 Hz, 2H), 6.83 (d, J = 8.6 Hz, 2H), 5.22 (d, J = 5.5Hz, 1H), 4.26 (d, J = 11.8 Hz, 1H), 4.18 (d, J = 11.8 Hz, 1H), 3.89 (dt, J = 7.9, 5.0 Hz, 1H), 3.81 (s, 3H), 3.79−3.71 (m, 1H), 3.41 (s, 3H), 3.32 (dd, J = 7.6, 4.2 Hz, 1H), 3.26 (t, J = 5.3 Hz, 2H), 3.18 (dd, J = 10.1, 4.2 Hz, 1H), 2.05 (t, J = 5.7 Hz, 2H), 1.47−1.38 (m, 4H), 1.10 (d, J = 6.1 Hz, 1H), 1.08 (s, 9H), 0.88 (s, 9H), 0.05 (s, 3H), 0.04 (s, 3H).

Table 12 Δδ (δ_S– δ_R) data for (S)- and (R)-MTPA esters of propargylic alcohol **131R**

position	$\delta_{S\text{-ester}}$ (ppm)	$\delta_{R\text{-ester}}$ (ppm)	Δδ (δ_S– δ_R) (ppm)
1	4.18	4.21	-0.03
6	3.18	3.26	-0.08
7	3.76	3.77	-0.01
9	3.29	3.32	-0.03
10	3.07	3.18	-0.11
14	2.07	2.05	+0.02
15	1.43	1.42	+0.01

Mitsunobu inversion (conversion of 131R to 131S): To a suspension of triphenylphosphine (2.31 g, 8.79 mmol, 14.0 equiv) in anhydrous toluene (6 mL) at 0 °C was added diethyl azodicarboxylate (3.45 mL, *ca*. 2 M in solution toluene, 6.91 mmol, 11.0 equiv). The mixture was then stirred at 0 °C for 1 h. After that, the mixture was added a solution of **131R** (450.7 mg, 0.62 mmol, 1.0 equiv) in anhydrous toluene (3 mL), followed by acetic acid (500 μL, 8.79 mmol, 14.0 equiv) at 0 °C. The reaction mixture was further stirred from 0 °C to room temperature for 1.5 h before being quenched with H_2O (5 mL). The aqueous layer was extracted with EtOAc (3 × 10 mL). The combined organic layers were washed with brine, dried over anhydrous Na_2SO_4 and concentrated *in vacuo*. The crude residue was purified by column chromatography (100% hexanes–5% EtOAc/hexanes) to afford acetate ester intermediate as a colorless oil (395.9 mg, 83%, R_f = 0.40 (5% EtOAc/hexanes)). Methanolysis of the acetate ester intermediate (395.9 mg, 0.52 mmol, 1.0 equiv) was later performed by using the general procedure for methanolysis. The crude residue was purified by column chromatography (10−20% EtOAc/CH_2Cl_2) to give the desired propargylic alcohol antipode **131S** (350.5 mg, 94%).

145

Z-Allylic alcohol 145: To a solution of propargylic alcohol **131***S* (620.7 mg, 0.87 mmol, 1.0 equiv) in EtOAc (8.7 mL, 0.1 M) at room temperature was added 5% Pd/CaCO$_3$ (276.3 mg, 0.13 mmol, 0.15 equiv), followed by quinoline (205 µL, 1.73 mmol, 2.0 equiv). The reaction mixture was stirred under H$_2$ atmosphere for 1.5 h. The mixture was then filtered through a pad of Celite and washed with EtOAc. The filtrate was washed with 50 mL of 1 M HCl (100 mL). The organic layer was separated and concentrated *in vacuo*. The crude residue was purified by column chromatography (10−20% EtOAc/hexanes) to yield allylic alcohol **145** as a colorless oil (554.0 mg, 89%): R_f = 0.45 (20% EtOAc/hexanes); $[\alpha]_D^{24}$ = –8.08 (*c* 1.00, CHCl$_3$); ^{1}H NMR (300 MHz, CDCl$_3$) δ 7.84–7.763 (m, 4H), 7.52–7.30 (m, 6H), 7.15 (d, *J* = 8.4 Hz, 2H), 6.85 (d, *J* = 8.4 Hz, 2H), 5.39 (dt, *J* = 10.8, 7.1 Hz, 1H), 5.34–5.17 (m, 1H), 4.35 (m, 2H), 3.97 (dd, *J* = 8.6, 6.0 Hz, 1H), 3.85–3.72 (m, 1H), 3.82 (s, 3H), 3.88–3.78 (m, 1H), 3.40 (d, *J* = 5.1 Hz, 2H), 3.26 (dd, *J* = 8.4, 4.5 Hz, 1H), 3.06–2.92 (m, 1H), 1.91 (brs, 1H), 1.84–1.59 (m, 2H), 1.41–1.22 (m, 4H), 1.17–0.98 (m, 12H), 0.91 (s, 9H), 0.06 (s, 3H), 0.05 (s, 3H); ^{13}C NMR (75 MHz, CDCl$_3$) δ 159.4, 136.2, 136.1, 134.4, 134.2, 133.6, 130.1, 129.8, 129.7, 129.4, 127.6, 127.5, 127.4, 113.8, 73.2, 71.9, 71.2, 68.6, 65.6, 60.3, 60.1, 55.4, 39.4, 27.8, 27.1, 26.0, 25.7, 25.7, 19.5, 18.2, –4.2, –4.6; IR (thin film): 3421, 2931, 2857, 1515, 1249, 1112 cm^{-1}; HRMS (ESI) *m/z* calcd for C$_{42}$H$_{62}$NaO$_6$Si$_2$ (M+Na)$^+$ 741.3983, found 741.3984.
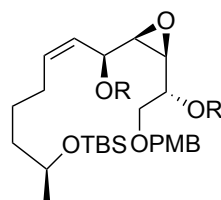
165 R = TBDPS

TBDPS ether 165: Silyl ether **165** was prepared from allylic alcohol **145** (550.8 mg, 0.77 mmol) using a general procedure for TBDPS protection. The crude residue was purified by column chromatography (2−10% EtOAc/hexanes) to yield TBDPS ether

165 as a colorless oil (645.4 mg, 88%): R_f = 0.73 (5% EtOAc/hexanes); $[\alpha]_D^{25}$ = –8.56 (*c* 1.00, CHCl$_3$); ^{1}H NMR (300 MHz, CDCl$_3$) δ 7.69 (d, *J* = 7.2 Hz, 2H) 7.67–7.56 (m, 6H), 7.43–7.25 (m, 6H), 7.24–7.12 (m, 6H), 7.02 (d, *J* = 8.7 Hz, 2H), 6.80 (d, *J* = 8.7 Hz, 2H), 5.31–5.19 (m, 1H), 4.98 (dt, *J* = 11.1, 7.2 Hz, 1H), 4.23 (d, *J* = 11.4 Hz, 1H), 4.16 (d, *J* = 11.4 Hz, 1H), 4.02–3.91 (m, 1H), 3.80 (s, 3H), 3.57–3.46 (m, 1H), 3.36–3.26 (m, 2H), 3.26–3.07 (m, 3H), 1.74–1.57 (m, 1H), 1.08 (s, 9H), 1.036 (s, 9H), 0.98 (d, *J* = 6.1 Hz, 3H), 0.88 (s, 9H), 0.82–0.72 (m, 4H), 0.66–0.52 (m, 1H), 0.02 (s, 3H), 0.00 (s, 3H); ^{13}C NMR (75 MHz, CDCl$_3$) δ 159.2, 136.3, 136.2, 136.15, 136.11, 134.4, 134.2, 133.7, 133.2, 130.4, 129.7,129.6, 129.5, 129.4, 129.3, 127.6, 127.4, 126.8, 113.7, 73.1, 72.4, 72.3, 69.5, 68.7, 61.3, 58.5, 55.4, 39.5, 27.2, 27.0, 26.1, 25.4, 24.0, 19.6, 18.2, –4.3, –4.5`; IR (thin film): 2932, 2858, 1699, 1427, 1112, 1066 cm^{-1}; HRMS (ESI) *m/z* calcd for C$_{58}$H$_{81}$O$_6$Si$_3$ (M+H)$^+$ 979.5160, found 979.5166.
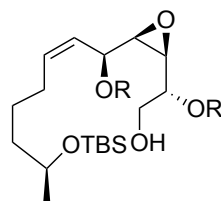
146 R = TBDPS

Alcohol 146: Alcohol **146** was prepared from PMB ether **165** (682.2 mg, 0.71 mmol) using a general procedure for PMB deprotection. The crude residue was purified by column chromatography (5−15% EtOAc/hexanes) to yield alcohol **146** as a light yellow oil (507.1 mg, 85%): R_f = 0.47 (5% EtOAc/hexanes); $[\alpha]_D^{24}$ = –16.60 (*c* 1.00, CHCl$_3$); ^{1}H NMR (300 MHz, CDCl$_3$) δ 7.79–7.57 (m, 8H), 7.47–7.35 (m, 4H), 7.33–7.17 (m, 8H), 5.45–5.31 (m, 1H), 5.23–5.10 (m, 1H), 4.06–3.94 (m, 1H), 3.65–3.48 (m, 1H), 3.40–3.20 (m, 5H), 1.40–1.27 (m, 2H), 1.14 (s, 9H), 1.05 (s, 9H), 1.03 (d, *J* = 6.1 Hz, 3H), 0.98–0.94 (m, 2H), 0.90 (s, 9H), 0.87–0.78 (m, 2H), 0.05 (s, 3H), 0.02 (s, 3H); ^{13}C NMR (75 MHz, CDCl$_3$) δ 136.2, 135.9, 134.0, 133.7, 133.6, 133.2, 133.1, 130.0, 129.7, 129.6, 127.9, 127.7, 127.6, 127.4, 126.9, 73.6, 69.4, 68.6, 64.7, 61.1, 58.2, 39.4, 27.3, 27.2, 27.0, 26.0, 25.3, 23.9, 19.5, 19.4, 18.2, –4.3, –4.6; IR (thin film): 3609, 2931, 2857, 1277, 1112 cm^{-1}; HRMS (ESI) *m/z* calcd for C$_{50}$H$_{75}$NaO$_5$Si$_3$ (M+Na)$^+$ 859.4585, found 859.4576.
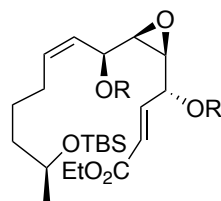
147 R = TBDPS

Ester 147: Alcohol **146** (350.1 mg, 0.42 mmol) was first transformed to aldehyde intermediate using a general procedure for DMP oxidation. The crude residue was purified by column chromatography (5−10% EtOAc/hexanes) to furnish the corresponding aldehyde intermediate as a colorless oil (328.3 mg, 94%) which was immediately subjected to Wittig olefination using a general procedure for Wittig olefination. The crude residue was purified by column chromatography (2−5% EtOAc/hexanes) to yield α,β-unsaturated ester **147** as a colorless oil (316.7 mg, 89%): R_f = 0.54 (5% EtOAc/hexanes); $[\alpha]_D^{25}$ = +25.40 (*c* 1.00, CHCl$_3$); ^{1}H NMR (500 MHz, CDCl$_3$) δ 7.71 (d, *J* = 7.0 Hz, 2H), 7.57 (d, *J* = 7.0 Hz, 4H), 7.52 (d, *J* = 7.5 Hz, 4H), 7.41 (t, *J* = 7.0 Hz, 1H), 7.37–7.25 (m, 5H), 7.21 (t, *J* = 7.0 Hz, 2H), 7.16 (t, *J* = 7.5 Hz, 2H), 7.09 (t, *J* = 7.5 Hz, 2H), 6.47 (dd, *J* = 15.5, 3.5 Hz, 1H), 6.03 (dd, *J* = 15.5, 1.0 Hz, 1H), 5.37 (t, *J* = 10.5 Hz, 1H), 5.24–5.16 (m, 1H), 4.15–4.03 (m, 2H), 3.97 (t, *J* = 8.0 Hz, 1H), 3.87–3.80 (m, 1H), 3.54–3.46 (m, 1H), 3.22 (dd, *J* = 8.0, 4.5 Hz, 1H), 3.03 (dd, *J* = 7.5, 4.5 Hz, 1H) 1.22 (t, *J* = 7.1 Hz, 3H), 1.10 (s, 9H), 1.08–1.02 (m, 2H), 1.00 (s, 9H), 0.97 (d, *J* = 5.6 Hz, 1H), 0.89–0.80 (m, 4H), 0.86 (s, 9H), –0.00 (s, 3H), –0.02 (s, 3H) ; ^{13}C NMR (125 MHz, CDCl$_3$) δ 166.1, 145.1, 136.2, 136.1, 136.0, 133.8, 133.6, 133.4, 133.2, 133.1, 130.0, 129.9, 129.7, 129.6, 127.7, 127.6, 127.5, 127.4, 126.7, 122.4, 72.0, 69.1, 68.6, 60.7, 60.4, 59.9, 39.4, 27.5, 27.2, 27.0, 26.0, 25.3, 23.9, 19.5, 19.4, 18.2, 14.3, –4.3, –4.6; IR (thin film): 2957, 2931, 2857, 1723, 1112, 1065 cm^{-1}; HRMS (ESI) *m/z* calcd for C$_{54}$H$_{76}$NaO$_6$Si$_3$ (M+Na)$^+$ 927.4847, found 927.4838.
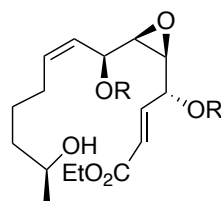
148 R = TBDPS

Alcohol 148: Alcohol **148** was prepared from ester **147** (220.4 mg, 0.24 mmol) using a general procedure for TBS deprotecton. The crude residue was purified by column

chromatography (20−40% EtOAc/hexanes) to yield alcohol **148** as a colorless oil (161.8 mg, 84%): R_f = 0.73 (50% EtOAc/hexanes); $[\alpha]_D^{25}$ = +9.06 (*c* 1.00, CHCl$_3$); ^{1}H NMR (500 MHz, CDCl$_3$) δ 7.72 (d, *J* = 7.5 Hz, 2H), 7.58 (d, *J* = 7.0 Hz, 5H), 7.53 (d, *J* = 7.5 Hz, 2H), 7.41 (t, *J* = 7.0 Hz, 1H), 7.37–7.25 (m, 6H), 7.25–7.20 (m, 2H), 7.18 (t, *J* = 7.5 Hz, 2H), 7.08 (t, *J* = 7.5 Hz, 2H), 6.45 (dd, *J* = 15.5, 3.5 Hz, 1H), 6.02 (dd, *J* = 15.5, 1.0 Hz, 1H), 5.44–5.35 (m, 1H), 5.20 (dt, *J* = 10.5, 6.5 Hz, 1H), 4.15–4.03 (m, 2H), 3.97 (t, *J* = 8.5 Hz, 1H), 3.87–3.82 (m, 2H), 3.50–3.40 (m, 1H), 3.23 (dd, *J* = 7.5, 4.5 Hz, 1H), 3.05 (dd, *J* = 8.0, 4.5 Hz, 1H), 1.22 (t, *J* = 7.1 Hz, 3H), 1.11 (s, 9H), 1.00 (s, 12H), 0.98–0.91 (m, 3H), 0.90–0.80 (m, 3H); ^{13}C NMR (125 MHz, CDCl$_3$) δ 166.2, 145.1, 136.2, 136.18, 136.10, 133.9, 133.4, 133.3, 133.2, 130.0, 129.96, 129.91, 129.7, 129.6, 127.7, 127.6, 127.5, 127.4, 127.0, 122.5, 72.1, 69.1, 67.8, 60.7, 60.5, 59.9, 38.8, 27.2, 27.0, 25.0, 23.3, 19.6, 19.5, 14.3; IR (thin film): 3431, 2932, 2858, 1720, 1427, 1112 cm^{-1}; HRMS (ESI) *m/z* calcd for C$_{48}$H$_{63}$O$_6$Si$_2$ (M+H)$^+$ 791.4163, found 791.4160.
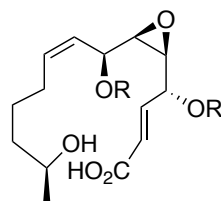
130 R = TBDPS

Seco acid 130: Seco acid **130** was prepared from alcohol **148** (240.8 mg, 0.30 mmol) using a general procedure for hydrolysis. The crude residue was purified by column chromatography (30% EtOAc/hexanes−100% EtOAc) to give seco acid **130** as a colorless oil (182.6 mg, 77%): R_f = 0.33 (50% EtOAc/hexanes); $[\alpha]_D^{25}$ = +9.64 (*c* 1.00, CHCl$_3$); ^{1}H NMR (500 MHz, CDCl$_3$) δ 7.73 (d, *J* = 7.5 Hz, 2H), 7.59 (t, *J* = 6.0 Hz, 4H), 7.53 (d, *J* = 7.5 Hz, 2H), 7.43 (t, *J* = 7.0 Hz, 1H), 7.38–7.26 (m, 5H), 7.26–7.22 (m, 2H), 7.18 (t, *J* = 7.5 Hz, 2H), 7.10 (t, *J* = 7.5 Hz, 2H), 6.50 (dd, *J* = 15.5, 3.0 Hz, 1H), 6.02 (d, *J* = 15.5 Hz, 1H), 5.40 (t, *J* = 10.5 Hz, 1H), 5.19 (dt, *J* = 10.5, 6.5 Hz, 1H), 3.95 (t, *J* = 8.5 Hz, 1H), 3.88–3.80 (m, 1H), 3.55–3.41 (m, 1H), 3.25 (dd, *J* = 7.5, 4.5 Hz, 1H), 3.08 (dd, *J* = 7.5, 4.5 Hz, 1H), 1.32–1.23 (m, 1H), 1.12 (s, 9H), 1.02 (s, 12H), 0.99–0.91 (m, 2H), 0.91–0.80 (s, 3H); ^{13}C NMR (125 MHz, CDCl$_3$) δ 170.2, 147.1, 136.2, 136.0, 133.8, 133.4, 133.3, 133.0, 132.9, 130.0, 129.9, 129.7, 129.6, 129.5, 127.7, 127.6, 127.5, 127.4, 126.9, 121.9, 72.1, 68.9, 68.1, 60.6, 59.7, 38.5, 27.1, 27.0,

26.9, 24.9, 23.1, 19.5, 19.4; IR (thin film): 3421, 2931, 2858, 1701, 1427, 1112 cm^{-1}; HRMS (ESI) m/z calcd for $C_{42}H_{60}NaO_6Si_2$ (M+Na)$^+$ 785.3670, found 785.3666.
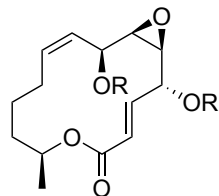
149 R = TBDPS

Macrolactone 149: Macrolactone **149** was prepared from seco acid **130** (200.3 mg, 0.26 mmol) using a general procedure for Shiina macrolactonization. The crude residue was purified by column chromatography (5−10% EtOAc/hexanes) to yield macrolactone **149** as a colorless oil (124.4 mg, 65%): R_f = 0.52 (5% EtOAc/hexanes); $[\alpha]_D^{25}$ = −12.50 (c 1.00, CHCl$_3$); ^{1}H NMR (500 MHz, CDCl$_3$) δ 7.73 (d, J = 7.2 Hz, 2H), 7.57 (d, J = 7.2 Hz, 2H), 7.44 (t, J = 7.4 Hz, 2H), 7.38 (t, J = 7.4 Hz, 2H), 7.36–7.23 (m, 6H), 7.15 (t, J = 7.5 Hz, 2H), 7.03 (t, J = 7.5 Hz, 2H), 6.32 (dd, J = 15.5, 7.1 Hz, 1H), 5.38–5.30 (m, 1H), 5.20 (d, J = 15.5 Hz, 2H), 5.18–5.12 (m, 1H), 4.92–4.82 (m, 1H), 3.87–3.81 (m, 1H), 3.77–3.70 (m, 1H), 3.24 (t, J = 4.6 Hz, 1H), 3.00 (dd, J = 8.8, 4.2 Hz, 1H), 1.87–1.81 (m, 1H), 1.76–1.56 (m, 2H), 1.52–1.43 (m, 2H), 1.12 (d, J = 6.2 Hz, 3H), 1.08 (s, 9H), 1.00 (s, 9H), 0.96–0.87 (m, 1H); ^{13}C NMR (125 MHz, CDCl$_3$) δ 165.7, 143.0, 136.3, 136.1, 133.8, 133.7, 133.4, 133.3, 132.9, 130.1, 129.9, 129.6, 129.5, 128.2, 127.8, 127.7, 127.44, 127.40, 123.1, 73.8, 71.9, 66.8, 62.8, 59.4, 33.2, 30.4, 28.0, 27.0, 26.9, 25.7, 24.7, 19.8, 19.6, 19.3; IR (thin film): 2930, 2857, 1723, 1472, 1112, 1065 cm^{-1}; HRMS (ESI) m/z calcd for $C_{46}H_{56}NaO_5Si_2$ (M+Na)$^+$ 767.3564, found 767.3569.
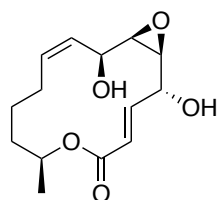
seiricuprolide (**13**)   **150** R = TBDPS
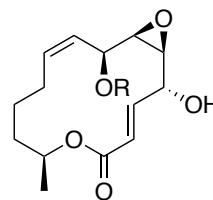
Seiricuprolide (13) and macrolactone 150: Macrolactones **13** and **150** were obtained from macrolactone **149** (55.7 mg, 0.07 mmol) using a general procedure for global TBDPS deprotection. The crude residue was purified by column chromatography (20−80% EtOAc/hexanes) to give compounds **13** and **150**.

Seiricuprolide (13): White solid (9.8 mg, 49%): R_f = 0.16 (50% EtOAc/hexanes); mp 126.5–127.9 °C; $[\alpha]_D^{25}$ = +48.12 (c 2.70, MeOH); ^{1}H NMR (500 MHz, CDCl$_3$) δ 6.85 (dd, J = 15.5, 6.5 Hz, 1H), 6.15 (dd, J = 15.5, 0.5 Hz, 1H), 5.57 (ddd, J = 11.5, 9.5, 1.0 Hz, 1H), 5.39 (ddd, J = 11.5, 9.5, 1.5 Hz, 1H), 5.00–4.91 (m, 1H), 4.36–4.29 (m, 1H), 4.27–4.20 (m, 1H), 3.28–3.24 (m, 1H), 3.03 (dd, J = 8.5, 4.5 Hz, 1H), 2.55 (brs, 1H), 2.51–2.39 (m, 1H), 2.16 (brs, 1H), 2.14–2.04 (m, 1H), 1.94–1.85 (m, 1H), 1.85–1.75 (m, 1H), 1.46 (ddd, J = 14.5, 9.0 Hz, 1.5H), 1.29 (d, J = 6.5 Hz, 1H), 1.27–1.21 (m, 1H); ^{13}C NMR (125 MHz, CDCl$_3$) δ 166.1, 143.0, 135.6, 127.4, 123.7, 73.3, 71.9, 64.4, 62.6, 59.0, 33.6, 29.0, 25.2, 20.0; IR (thin film): 3477, 2932, 2859, 1722, 1242, 1111, 1048 cm^{-1}; HRMS (ESI) m/z calcd for C$_{14}$H$_{20}$NaO$_5$ (M+Na)$^+$ 291.1208, found 291.1180.

Macrolactone 150: Light yellow oil (4.5 mg, 12%): R_f = 0.34 (20% EtOAc/hexanes); $[\alpha]_D^{25}$ = +39.08 (c 1.00, CHCl$_3$); ^{1}H NMR (500 MHz, CDCl$_3$) δ 7.77 (d, J = 6.8 Hz, 2H), 7.68 (d, J = 6.8 Hz, 2H), 7.48–7.35 (m, 6H), 6.45 (dd, J = 15.5, 5.4 Hz, 1H), 5.62 (dd, J = 15.5, 1.0 Hz, 1H), 5.44 (t, J = 9.7 Hz, 1H), 5.34–5.27 (m, 1H), 4.93–4.85 (m, 1H), 3.98 (t, J = 9.0 Hz, 1H), 3.21 (t, J = 6.2 Hz, 1H), 3.03 (dd, J = 8.7, 4.3 Hz, 1H), 3.01–2.97 (m, 1H), 1.93–1.80 (m, 1H), 1.81–1.65 (m, 2H), 1.65–1.55 (m, 1H), 1.51–1.40 (m, 1H), 1.32–1.23 (m, 2H), 1.21 (d, J = 6.3 Hz, 1H), 1.07 (s, 9H); ^{13}C NMR (125 MHz, CDCl$_3$) δ 165.9, 142.6, 136.6, 136.2, 134.0, 133.9, 133.8, 130.0, 129.8, 128.4, 127.7, 127.5, 123.5, 72.7, 72.0, 66.3, 61.6, 59.1, 33.7, 28.7, 27.1, 25.2, 20.0, 19.6; IR (thin film): 3421, 2931, 2857, 1717, 1260, 1112, 1055 cm^{-1}; HRMS (ESI) m/z calcd for C$_{30}$H$_{38}$NaO$_5$Si (M+Na)$^+$ 529.2386, found 529.2380.
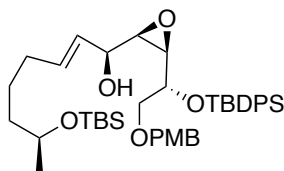
156

***E*-Allylic alcohol 156:** To a solution of propargylic alcohol **131S** (358.3 mg, 0.49 mmol, 1.0 equiv) in anhydrous THF (10 mL, 0.05 M) at 4 °C was added sodium bis(2-methoxyethoxy)aluminium hydride (Red-Al, 3.6 M solution in toluene, 700 μL, 2.49 mmol, 5.0 equiv). After being maintained at this temperature for 5 h, the reaction mixture was quenched with saturated aqueous potassium sodium tartrate solution (10

mL). The aqueous phase was extracted with EtOAc (2 × 10 mL). The combined organic layers were washed with brine, dried over anhydrous Na_2SO_4, and concentrated *in vacuo*. The crude residue was purified by column chromatography (2−10% EtOAc/hexanes) to give *E*-allylic alcohol **156** as a colorless oil (265.9 mg, 74%): R_f = 0.46 (20% EtOAc/hexanes); $[\alpha]_D^{25}$ = –16.30 (*c* 1.00, CHCl₃); ¹H NMR (300 MHz, CDCl₃) δ 7.75 (d, *J* = 7.5 Hz, 2H), 7.72 (d, *J* = 7.5 Hz, 2H), 7.44 (t, *J* = 7.0 Hz, 2H), 7.41–7.35 (m, 3H), 7.14 (d, *J* = 8.5 Hz, 2H), 6.85 (d, *J* = 8.5 Hz, 2H), 5.53 (dt, *J* = 15.5, 6.5 Hz, 1H), 5.34 (dd, *J* = 15.5, 5.5 Hz, 1H), 4.37–4.30 (m, 2H), 3.85 (dt, *J* = 8.3, 5.4 Hz, 1H), 3.81 (s, 3H), 3.78–3.71 (m, 1H), 3.66 (t, *J* = 6.0 Hz, 1H), 3.47–3.39 (m, 2H), 3.26 (dd, *J* = 8.5, 4.5 Hz, 1H), 3.00–2.97 (m, 1H), 1.96 (brs, 1H), 1.90–1.84 (m, 2H), 1.45–1.21 (m, 4H), 1.11 (s, 12H), 0.90 (s, 9H), 0.05 (s, 3H), 0.04 (s, 3H) ;¹³C NMR (75 MHz, CDCl₃) δ 159.4, 136.3, 136.1, 134.2, 133.6, 133.3, 130.0, 129.9, 129.8, 129.4, 128.1, 127.6, 127.5, 113.9, 73.1, 71.9, 69.8, 68.6, 60.6, 60.3, 55.3, 39.3, 32.4, 25.3, 23.9, 19.5, 18.2, –4.3, –4.6; IR (thin film): 3420, 2932, 2858, 1699, 1427, 1112, 1066 cm⁻¹; HRMS (ESI) *m/z* calcd for $C_{42}H_{62}NaO_6Si_2$ (M+Na)⁺ 741.3983, found 741.3995.
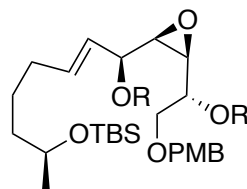
166 R = TBDPS

Silyl ether 166: Silyl ether **166** was prepared from allylic alcohol **156** (110.5 mg, 0.15 mmol) using a general procedure for TBDPS protection. The crude residue was purified by column chromatography (2−10% EtOAc/hexanes) to give siyl ether **166** as a colorless oil (133.9 mg, 91%): R_f = 0.76 (5% EtOAc/hexanes); $[\alpha]_D^{24}$ = –4.24 (*c* 1.00, CHCl₃); ¹H NMR (500 MHz, CDCl₃) δ 7.68 (d, *J* = 7.5 Hz, 2H), 7.63–7.52 (m, 6H), 7.44–7.30 (m, 5H), 7.28–7.24 (m, 2H), 7.23–7.17 (m, 3H), 7.14 (t, *J* = 7.6 Hz, 2H), 7.00 (d, *J* = 8.5 Hz, 2H), 6.78 (d, *J* = 8.5 Hz, 2H), 5.15 (dd, *J* = 15.5, 7.1 Hz, 1H), 4.87 (dt, *J* = 15.5, 6.8 Hz, 1H), 4.19 (d, *J* = 11.7 Hz, 1H), 4.13 (d, *J* = 11.7 Hz, 1H), 3.79 (s, 3H), 3.70–3.64 (m, 1H), 3.61 (t, *J* = 7.4 Hz, 1H), 3.40–3.34 (m, 1H), 3.27 (dd, *J* = 8.5, 4.4 Hz, 1H), 3.23 (dd, *J* = 10.4, 5.0 Hz, 1H), 3.15 (*J* = 7.4, 4.4 Hz, 2H), 1.65–1.52 (m, 4H), 1.30–1.22 (m, 1H), 1.20–1.12 (m, 1H), 1.06 (s, 9H), 1.05 (s, 12H), 0.88 (s, 9H), 0.03 (d, *J* = 10.4 Hz, 1H); ¹³C NMR (125 MHz, CDCl₃) δ 159.1, 136.3, 136.2, 136.0,

135.3, 134.9, 134.3, 133.9, 133.7, 133.4, 130.3, 129.8, 129.6, 129.57, 129.50, 129.4, 129.1, 127.9, 127.7, 127.5, 127.4, 127.3, 113.7, 74.0, 72.8, 72.2, 72.1, 68.5, 61.0, 58.6, 55.4, 39.3, 32.2, 27.1, 27.0, 26.7, 24.9, 23.9, 19.6, 19.4, 18.3, –4.2, –4.6; IR (thin film): 2932, 2858, 1699, 1427, 1112, 1066 cm^{-1}; HRMS (ESI) m/z calcd for $C_{58}H_{80}NaO_6Si_3$ (M+Na)$^+$ 979.5160, found 979.5171.

158 R = TBDPS
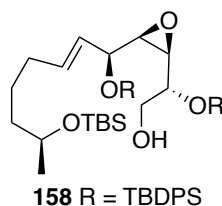
Alcohol 158: Alcohol **158** was prepared from PMB ether **166** (298.9 mg, 0.31 mmol) using a general procedure for PMB deprotection. The crude residue was purified by column chromatography (5–15% EtOAc/hexanes) to yield alcohol **158** as a colorless oil (240.4 mg, 92%): R_f = 0.47 (5% EtOAc/hexanes); $[\alpha]_D^{24}$ = +9.02, c 1.00, CHCl$_3$); ^{1}H NMR (500 MHz, CDCl$_3$) δ 7.66 (d, J = 7.4 Hz, 4H), 7.56 (t, J = 8.0 Hz, 4H), 7.42–7.34 (m, 4H), 7.27–7.20 (m, 8H), 5.23 (dd, J = 15.5, 8.0 Hz, 1H), 4.78 (dt, J = 15.5, 6.6 Hz, 1H), 3.73–3.66 (m, 1H), 3.57 (t, J = 7.8 Hz, 1H), 3.36–3.29 (m, 2H), 3.29–3.23 (m, 2H), 3.19 (dd, J = 7.6, 4.2 Hz, 1H), 1.89–1.80 (brs, 1H), 1.74–1.66 (m, 2H), 1.34–1.14 (m, 4H), 1.10 (s, 9H), 1.07 (d, J = 6.2 Hz, 3H), 1.05 (s, 9H), 0.04 (d, J = 9.9 Hz, 3H); ^{13}C NMR (125 MHz, CDCl$_3$) δ 136.2, 136.16, 136.12, 135.8, 134.4, 134.1, 133.8, 133.7, 132.9, 129.9, 129.8, 129.6, 129.5, 127.9, 127.6, 127.5, 127.4, 74.3, 73.1, 68.5, 64.6, 60.9, 57.8, 39.3, 32.2, 27.1, 27.2, 26.0, 24.9, 23.9, 19.5, 19.4, 18.2, –4.3, –4.6; IR (thin film): 3613, 2930, 2857, 1457, 1112, 1052 cm^{-1}; HRMS (ESI) m/z calcd for $C_{50}H_{75}NaO_5Si_3$ (M+Na)$^+$ 859.4585, found 859.4591.

159 R = TBDPS
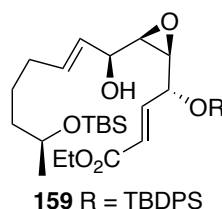
Ester 159: Alcohol **158** (200.1 mg, 0.24 mmol) was first transformed to aldehyde intermediate using a general procedure for DMP oxidation. The crude residue was purified by column chromatography (10−20% EtOAc/hexanes) to furnish the corresponding aldehyde intermediate as a colorless oil (175.7 mg, 88%) which was

immediately subjected to Wittig olefination using a general procedure for Wittig olefination. The crude residue was purified by column chromatography (2–10% EtOAc/hexanes) to yield ester **159** as a colorless oil (179.0 mg, 94%): R_f = 0.55 (5% EtOAc/hexanes); $[\alpha]_D^{25}$ = +8.40 (*c* 1.00, CHCl$_3$); ^{1}H NMR (500 MHz, CDCl$_3$) δ 7.65 (d, *J* = 7.2 Hz, 2H), 7.60 (d, *J* = 7.2 Hz, 2H), 7.54–7.49 (m, 4H), 7.41–7.29 (m, 4H), 7.26–7.16 (m, 8H), 6.51 (dd, *J* = 15.7, 4.7 Hz, 1H), 5.78 (d, *J* = 15.7 Hz, 1H), 5.22 (dd, *J* = 15.5, 7.7 Hz, 1H), 4.88 (dt, *J* = 15.5, 6.6 Hz, 1H), 4.15–4.04 (m, 2H), 3.88–3.81 (m, 1H), 3.73–3.64 (m, 1H), 3.59 (t, *J* = 7.7 Hz, 1H), 3.15 (dd, *J* = 7.8, 4.4 Hz, 1H), 3.03 (dd, *J* = 7.9, 4.4 Hz, 1H), 1.78–1.69 (m, 2H), 1.36–1.25 (m, 4H), 1.22 (t, *J* = 7.1 Hz, 1H), 1.08 (s, 9H), 1.06 (d, *J* = 6.1 Hz, 3H), 1.02 (s, 9H), 0.88 (s, 9H), 0.03 (s, 3H), 0.02 (s, 3H); ^{13}C NMR (125 MHz, CDCl$_3$) δ 166.0, 144.7, 136.2, 136.1, 134.8, 134.0, 133.8, 133.2, 133.1, 129.9, 127.7, 127.6, 127.57, 127.50, 127.4, 122.6, 74.0, 72.1, 68.5, 60.5, 60.4, 59.6, 39.3, 32.1, 24.8, 23.9, 19.5, 19.4, 18.3, 14.3, –4.3, –4.6; IR (thin film): 3431, 2932, 2858, 1720, 1427, 1112 cm^{-1}; HRMS (ESI) *m/z* calcd for C$_{54}$H$_{76}$NaO$_6$Si$_3$ (M+Na)$^+$ 927.4847, found 927.4854.
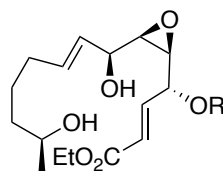
160 R = TBDPS

Alcohol 160: Alcohol **160** was prepared from ester **159** (160.7 mg, 0.18 mmol) using a general procedure for TBS deprotecton. The crude residue was purified by column chromatography (20–40% EtOAc/hexanes) to yield alcohol **160** as a colorless oil (130.2 mg, 81%): R_f = 0.73 (50% EtOAc/hexanes); $[\alpha]_D^{24}$ = +31.04 (*c* 1.00, CHCl$_3$); ^{1}H NMR (500 MHz, CDCl$_3$) δ 7.66 (d, *J* = 7.1 Hz, 2H), 7.59 (d, *J* = 7.2 Hz, 2H), 7.54–7.49 (m, 4H), 7.41–7.31 (m, 5H), 7.28–7.23 (m, 3H), 7.21–7.16 (m, 4H), 6.51 (dd, *J* = 15.6, 4.4 Hz, 1H), 5.86 (d, *J* = 15.6 Hz, 1H), 5.24 (dd, *J* = 15.5, 7.8 Hz, 1H), 4.81 (dt, *J* = 15.5, 6.7 Hz, 1H), 4.15–4.04 (m, 2H), 3.89–3.82 (m, 1H), 3.72–3.67 (m, 1H), 3.57 (t, *J* = 7.9 Hz, 1H), 3.16 (dd, *J* = 7.8, 4.4 Hz, 1H), 3.03 (dd, *J* = 7.9, 4.4 Hz, 1H), 1.86–1.65 (m, 4H), 1.28–1.20 (m, 2H), 1.22 (t, *J* = 7.2 Hz, 1H), 1.11 (d, *J* = 6.2 Hz, 3H), 1.08 (s, 9H), 1.02 (s, 9H); ^{13}C NMR (125 MHz, CDCl$_3$) δ 166.4, 145.2, 136.2, 136.1, 136.0, 134.7, 134.1, 133.7, 133.2, 133.0, 129.9, 129.7, 129.6, 127.7, 127.6, 127.5, 127.4, 122.5, 74.2,

72.1, 67.8, 60.7, 60.4, 59.6, 38.9, 32.1, 27.1, 27.0, 24.9, 23.3, 19.5, 19.4, 14.3; IR (thin film): 3421, 2931, 2857, 1699, 1112, 1065 cm^{-1}; HRMS (ESI) m/z calcd for C$_{48}$H$_{62}$NaO$_6$Si$_2$ (M+Na)$^+$ 813.3983, found 813.3990.
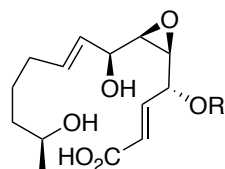
129 R = TBDPS

Seco acid 129: Seco acid **129** was prepared from alcohol **160** (118.7 mg, 0.15 mmol) using a general procedure for hydrolysis. The crude residue was purified by column chromatography (30% EtOAc/hexanes–100%EtOAc) to yield seco acid **129** as a colorless oil (80.7 mg, 69%): R_f = 0.33 (50% EtOAc/hexanes); [α]$_D^{25}$ = +34.94 (c 1.00, CHCl$_3$); ^{1}H NMR (500 MHz, CDCl$_3$) δ 7.67 (d, J = 7.2 Hz, 2H), 7.57 (d, J = 7.2 Hz, 2H), 7.51 (d, J = 7.3 Hz, 4H), 7.42–7.37 (m, 1H), 7.37–7.31 (m, 3H), 7.28–7.23 (m, 2H), 7.23–7.13 (m, 6H), 6.54 (dd, J = 15.5, 4.5 Hz, 1H), 5.83 (d, J = 15.5 Hz, 1H), 5.24 (dd, J = 15.5, 7.9 Hz, 1H), 4.79 (dt, J = 15.5, 6.7 Hz, 1H), 4.75–4.53 (brs., 2H), 3.86–3.80 (m, 1H), 3.75–3.67 (m, 1H), 3.53 (t, J = 8.0 Hz, 1H), 3.16 (dd, J = 8.0, 4.4 Hz, 1H), 3.05 (dd, J = 7.7, 4.4 Hz, 1H), 1.84–1.72 (m, 1H), 1.71–1.61 (m, 1H), 1.25 (s, 4H), 1.08 (s, 12H), 1.01 (s, 9H); ^{13}C NMR (125 MHz, CDCl$_3$) δ 169.2, 146.6, 136.2, 136.1, 136.09, 136.04, 134.8, 134.0, 133.6, 133.1, 133.0, 129.9, 129.6, 129.5, 127.7, 127.6, 127.5, 127.4, 122.1, 74.0, 72.2, 68.3, 60.2, 59.8, 38.6, 32.1, 27.1, 27.0, 24.9, 22.9, 19.5, 19.4; IR (thin film): 3431, 2931, 2857, 1699, 1112, 1065 cm^{-1}; HRMS (ESI) m/z calcd for C$_{46}$H$_{58}$NaO$_6$Si$_2$ (M+Na)$^+$ 785.3670, found 785.3662.
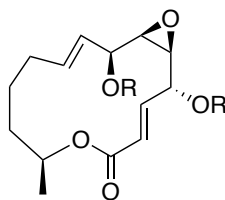
161 R = TBDPS

Macrolactone 161: Macrolactone **161** was prepared from seco acid **129** (74.8 mg, 0.10 mmol) using a general procedure for Shiina macrolactonization. The crude residue was purified by column chromatography (5–10% EtOAc/hexanes) to yield macrolactone **161** as a colorless oil (42.1 mg, 59%): R_f = 0.59 (5% EtOAc/hexanes); [α]$_D^{25}$ = +33.44, (c 1.00, CHCl$_3$); ^{1}H NMR (300 MHz, CDCl$_3$) δ 7.77–7.70 (m, 2H), 7.59–7.51 (m, 6H),

7.47–7.28 (m, 8H), 7.18 (t, J = 7.6 Hz, 2H), 7.06 (t, J = 7.6 Hz, 2H), 6.51 (dd, J = 15.3, 4.2 Hz, 1H), 5.93 (dd, J = 15.3, 1.6 Hz, 1H), 5.37 (dt, J = 15.5, 5.6 Hz, 1H), 5.22–5.10 (m, 1H), 4.72–4.59 (m, 1H), 4.01–3.95 (m, 1H), 3.56 (t, J = 8.2 Hz, 1H), 3.13–3.05 (m, 2H), 1.99–1.86 (m, 1H), 1.77–1.55 (m, 4H), 1.34–1.29 (m, 1H), 1.15 (d, J = 6.3 Hz, 3H), 1.12 (s, 9H), 1.02 (s, 9H); ^{13}C NMR (75 MHz, CDCl$_3$) δ 165.8, 145.6, 136.2, 136.1, 136.0, 135.0, 134.1, 133.4, 133.1, 130.0, 129.9, 129.6, 129.5, 129.0, 127.8, 127.4, 127.3, 121.6, 73.5, 72.8, 71.9, 61.8, 58.9, 34.4, 33.0, 27.1, 27.0, 24.3, 20.1, 19.5, 19.4; IR (thin film): 293, 2857, 1719, 1259, 1112, 1065 cm^{-1}; HRMS (ESI) m/z calcd for C$_{46}$H$_{56}$NaO$_5$Si$_2$ (M+Na)$^+$ 767.3564, found 767.3567.
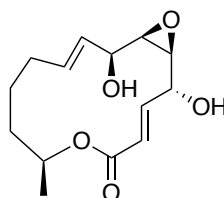
pestalotioprolide B (**14**)

Pestalotioprolide B (14): Pestalotioprolide B (**14**) was obtained from macrolactone **161** (42.1 mg, 0.06 mmol) using a general procedure for global deprotection. The crude residue was purified by column chromatography (20–80% EtOAc/hexanes) to give macrolactone **14** (8.9 mg, 59%) as a white solid: R_f = 0.17 (50% EtOAc/hexanes); mp 109.6–111.3 °C; [α]$_D^{25}$ = +75.96, (c 1.00, CHCl$_3$); ^{1}H NMR (500 MHz, acetone-d_6) δ 7.11 (dd, J = 15.5, 3.6 Hz, 1H), 5.99 (dd, J = 15.5, 1.8 Hz, 1H), 6.03–5.90 (m, 1H), 5.55 (dd, J = 15.5, 7.8 Hz, 1H), 5.01 (brs, 1H), 4.69–4.62 (m, 1H), 4.21 (brs, 1H), 4.35–4.28 (brs, 1H), 3.97–3.91 (m, 1H), 2.94 (dd, J = 8.9, 4.5 Hz, 1H), 2.93–2.89 (m, 1H), 2.16–2.08 (m, 1H), 2.03–1.93 (m, 1H), 1.89–1.75 (m, 2H), 1.60–1.50 (m, 1H), 1.21 (d, J = 6.2 Hz, 3H), 1.16–1.09 (m, 1H); ^{13}C NMR (125 MHz, acetone-d_6) δ 166.1, 148.2, 135.2, 130.9, 120.8, 72.3, 71.7, 71.4, 61.7, 59.2, 35.1, 33.7, 25.3, 20.3; IR (thin film): 3369, 2930, 2857, 1722, 1242, 1112, 1048 cm^{-1}; HRMS (ESI) m/z calcd for C$_{14}$H$_{20}$NaO$_5$ (M+Na)$^+$ 291.1208, found 291.1190.

4.3 Cytotoxicity assay

The evaluation of cytotoxic activity against the HCT116 colon cancer and non-cancerous (Vero) cells of **13** and **14** was measured using 3-(4,5-dimethyl-2-thiazolyl)-2,5-diphenyl-2H-tetrazolium bromide (MTT) assay following a procedure previously described (Thiraporn et al., 2022) by the laboratory of Prof. Dr. Chatchai Muanprasat of Chakri Naruebadin Medical Institute, Faculty of Medcine Ramathibodi Hospital, Mahidol University.

4.4 CFTR inhibition assay

The evaluation of inhibitory effect on CFTR in human intestinal epithelial (T84) cells of **4** and **5** was measured using short-circuit current analysis following a procedure previously described (Muangnil et al., 2018 and Thiraporn et al., 2022) by the laboratory of Prof. Dr. Chatchai Muanprasat of Chakri Naruebadin Medical Institute, Faculty of Medcine Ramathibodi Hospital, Mahidol University.

REFERENCES

Adam, W.; Stegmann, V. R.; Saha-Möller, C. R. 1999. Regio- and Diastereoselective Epoxidation of Chiral Allylic Alcohols Catalyzed by Manganese(salen) and Iron(porphyrin) Complexes. J. Am. Chem. Soc. 121, 1879−1882.

Albert, B. J.; Sivaramanabhan, A.; Naka, T.; Czaicki, N. L.; Koide, K. 2007. Total Syntheses, Fragmentation Studies, and Antitumor/Antiproliferative Activities of FR901464 and Its Low Picomolar Analogue. J. Am. Chem. Soc. 129, 2648−2659.

Baikadi, K.; Talakokkula, A.; Narsaiah, V. 2019. Studies Towards the Stereoselective Total Synthesis of 7-O-methylnigrosporolide. Chemistry Select. 4, 5531–5534.

Ballio, A.; Evident, A.; Graniti, A.; Randazzo, G.; Sparapano, L. 1998. Seiricuprolide, a New Phytotoxic Macrolide from a Strain of Seiridium Cupressi Infecting Cypress. Phytochemistry 27 (10), 3117–3121.

Baltas, M.; Sugisaki, C. H.; Ruland, Y. 2003. Direct Access to Furanosidic Eight-Membered Ulosonic Esters from cis-α,β-Epoxy Aldehydes. Eur. J. Org. Chem. 2003, 672–688.

Bartolucci, C.; Cerrini, S.; Lamba, D.; Evident, A.; Randazzo, G. 1992. Absolute Configuration of Seiricuprolide, a New Phytotoxin from *Seiridium cupressi*. Acta. Cryst. C48, 83–86.

Bode, H. B.; Walker, M.; Zeeck, A. 2000. Structure and Biosynthesis of Mutolide, a Novel Macrolide from a UV Mutant of the Fungus F-24′707. Eur. J. Org. Chem. 2000, 1451–1456.

Bodugam, M.; Javed, S.; Ganguly, A.; Torres, J.; Hanson, P. R. 2016. A Pot-Economical Approach to the Total Synthesis of Sch-725674. Org. Lett. 18, 516–519.

Bressin, R. K.; Osman, S.; Pohorilets, I.; Basu, U.; Koide K. 2020. Total Synthesis of Meayamycin B. J. Org. Chem. 85, 4637−4647.

Chu, D. T. W. 1995. Section Review Anti-Infectives: Recent Developments in 14- and 15- Membered Macrolides. Expert Opin. Invest. Drugs. 4 (2), 65–94.

Cid, M. B.; Alfonso, F.; Alonso, I.; Martìn-Lomas, M. 2009. On the origin of the regioselectivity in glycosylation reactions of 1,2-diols. Org. Bimol. Chem. 7, 1471–1481.

Freccero, M.; Gandolfi, R.; Sarzi-Amadè, M.; Rastelli, A. 2000. Epoxidation of Acyclic Chiral Allylic Alcohols with Peroxy Acids: Spiro or Planar Butterfly Transition Structures? A Computational DFT Answer. J. Org. Chem. 65, 2030−2042.

Fürstner, A.; Flügge, S.; Larionov, O.; Takahashi, Y.; Kubota, T.; Kobayashi, J. 2009. Total Synthesis and Biological Evaluation of Amphidinoline V and Analouges. Chem. Eur. J. 15, 4011–4029.

Galvidis, I.; Lapa, G.; Burkin, M. 2015. Group Determination of 14-Membered Macrolide Antibiotics and Azithromycin Using Antibodies Common Epitopes. Anal. Biochem. 468, 75–82.

Gao, Y.; Stuhldreier, F.; Schmitt, L.; Wesselborg, S.; Wang, L.; Müller, W. E. G.; Kalscheuer, R.; Guo, Z.; Zou, K.; Liu, Z.; Proksch, P. 2020. Sesterterpenes and Macrolide Derivatives from the Endophytic fungus *Aplosporella javeedii*. Fitoterapia. 146, 104652.

Garbaccio, R. M.; Stachel, S. J.; Baeschlin, D. K.; Danishefsky, S. J. 2001. Concise Asymetric Syntheses of Radicicol and Monocillin I. J. Am. Chem. Soc. 123, 10903–10908.

Goswami, R.; Tsutomu K.; Sharpless, B. 1980. The First Practical Method for Asymmetric Epoxidation. J. Am. Chem. Soc. 102, 5974–5976.

Gucchait, A.; Kundu, M.; Misra, A. K. 2021. Synthesis of Pentasaccharide Repeating Unit Corresponding to the Cell Wall *O*-Polysaccharide of *Salmonella enterica* O55 Strain Containing a Rare Sugar 3-Acetamido-3-deoxy-d-fucose. Synthesis 53, 3613−3620.

Hoffmann, R. W. 1989. Allylic 1,3-strain as a controlling factor in stereoselective transformations. Chem. Rev. 89, 1841−1860.

Ikeuchi, K.; Murasawa, K.; Yamada, H. 2019. A simple method for preparation of stainless and highly pure trichloroacetimidate. Synlett 30, 1308−1312.

Isaacs, J. S.; Xu, W.; Neckers, L. 2003. Heat Shock Protein 90 as a Molecular Target for Cancer Therapeutics. Cancer Cell 3, 213–217.

Isaka, M.; Suyarnsestakorn, C.; Tanticharoen, M.; Kongsaeree, P.; Thebtaranonth, Y. 2002. Aigialomycins A-E, New Resorcylic Macrolides from the Marine Mangrove Fungus *Aigialus parvus*. J. Org. Chem. 67, 1561–1566.

Kanfer, I.; Skinner, M. F.; Walker, R. B. 1998. Analysis of Macrolide Antibiotics. J. Chromatogr. A. 812, 255–286.

Kim, H. J.; Pongdee, R.; Wu, Q.; Hong, L.; Liu, H.-W. 2007. The Biosynthesis of Spinosyn in Saccharopolyspora spinosa: Synthesis of the Cross-Bridging Precursor and Identification of the Function of SpnJ. J. Am. Chem. Soc. 129, 14582–14584.

Kurmar, A. S.; Kurmar, J. N.; Kanth, B. S.; Shinde, D. B.; Das, B. 2018. Stereoselective Total Synthesis of Proposed Structure of Stagonolide D. Organic Chem. Curr. Res. 7 (1), 1000186.

Kurmar, A. S.; Kurmar, J. N.; Kanth, B. S.; Shinde, D. B.; Das, B. *Organic Chem*. *Curr*. *Res*. **2018**, *7*, 1000186.

Li, J.; Park, S.; Miller, R. L.; Lee, D. 2009. Tandem Enyne Metathesis-Metallotropic [1,3]-Shift for a Concise Total Syntheses of (+)-Asperpentyn, (–)-Harveynone, and (–)-Tricholomenyn A. Org. Lett. 11, 571−574.

Liu, S.; Dai, H.; Makhloufi, G.; Heering, C.; Janiak, C.; Hartmann, R.; Mándi, A.; Kurtán, T.; Müller, W. E. G.; Kassack, M. U.; Lin, W.; Liu, Z.; Proksch, P. 2016. Cytotoxic 14-Membered Macrolides from a Mangrove-Derived Endophytic Fungus, *Pestalotiopsis microspora*. J. Nat. Prod. 79, 2332−2340.

Matsumoto, K.; Katsuki, T. 2012. Oxidation: Epoxidation (Allylic Alcohol, Homoallylic alcohol, Simple C=C, Electron Deficient C=C). Comprehensive Chirality. 15, 69–117.

McGuire, J. M.; Bunch, R. L.; Anderson, R. C.; Boaz, H. E.; Flynn, E. H.; Powell, H. M.; Smith, J. W. 1952. Ilotycin, a New Antibiotic. Antibiot. Chemother. 2, 281–283.

McKenzie, N. C.; Scott, N. E.; John, A.; White, J. M.; Goddard-Borger, E. D. 2018. Synthesis and use of 6,6,6-trifluoro-L-fucose to block core-fucosylation in hybridoma cell lines. Carbohydr. Res. 465, 4−9.

McLellan, C. A.; Turbyville, T. J.; Kithsiri W. E. M.; Kerschen, A.; Vier-ling, E.; Queitsch, C.; Whitesell, L.; Leslie Gunatilaka, A. A. 2007. A Rhizosphere Fungus Enhances Arabidopsis Thermotolerance through Production of an HSP90 Inhibitor. Plant Physiol.145, 174–182.

Mejia, E. J.; Loveridge, S. T.; Stepan, G.; Tsai, A.; Jones, G. S.; Barnes, T.; White, K. N.; Draškoviç, M.; Tenny K.; Tsiang, M.; Geleziunas, R.; Chihlar, T.; Pagratis, N.; Tain, Y.; Yu, H.; Crews, P. 2014. Study of Marine Natural Products including Resorcylic Acid Lactones from Humicola fuscoatra that Reactivate Latent HIV-1 Expression in an in vitro Model of Central Memory CD4 + T cells. J. Nat. Prod. 77, 618–624.

Meta, C. T.; Koide, K. 2004. Trans-Selective Conversions of γ-Hydroxy-α,β-Alkynoic Esters to γ-Hydroxy-α,β-Alkenoic Esters. Org. Lett. 6, 1785−1787.

Migawa, M. T.; Prakash, T. P.; Vasquez, G.; Seth, P. P.; Swayze, E. E. 2013. Synthesis and Biophysical Properties of Constrained D-Altritol Nucleic Acids (cANA). 15 (17), 4316–4319.

Migawa, M. T.; Prakash, T. P.; Vasquez, G.; Seth, P. P.; Swayze, E. E. *Org. Lett*. **2013**, *15*, 4316–4319.

Nair, M. S. R.; Carey, S. T. 1980. Metabolites of Pyrenomycetes XIII: Structure of (+)-Hypothemycin, an Antibiotic Macrolide from *Hypomyces trichothecoides*. Tetrahedron Lett. 21, 2011–2012.

Nurula, A. S. 1983. Stereoselective Introduction of Chiral Centres in Acyclic Precursors: a Probe into the Transition State of *m*-chloroperbenzoic (*m*-CPBA) acid Epoxidation of Acyclic Allylic Alcohols and its Synthetic Implications. Tetrahedron Lett. 24, 5421−5424.

Palframan, M. J.; Kociok-Köhn, G.; Lewis, S. E. 2012. Photooxygenation of a Microbial Arene Oxidation Product and Regioselective Kornblum–DeLaMare Rearrangement: Total Synthesis of Zeylenols and Zeylenones. Chem. Eur. J. 18, 4766–4774.

Paranagama, P. A.; Kithsiri, W. E. M.; Leslie, G. A. A. 2007. Uncovering Biosynthetic Potential of Plant-Associated Fungi: Effect of Culture Conditions on Metabolite Production by *Paraphae-osphaeria quadriseptata* and *Chaetomium chiversii*. J. Nat. Prod. 70, 1939–1945.

Park, J. W.; Yoon, Y. J. 2019. Recent Advances in the Discovery and Combinatorial Biosynthesis of Microbial 14-Membered Macrolides and Macrolactones. J. Ind. Microbiol. Biotechnol. 46, 445–458.

Paul, D.; Saha, P.; Goswami, R. K. 2018. Total Synthesis of Pestalotioprolide E and Structural Revision of Pestalotioprolide F. Org. Lett. 20, 4606–4609.

Reddy, C. R.; Dharmapuri, G.; RaO, N. N. 2009. Synthesis of the Macrocyclic Core of Iriomoteolide 3a. Org. Lett. 11 (24), 5730–5733.

Rossiter, B. E.; Verhoeven, T. R.; Shrapless, K. B. 1979. Stereoselective Epoxidation of Acyclic Aalcohols. A Correction of our Previous Work. Tetrahedron Lett. 20, 4733−4736.

Rukachaisirikul, V.; Rodglin, A.; Phongpaichit, S.; Buatong, J.; Sakayaroj, J. 2012. α-Pyrone and Seiricuprolide Derivatives from the Mangrove-derived Fungi *Pestalotiopsis* spp. PSU-MA92 and PSU-MA119. Phytochem. Lett. 5, 13–17.

Sellès, P.; Lett, R. 2002a. Convergent Stereospecific Synthesis of C292 (or LL-Z1640-2), and Hypothemycin. Part 1. Tetrahedron Lett. 43, 4621–4625.

Shah, M.; Deshmukh, S. K.; Verekar, S. A.; Gohil, A.; Kate, A. S.; Rekha, V.; Kulkarni-Almeida, A. 2015. Anti-Inflammatory Properties of Mutolide Isolated from the Fungus Lepidosphaeria Species (PM0651419). Springerplus. 4, 706, DOI 10.1186/s40064-015-1493-6.

Shinonaga, H.; Kawamura, Y.; Ikeda, A.; Aoki, M.; Sakai, N.; Fujimoto, N.; Kawashima, A. 2009a. Pochonins K-P: New Radicicol Analogues from *Pochonia chlamydosporia* var. *chlamydosporia* and their WNT-5A Expression Inhibitory Activities. Tetrahedron 65, 3446– 3453.

Sun, Z.; Yang, S.; Xu, C.; Yi, F.; Cao, L; Tian, Y.; Lin, J.; Xu, X. 2021. Concise total synthesis of (+)-Zeylenone with antitumor activity and the structure–activity relationship of its derivatives. Bioorg. Chem. 116, 105333.

Tadpetch, K.; Jeanmard, L.; Rukachaisirikul, V. 2015. Total Synthesis of the Proposed Structure of Pestalotioprolide A. Tetrahedron:Asymmetry. 26 (17), 918–923.

Thiraporn, A.; Iawsipo, P.; Tadpetch, K. 2022. Total Synthesis and Cytotoxic Activity of 7-*O*-Methylnigrosporolide and Pestalotioprolide D. Synlett 33, 1341−1346.

Thiraporn, A.; Saikachain, N; Khumjiang, R.; Muanprasat, C.; Tadpetch, K. 2022. Total Synthesis and Biological Evaluation of Mutolide and Analogues. Chem Asian J. 17, e202200329.

Thirupathi, B.; Mohapatra, D. K. 2016. Gold-Catalyzed Hosomi-Sakurai Type Reaction for the Total Synthesis of Herboxidiene. Org. Biomol. Chem. 14 (26). 6212–6224.

Trost, B. M.; Bartlett, M. J.; Weiss, A. H.; von Wangelin, A. J.; Chan, V. S. 2012. Development of Zn–ProPhenol-Catalyzed Asymmetric Alkyne Addition: Synthesis of Chiral Propargylic Alcohols. Chem. Eur. J. 18, 16498−16509.

Trost, B. M.; Weiss, A. H.; von Wangelin, A. J. 2006. Dinuclear Zn-Catalyzed Asymmetric Alkynylation of Unsaturated Aldehydes. J. Am. Chem. Soc. 128, 8−9.

Turbyville, T. J.; Wijeratne, E. M. K.; Liu, M. X.; Burns, A. M.; Seliga, C. J.; Leuvano, L. A.; David, C. L.; Faeth, S. H.; Whitesell, L.; Gunatilaka, A. A. L. 2006. Search for Hsp90 Inhibitors with Potent Anticancer Activity: Isolation and SAR Studied of Radicicol and Monocillin I from Two Plant-Associated Fungi of the Sonoran Desert. J. Nat. Prod. 69, 178–184.

Vinaykumar, A.; Maniraju, C.; Rao, B. V. 2017. Stereoselective total synthesis of (–)-zeylenol, a key intermediate for the synthesis of (+)-pipoxide, (–)-uvarigranol G and (–)-tonkinenin A. Tetrahedron Lett. 58 (11), 1075–1077.

Wang, Y.; Liu, Q.-F.; Xue, J.-J.; Zhou, Y.; Yu, H.-C.; Yang, S.-P.; Zhang, B.; Zuo, J.-P.; Li, Y.; Yue, J.-M. 2014. Ivorenlide B, an Immunosuppressive 17-Membered Macrolide from *Khaya ivorensis*: Structural Determination and Total Synthesis. Org. Lett. 16, 2062–2065.

Wee, J. L.; Sundermann, K.; Licari, P.; Galazzo, J. 2006. Cytotoxic Hypothemycin Analogues from *Hypomyces subiculosus*. J. Nat. Prod. 69, 1456–1459.

Yang S. W.; Chan, T. M.; Terracciano, J.; Loebenberg, D.; Patel, M.; Chu, M. 2005. Structure Elucidation of Sch 725674 from *Aspergillus* sp. J. Antibot. 58 (8), 535–538.

Yu, L.; Zhang, R.; Wang, Z. 2001. A New and Efficient Route to Derivatives of (R)-4-Hydroxycyclohex-2-enone. J. Chem. Soc., Perkin Trans. 1, 2958−2961.

Zhao, A.; Lee, S. H.; Mojena, M.; Jenkins, R. G.; Patrick, D. R.; Huber, H. E.; Goetz, M. A.; Hensens, O. D.; Zink, D. L.; Vilella, D.; Dombrowski, A. W.; Lingham, R. B.; Huang, L. 1999. Resorcylic Acid Lactones: Naturally Occurring Potent and Selective Inhibitors of MEK. J. Antibiot. 52, 1086–1094.

Zhao, Y.; Huang, Z. J.; Rahman, M.; Luo, Q.; Thorlacius, H. 2013. Radicicol, an Hsp90 Inhibitor, Inhibits intestinal Inflammation and Leakage in Abdominal Sepsis. J. Surg. Res. 182, 312–318.

Zhanel, G. G.; Dueck, M.; Hoban, D. J.; Vercaigne, L. M.; Embil, J. M.; Gin, A. S.; Karlowsky, J. A. 2001. Review of Macrolides and Ketolides: Focus on Respiratory Tract Infections. Drugs. 61 (4), 443–498.

APPENDIX

Total Synthesis and Biological Evaluation of Seiricuprolide and Pestalotioprolide B

Pitipat Sanphetchaloemchok,[a] Nongluk Saikachain,[b] Rungtiwa Khumjiang,[b] Chatchai Muanprasat,[b] and Kwanruthai Tadpetch*[a]

The first total syntheses of seiricuprolide and pestalotioprolide B, rare 14-membered α,β-unsaturated macrolides embedding a chiral epoxide motif, were achieved in 17 steps with 1.9% and 1.6% overall yields, respectively. Our synthesis featured the key Shiina macrolactonization to construct the 14-membered macrocyclic skeleton, Wittig olefination to generate the (E)-α,β-unsaturated ester and selective reduction of advanced chiral propargylic alcohol intermediate to enable the exclusive formation of Z- or E-olefin at C8–C9. Synthetic seiricuprolide and pestalotioprolide B were evaluated for their cytotoxic activity against the HCT116 colon cancer cell line as well as their inhibitory effect on CFTR chloride channel activity in human intestinal epithelial (T84) cells. Preliminary structure–activity relationship suggested that the C5–C6 β-epoxide moiety suppressed both biological activities.

Introduction

14-Membered macrolactones are a significant class of polyketide metabolites exhibiting a broad range of biological activities and diverse architectural features. Because of this, these macrolides have received a great deal of interest from organic chemists.[1] A rare subgroup of 14-membered macrolides are those containing chiral epoxides. This subgroup of macrolides can be divided into two group based on the presence of a β-resorcylic acid subunit. The prominent examples of resorcylic acid lactones (RALs) containing epoxide motif are depicted in Figure 1A. Radicicol (1),[2a–c] monocillin I (2)[2a,b] and hypothemycin (3)[2d] were isolated from various strains of fungi and are shown to display a wide range of biological activities such as cytotoxic,[3] antifungal,[2a] antibiotic,[4] antimalarial[2d] and HSP90 inhibitory activities.[5] Owing to their promising biological activities, the syntheses of RALs 1–3 were reported by many research groups.[6] Another group of 14-membered macrolides bearing epoxide moiety are those lacking the β-resorcylic acid which are very rare in nature and, to the best of our knowledge, only two examples have been reported (Figure 1B). Seiricuprolide (4) was originally isolated from a fungus *Seiridium cupressi* by Sparapano et al. in 1988.[7] The Sparapano group also reported the phytotoxic activity of macrolide 4. Structurally, seiricuprolide (4) is a 14-membered α,β-unsaturated lactone containing β-epoxide at C5–C6, Z-double bond at C8–C9 as well as three alcohol stereogenic centers. The structure and the absolute configurations of 4 were later confirmed by single-crystal X-ray diffraction analysis by the Lamba group in 1992,[8] rendering 4 a β-epoxide analogue of nigrosporolide (7, Figure 1C), a known 14-membered macrolactone of which the first total synthesis was disclosed by our research group.[9] Pestalotioprolide B (5), the other known macrolactone of this subclass, was first discovered as a diacetate derivative 6 from mangrove-derived endophytic fungus *Pestalotiopsis* sp. PSU-MA119 by Rukachaisirikul et al. in 2012.[10] In 2016, macrolides 4 and 5 were reisolated from the mangrove-derived endophytic fungus *Pestalotiopsis microspora* by Liu and Proksch and co-workers.[11] The Liu and Proksch group also verified the structures and the absolute configurations of macrolide 5 by single-crystal X-ray diffraction analysis. Pestalotioprolide B (5) is structurally nearly identical to 4 except for the configuration of double bond at C8–C9, which also makes 5 a β-epoxide analogue of previously reported (4S,7S,13S)-4,7-dihydroxy-13-tetradeca-2,5,8-trienolide (8, Figure 1C).[9] Although macrolactones 4 and 5 were reported to have no cytotoxicity against the L5178Y murine lymphoma and the A2780 human ovarian cancer cell lines by the Liu and Proksch group, their novel structures and unprecedented chemical syntheses sparked our interest. As part of our ongoing program on total syntheses and anticancer drug discovery of 14-membered macrolides, we report herein the first total syntheses of seiricuprolide (4) and pestalotioprolide B (5) as well as evaluation of their cytotoxic activity against the HCT116 colon cancer cells and inhibitory activity against cystic fibrosis transmembrane regulator (CFTR). In addition, the preliminary structure-activity relationship of this subgroup of 14-membered macrolactones was suggested in this work.

[a] P. Sanphetchaloemchok, Dr. K. Tadpetch
Division of Physical Science and
Center of Excellence for Innovation in Chemistry
Faculty of Science, Prince of Songkla University
Hat Yai, Songkhla 90110 (Thailand)
E-mail: kwanruthai.t@psu.ac.th
[b] N. Saikachain, R. Khumjiang, Prof. Dr. C. Muanprasat
Chakri Naruebodindra Medical Institute
Faculty of Medicine Ramathibodi Hospital
Mahidol University
Bang Pla, Bang Pli, Samut Prakan 10540 (Thailand)
Supporting information for this article is available on the WWW under
https://doi.org/10.1002/ejoc.202300034

EurJOC
European Journal of Organic Chemistry

Research Article
doi.org/10.1002/ejoc.202300034

**Chemistry
Europe**
European Chemical
Societies Publishing
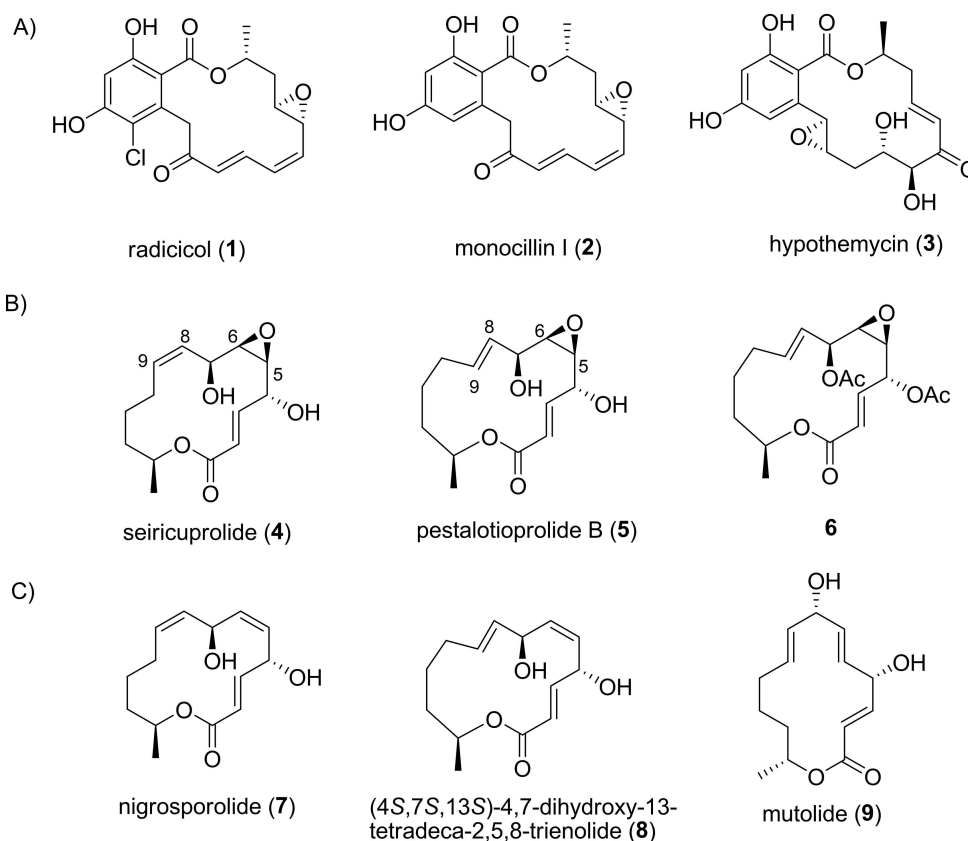
Figure 1. A) Selected examples of RALs containing epoxide moiety B) 14-membered α,β-unsaturated macrolides containing epoxide moiety C) 14-membered α,β-unsaturated macrolides of which total syntheses were reported by our research group.

Results and Discussion

Since seiricuprolide (**4**) and pestalotioprolide B (**5**) are structurally similar to those of nigrosporolide (**7**) and (4*S*,7*S*,13*S*)-4,7-dihydroxy-13-tetradeca-2,5,8-trienolide (**8**), we anticipated that our previously described key bond formation strategy employed in the syntheses of **7** and **8** would be applicable for syntheses of **4** and **5**.[9] However, the challenging part of syntheses of **4** and **5** is the installation of the β-epoxide moiety since epoxides are sensitive functional group and late stage installation of epoxides would be preferable. Ideally, macrolactone targets **4** and **5** should be directly obtained via selective epoxidation of macrolides **7** and **8**. Nevertheless, this strategy posed a challenge due to the presence of two olefins in the molecules of **7** and **8** in addition to the facial selectivity of the epoxidation step. Thus, our bond disconnections would rely on installing the epoxide moiety in an early stage to avoid such challenges. The retrosynthetic analysis of **4** and **5** is outlined in Scheme 1. Our approach would still rely on the same key disconnection strategy to our previous reports on the total syntheses of the closely-related analogues.[9] Shiina macrolactonization of seco acids **10** and **11** would be utilized to assemble the macrocycles. Wittig olefination would be employed to generate the C2–C3 (*E*)-α,β-unsaturated ester moiety of both **10** and **11**. The *Z*- or *E*-double bond at C8–C9 (of **10** or

11, respectively) would be derived from selective reduction of chiral propargylic alcohol **12**, which would in turn be elaborated from acetylide addition of known chiral alkyne **13**[9,16] prepared from (*S*)-propylene oxide to chiral epoxy aldehyde **14**. It was anticipated that the adjacent chiral epoxide of aldehyde **14** would direct the stereoselectivity of this acetylide addition step.[12] Chiral epoxy aldehyde **14** would then be prepared from substrate-controlled and selective epoxidation of our previously reported chiral *Z*-allylic alcohol **15** via the Baltas's protocol.[13] In 2003, Baltas and co-workers reported the substrate-controlled *m*-CPBA-mediated epoxidation of *Z*-allylic alcohols bearing adjacent (*S*)-silyloxy stereogenic centers (**16** and **17**) which provided good *erythro* selectivity leading to β-epoxides as major products (Scheme 2A). Since our chiral *Z*-allylic alcohol substrate **15** is nearly identical to **16** and **17**, we expected that *m*-CPBA epoxidation of **15** would provide the desired β-selectivity. The Baltas group also observed a particular trend in vicinal coupling constants of methine protons in the chiral epoxides α to silyloxy stereogenic centers ($J_{3/4}$) i.e. *threo* products generally have higher values of $J_{3/4}$ vicinal coupling constants compared to those of the *erythro* counterparts. This information could be used as a guideline to verify the absolute configurations of chiral epoxides bearing adjacent silyloxy stereogenic centers. Nevertheless, the rationale of the stereoselectivity of epoxidation of this particular substrate was not

EurJOC
European Journal of Organic Chemistry

Research Article
doi.org/10.1002/ejoc.202300034

Chemistry Europe
European Chemical Societies Publishing
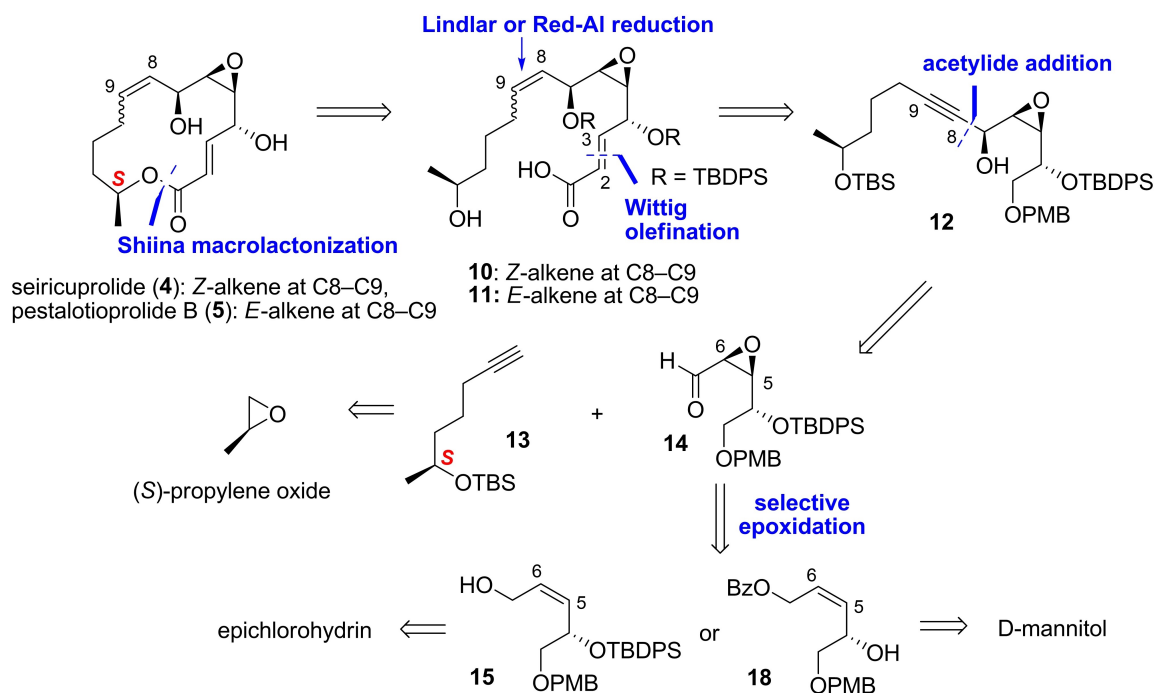
Scheme 1. Retrosynthetic analysis of sericuprolide (**4**) and pestalotioprolide B (**5**)
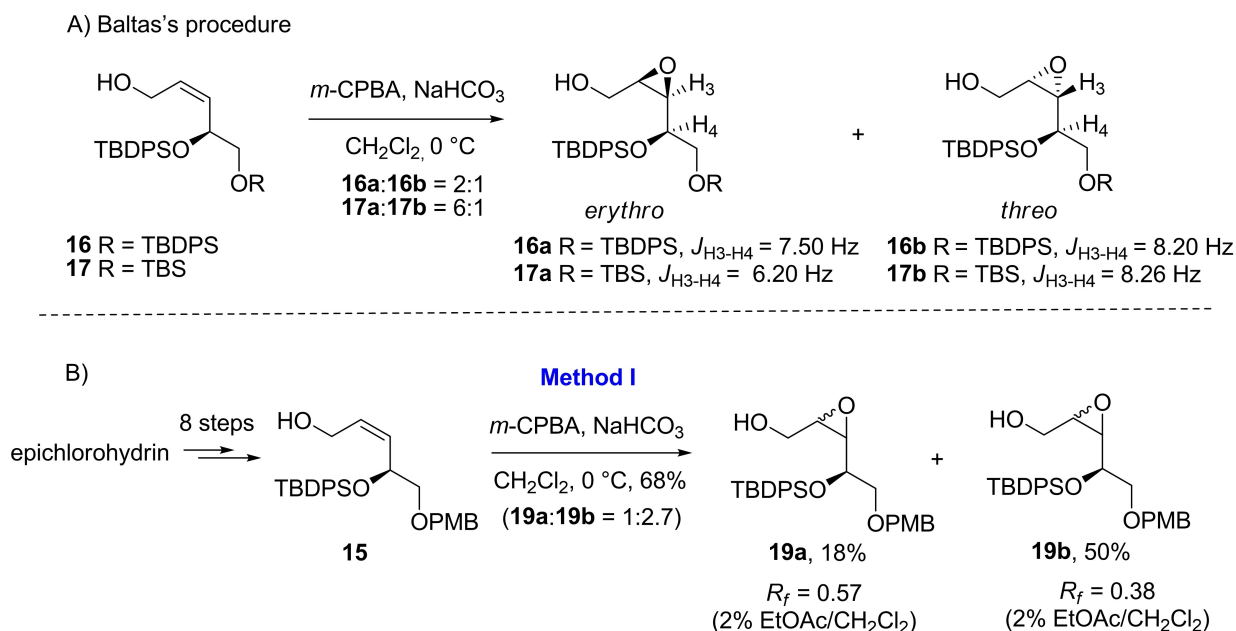
Scheme 2. A) Previously reported *m*-CPBA epoxidation by Baltas et al. B) *m*-CPBA epoxidation of *Z*-allylic alcohol **15** using Baltas's protocol (Method I).

discussed. Alternatively, we envisioned that β-epoxide **14** could be obtained via chiral OH-directed *m*-CPBA epoxidation of **18**.[14] The modified *Z*-Allylic alcohol **18** would be synthesized from D-mannitol, a commercially available and inexpensive chiral building block.[13,15]

Synthesis of macrolides **4** and **5** started with preparation of chiral epoxy aldehyde **14**. The first method was the use of our previously reported *Z*-allylic alcohol intermediate **15**, which was

obtained from epichlorohydrin in 8 steps via the key Jacobsen hydrolytic kinetic resolution and Still-Gennari olefination,[16] as epoxidation substrate according to Baltas's protocol.[13] *Z*-Allylic alcohol **15** was therefore subjected to *m*-CPBA in the presence of NaHCO$_3$ at 0 °C to provide the separable epoxy alcohol diastereomers **19a** (18%, $R_f = 0.57$ in 2% EtOAc/CH$_2$Cl$_2$) and **19b** (50%, $R_f = 0.38$ in 2% EtOAc/CH$_2$Cl$_2$) in 68% combined yield (dr = 1:2.7) (Method I, Scheme 2B). Unfortunately, the

EurJOC
European Journal of Organic Chemistry

Research Article
doi.org/10.1002/ejoc.202300034

Chemistry Europe
European Chemical Societies Publishing

absolute configuration of newly formed epoxides could not be determined by comparison of $J_{3/4}$ vicinal coupling constants due to unclear multiplicity of H3 and H4 signals of the major product **19b**. However, we observed the $J_{3/4}$ vicinal coupling constant in the minor product **19a** to be 8.40 Hz, which was comparable to the values observed for *threo* products in Baltas's report. Since *m*-CPBA epoxidation of **15** provided the modest diastereomeric ratio, allylic alcohol substrate **15** may not be suitable for gram-scale synthesis. In addition, although our reported preparation of **15** is efficient, it is somewhat lengthy and requires the use of some relatively expensive reagents,[16] leading us to screen another method to efficiently access the requisite β-epoxide.

Synthesis of the modified epoxidation precursor, *Z*-allylic alcohol **18**, began with conversion of D-mannitol to known allylic alcohol **20** in 4 steps in a 10-gram scale via the key Wittig olefination following a protocol reported by Baltas et al.[13] and Chu et al.[15] (Scheme 3). Allylic alcohol **20** was then transformed to diol **22** in 2 steps via benzoylation to give benzoate ester **21** in 89% yield, followed by acetonide deprotection by treatment with 2 M HCl in acetonitrile. The next task was regioselective protection of primary alcohol of diol **22** with a *p*-metheoxybenzyl (PMB) group. We decided to convert diol **22** to stannylene acetal by using dibutyltin oxide, followed by employment of PMBCl in the presence of tetrabutylammonium bromide (TBAB) to provide the desired PMB ether **18** in 71% yield along with 24% of undesired PMB ether regioisomer.[17] It should be noted that using typical conditions for PMB protection (NaH, PMBCl) or using the more reactive 4-methoxybenzyl 2,2,2-trichloroacetimidate[18] gave the undesired PMB ether regioisomer as a major product. Next, *m*-CPBA epoxidation of allylic alcohol **18** was then performed to give inseparable

diastereomeric epoxy alcohols in 78% combined yield. We decided to elaborate this mixture to epoxy alcohols **19a** and **19b** in order to determine the stereoselectivity outcome compared to Method I. Ensuing 2-step transformations, including TBDPS protection and methanolysis, proceeded smoothly to give separable epoxy alcohol diastereomers **19a** and **19b** in a combined 79% yield and an excellent diastereomeric ratio of 16:1, in which ¹H and ¹³C NMR spectroscopic data as well as retention factor values (0.57 and 0.38 in 2% EtOAc/CH₂Cl₂) of **19a** and **19b** from these conditions were identical to those of epoxy alcohol products from Method I.

According to contrastively observed results from Methods I and II, we therefore proposed the conformational models to rationalize the stereoselectivity observed in each chiral substrate based on Sharpless model, which requires conformation alignment of the O–C–C=C dihedral angle (α) estimated to be 120° (Scheme 4).[19] In the case of chiral allylic alcohol substrate **18** (Method II), the major product, β-epoxide **23 erythro**, would result from *m*-CPBA epoxidation directed by the adjacent chiral hydroxyl group via the lower-energy transition state **TS1** due to minimization of 1,3-allylic strain[20] whereas the other transition state **TS2** leading to α-epoxide **23 threo** would suffer from 1,3-allylic strain. On the other hand, *m*-CPBA epoxidation of allylic alcohol substrate **15** bearing adjacent (*S*)-silyloxy stereogenic center provided a reversed diastereoselectivity. Since the allylic hydroxyl group of **15** contains no chiral entity to differentiate the facial selectivity of epoxidation via hydrogen bonding, we proposed that the observed stereoselectivity in the epoxidation of **15** would derive from the minimization of 1,3-allylic strain controlled by the bulky adjacent silyloxy stereogenic center as shown in transition states **TS3** and **TS4**. **TS4** would be preferred due to the minimized 1,3-allylic strain compared to **TS3**
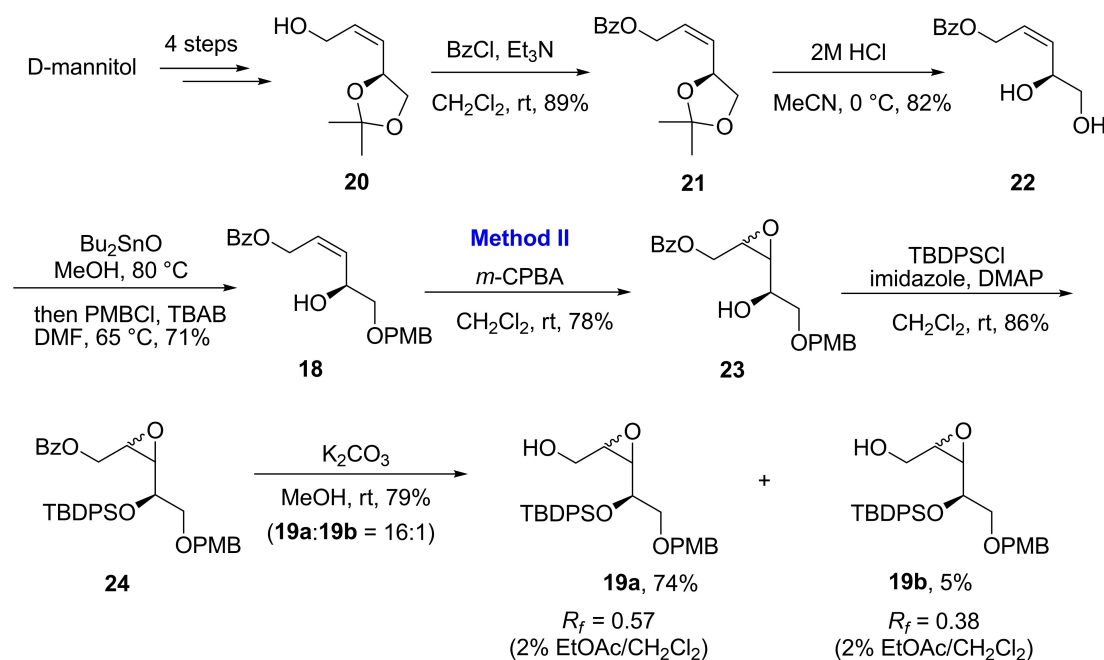
Scheme 3. Synthesis of *Z*-allylic alcohol **18** and *m*-CPBA epoxidation of *Z*-allylic alcohol **18** using Baltas's protocol (Method II).

EurJOC
European Journal of Organic Chemistry

Research Article
doi.org/10.1002/ejoc.202300034

Chemistry
Europe
European Chemical
Societies Publishing
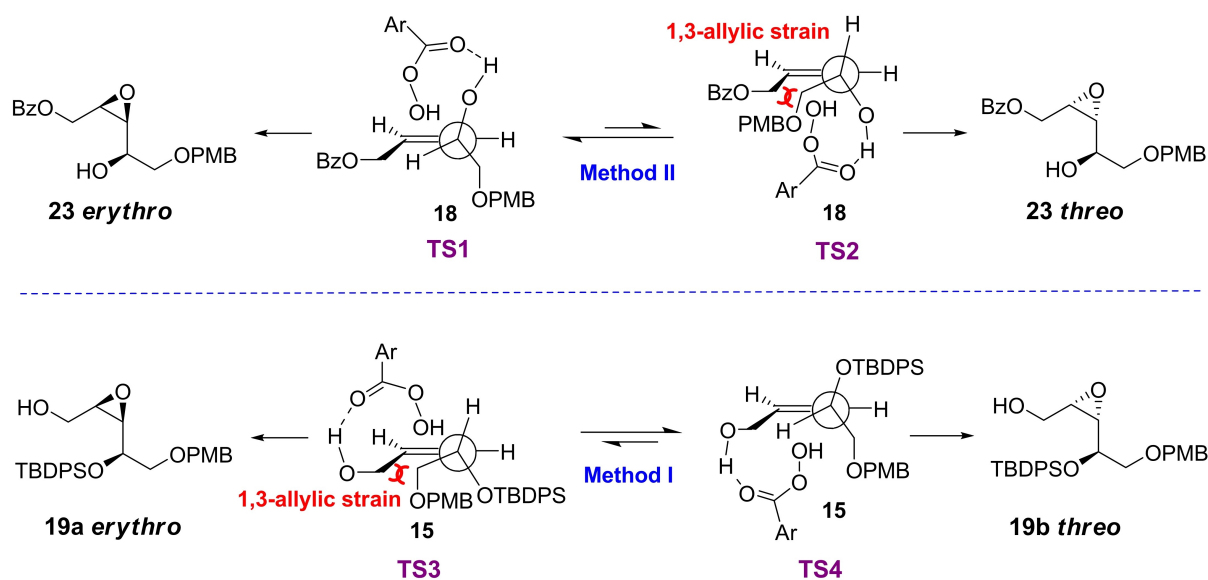
Scheme 4. Proposed rationale for observed diasteroselectivities in the epoxidation of Z-allylic alcohols **15** (Method I) and **18** (Method II).

rendering the epoxidation to occur on the alkene face opposite to the bulky OTBDPS group and delivered α-epoxide **19b** *threo* as a major product. This proposed rationale would be contradictory to the previously reported results by the Baltas group. To verify our proposed rationale, we therefore converted the minor epoxy alcohol **19b** to Baltas's epoxy alcohol intermediate (**17a** or **17b**) in 4 steps (Scheme S1A in the Supporting Information). To our surprise, the ^{1}H and ^{13}C NMR data of this derivative matched those reported by the Baltas group for 'erythro' intermediate **17a** which was their major product. In addition, we further converted the major epoxy alcohol **19a** to Baltas's intermediate (Scheme S1B in the Supporting Information) and found that the ^{1}H and ^{13}C NMR data of this compound were identical to those reported for the minor 'threo' product by the Baltas group. Even though the absolute configuration of each epoxy alcohol could not be unambiguously confirmed at this stage, we were certain, based on these results, that the α-epoxide *threo* product would predominate from *m*-CPBA

epoxidation of Z-allylic alcohol containing (S)-α-silyloxy stereogenic center for example **15**. Thus, we decided to proceed with epoxy alcohol **19a**, a major diastereomer from Method II, due to its availability in larger quantity and the excellent *erythro* diastereoselectivity rationalized above.

With the proposed β-epoxy alcohol **19a** in hand, we then proceeded to assemble the key fragments as shown in Scheme 5. β-Epoxy alcohol **19a** was subjected to oxidation mediated by IBX to yield the requisite epoxy aldehyde **14** in 81% yield. The next task was coupling of chiral epoxy aldehyde **14** with known alkyne **13** via acetylide addition. Epoxy aldehyde **14** was exposed to a premixed solution of alkyne **13** and *n*-butyl lithium at -78°C in THF. After warming to 0°C for 2 h, propargylic alcohols **12a** and **12b** were obtained in respective 21% and 56% yields upon purification by column chromatography. The absolute configuration of the newly formed alcohol stereogenic center of each diastereomer was assigned by Mosher's ester analysis. Although the β-epoxide moiety of **14**
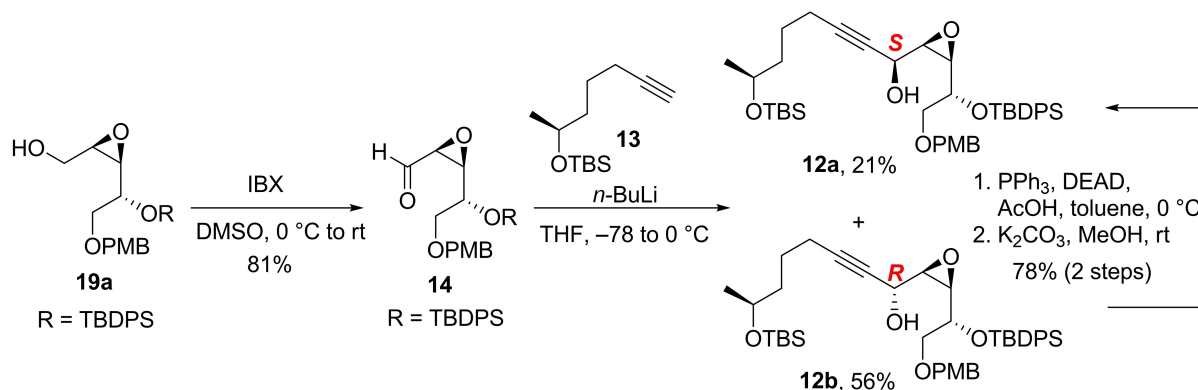
Scheme 5. Coupling of the key fragments **13** and **14**.

Research Article
doi.org/10.1002/ejoc.202300034

did not lead to the desired (S)-propargylic alcohol **12a** as a major product as anticipated, we were delighted to find that the undesired (R)-propargylic alcohol **12b** could be smoothly transformed to **12a** in 2 steps via Mitsunobu inversion[12] with acetic acid, followed by methanolysis. Attempts to perform this coupling in asymmetric fashion using Trost's asymmetric Zn-mediated alkynylation[21] were unsuccessful in our hands as substrates **13** and **14** were inert to such conditions.

Having successfully obtained the requisite chiral propargylic alcohol **12a**, we next continued to complete the synthesis of seiricuprolide (**4**) using our previously established sequence[9] as shown in Scheme 6. The synthesis commenced with Z-selective reduction of propargylic alcohol **12a**, which was carried out via Lindlar hydrogenation in ethyl acetate to exclusively furnish Z-allylic alcohol **25** in 89% yield. The Z-geometry of **25** was confirmed on the basis of a coupling constant of 10.8 Hz between H8 and H9. Subsequent protection of allylic alcohol of **25** with TBDPSCl provided silyl ether **26** in 88% yield. The next task was to install the requisite 2-carbon α,β-unsaturated ester fragment which was performed in 3 steps. Removal of a PMB protecting group of **26** by treatment with DDQ afforded primary alcohol **27** in 85% yield. Subsequent oxidation of **27** mediated by Dess-Martin periodinane, followed by Wittig olefination with Ph$_3$P=CHCO$_2$Et furnished (E)-α,β-unsaturated ester **28** as a single isomer in excellent 85% yield over 2 steps. The E-geometry of the newly formed olefin was verified by a coupling constant of 15.5 Hz between H2 and H3. With the advanced intermediate with all 14 carbons of seiricuprolide in

hand, our remaining task was to elaborate **28** to the macro-lactonization precursor, seco acid **10**. Ester **28** was then subjected to selective deprotection of TBS protecting group using 4 equivalents of weakly acidic PPTS to give alcohol **29** in 84% yield. Gratifyingly, the β-epoxide remained untouched and deprotection of TBDPS protecting groups was not observed. Ensuing ester hydrolysis and acidic workup also smoothly furnished seco acid **10** in 77% yield without affecting the epoxide moiety. Shiina macrolactonization of seco acid **10** was then performed using 2-methyl-6-nitrobenzoic anhydride (MNBA) in the presence of 6 equivalents of DMAP in toluene at room temperature to achieve macrolactone **30** in 65% yield. Final global deprotection of **30** was achieved using our established conditions i.e. 10 equivalents of TBAF buffered with AcOH (4 mol%) in THF at 60 °C to provide seiricuprolide (**4**) in 49% yield as a white solid along with monoprotected analogue **31** (12%). The ^{1}H and ^{13}C NMR spectroscopic data as well as the melting point of synthetic **4** were identical to those reported for natural **4**.[7] Moreover, a specific rotation of synthetic **4** as $[\alpha]_D^{25} = +48.12$ (c 2.70, MeOH) was in good agreement with the reported value for natural product **4** ($[\alpha]_D^{20} = +40$, c 2.7, MeOH),[11] which unambiguously confirmed the absolute configuration of β-epoxide intermediate **19a** and verified our rationale for the diastereoselectivity of m-CPBA epoxidation. Remarkably, β-epoxide **19a** proved to be a very robust substrate for the total synthesis, leading us to utilize **12a** for completion of the other targeted natural product pestalotioprolide B.
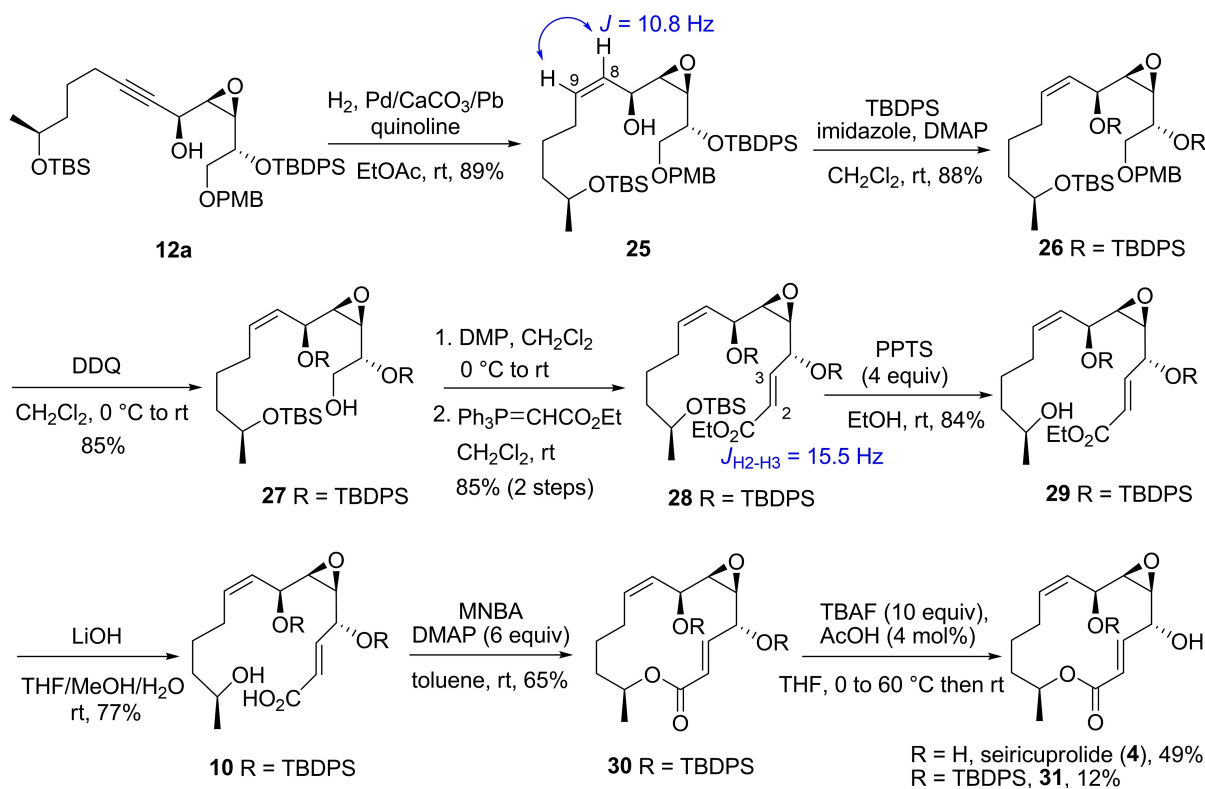
Scheme 6. Completion of synthesis of seiricuprolide (**4**).

EurJOC
European Journal of Organic Chemistry

Research Article
doi.org/10.1002/ejoc.202300034

Chemistry Europe
European Chemical Societies Publishing

Our attention focused then on completion of synthesis of pestalotioprolide B (**2**). The synthesis began with optimization of *E*-selective reduction of propargylic alcohol **12a** mediated by sodium(2-methoxyethoxy)aluminium hydride (Red-Al) as a reducing agent (Table 1). Propargylic alcohol **12a** was initially treated with 1.2 or 3.0 equivalents of Red-Al in THF from 0 °C to room temperature (entries 1 and 2).[22] Disappointingly, these conditions gave no desired product, and the starting material was recovered. Increasing Red-Al to 5 equivalents under the same conditions provided an inseparable mixture of the desired **32** and overreduced product **33** in 53 % combined yield and a ratio of 1:2.1 as determined by ^{1}H NMR spectroscopy (entry 3). Further optimization was then performed by changing the solvent to toluene (entry 4) or ether (entry 5) under the same conditions as entry 3. Unfortunately, only the starting material **12a** was observed from both conditions. These results suggested that THF should be the appropriate solvent for Red-Al-mediated reduction of **12a**. Formation of overreduced product **33** observed in entry 3 thus prompted us to perform this reaction at lower temperature. After slowly warming the reaction mixture from −30 °C to 0 °C for 6.5 h, no undesired overreduced product **33** was obtained under these conditions and the desired **32** was observed (40 %) along with unreacted starting material **12a** (39 %) as an inseparable 1:1 mixture as determined by ^{1}H NMR spectroscopy (entry 6).[23] Further optimization was then performed by slightly increasing the reaction temperature to 4 °C. Gratifyingly, after maintaining the reaction at this temperature for 5 h, starting **12a** was completely consumed and the desired *E*-allylic alcohol **32** was observed in 74 % yield without the overreduced counterpart. The *E*-geometry of **32** was again confirmed by a coupling constant of 15.5 Hz between H8 and H9.

With the requisite intermediate **32** in hand, the remaining installation of (*E*)-α,β-unsaturated ester as well as the construction of macrocyclic core of **5** were accomplished by transformation of **32** to **38** in 7 steps via the same synthetic sequence established in the synthesis of **4**. The global deprotection of **38** was also performed under the same conditions employed for **4** to deliver expected **5** in slightly

higher yield (56 %) as a white solid (Scheme 7). The ^{1}H and ^{13}C NMR spectroscopic data as well as HRMS data and melting point of synthetic **5** were in excellent agreement with those reported for natural **5**.[11] Moreover, the observed specific rotation of synthetic **5**, $[\alpha]_D^{25} = +75.96$ (*c* 1.00, CHCl$_3$), was essentially identical to that of natural product **5**, ($[\alpha]_D^{20} = +72$, *c* 1.0, CHCl$_3$).[11] These results once again verified the absolute configuration of β-epoxide intermediate **19a**, thereby rendering its diastereomer **19b** an α-epoxide antipode.

Our research group has recently reported the in vitro cytotoxic activity of synthetic analogues of **4** and **5**, i.e. nigrosporolide (**7**), (4*S*,7*S*,13*S*)-4,7-dihydroxy-13-tetradeca-2,5,8-trienolide (**8**) and mutolide (**9**) against three human cancer cell lines including HCT116 colorectal carcinoma, MCF-7 breast adenocarcinoma and Calu-3 lung adenocarcinoma using the MTT assay.[9] It was discovered that synthetic mutolide (**9**) was significantly active against the HCT116 colon cancer cells (IC$_{50}$ = 12 μM) and was essentially inactive against the other two cell lines (IC$_{50}$ > 50 μM), whereas macrolactone analogues **7** and **8** showed no cytotoxic effects on all three cancer cell lines tested. Therefore, the HCT116 colon cancer cell line was selected for screening of cytotoxic activity of synthetic **4** and **5** (Figure S75 in the Supporting Information). In addition, cytotoxicity against non-cancerous (Vero) cells of **4** and **5** was evaluated using MTT assay (Figure S76 in the Supporting Information). The dose-response experiments of compounds **4** and **5** were then performed on both cell lines at 0, 10, 20, 50 and 100 μM at 24, 48 and 72 h of incubation. It was found that both compounds showed no cytotoxic effects on the HCT116 colon cancer cells even at 100 μM and prolonged incubation time of 72 h. Similar results were observed for seiricuprolide (**4**) on Vero cells viability, whereas pestalotioprolide B (**5**) inhibited the viability of Vero cells in a more dose-dependent manner. The latter observation suggested that macrolide **5** was more cytotoxic to Vero cells to other related analogues **4** and **7–9**. On the basis of the cytotoxic activity results, it can be roughly concluded that the β-epoxide moiety at C5–C6 of this group of macrolides suppressed the cytotoxicity against HCT116 cancer cells. This preliminary structure-activity relationship is in accordance with

Table 1. Optimization of *E*-selective reduction of propargylic alcohol **12a** mediated by Red-Al.

entry	Red-Al (equiv.)	solvent	temp	time [h]	results
1	1.2	THF	0 °C to rt	6	no reaction
2	3.0	THF	0 °C to rt	20	no reaction
3	5.0	THF	0 °C to rt	4.5	**32:33** = 1:2.1 (53 % combined yield)
4	5.0	toluene	0 °C to rt	5	no reaction
5	5.0	ether	0 °C to rt	5	no reaction
6	5.0	THF	−30 °C to 0 °C	6.5	**32** (40 %)[a] and **12a** (39 %)[a]
7	5.0	THF	4 °C	5	**32** (74 % yield)

[a] Determined by the integration ratio of ^{1}H NMR data.

EurJOC
European Journal of Organic Chemistry

Research Article
doi.org/10.1002/ejoc.202300034

Chemistry Europe
European Chemical
Societies Publishing
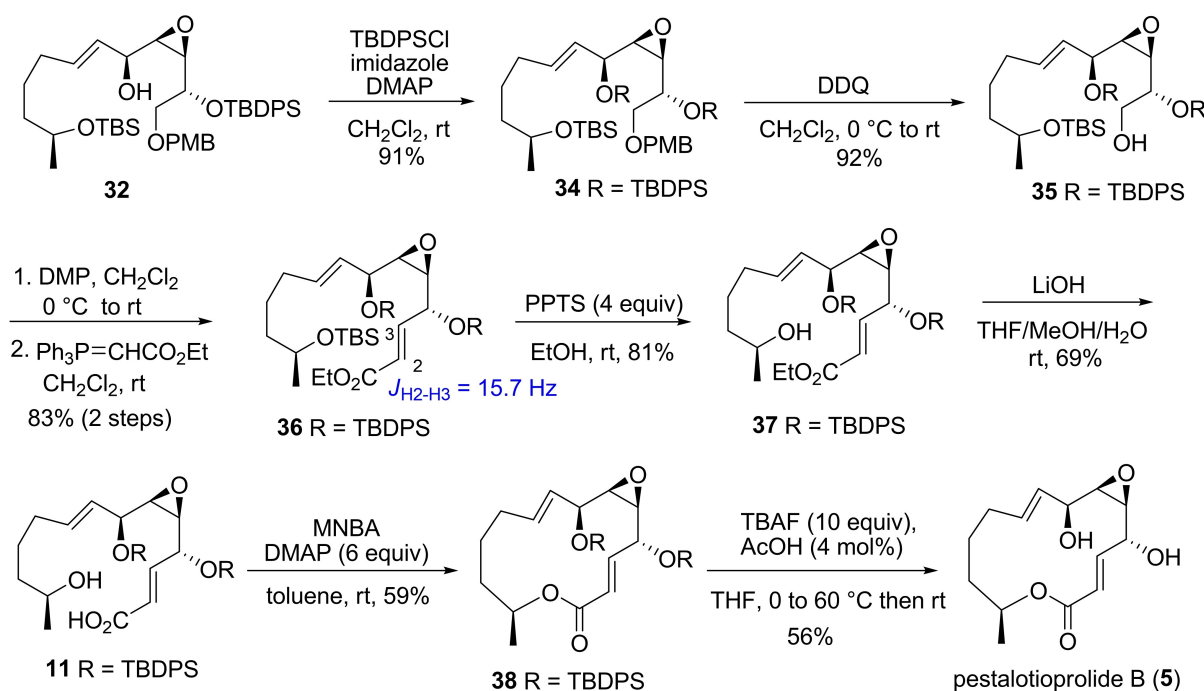
Scheme 7. Completion of synthesis of pestalotioprolide B (**5**).

Liu and Proksch's report that the β-epoxide group of natural products **4** and **5** decreased cytotoxic activities against the L5178Y mouse lymphoma cells compared to natural products **7** and **8** which possess the Z-olefin at this emplacement.[11]

Synthetic seiricuprolide (**4**) and pestalotioprolide B (**5**) were further subjected to evaluation on inhibitory activity on cystic fibrosis transmembrane regulator (CFTR)-mediated chloride secretion in human intestinal epithelial (T84) cells using short-circuit current analysis (I_{sc}). Our group has also recently disclosed the CFTR inhibitory activity of synthetic macrolide **7**–**9**, in which mutolide (**9**) showed stronger inhibition (~70% inhibition) compared to analogues **7** (40% inhibition) and **8** (30% inhibition) at the same concentration of 5 μM.[9] Disappointingly, synthetic **4** and **5** were found to show no effects on CFTR-mediated chloride secretion in T84 cells stimulated by forskolin (a cAMP donor) at both 5 and 10 μM compared to a positive control, CFTR(inh)-172 (Figure S77 in the Supporting Information). Therefore, the β-epoxide moiety of macrolides **4** and **5** apparently suppressed the CFTR inhibitory activity compared to compounds **7** and **8**, which are their C5–C6 Z-olefin counterparts.

Conclusion

In conclusion, we have accomplished the first and convergent total synthesis of seiricuprolide (**4**) and pestalotioprolide B (**5**) starting from known alkyne **13** and chiral Z-allylic alcohol **18**, in which **18** derived from D-mannitol, an inexpensive and commercially available chiral building block. The synthetic macrolides **4** and **5** were achieved in a longest linear sequence

of 17 steps and a total of 19 steps in 1.9 and 1.6% overall yields, respectively. The key strategies for our synthesis included Shiina macrolactonization to construct 14-membered skeleton, Wittig olefination to generate the (E)-α,β-unsaturated ester segment and selective reduction of propargylic alcohol to form Z- or E-olefin at C8–C9 for **4** and **5**. Our work also highlighted a highly stereoselective substrate-controlled m-CPBA epoxidation to install the C5–C6 β-epoxide at the early stage, which reaffirmed the remarkable robustness of this β-epoxide moiety of both natural products. Synthetic macrolides **4** and **5** were evaluated for their cytotoxic activity against the HCT116 colon cancer cells as well as their inhibitory effect on CFTR in human intestinal epithelial (T84) cells. These two synthetic macrolides were found to possess no reactivity of both biological activities tested. Preliminary structure-activity relationship suggested that the C5–C6 β-epoxide moiety of both **4** and **5** suppressed the cytotoxic activity against the HCT116 colon cancer cells as well as their CFTR inhibitory effect.

Experimental Section

General Information: Unless otherwise stated, all reactions were performed under a nitrogen or argon atmosphere in oven- or flamed-dried glassware. Solvents were used as received from suppliers or distilled before use using standard procedures. All other reagents were obtained from commercial sources and used without further purification. Column chromatography was carried out on Silica gel 60 (0.063–0.200 mm, Merk). Thin-layer chromatography (TLC) was carried out on Silica gel 60 F_{254} plates (Merk). ^{1}H, ^{13}C and 2D NMR spectroscopic data were recorded on 300 or 500 MHz Bruker FT NMR Ultra Shield spectrometers. Chemical shifts (δ) in the ^{1}H and ^{13}C NMR spectra are reported in ppm relative to

EurJOC
European Journal of Organic Chemistry

Research Article
doi.org/10.1002/ejoc.202300034

Chemistry Europe
European Chemical Societies Publishing

internal tetramethylsilane. The data are presented as follows: chemical shift, multiplicity (s = singlet, d = doublet, t = triplet, m = multiplet, br = broad), coupling constant(s) in hertz (Hz), and integration. Infrared (IR) spectra were recorded with a Perkin-Elmer 783 FTS165 FTIR spectrometer. High-resolution mass spectra were obtained on a Ultra-Performance Liquid Chromatography-High Resolution Mass Spectrometer (Agilent LC-QTOF 6500 system), Mae Fah Luang University or a High-Performance Liquid Chromatograph–Mass Spectrometer (Shimadzu LCMS-IT-TOF Model LC-20ADXR), Thammasat University. Melting points were measured using an Electrothermal IA9200 melting point apparatus and are uncorrected. The optical rotations were recorded on a JASCO P-2000 polarimeter. All cell lines for biological assay were purchased from the American Type Culture Collection (ATCC). Detailed experimental procedure, full characterization data and NMR spectra of new compounds can be found in the Supporting Information.

Cytotoxic Assay: evaluation of cytotoxic activity against the HCT116 colon cancer cell line and non-cancerous (Vero) cells of **4** and **5** was performed using 3-(4,5-dimethyl-2-thiazolyl)-2,5-diphenyl-2H-tetrazolium bromide (MTT) assay following the procedure previously described by our research group (cell viability assay for **7–9**).[9]

CFTR Inhibition Assay: inhibitory effect on CFTR in human intestinal epithelial (T84) cells of **4** and **5** was measured using short-circuit current analysis following the procedure previously described by our research group (for CFTR inhibition of **7–9**[9] or a fungal metabolite zearalenone[25]).

Acknowledgements

Conflict of Interest

The authors declare no conflict of interest.

Data Availability Statement

The data that support the findings of this study are available in the supplementary material of this article.

[1] a) G. G. Zhanel, M. Dueck, D. J. Hoban, L. M. Vercaigne, J. M. Embil, A. S. Gin, J. A. Karlowsky, *Drugs* **2001**, *61*, 443–498; b) A. Janas, P. Przybylski, *Eur. J. Med. Chem.* **2019**, *182*, 111662; c) H. Zhang, J. Zou, X. Yan, J. Chen, X. Cao, J. Wu, Y. Liu, T. Wang, *Mar. Drugs* **2021**, *19*, 180.

[2] a) W. A. Ayer, S. P. Lee, A. Tsuneda, Y. Hiratsuka, *Can. J. Microbiol.* **1980**, *26*, 766–773; b) D. T. Wicklow, A. M. Jordan, J. B. Gloer, *Mycol. Res.* **2009**, *113*, 1433–1442; c) C. A. McLellan, T. J. Turbyville, E. M. K. Wijeratne, A. Kerschen, E. Verling, C. Queitsch, L. Whitesell, A. A. L. Gunatilaka, *Plant Physiol.* **2007**, *145*, 174–182; d) M. Isaka, C. Suyarnsestakorn, M. Tanticharoen, *J. Org. Chem.* **2002**, *67*, 1561–1566.

[3] M. Isaka, P. Chinthanom, S. Veeranondha, S. Supothina, J. J. Luangsa-ard, *Tetrahedron* **2008**, *64*, 11028–11033.

[4] M. Arai, K. Yamanoto, I. Namatame, H. Tomoda, S. Omura, *J. Antibiotica* **2003**, *6*, 526–533.

[5] a) J. S. Isaacs, W. Xu, L. Neckers, *Cancer Cell* **2003**, *3*, 213–217; b) S. V. Sharma, T. Agatsuma, H. Nakano, *Oncogene* **1998**, *16*, 2639–2645.

[6] a) M. Lampilas, R. Lett, *Tetrahedron Lett.* **1992**, *33*, 777–780; b) I. Tichkowsky, R. Lett, *Tetrahedron Lett.* **2002**, *43*, 4003–4007; c) R. M. Gabaccio, S. J. Stachel, D. K. Baeschlin, S. J. Danishefsky, *J. Am. Chem. Soc.* **2001**, *123*, 10903–10908; d) P. Sellès, R. Lett, *Tetrahedron Lett.* **2002**, *43*, 4621–4625; e) P. Sellès, R. Lett, *Tetrahedron Lett.* **2002**, *43*, 4627–4631.

[7] A. Ballio, A. Evident, A. Graniti, G. Randazzo, L. Sparapano, *Phytochemistry* **1988**, *27*, 3117–3121.

[8] C. Bartolucci, S. Cerrini, D. Lamba, A. Evidente, G. Randazzo, *Acta Crystallogr.* **1992**, *C48*, 83–86.

[9] A. Thiraporn, N. Saikachain, R. Khumjiang, C. Muanprasat, K. Tadpetch, *Chem. Asian J.* **2022**, *17*, e202200329.

[10] V. Rukachaisirikul, A. Rodglin, S. Phongpaichit, J. Buatong, J. Sakayaroj, *Phytochem. Lett.* **2012**, *5*, 13–17.

[11] S. Liu, H. Dai, G. Makhloufi, C. Heering, C. Janiak, R. Hartmann, A. Mándi, T. Kurtán, W. E. G. Müller, M. U. Kassack, W. Lin, Z. Liu, P. Proksch, *J. Nat. Prod.* **2016**, *79*, 2332–2340.

[12] J. Li, S. Park, R. L. Miller, D. Lee, *Org. Lett.* **2009**, *11*, 571–574.

[13] C. H. Sugisaki, Y. Ruland, M. Baltas, *Eur. J. Org. Chem.* **2003**, *2003*, 672–688.

[14] N. Minami, S. S. Ko, Y. Kishi, *J. Am. Chem. Soc.* **1982**, *104*, 1109–1111.

[15] Y. Zhao, T. Yang, M. Lee, D. Lee, M. G. Newton, C. K. Chu, *J. Org. Chem.* **1995**, *60*, 5236–5242.

[16] A. Thiraporn, P. Iawsipo, K. Tadpetch, *Synlett* **2022**, *33*, 1341–1346.

[17] A. Gucchait, M. Kundu, A. K. Misra, *Synthesis* **2021**, *53*, 3613–3620.

[18] K. Ikeuchi, K. Murasawa, H. Yamada, *Synlett* **2019**, *30*, 1308–1312.

[19] a) B. E. Rossiter, T. R. Verhoeven, K. B. Sharpless, *Tetrahedron Lett.* **1979**, *20*, 4733–4736; b) A. S. Narula, *Tetrahedron Lett.* **1983**, *24*, 5421–5424; c) W. Adam, V. R. Stegmann, C. R. Saha-Möller, *J. Am. Chem. Soc.* **1999**, *121*, 1879–1882; d) M. Freccero, R. Gandolfi, M. Sarzi-Amadè, A. Rastelli, *J. Org. Chem.* **2000**, *65*, 2030–2042; e) R. K. Bressin, S. Osman, I. Pohorilets, U. Basu, K. Koide, *J. Org. Chem.* **2020**, *85*, 4637–4647.

[20] R. W. Hoffmann, *Chem. Rev.* **1989**, *89*, 1841–1860.

[21] a) B. M. Trost, A. H. Weiss, A. J. von Wangelin, *J. Am. Chem. Soc.* **2006**, *128*, 8–9; b) B. M. Trost, A. H. Weiss, *Org. Lett.* **2006**, *8*, 4461–4464; c) B. M. Trost, M. J. Bartlett, A. H. Weiss, A. J. von Wangelin, V. S. Chan, *Chem. Eur. J.* **2012**, *18*, 16498–16509.

[22] J. Li, S. Park, R. L. Miller, D. Lee, *Org. Lett.* **2009**, *11*, 571–574.

[23] a) B. J. Albert, A. Sivaramanabhan, T. Naka, N. L. Czaicki, K. Koide, *J. Am. Chem. Soc.* **2007**, *129*, 2648–2659; b) C. T. Meta, K. Koide, *Org. Lett.* **2004**, *6*, 1785–1787.

[24] T. R. Hoye, C. S. Jeffrey, F. Shao, *Nat. Protoc.* **2007**, *2*, 2451–2458.

[25] P. Muangnil, S. Satitsri, K. Tadpetch, P. Saparpakorn, V. Chatshuthipong, S. Hannongbua, V. Rukachaisirikul, C. Muanprasat, *Biochem. Pharmacol.* **2018**, *150*, 293–304.

^{1}H and ^{13}C NMR spectra

Figure 10 ^{1}H NMR (300 MHz, CDCl$_3$) spectrum of compound **27**
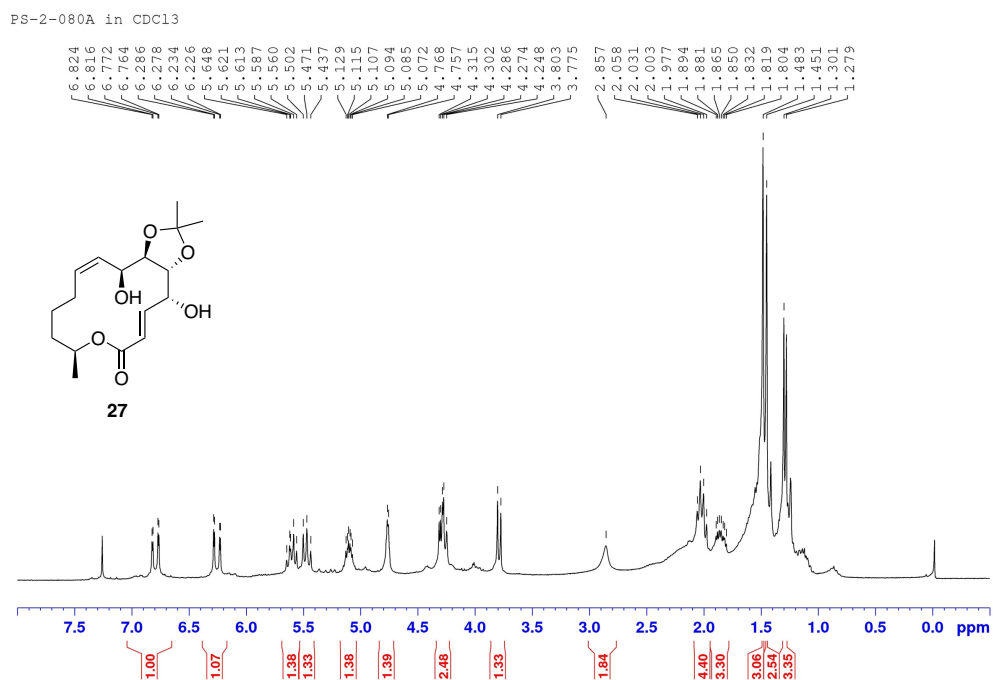
Figure 11 ^{13}C NMR (75 MHz, CDCl$_3$) spectrum of compound **27**
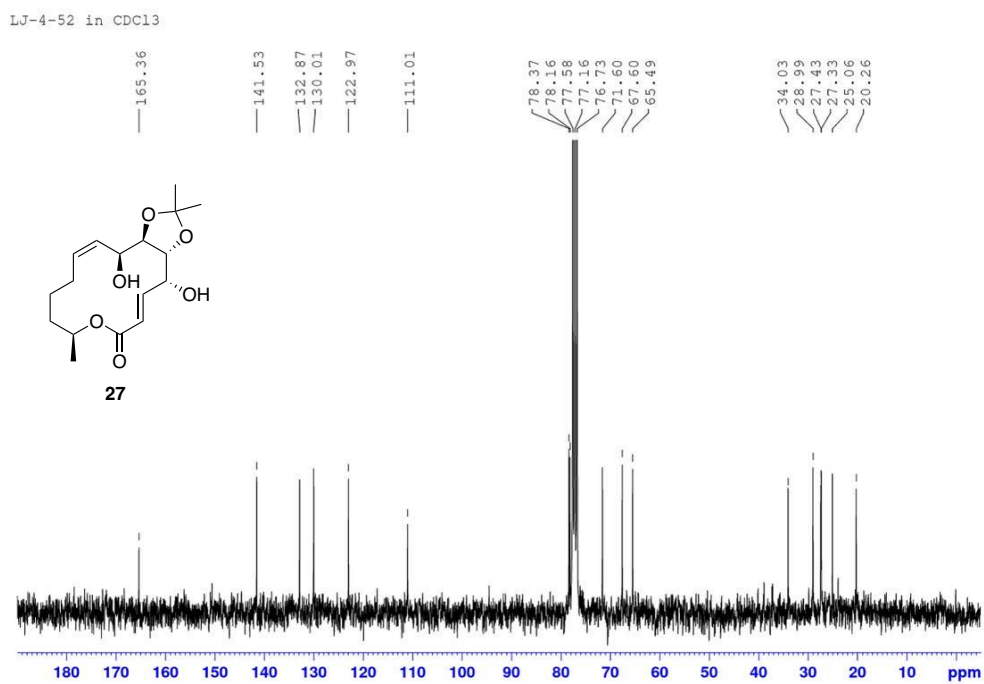
Figure 12 ^{1}H NMR (300 MHz, CDCl$_3$) spectrum of compound **28**
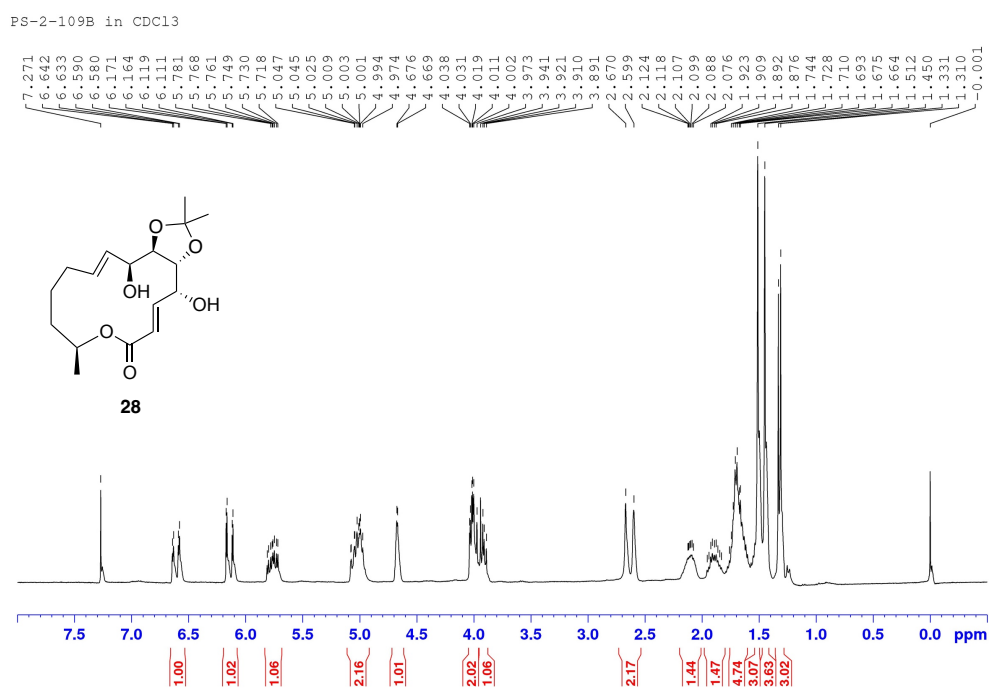
Figure 13 ^{13}C NMR (75 MHz, CDCl$_3$) spectrum of compound **28**
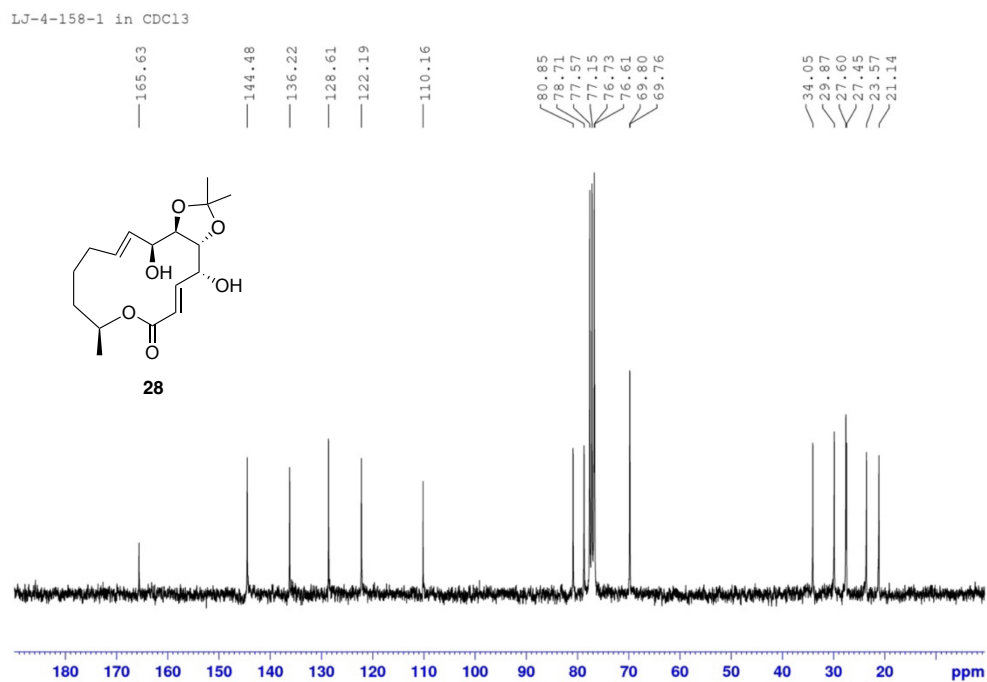
Figure 14 ^{1}H NMR (300 MHz, CDCl$_3$) spectrum of compound **102**
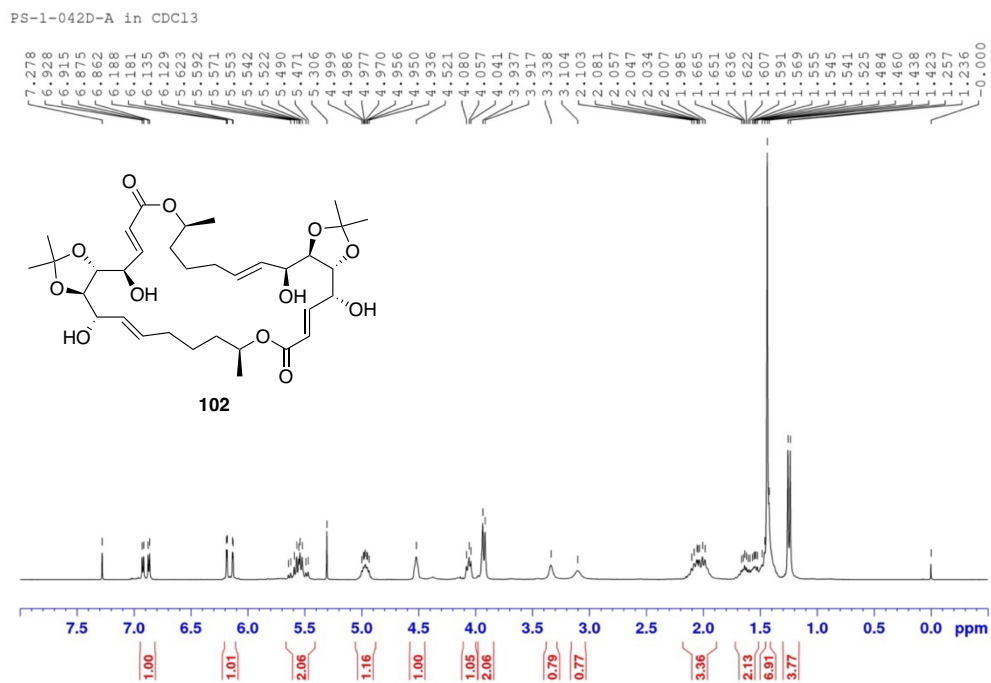
Figure 15 ^{13}C NMR (75 MHz, CDCl$_3$) spectrum of compound **102**
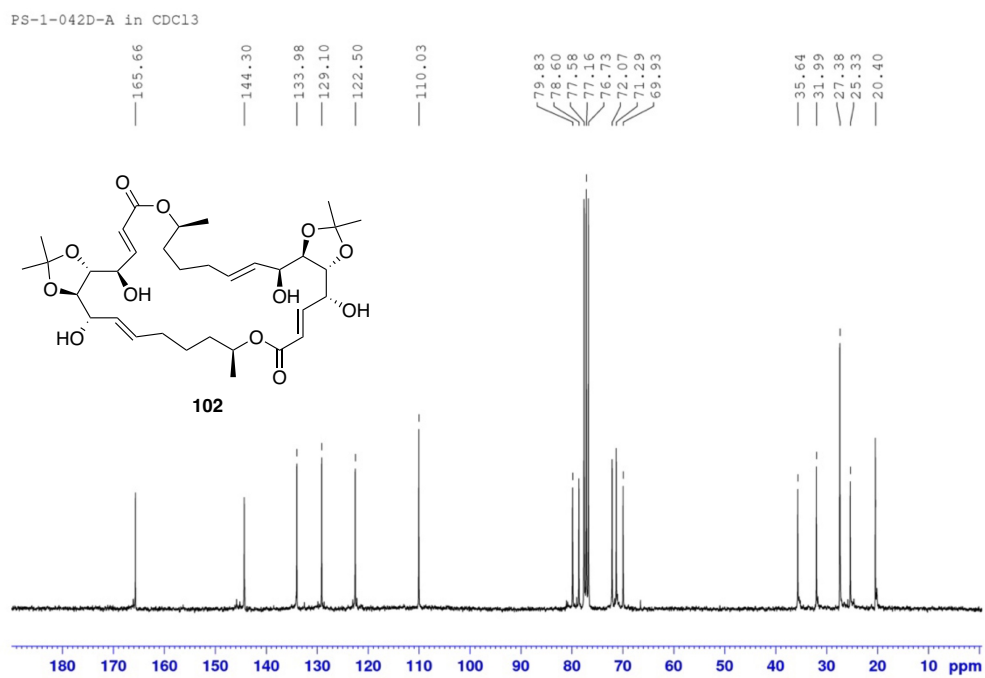
Figure 16 ¹H NMR (300 MHz, CDCl₃) spectrum of compound **103**
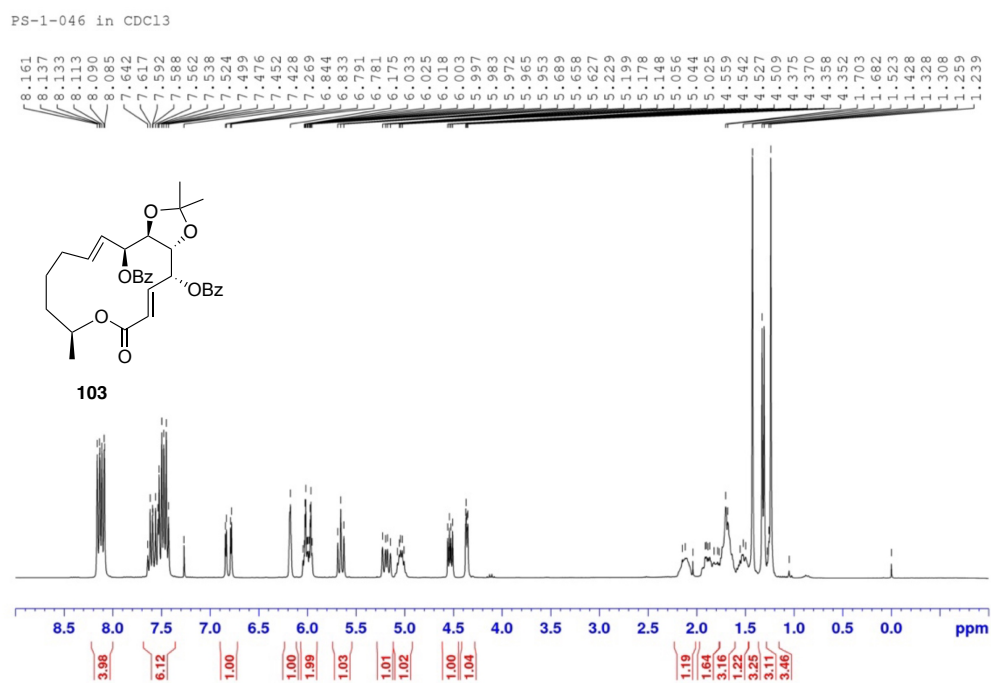
Figure 17 ¹³C NMR (75 MHz, CDCl₃) spectrum of compound **103**
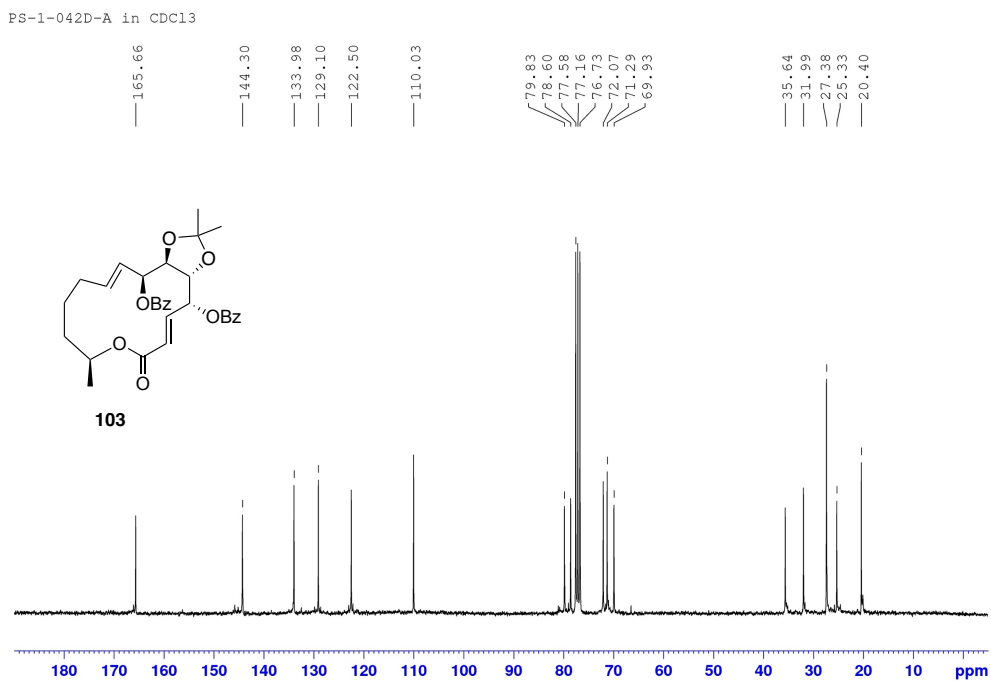
Figure 18 ^{1}H NMR (300 MHz, CDCl$_3$) spectrum of compound **104**
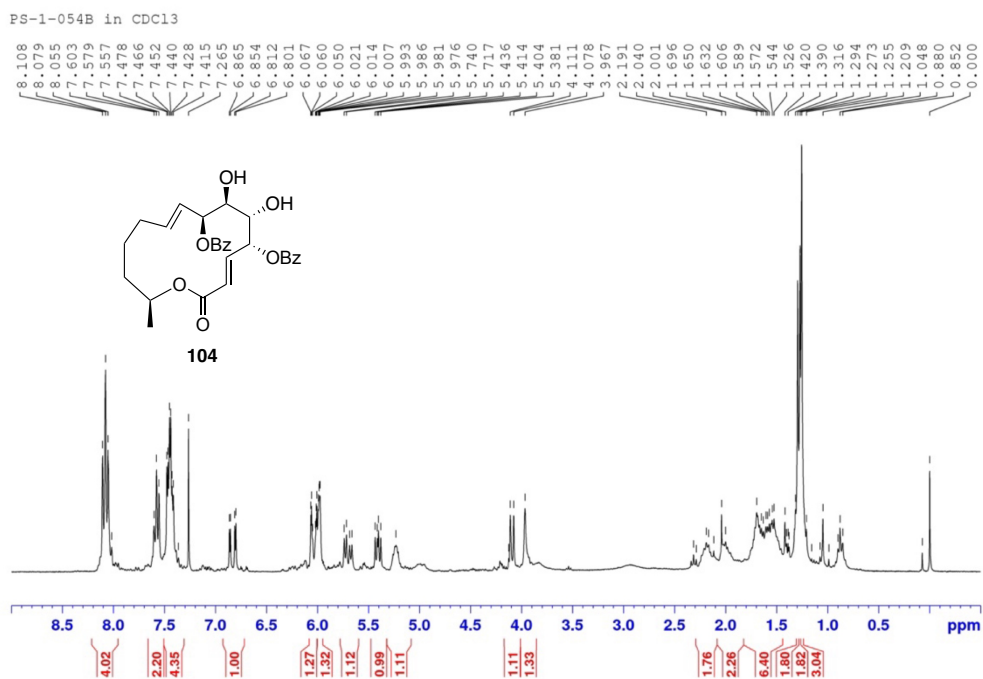
Figure 19 ^{13}C NMR (75 MHz, CDCl$_3$) spectrum of compound **104**
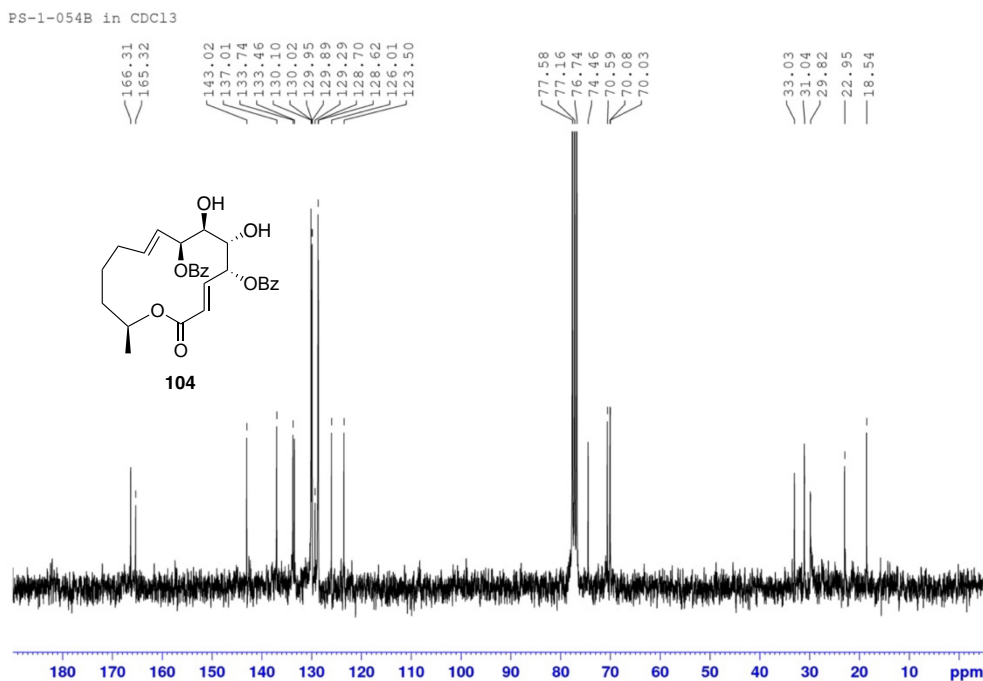
Figure 20 ^{1}H NMR (300 MHz, CDCl$_3$) spectrum of compound **110**
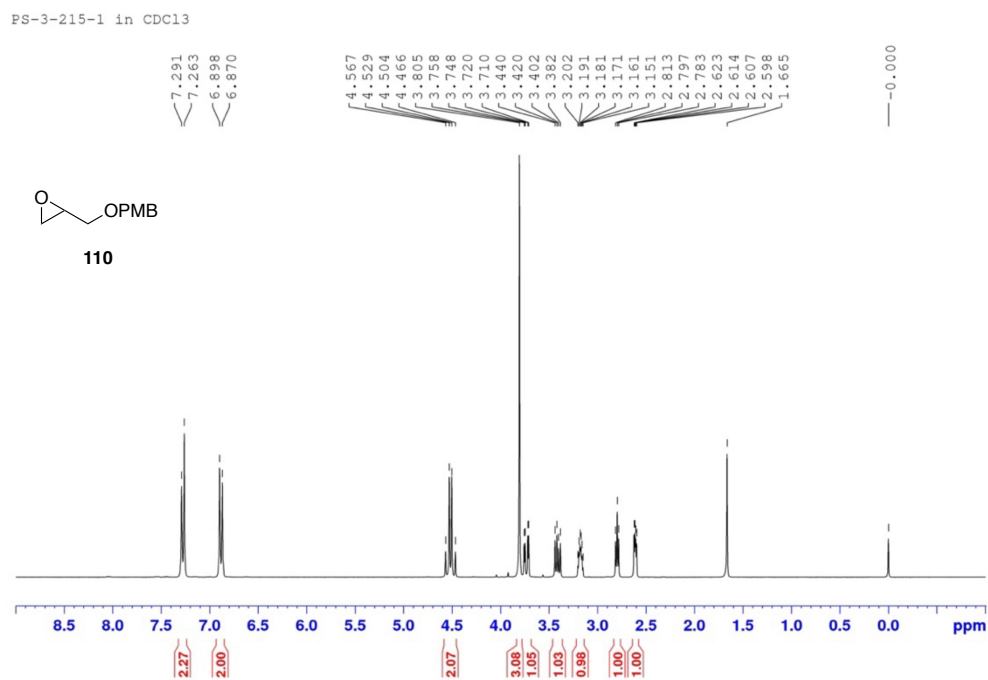
Figure 21 ^{1}H NMR (300 MHz, CDCl$_3$) spectrum of compound **110*S***
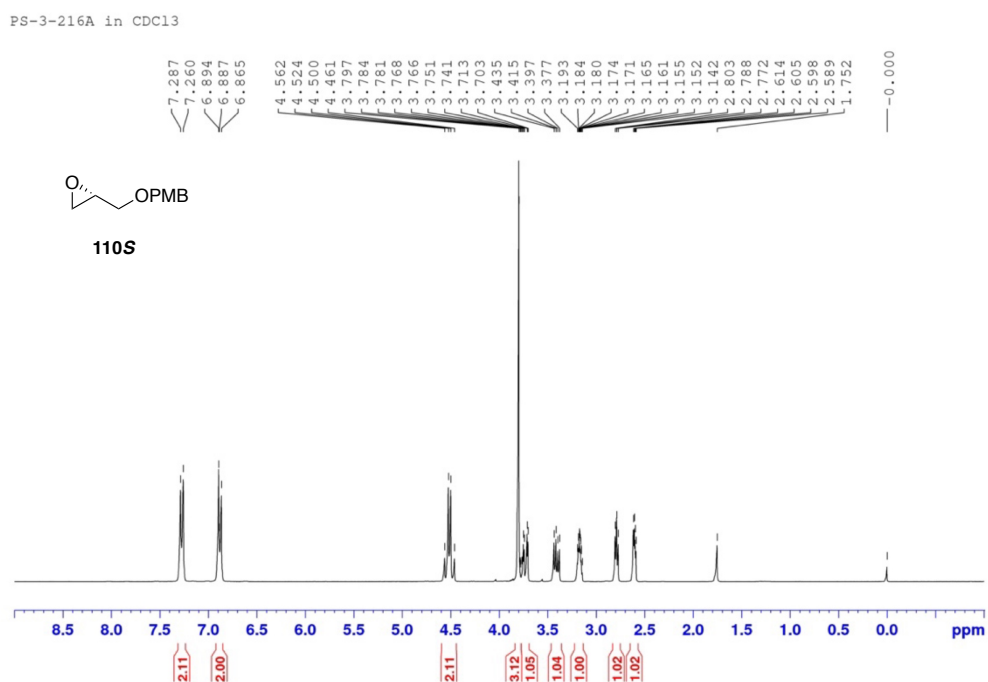
Figure 22 ^{1}H NMR (300 MHz, CDCl$_3$) spectrum of compound **162**
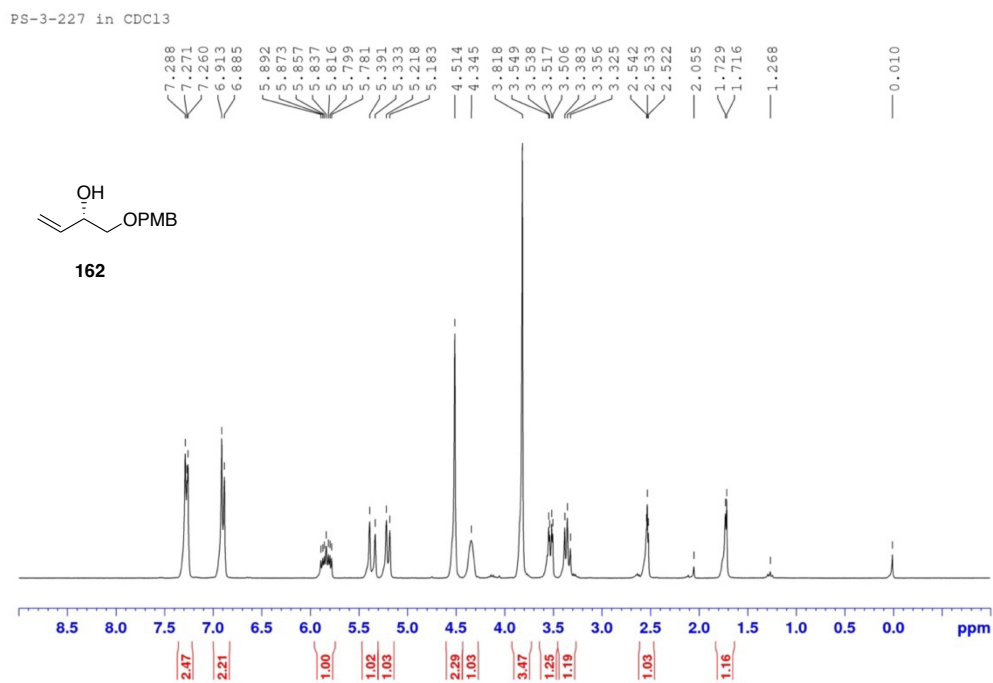
Figure 23 ^{1}H NMR (300 MHz, CDCl$_3$) spectrum of compound **112**
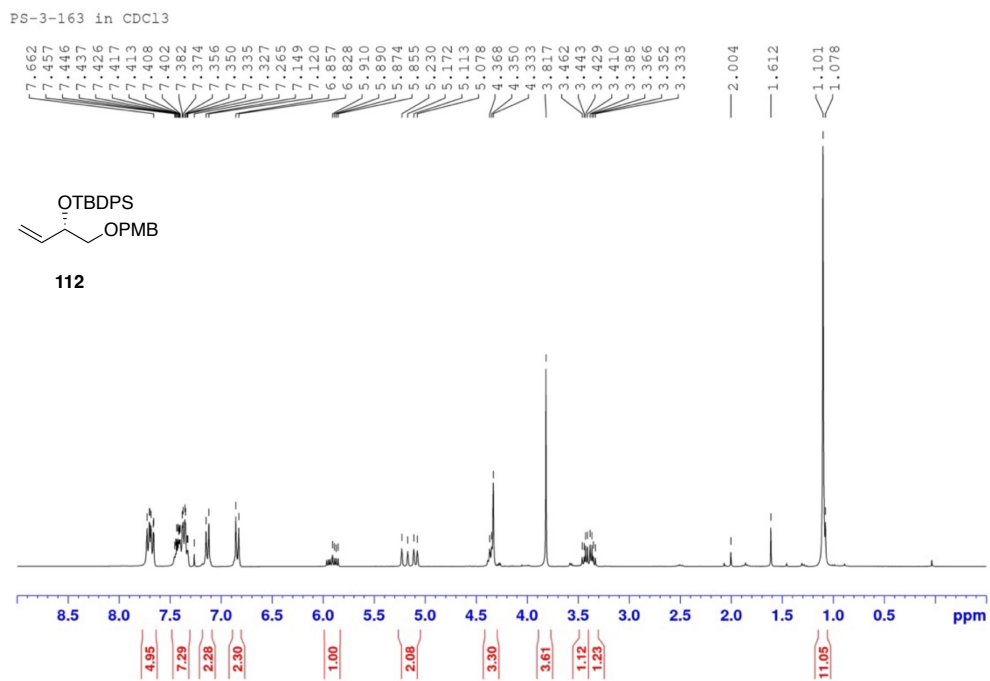
Figure 24 ^{1}H NMR (300 MHz, CDCl$_3$) spectrum of compound **113**
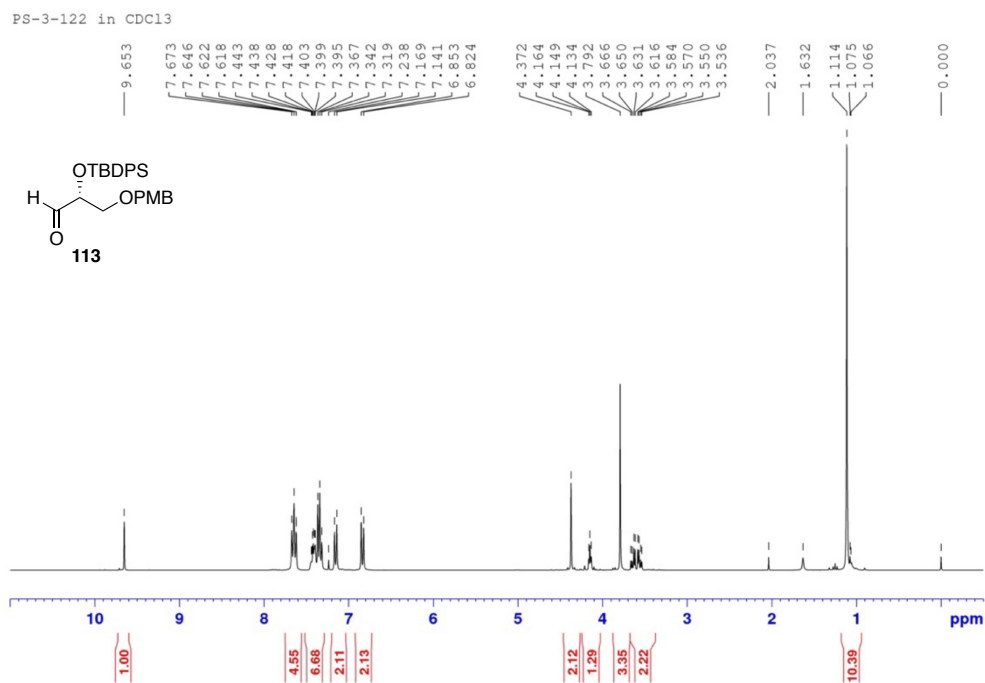
Figure 25 ^{1}H NMR (300 MHz, CDCl$_3$) spectrum of compound **115**
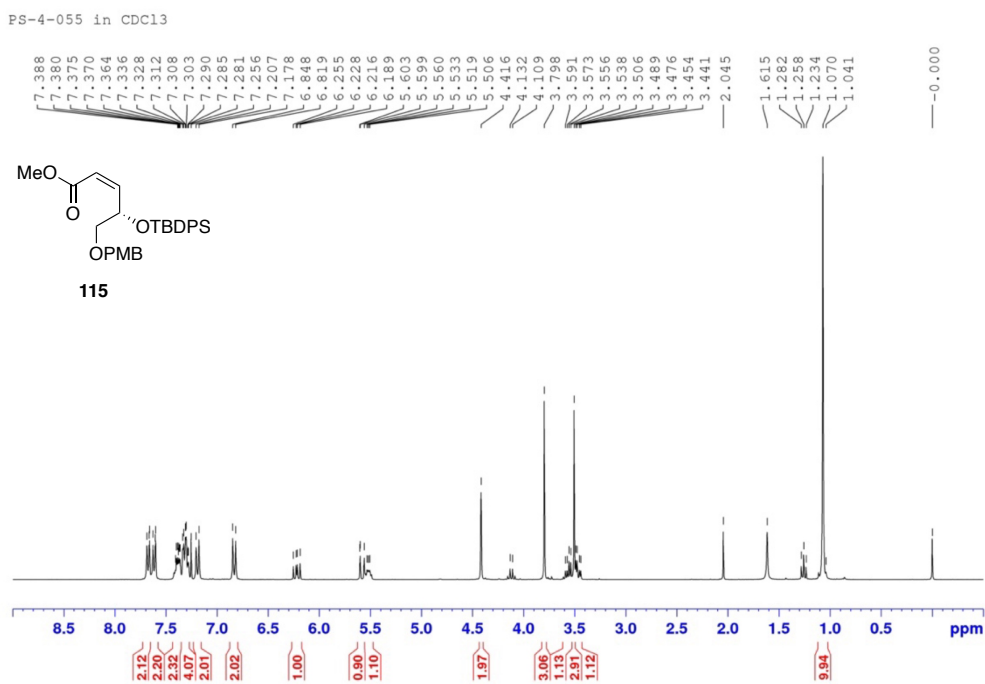
Figure 26 ^{1}H NMR (300 MHz, CDCl$_3$) spectrum of compound **108**
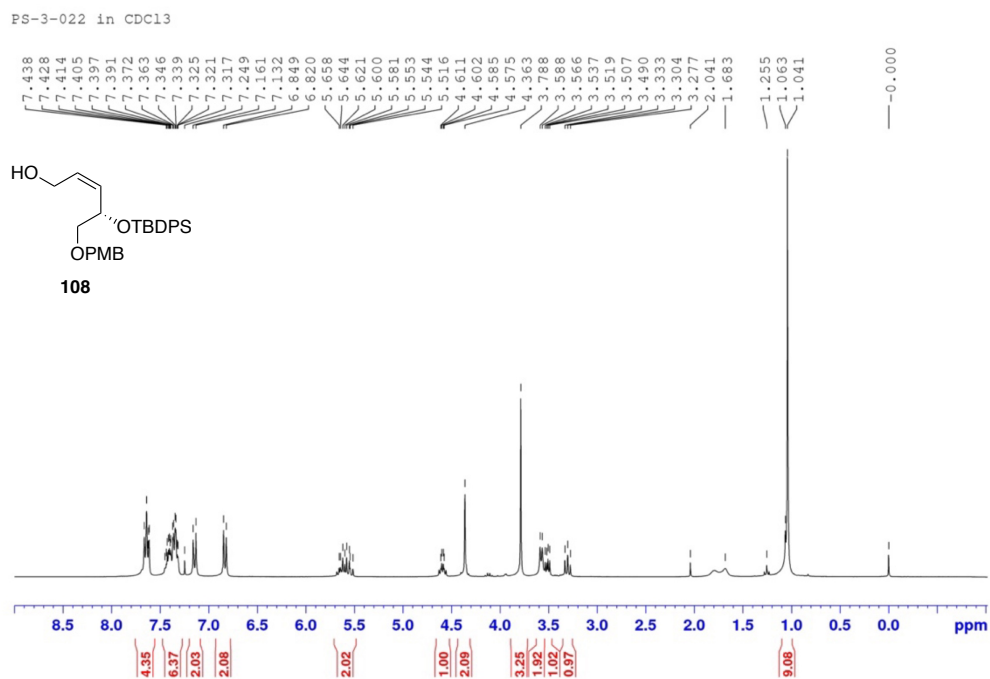
Figure 27 ^{1}H NMR (300 MHz, CDCl$_3$) spectrum of compound **1116a**
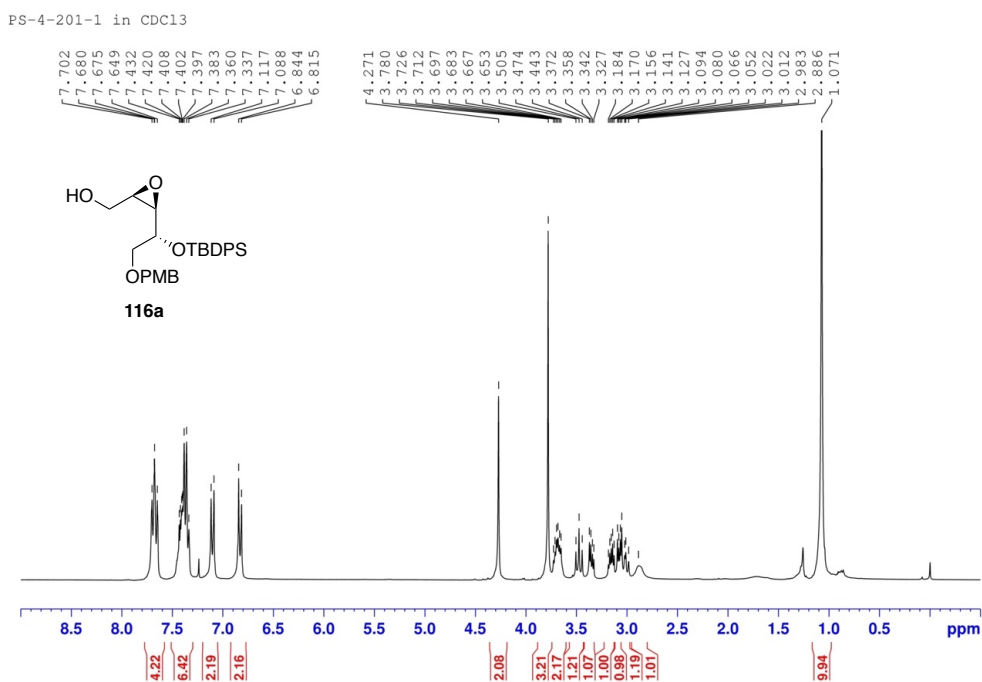
Figure 28 ^{13}C NMR (75 MHz, CDCl$_3$) spectrum of compound **116a**
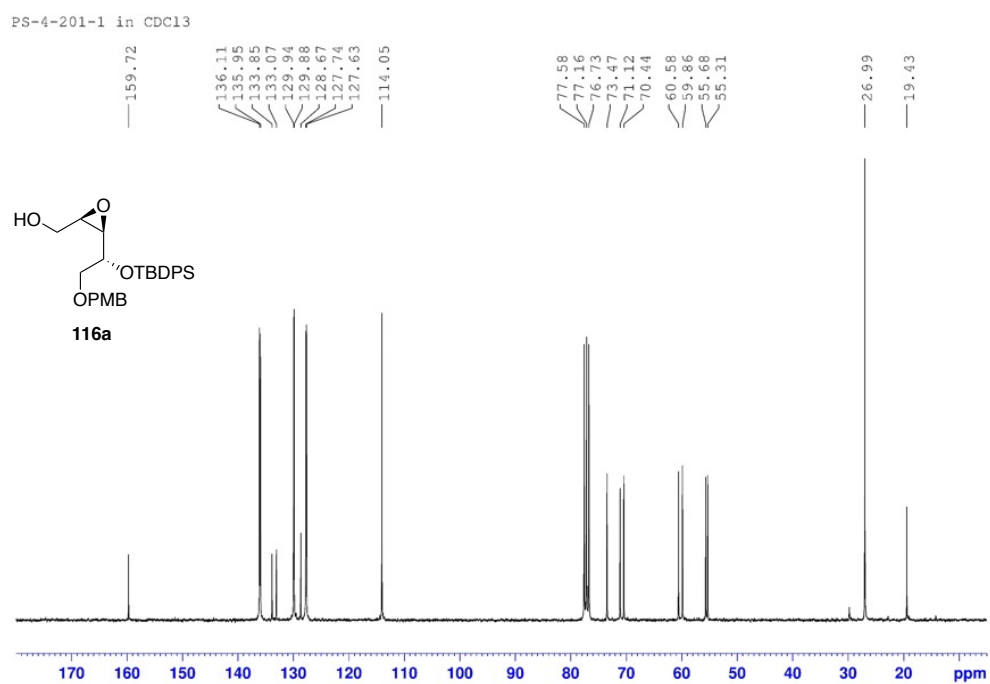
Figure 29 ^{1}H NMR (300 MHz, CDCl$_3$) spectrum of compound **1116b**

Figure 30 ^{13}C NMR (75 MHz, CDCl$_3$) spectrum of compound **116b**
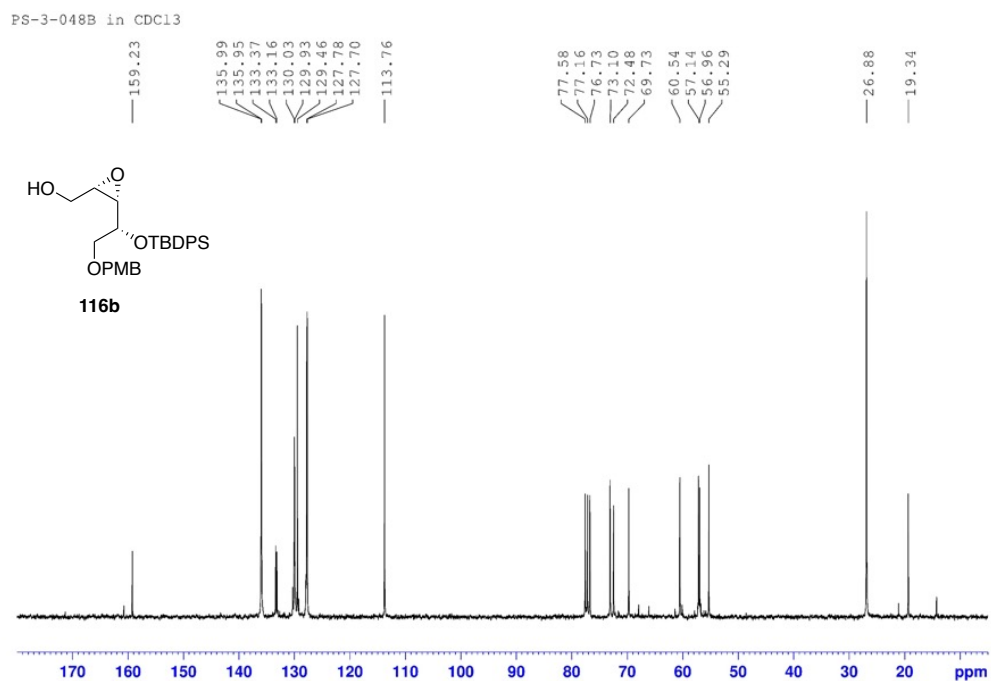
Figure 31 ^{1}H NMR (300 MHz, CDCl$_3$) spectrum of compound **117**
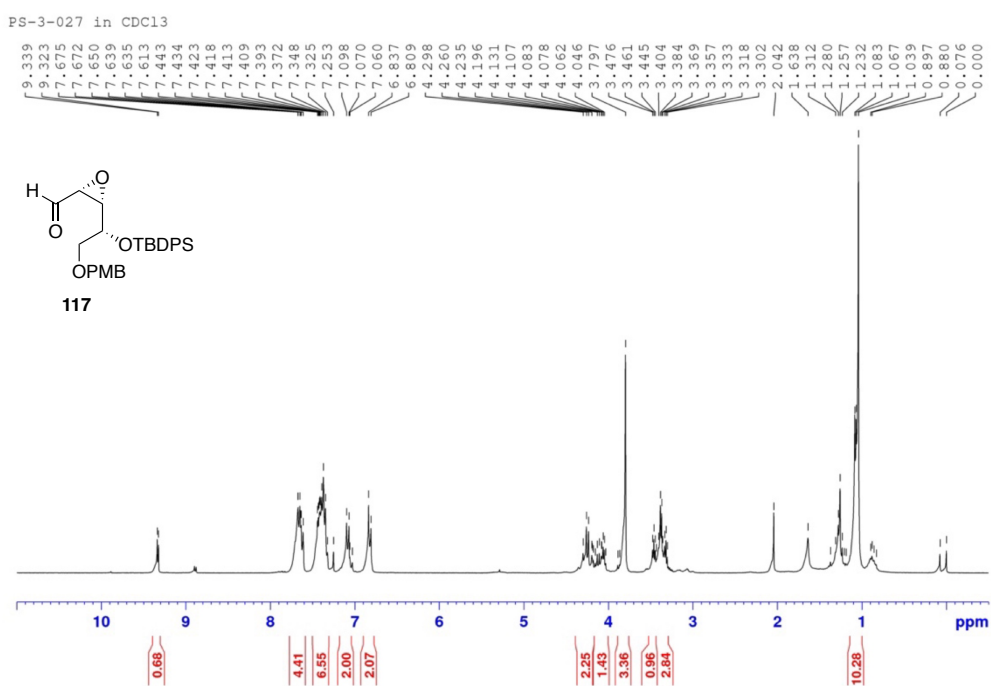
Figure 32 ^{13}C NMR (75 MHz, CDCl$_3$) spectrum of compound **117**
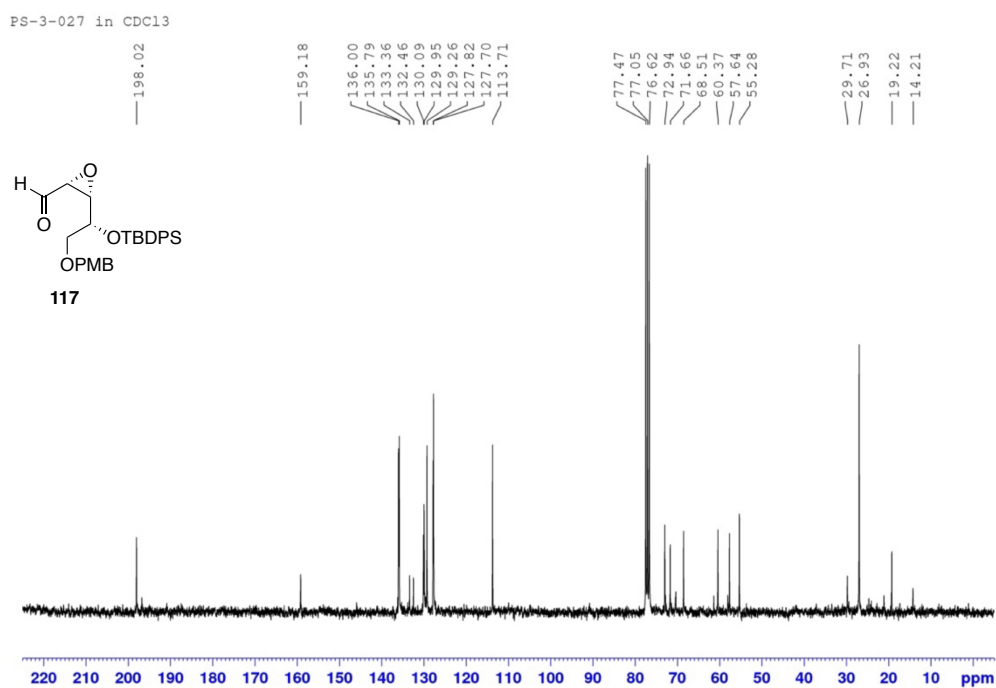
Figure 33 ^{1}H NMR (300 MHz, CDCl$_3$) spectrum of compound **118***S*
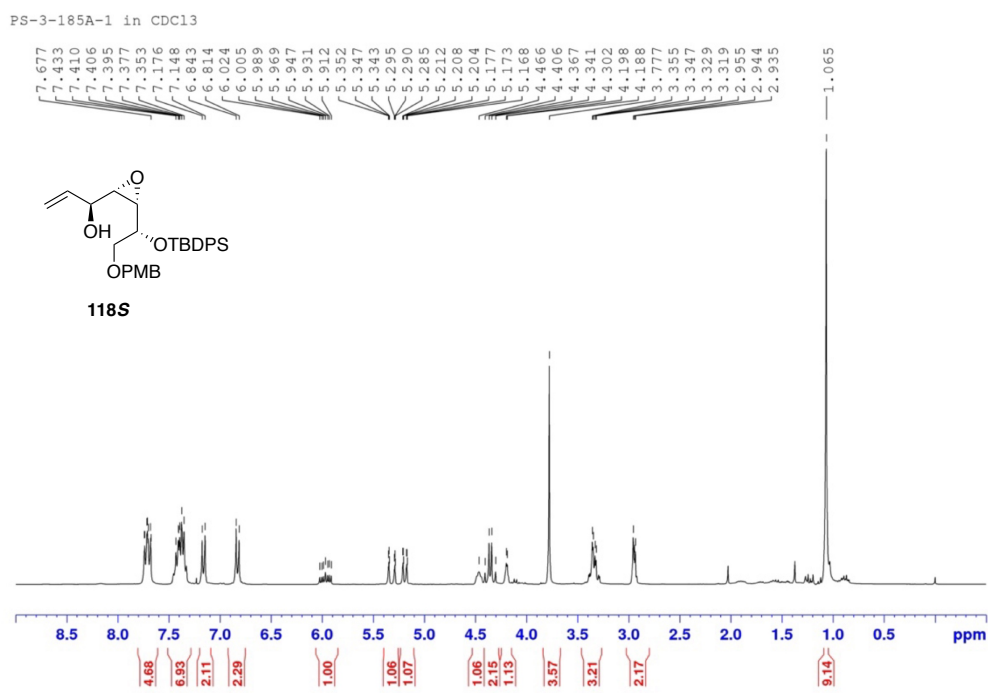
Figure 34 ^{13}C NMR (75 MHz, CDCl$_3$) spectrum of compound **118S**
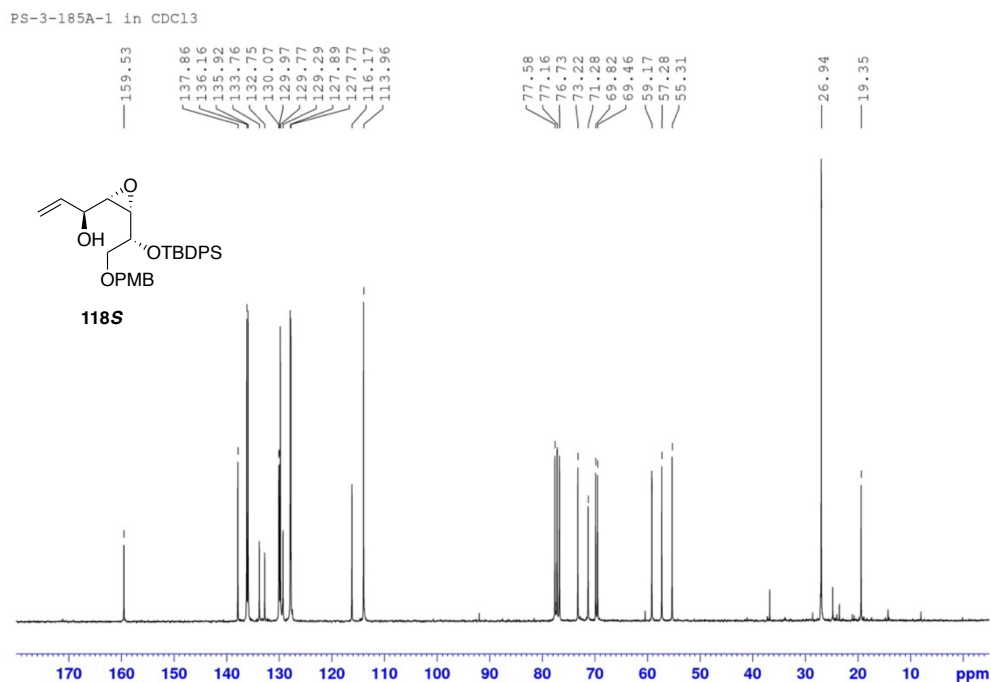
Figure 35 ^{1}H NMR (300 MHz, CDCl$_3$) spectrum of (S)-MTPA ester of **118S**
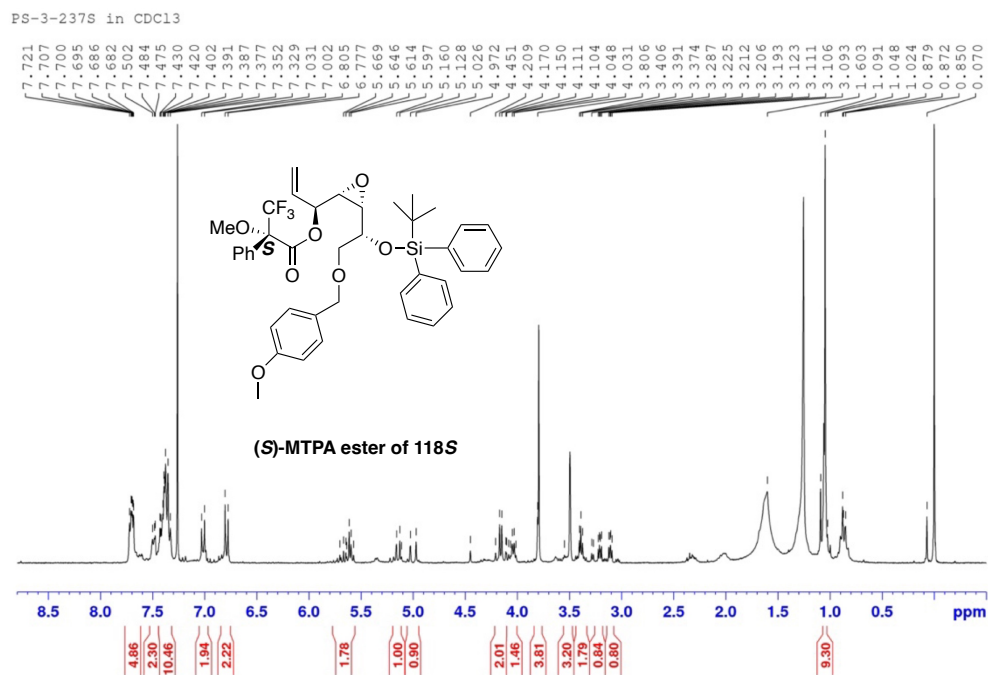
Figure 36 ^{1}H NMR (300 MHz, CDCl$_3$) spectrum of (R)-MTPA ester of **118S**
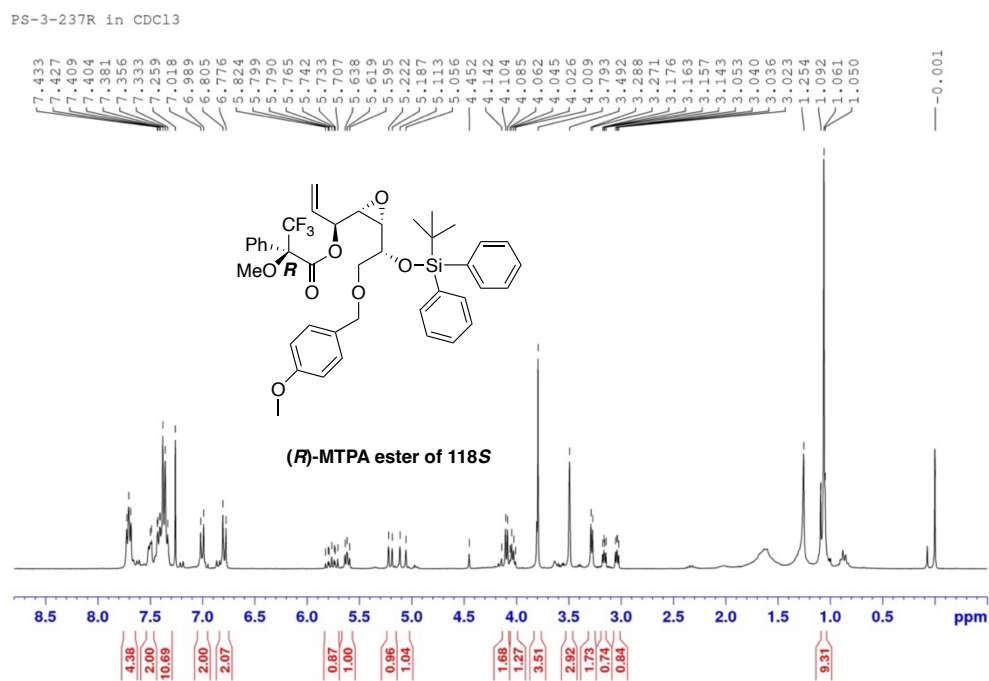
Figure 37 ^{1}H NMR (300 MHz, CDCl$_3$) spectrum of compound **118R**
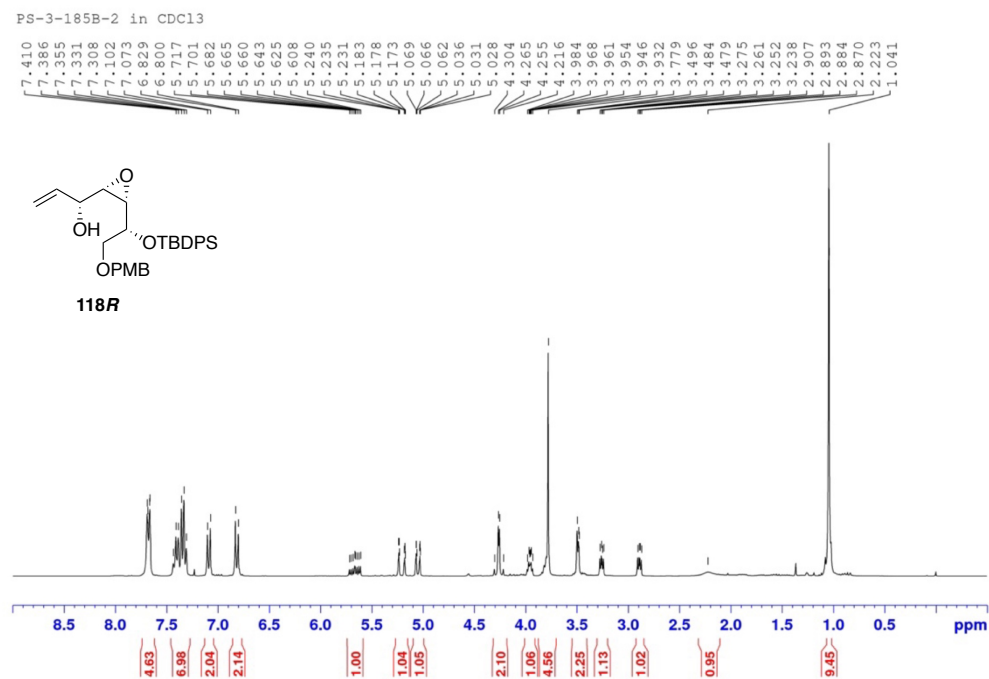
Figure 38 ^{13}C NMR (75 MHz, CDCl$_3$) spectrum of compound **118R**
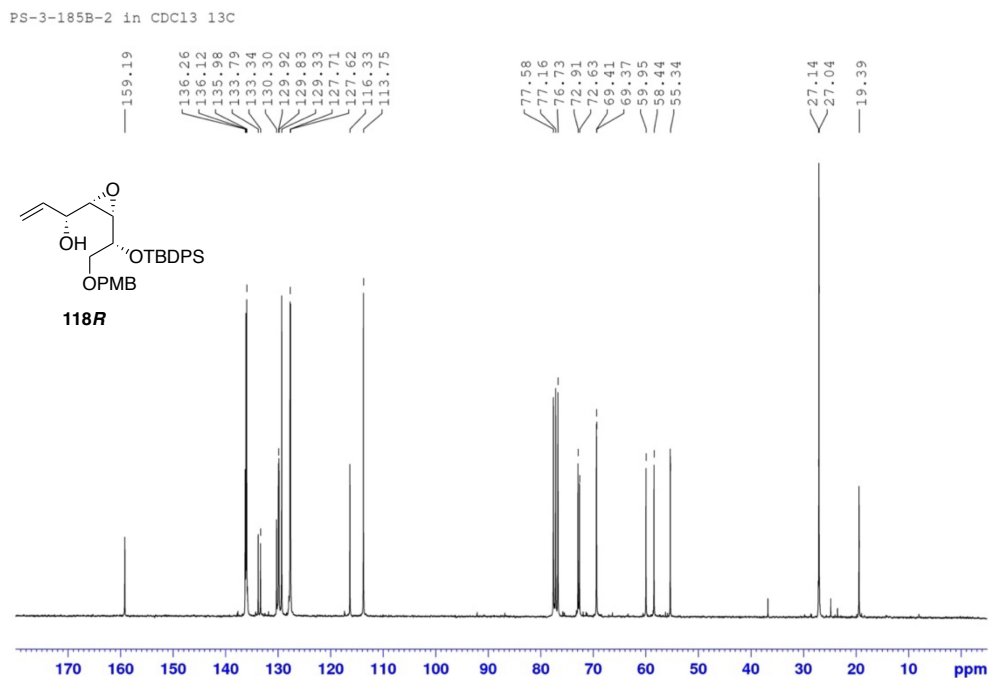
Figure 39 ^{1}H NMR (300 MHz, CDCl$_3$) spectrum of (*S*)-MTPA ester of **118R**
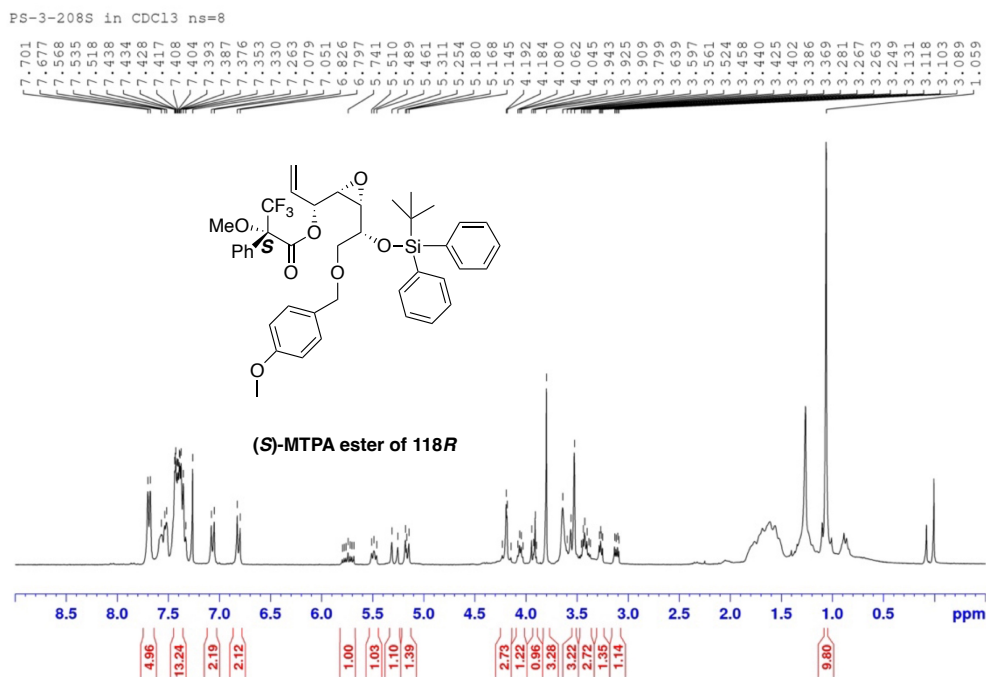
Figure 40 ^{1}H NMR (300 MHz, CDCl$_3$) spectrum of (R)-MTPA ester of **118R**
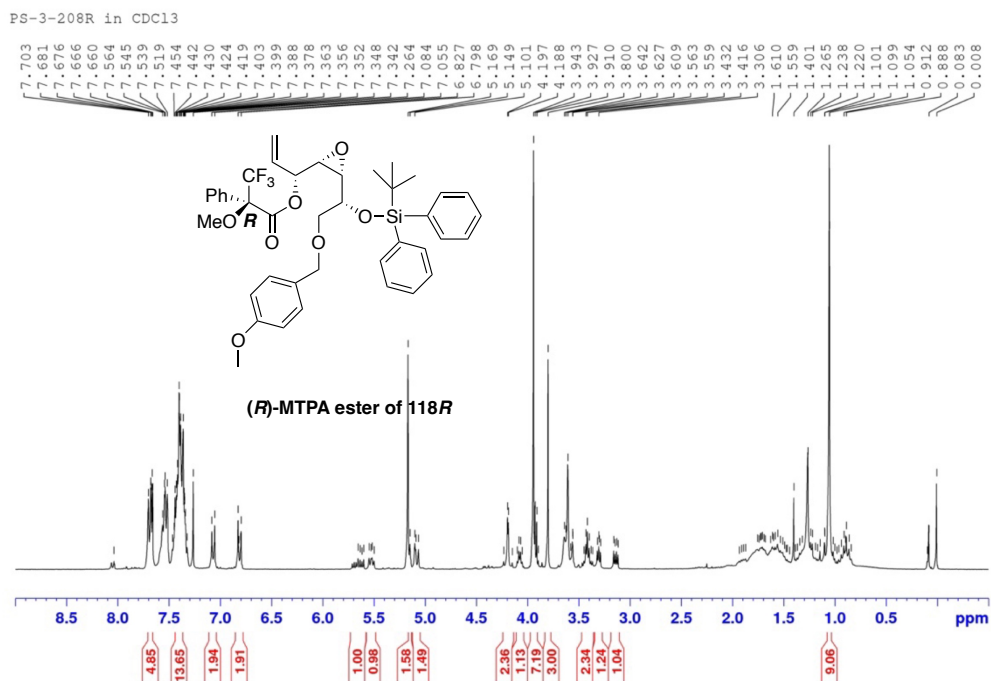
Figure 41 ^{1}H NMR (300 MHz, CDCl$_3$) spectrum of compound **119**
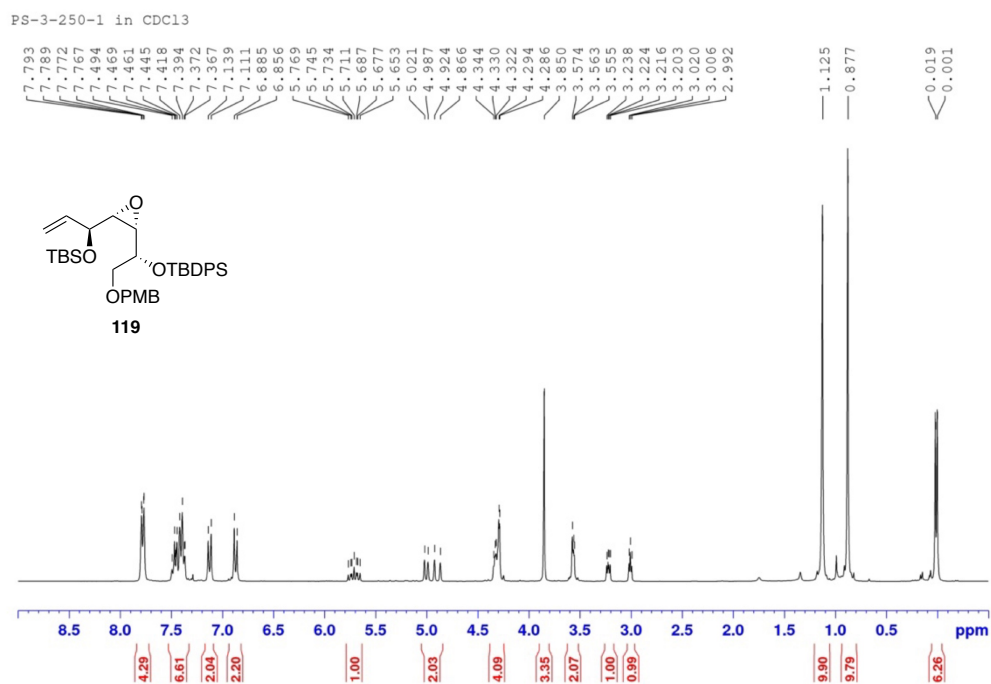
Figure 42 ^{13}C NMR (75 MHz, CDCl$_3$) spectrum of compound **119**
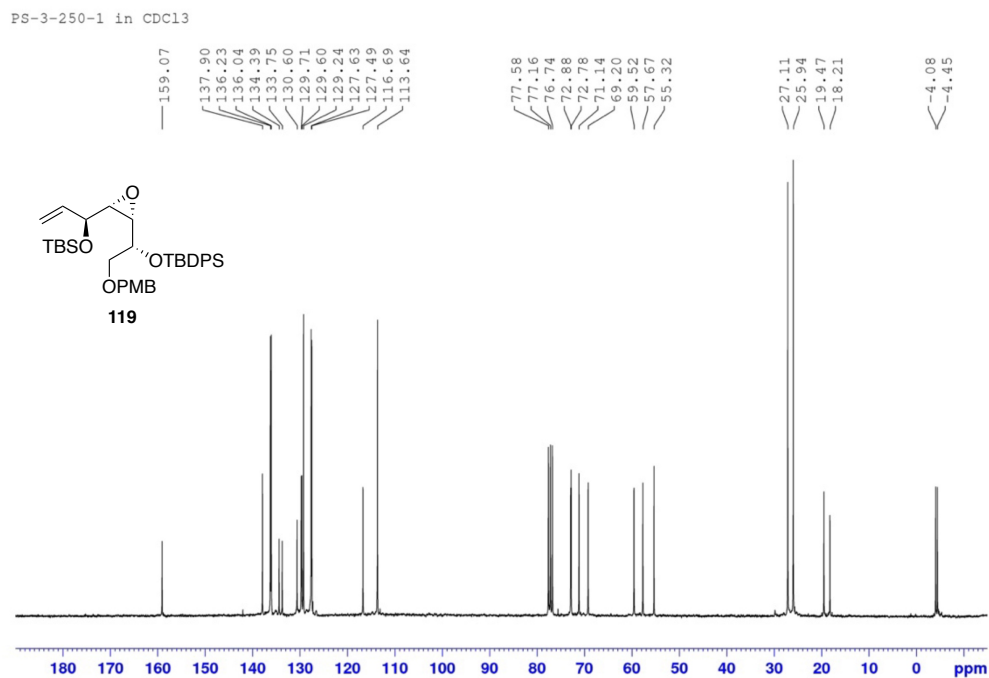
Figure 43 ^{1}H NMR (300 MHz, CDCl$_3$) spectrum of compound **163**
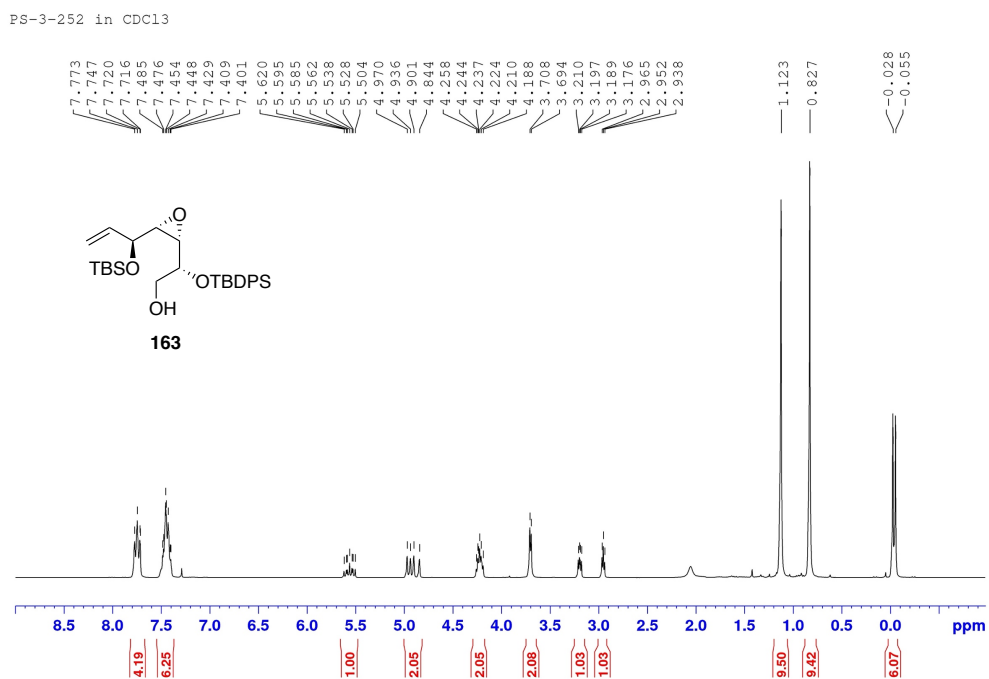
Figure 44 ^{13}C NMR (75 MHz, CDCl$_3$) spectrum of compound **163**
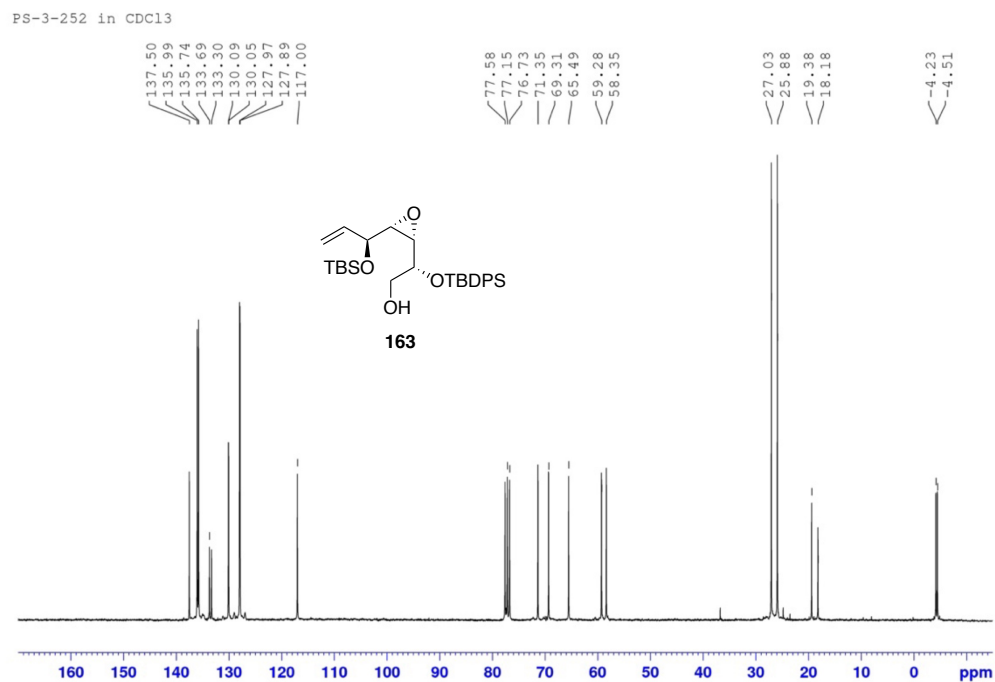
Figure 45 ^{1}H NMR (300 MHz, CDCl$_3$) spectrum of compound **121**
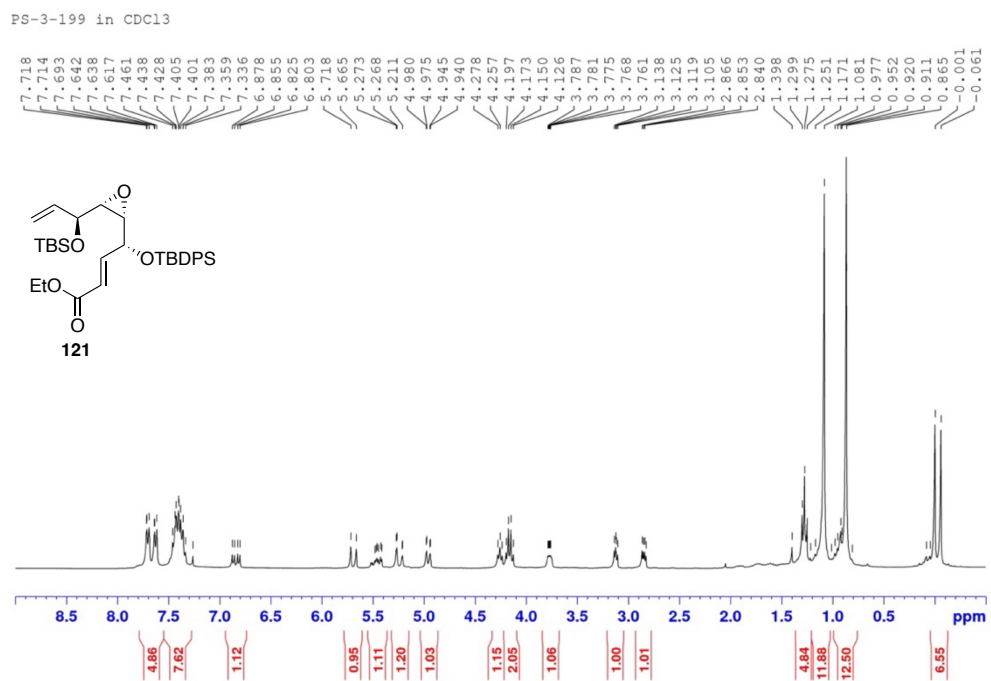
Figure 46 ^{13}C NMR (75 MHz, CDCl$_3$) spectrum of compound **121**
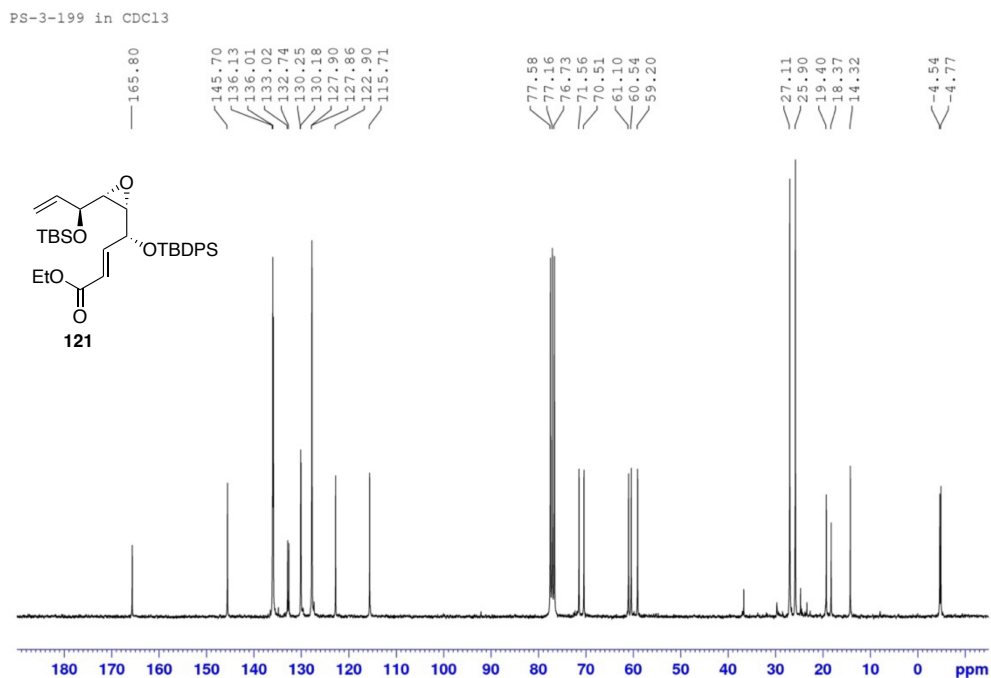
Figure 47 ^{1}H NMR (300 MHz, CDCl$_3$) spectrum of compound **122**
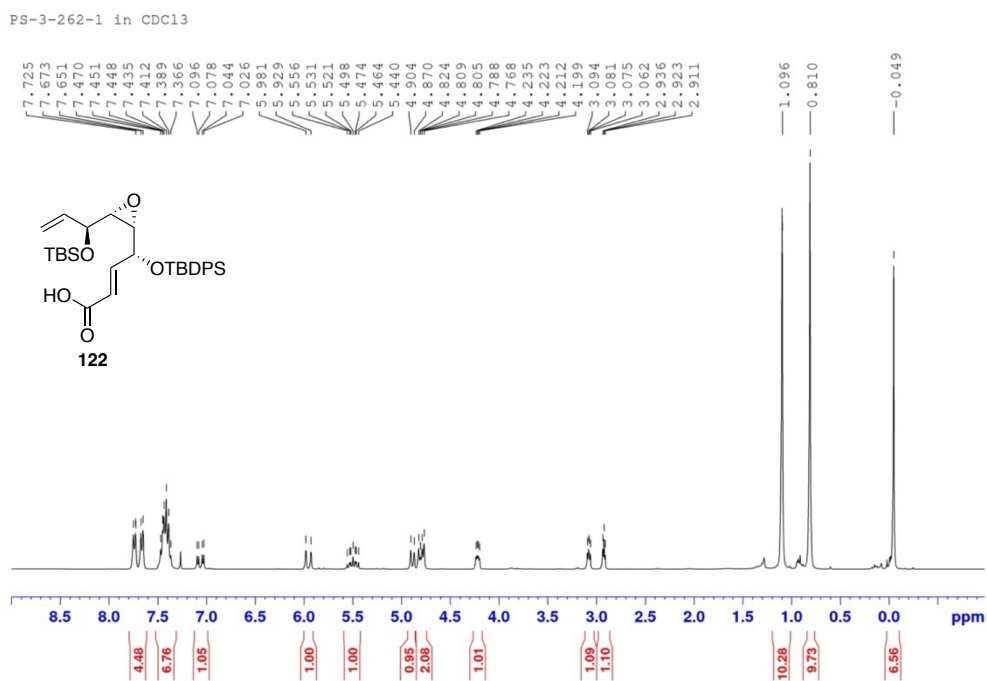
Figure 48 ^{13}C NMR (75 MHz, CDCl$_3$) spectrum of compound **122**
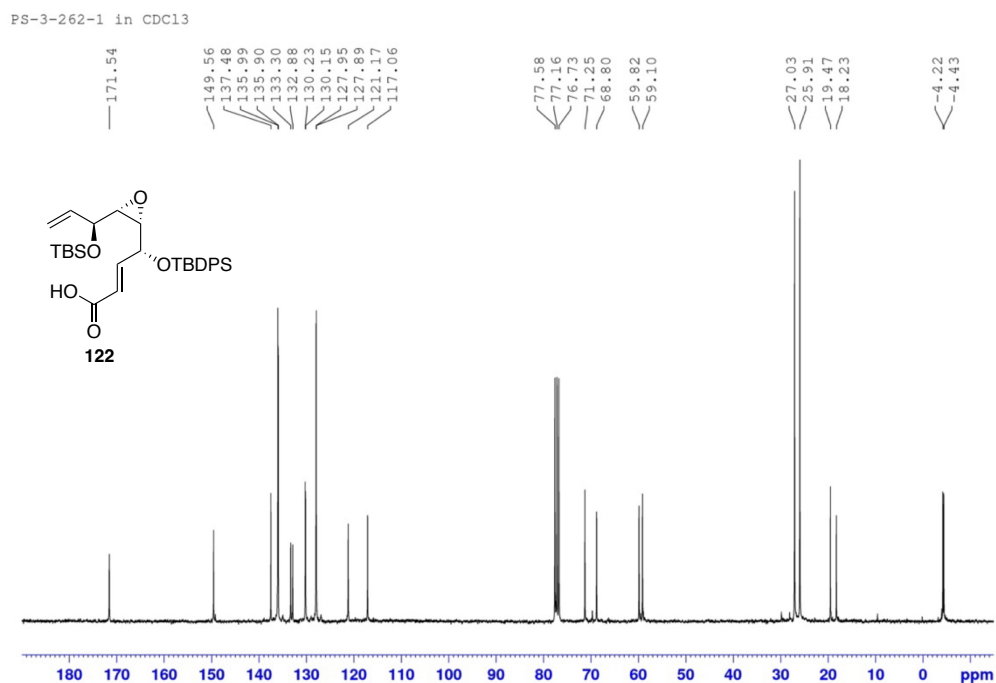
Figure 49 ^{1}H NMR (300 MHz, CDCl$_3$) spectrum of compound **123**
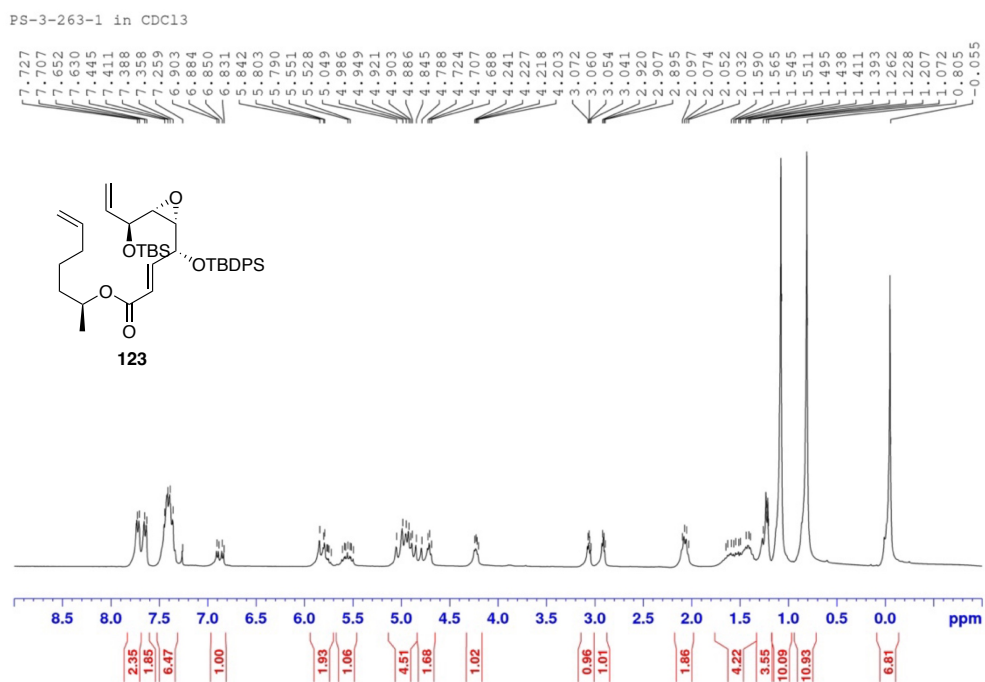
Figure 50 ^{13}C NMR (75 MHz, CDCl$_3$) spectrum of compound **123**
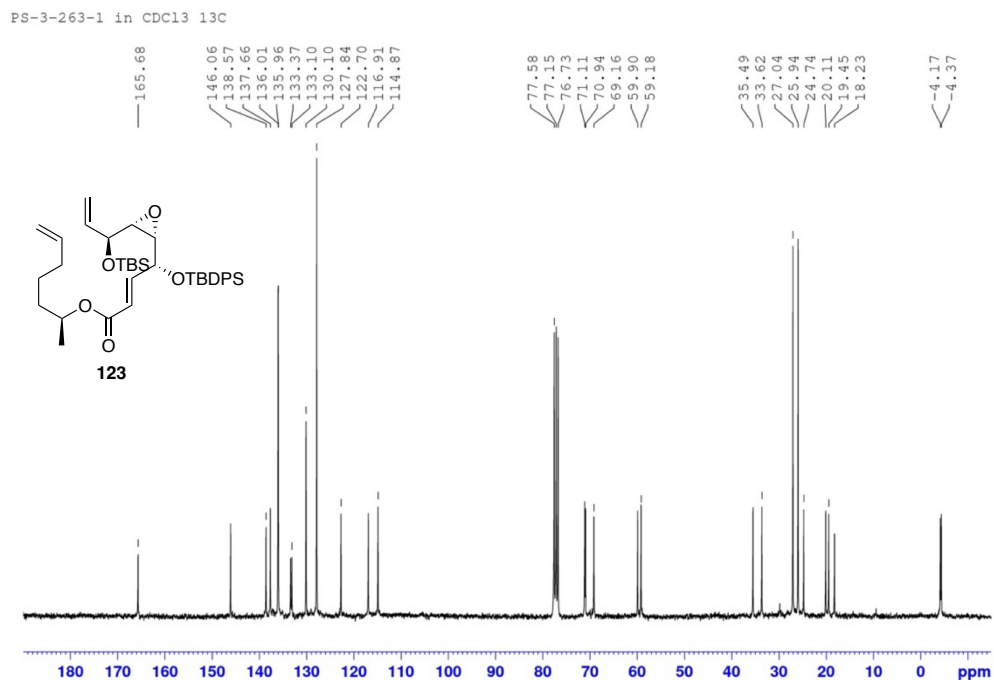
Figure 51 ^{1}H NMR (300 MHz, CDCl$_3$) spectrum of compound **124**
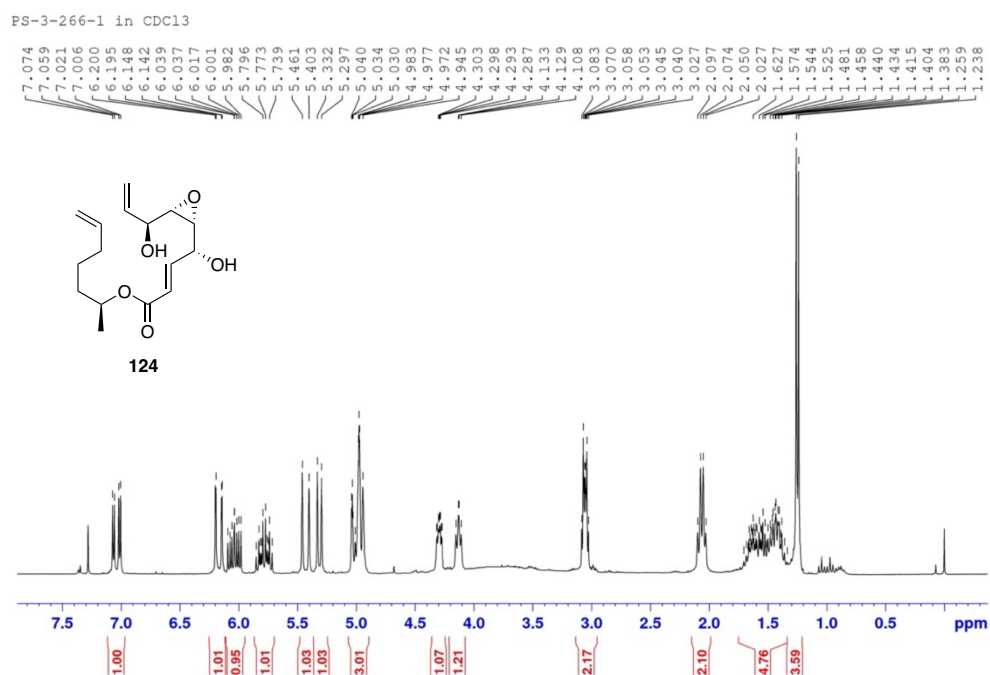
Figure 52 ^{13}C NMR (75 MHz, CDCl$_3$) spectrum of compound **124**
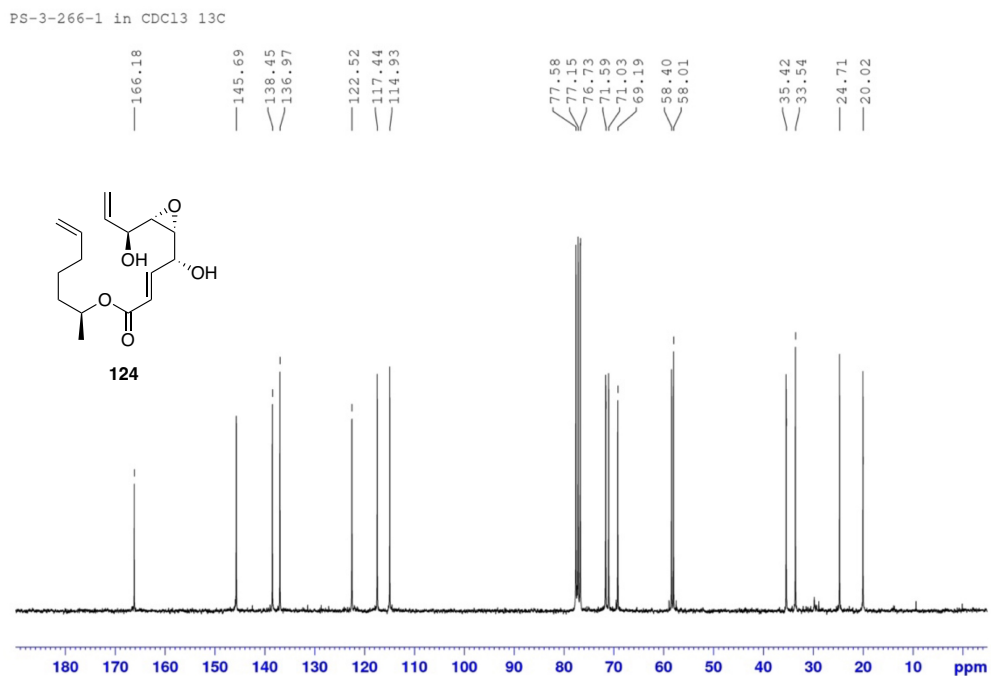
Figure 53 ^{1}H NMR (300 MHz, CDCl$_3$) spectrum of compound **152**
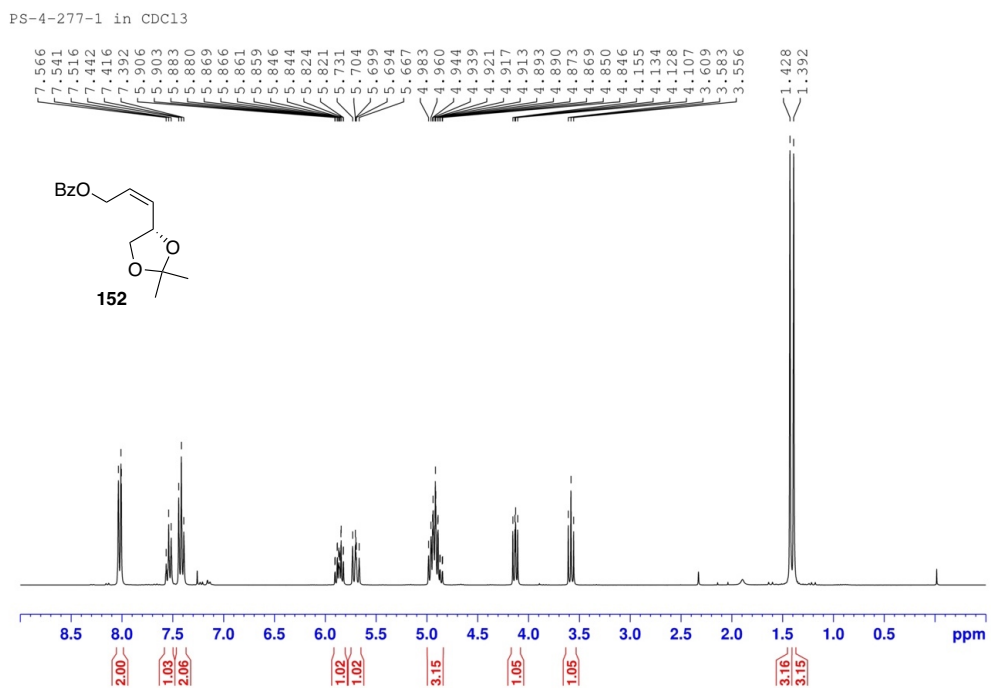
Figure 54 ^{13}C NMR (75 MHz, CDCl$_3$) spectrum of compound **152**
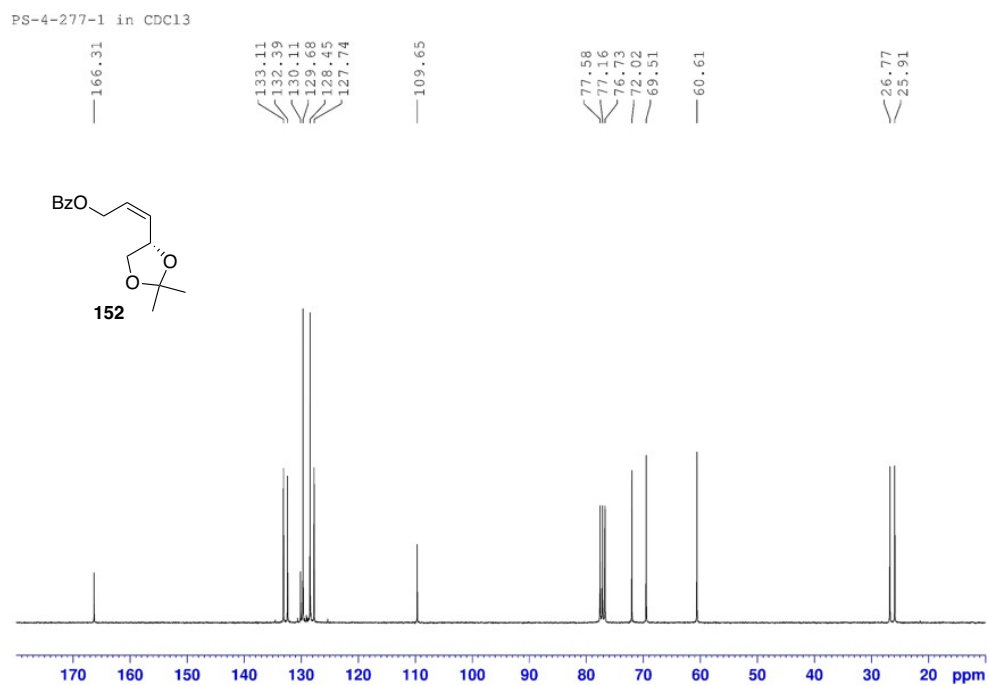
Figure 55 ^{1}H NMR (300 MHz, CDCl$_3$) spectrum of compound **153**
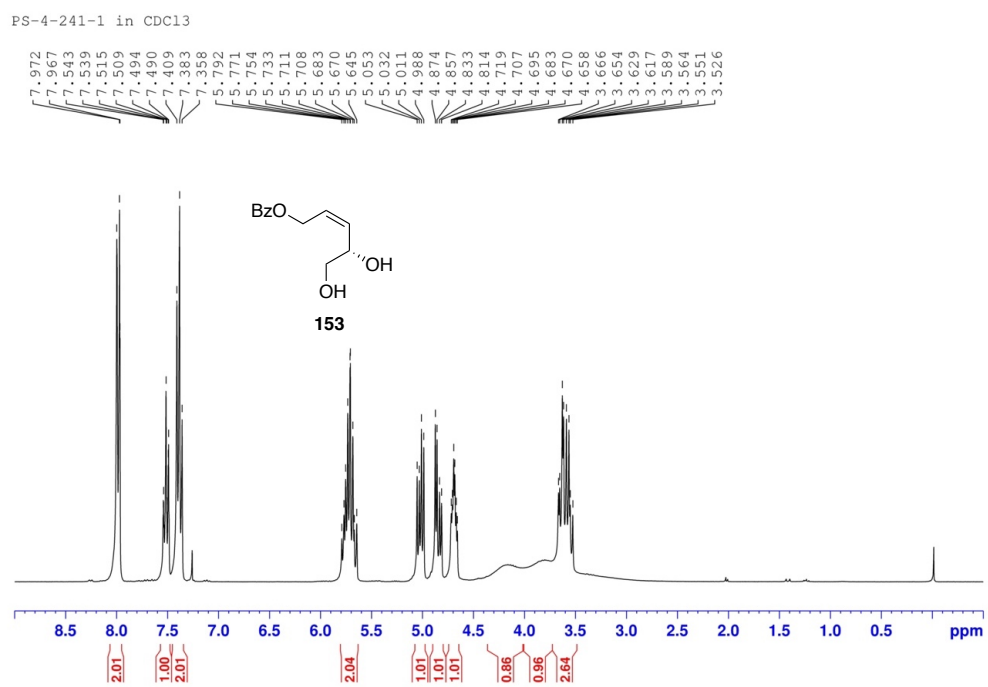
Figure 56 ^{13}C NMR (75 MHz, CDCl$_3$) spectrum of compound **153**
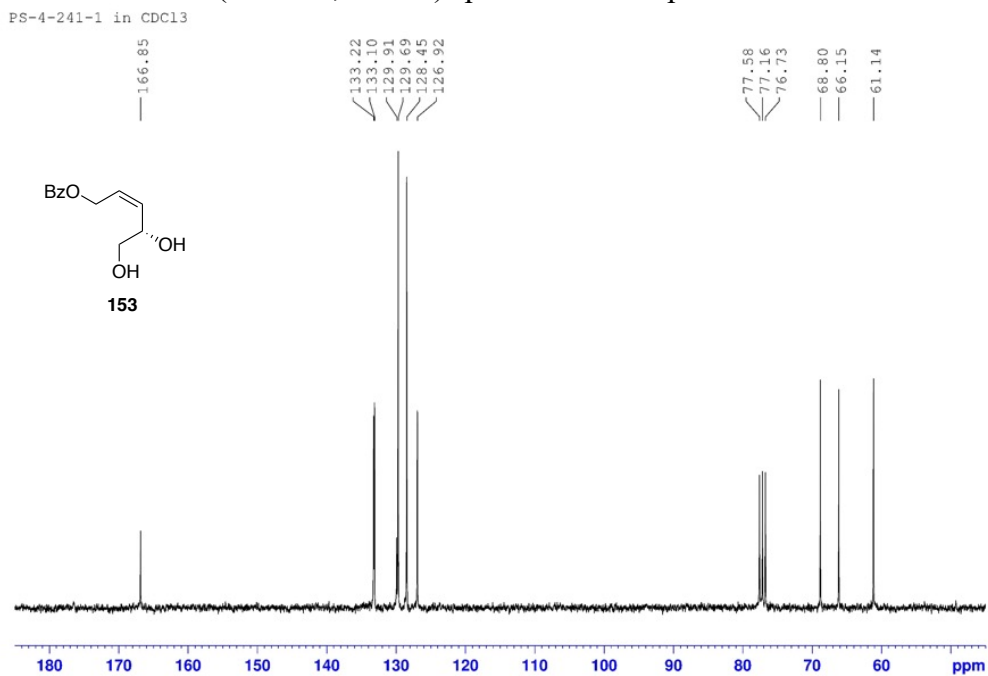
Figure 57 ^{1}H NMR (300 MHz, CDCl$_3$) spectrum of compound **134**
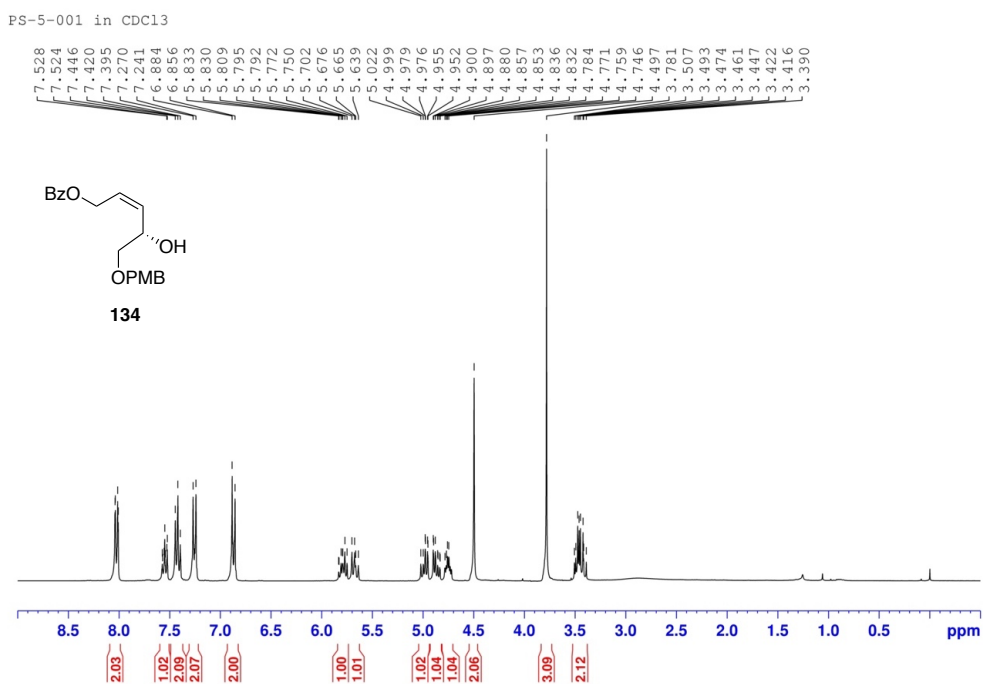
Figure 58 ^{13}C NMR (75 MHz, CDCl₃) spectrum of compound **134**
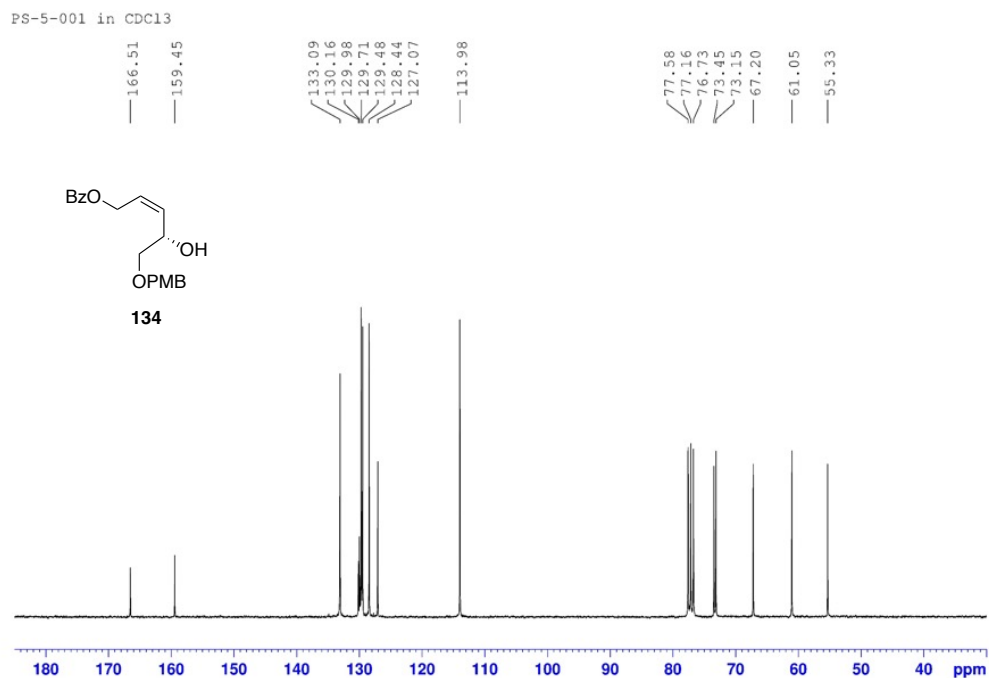
Figure 59 ^{1}H NMR (300 MHz, CDCl₃) spectrum of compound **136**
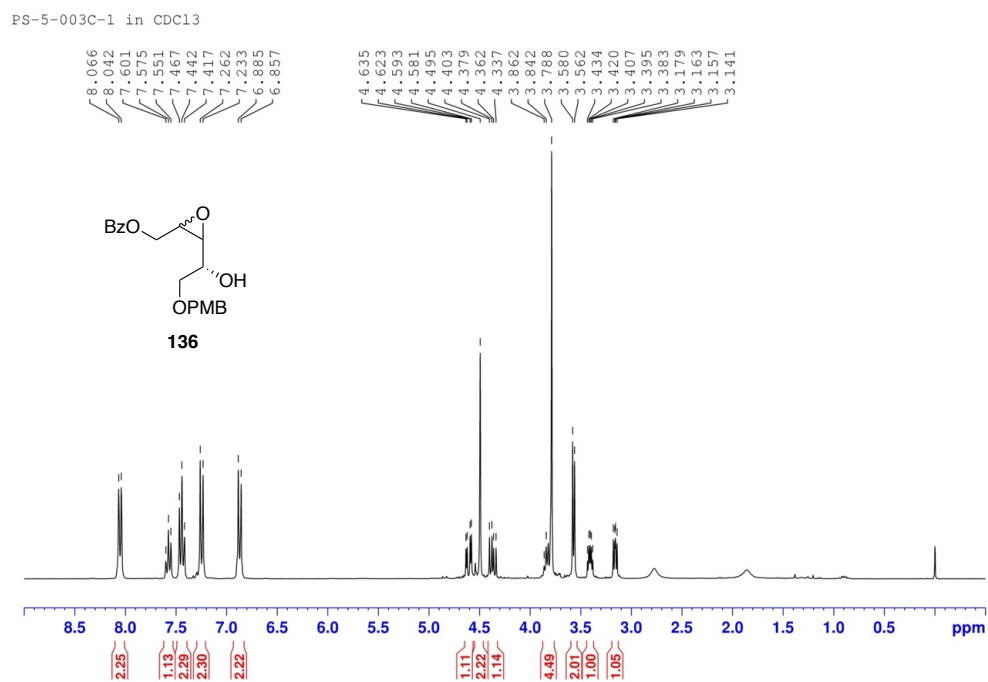
Figure 60 ^{13}C NMR (75 MHz, CDCl$_3$) spectrum of compound **136**
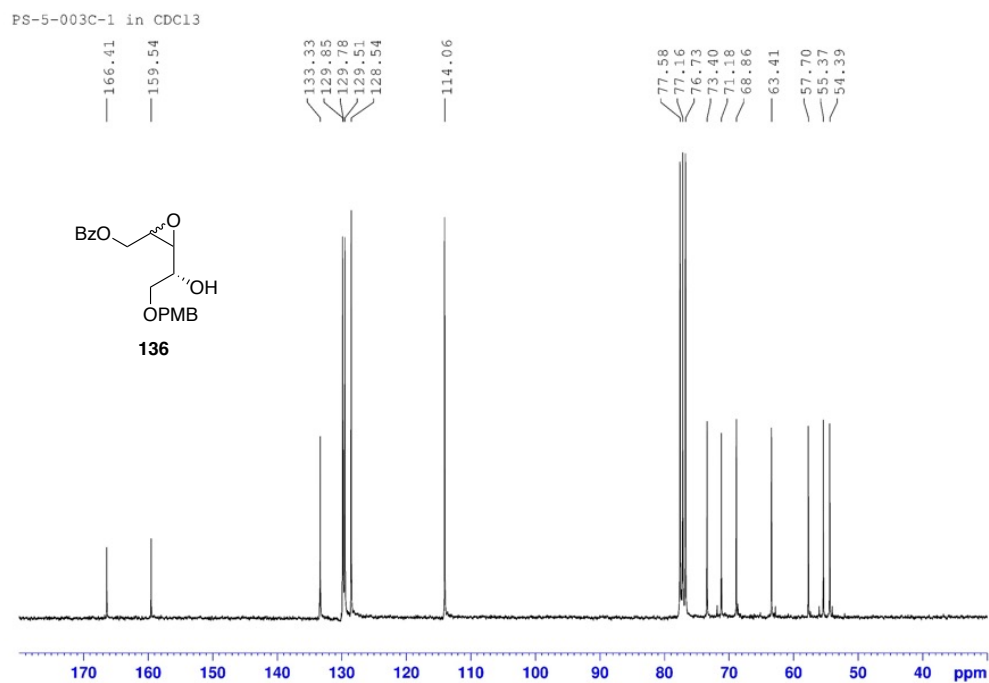
Figure 61 ^{1}H NMR (300 MHz, CDCl$_3$) spectrum of compound **164**
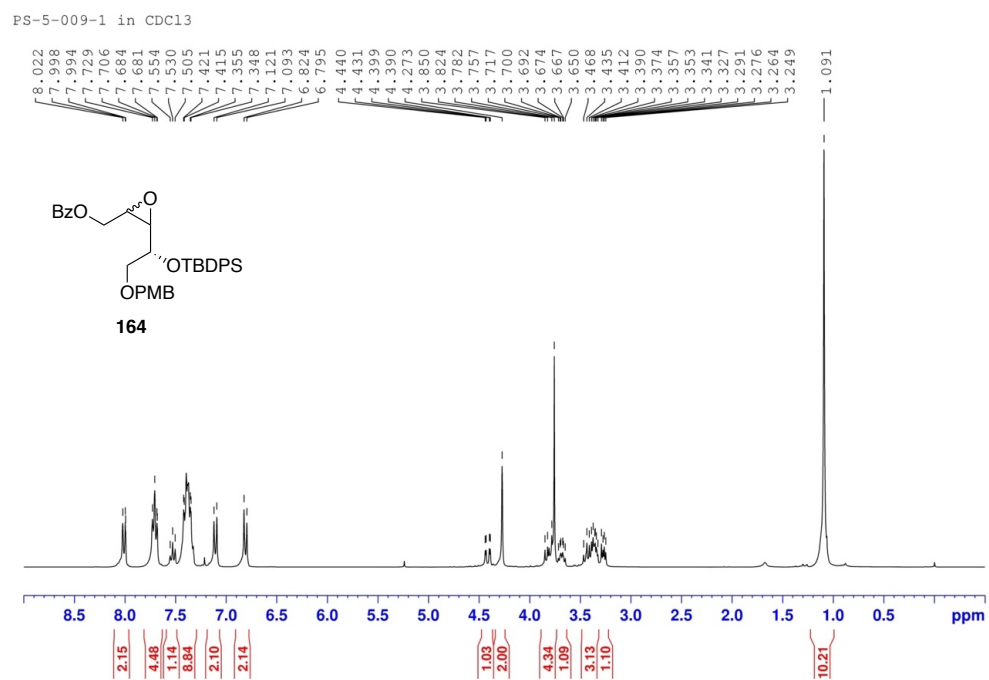
Figure 62 ^{13}C NMR (75 MHz, CDCl$_3$) spectrum of compound **164**
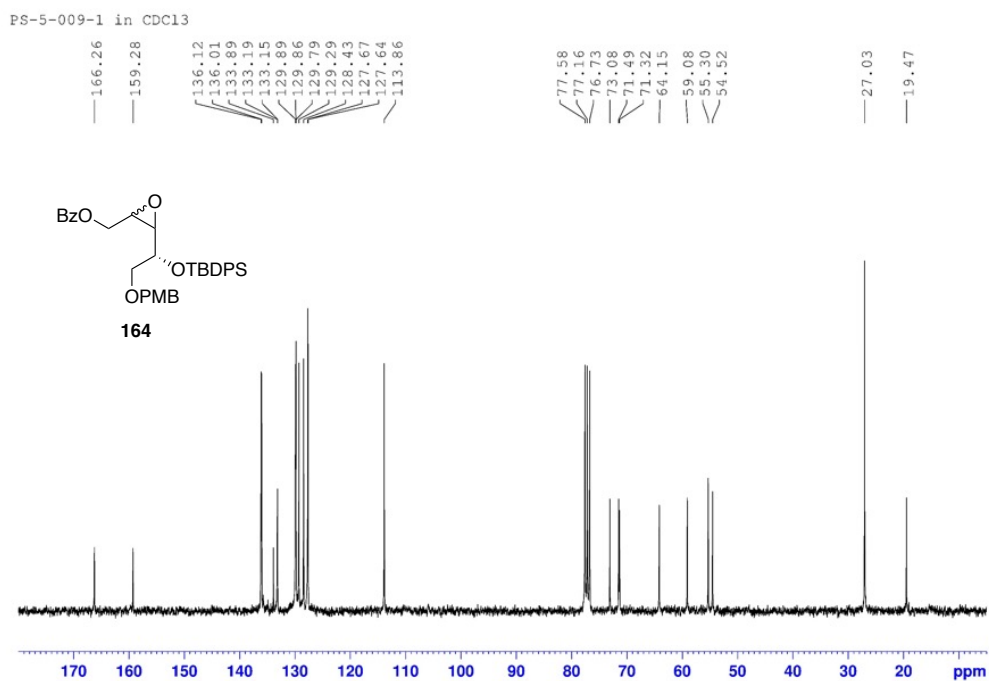
Figure 63 ^{1}H NMR (300 MHz, CDCl$_3$) spectrum of compound **137**
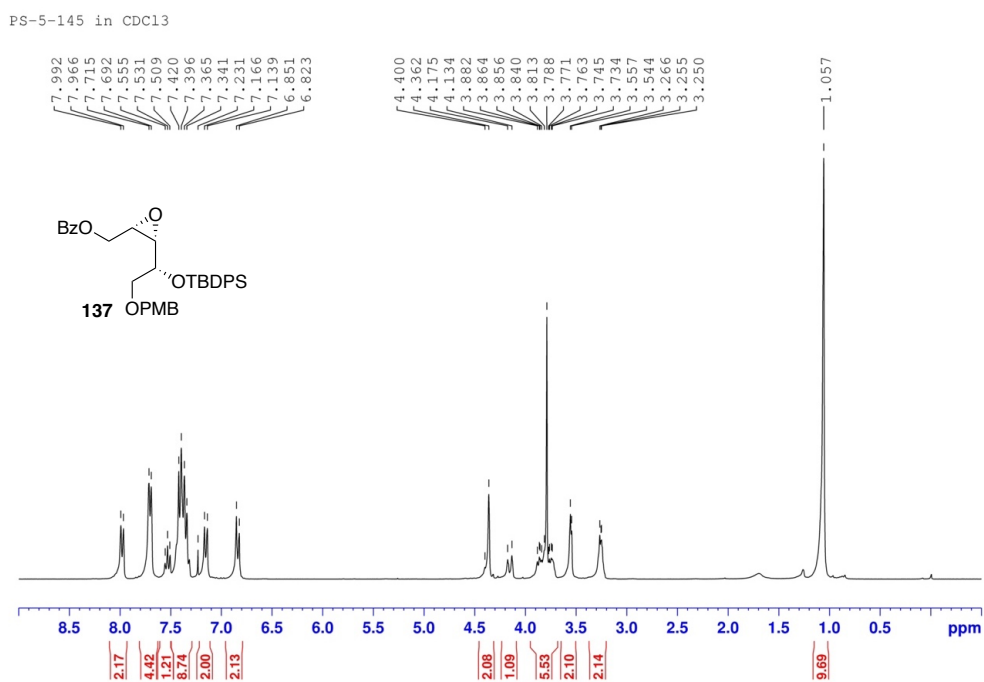
Figure 64 ^{13}C NMR (75 MHz, CDCl$_3$) spectrum of compound **137**
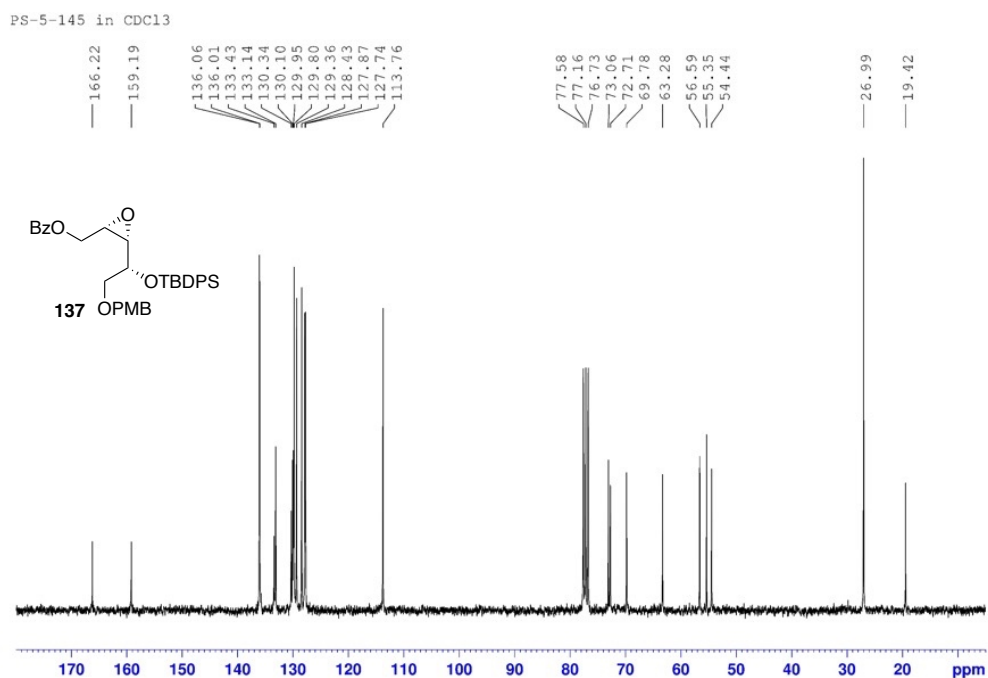
Figure 65 ^{1}H NMR (300 MHz, CDCl$_3$) spectrum of compound **138**
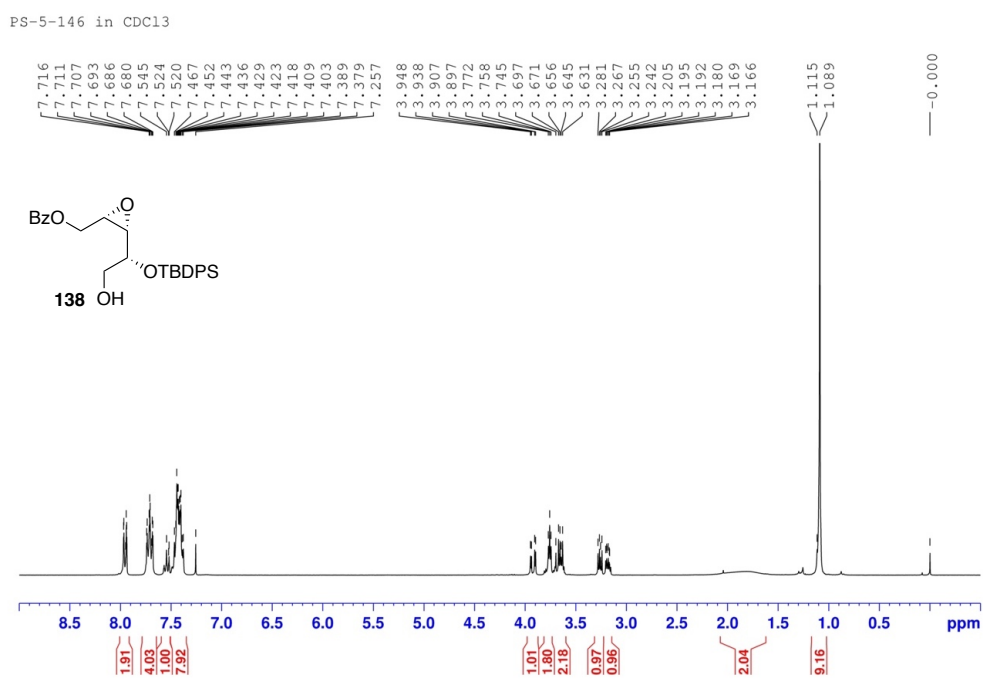
Figure 66 ^{13}C NMR (75 MHz, CDCl$_3$) spectrum of compound **138**
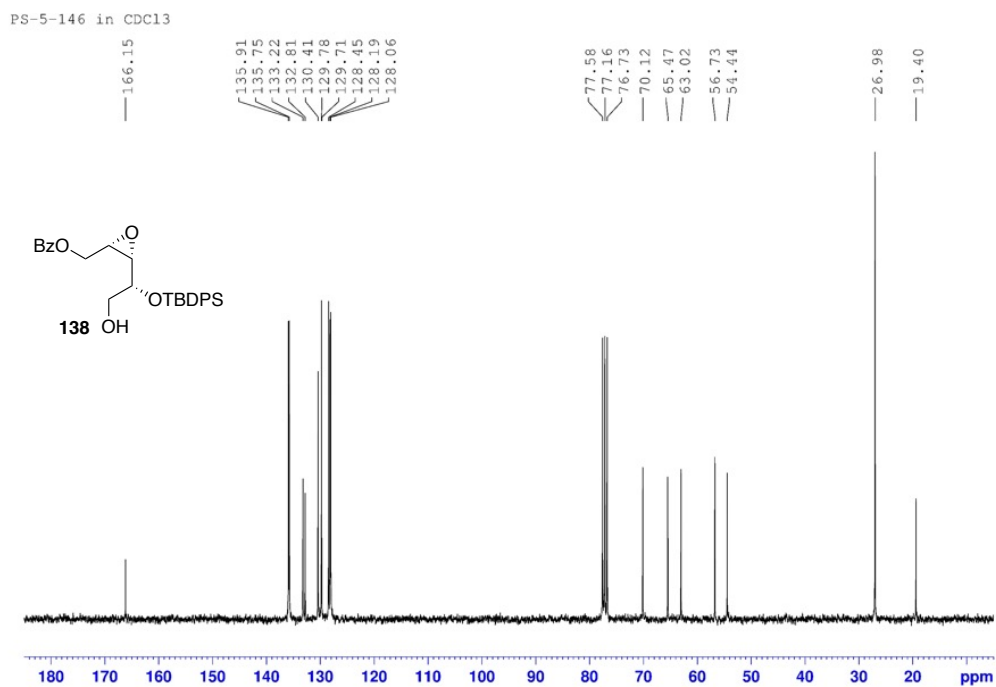
Figure 67 ^1H NMR (300 MHz, CDCl$_3$) spectrum of compound **139**
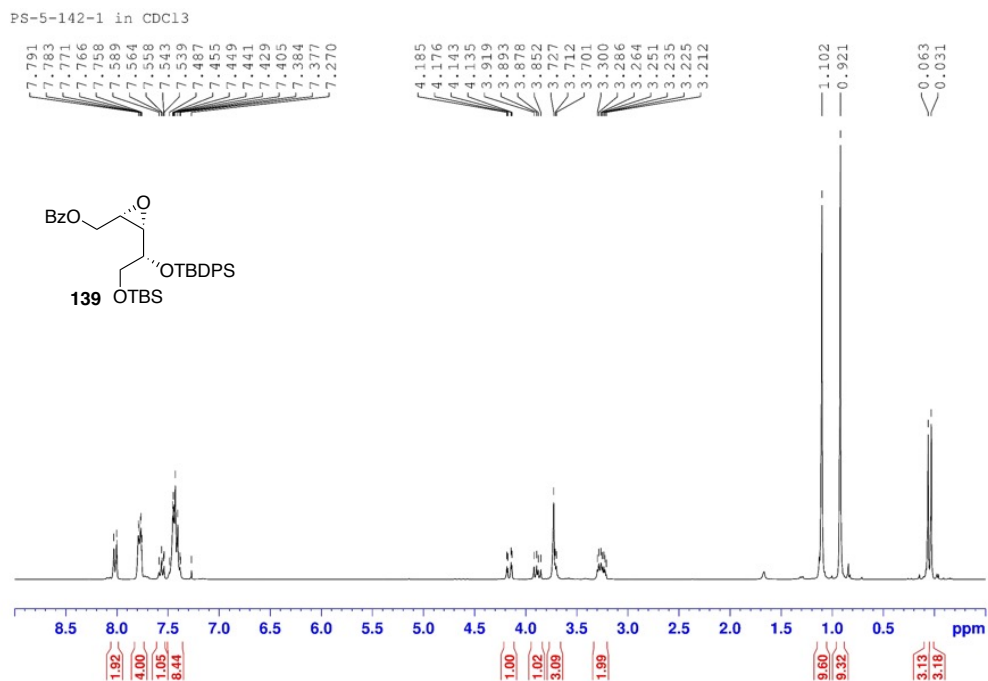
Figure 68 ^{13}C NMR (75 MHz, CDCl$_3$) spectrum of compound **139**
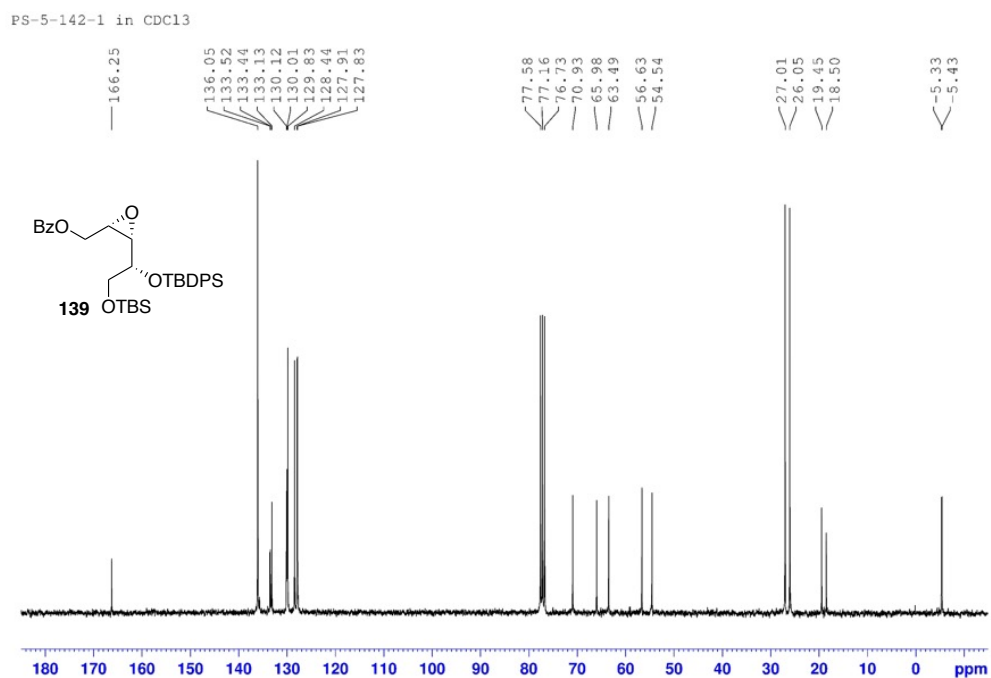
Figure 69 ^{1}H NMR (300 MHz, CDCl$_3$) spectrum of compound **140**

Figure 70 ^{13}C NMR (75 MHz, CDCl$_3$) spectrum of compound **140**

Figure 71 ^{1}H NMR (300 MHz, CDCl$_3$) spectrum of compound **141**
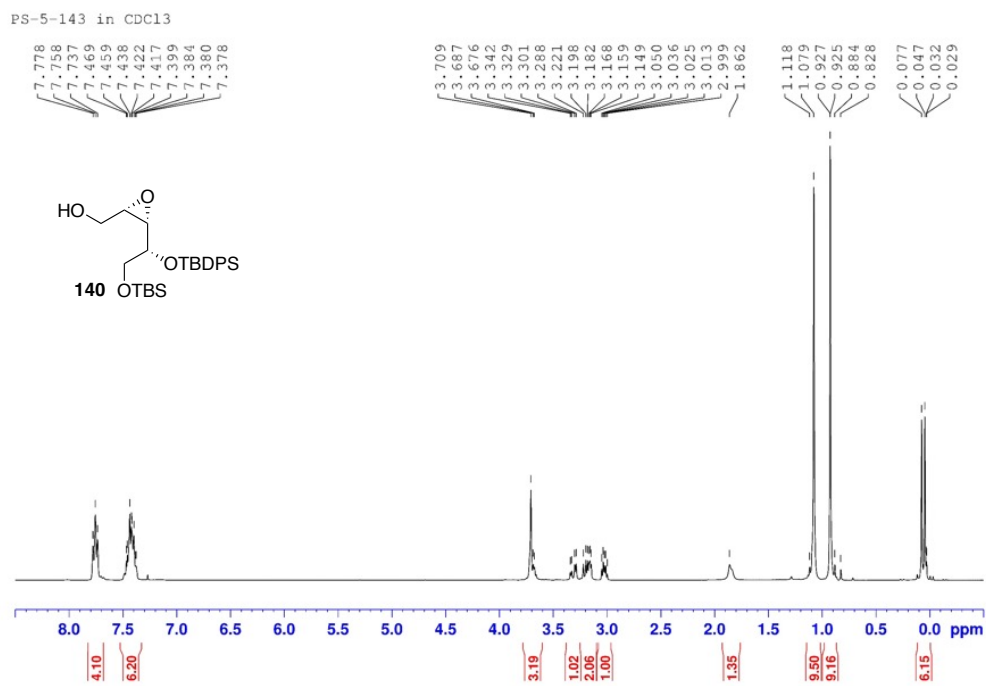
Figure 72 ^{13}C NMR (75 MHz, CDCl$_3$) spectrum of compound **141**
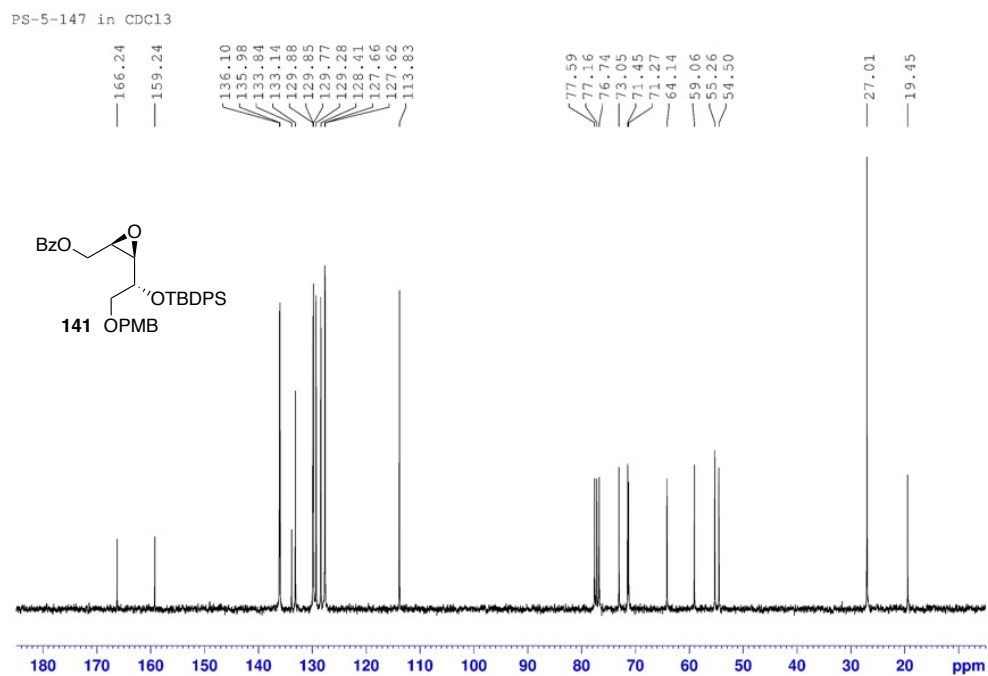
Figure 73 ^{1}H NMR (300 MHz, CDCl$_3$) spectrum of compound **142**
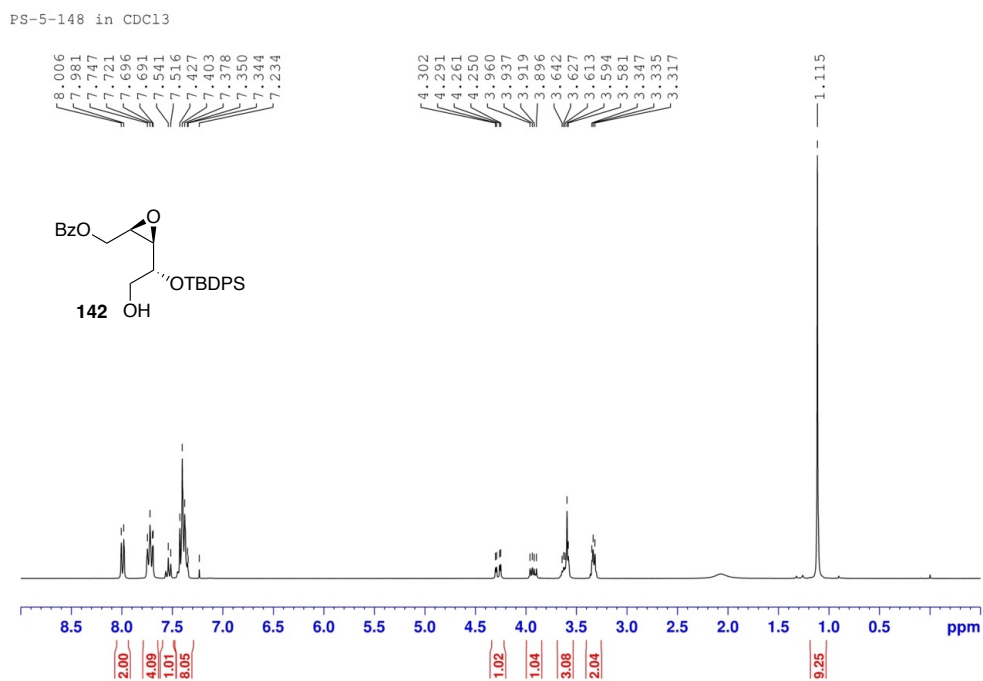
Figure 74 ^{13}C NMR (75 MHz, CDCl$_3$) spectrum of compound **142**
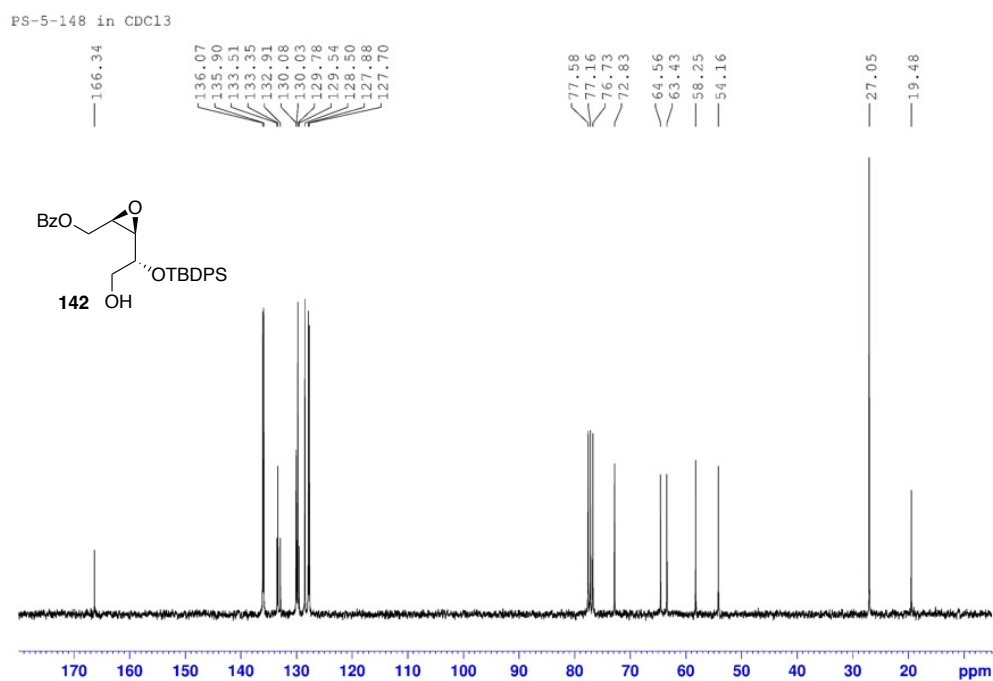
Figure 75 ^{1}H NMR (300 MHz, CDCl$_3$) spectrum of compound **143**
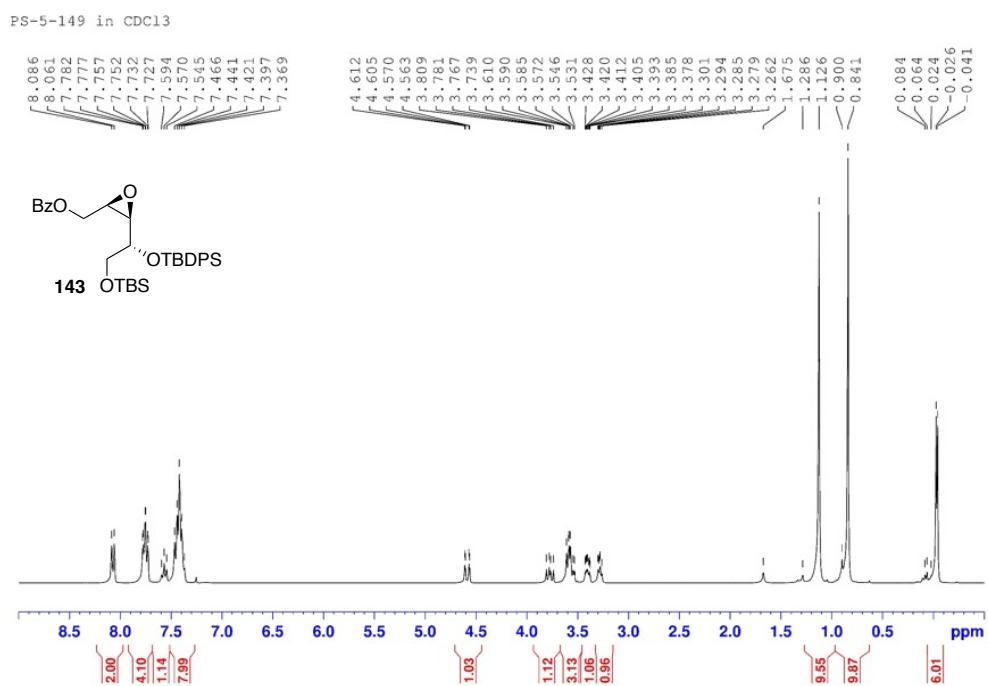
Figure 76 ^{13}C NMR (75 MHz, CDCl$_3$) spectrum of compound **143**
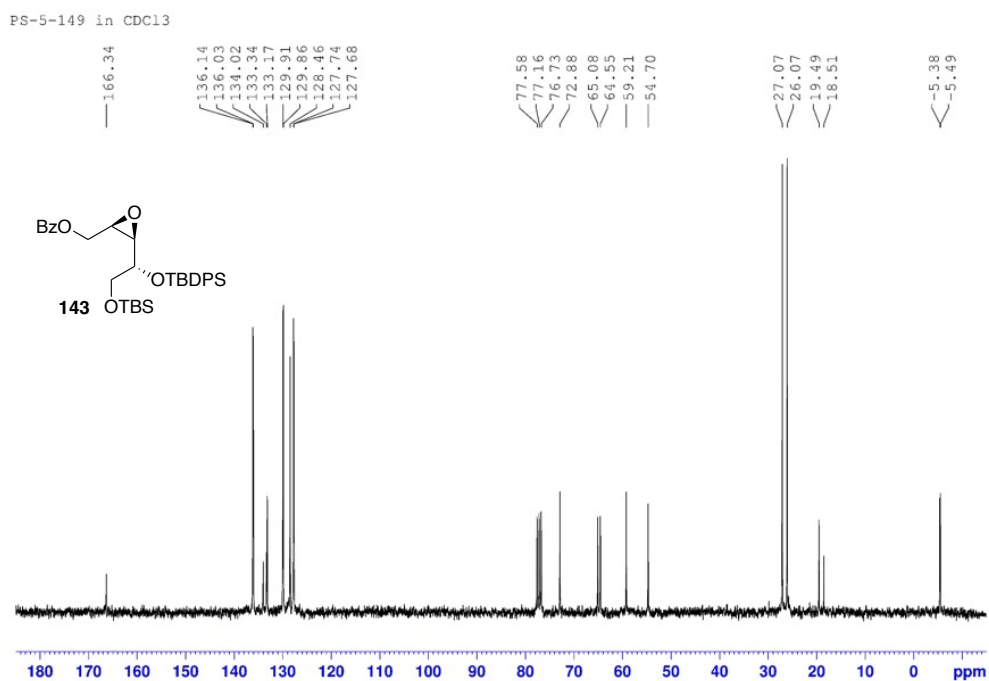
Figure 77 ^{1}H NMR (300 MHz, CDCl$_3$) spectrum of compound **144**

Figure 78 ^{13}C NMR (75 MHz, CDCl$_3$) spectrum of compound **144**

Figure 79 ^{1}H NMR (300 MHz, CDCl$_3$) spectrum of compound **107**
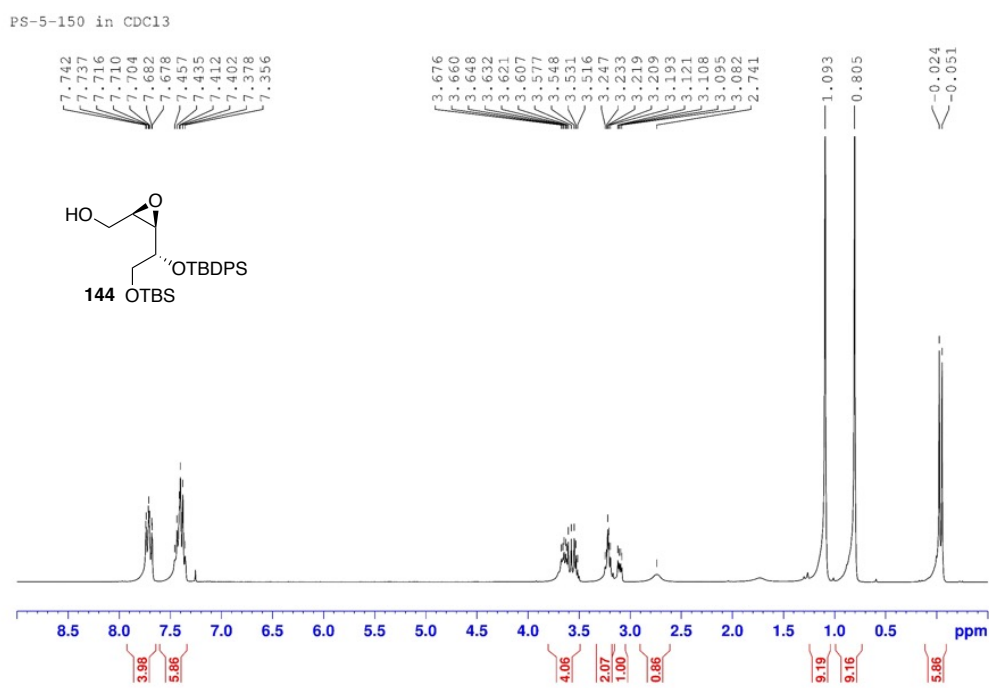
Figure 80 ^{13}C NMR (75 MHz, CDCl$_3$) spectrum of compound **107**
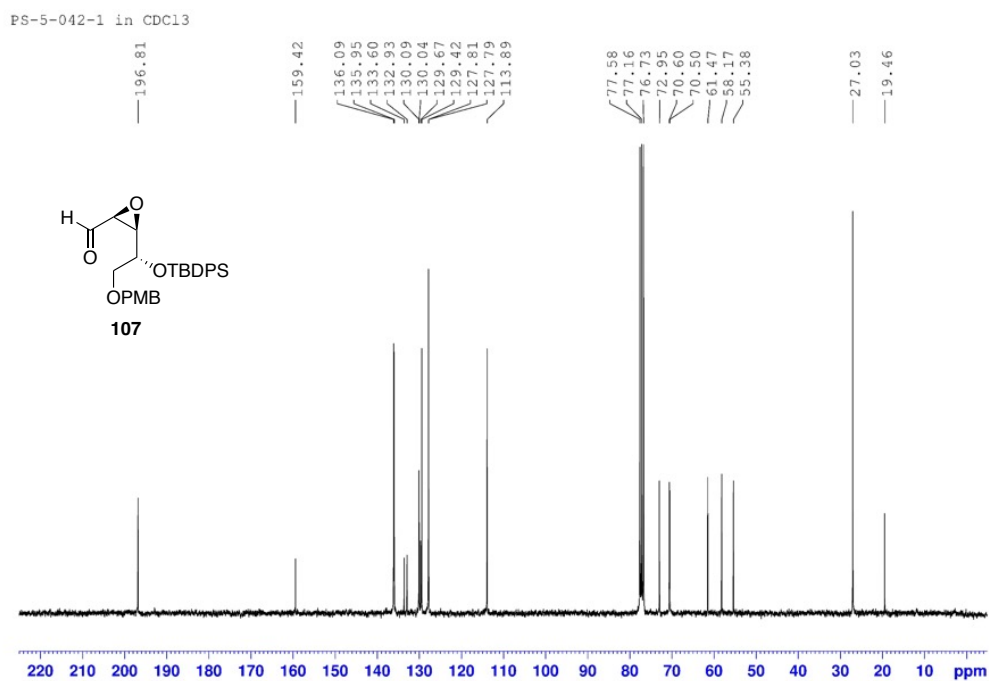
Figure 81 ^{1}H NMR (300 MHz, CDCl$_3$) spectrum of compound **131***S*
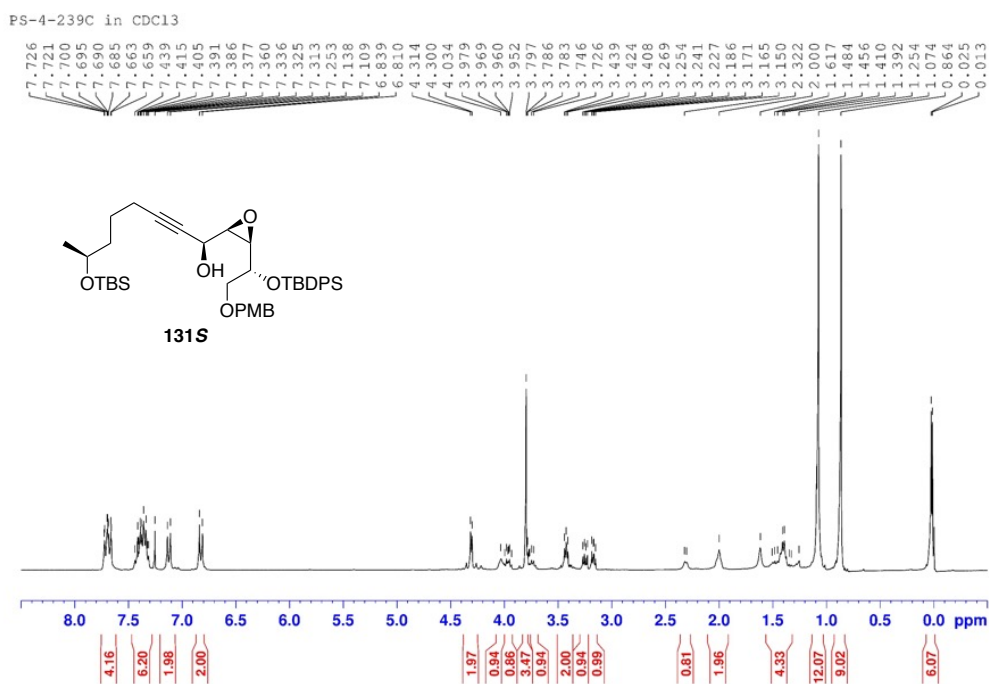
Figure 82 ^{13}C NMR (75 MHz, CDCl$_3$) spectrum of compound **131***S*
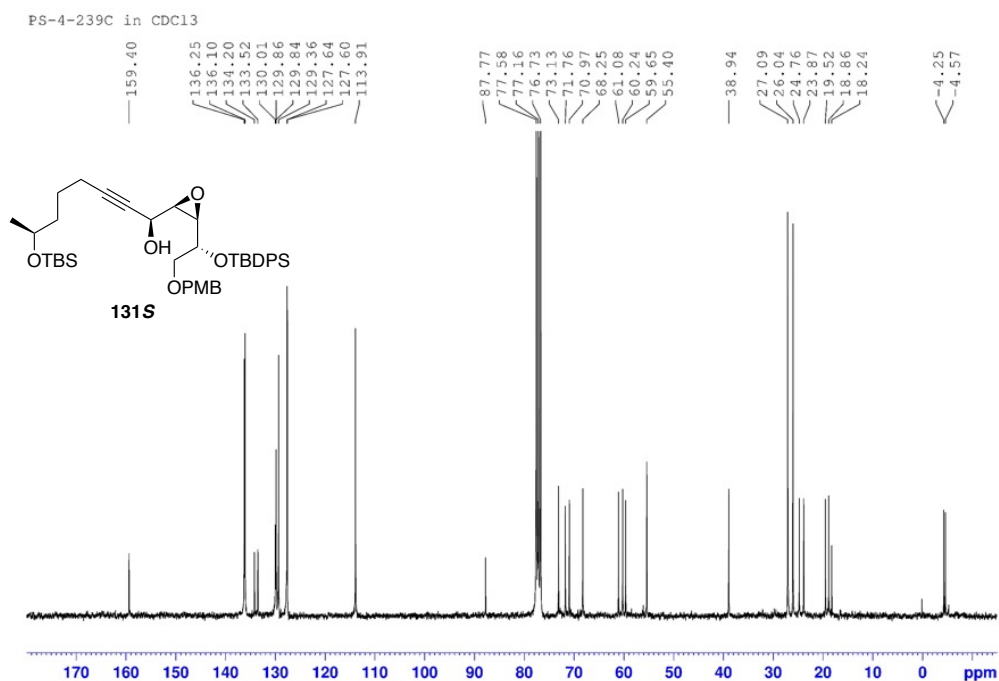
Figure 83 ^{1}H NMR (300 MHz, CDCl$_3$) spectrum of (*S*)-MTPA ester of **131***S*
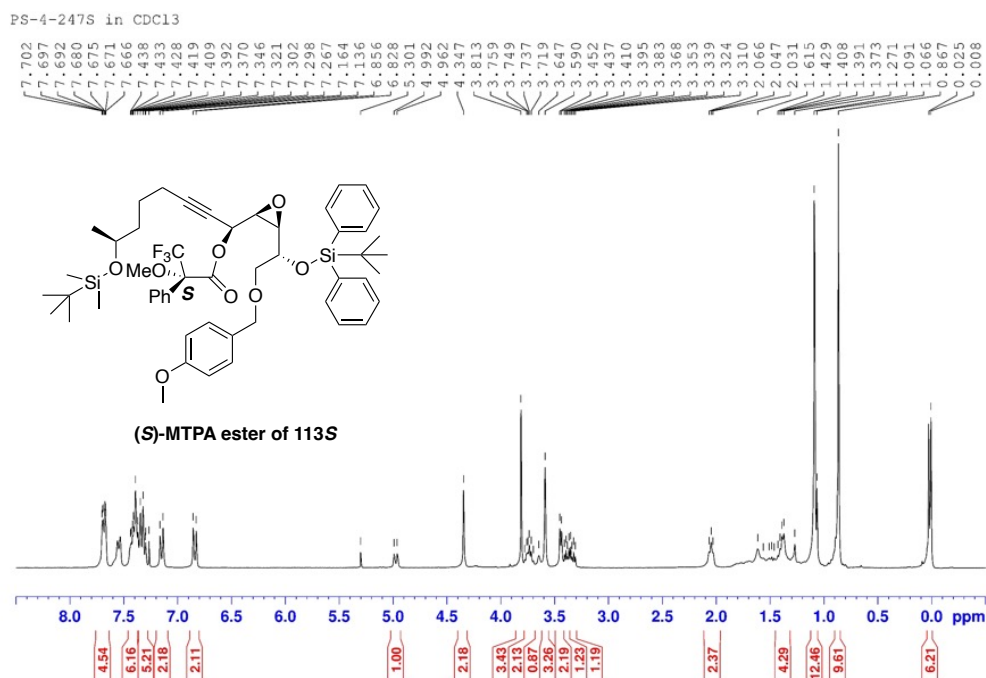
Figure 84 ^{1}H NMR (300 MHz, CDCl$_3$) spectrum of (*R*)-MTPA ester of **131*S***
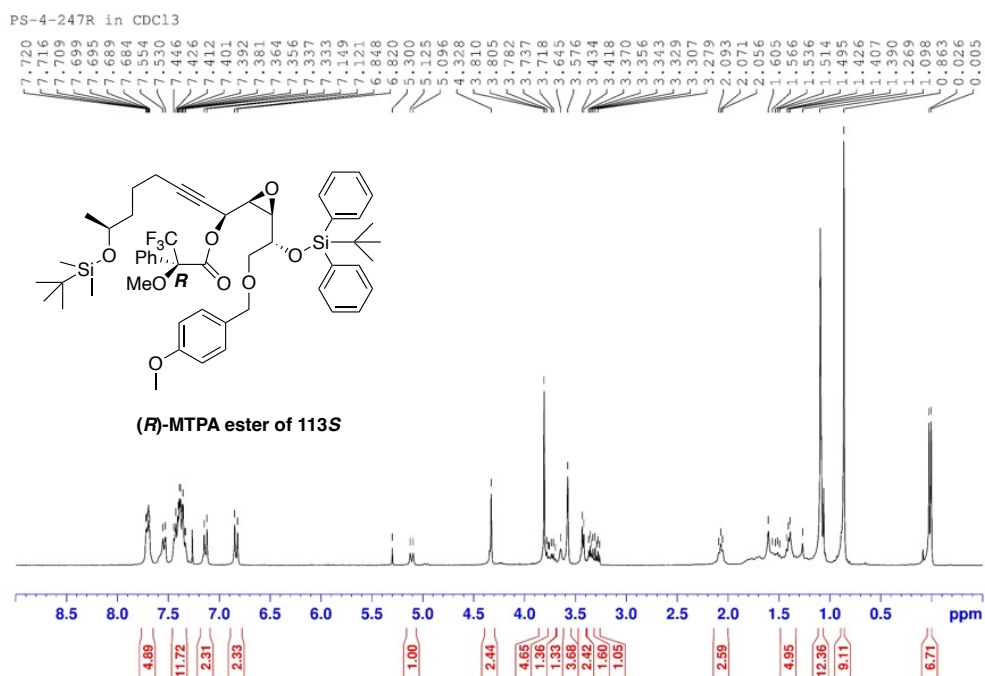
Figure 85 ^{1}H NMR (300 MHz, CDCl$_3$) spectrum of compound **131*R***
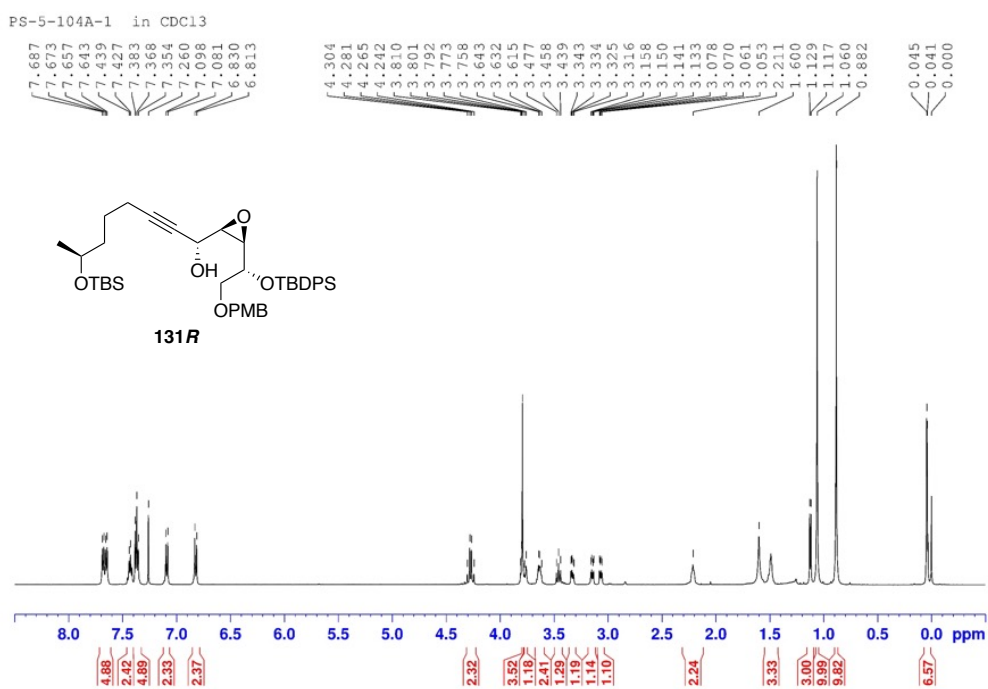
Figure 86 ^{13}C NMR (125 MHz, CDCl$_3$) spectrum of compound **131*R***
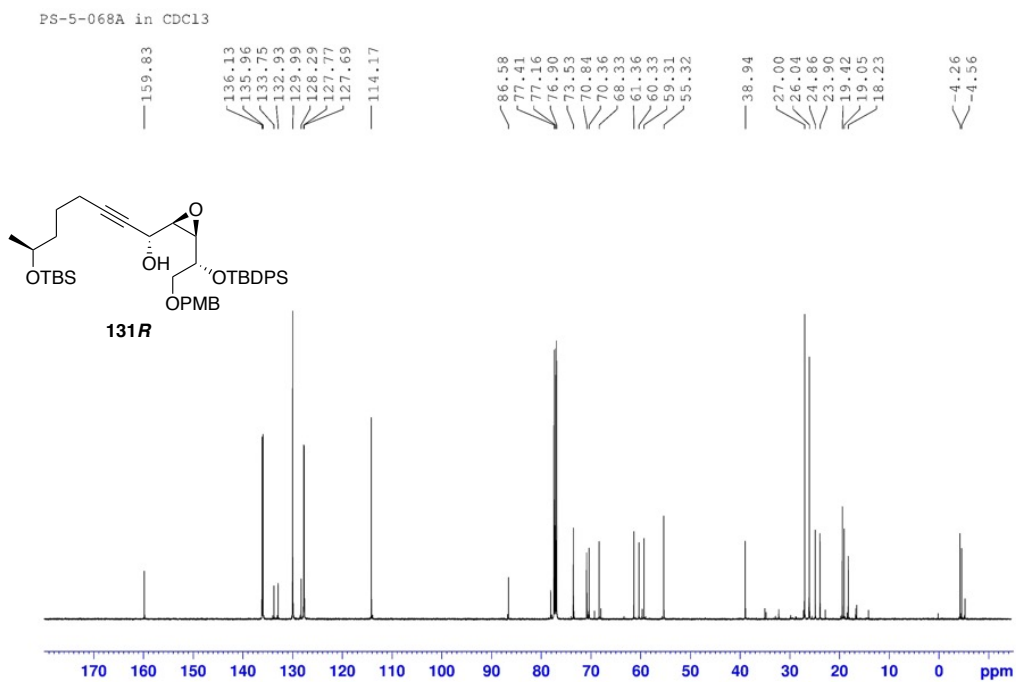
Figure 87 ^{1}H NMR (300 MHz, CDCl$_3$) spectrum of (*S*)-MTPA ester of **131*R***

162
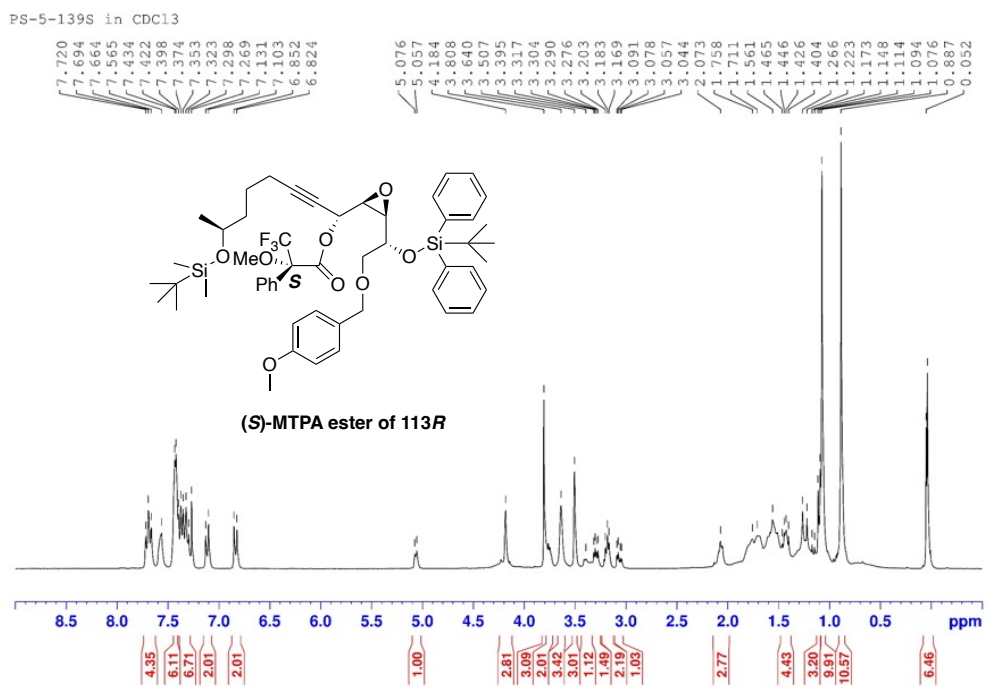
Figure 88 ^{1}H NMR (300 MHz, CDCl$_3$) spectrum of (R)-MTPA ester of **131R**

(*R*)-MTPA ester of 113*R*
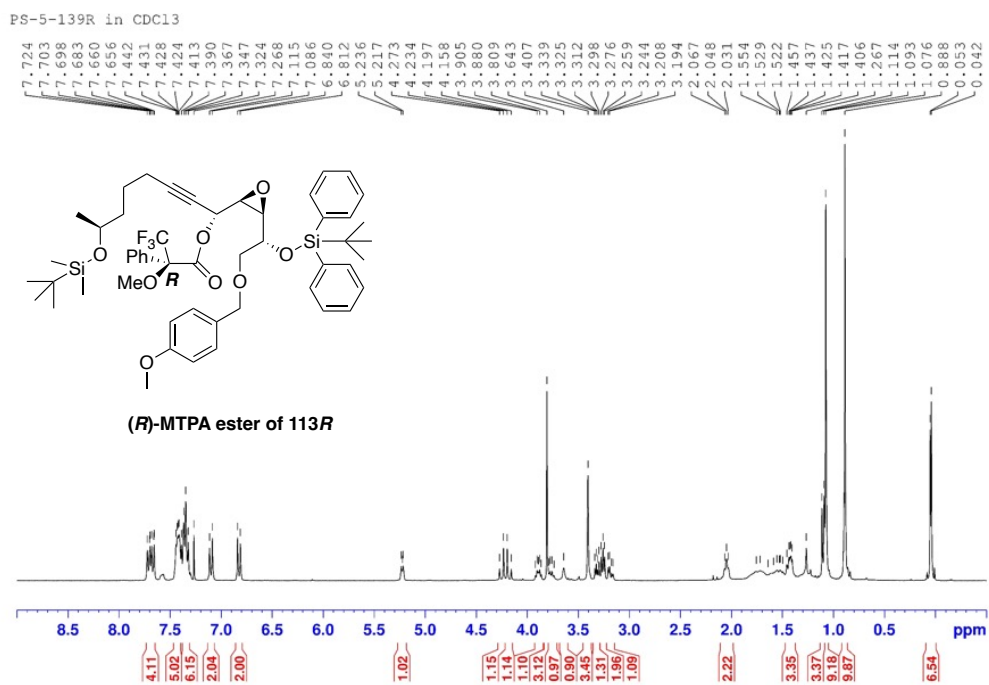
Figure 89 ^{1}H NMR (300 MHz, CDCl$_3$) spectrum of compound **145**

145
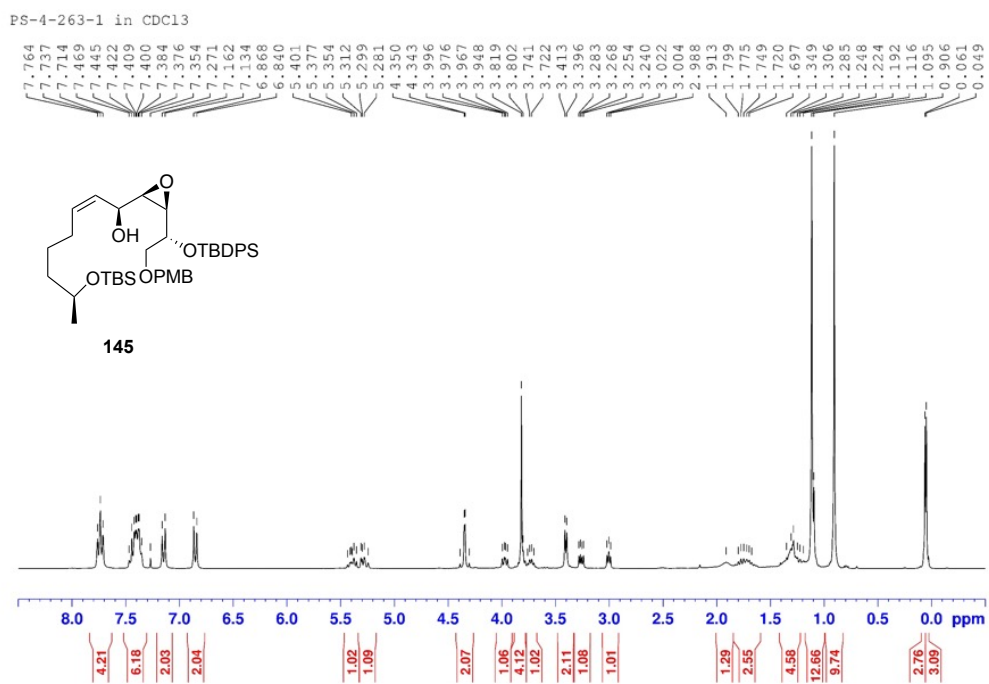
Figure 90 ^{13}C NMR (75 MHz, CDCl$_3$) spectrum of compound **145**
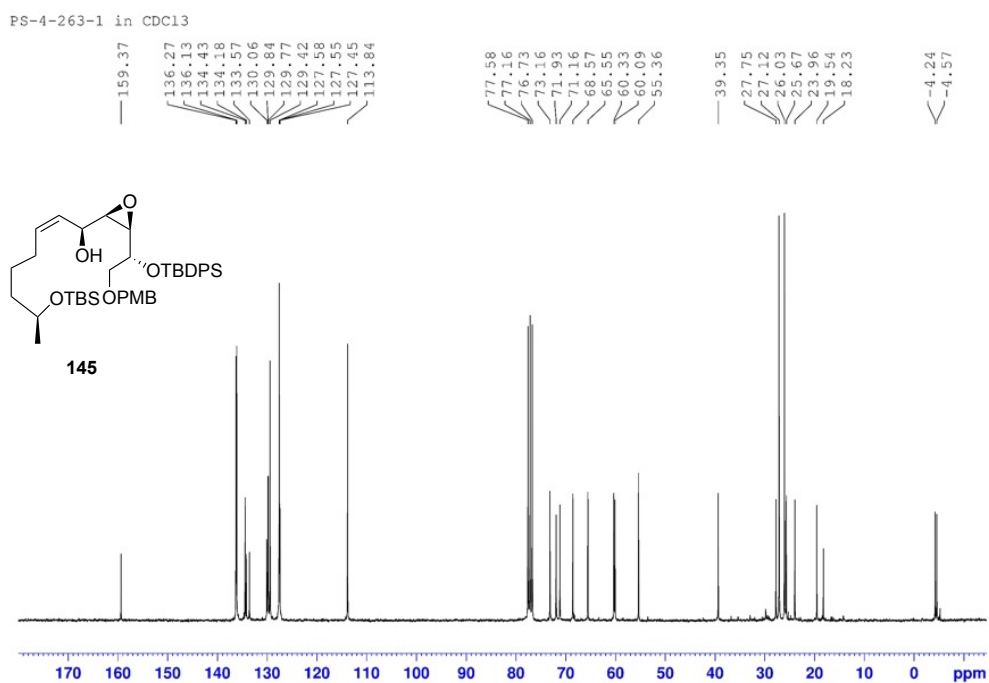
Figure 91 ^{1}H NMR (300 MHz, CDCl$_3$) spectrum of compound **165**

Figure 92 ^{13}C NMR (75 MHz, CDCl[3]) spectrum of compound **165**

Figure 93 ^{1}H NMR (300 MHz, CDCl[3]) spectrum of compound **146**

Figure 94 ^{13}C NMR (75 MHz, CDCl$_3$) spectrum of compound **146**

Figure 95 ^{1}H NMR (500 MHz, CDCl$_3$) spectrum of compound **147**

Figure 96 ^{13}C NMR (125 MHz, CDCl$_3$) spectrum of compound **147**

Figure 97 ^{1}H NMR (500 MHz, CDCl$_3$) spectrum of compound **148**
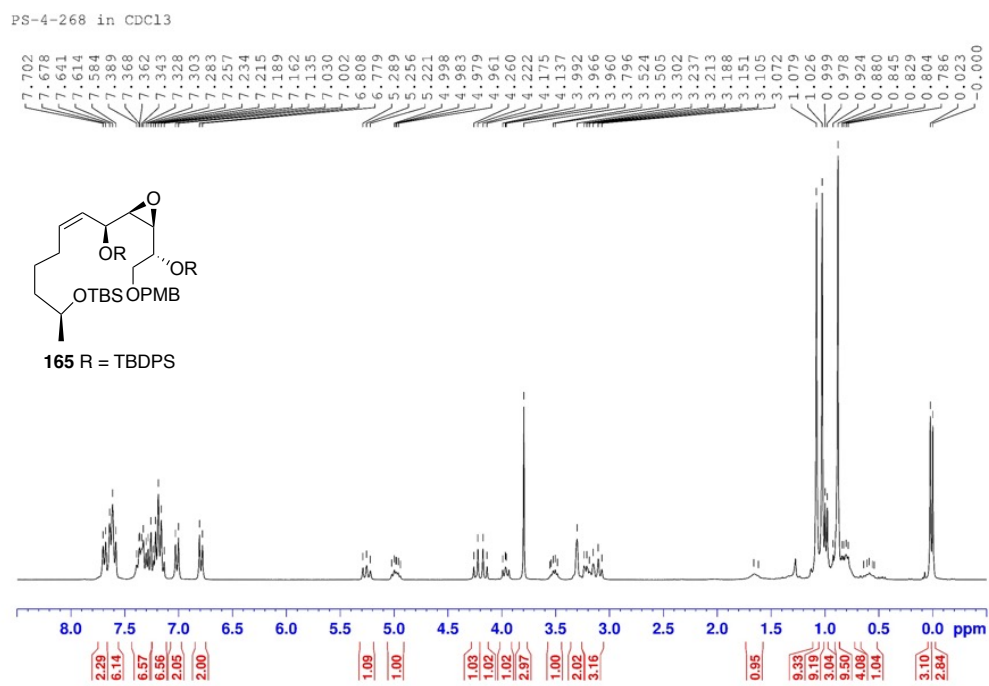
Figure 98 ^{13}C NMR (125 MHz, CDCl$_3$) spectrum of compound **148**
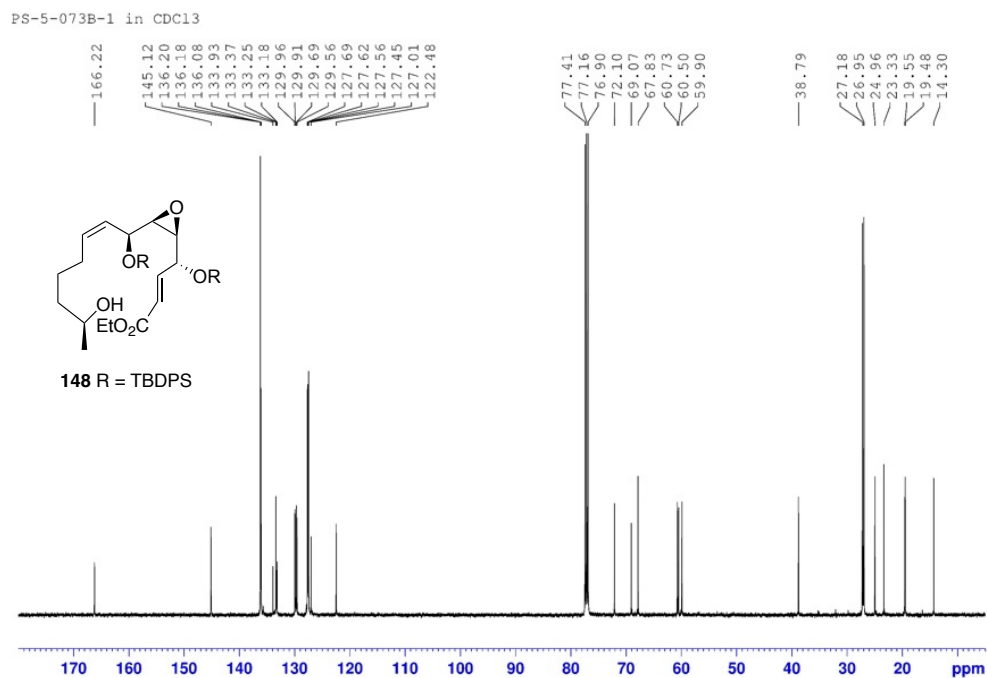
Figure 99 ^{1}H NMR (500 MHz, CDCl$_3$) spectrum of compound **130**

Figure 100 ^{13}C NMR (125 MHz, CDCl$_3$) spectrum of compound **130**

Figure 101 ^{1}H NMR (500 MHz, CDCl$_3$) spectrum of compound **149**
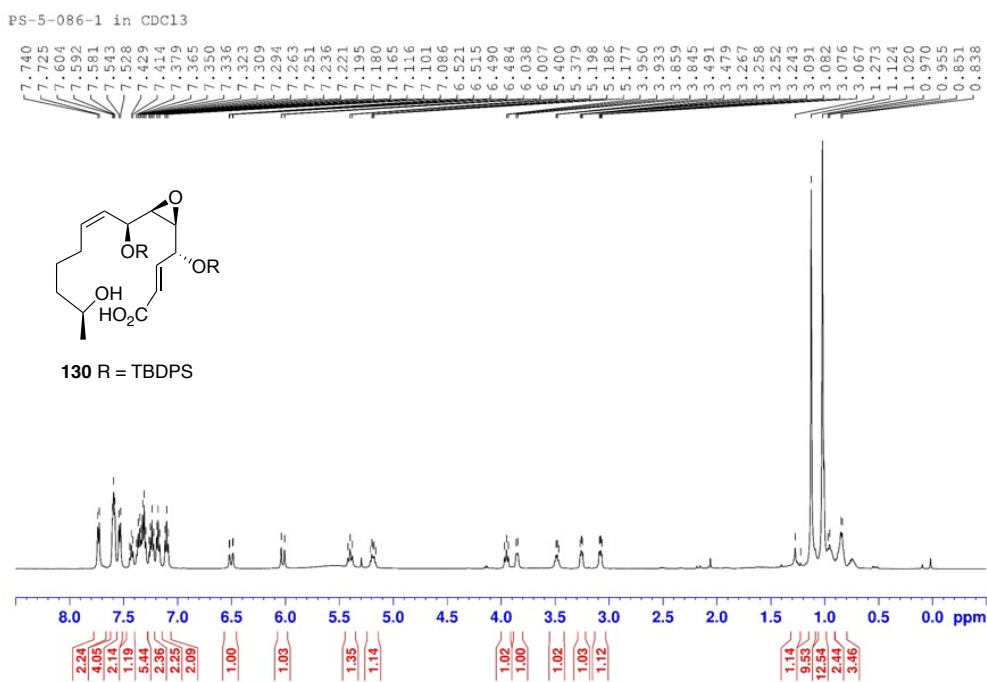
Figure 102 ^{13}C NMR (125 MHz, CDCl$_3$) spectrum of compound **149**
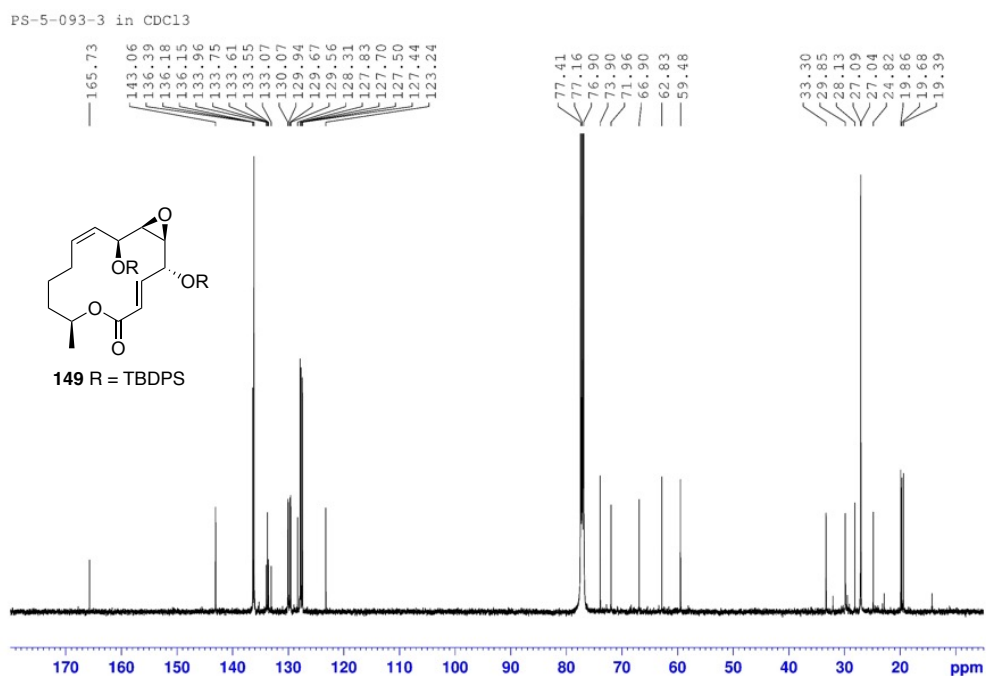
Figure 103 ^{1}H NMR (500 MHz, CDCl$_3$) spectrum of compound **13**
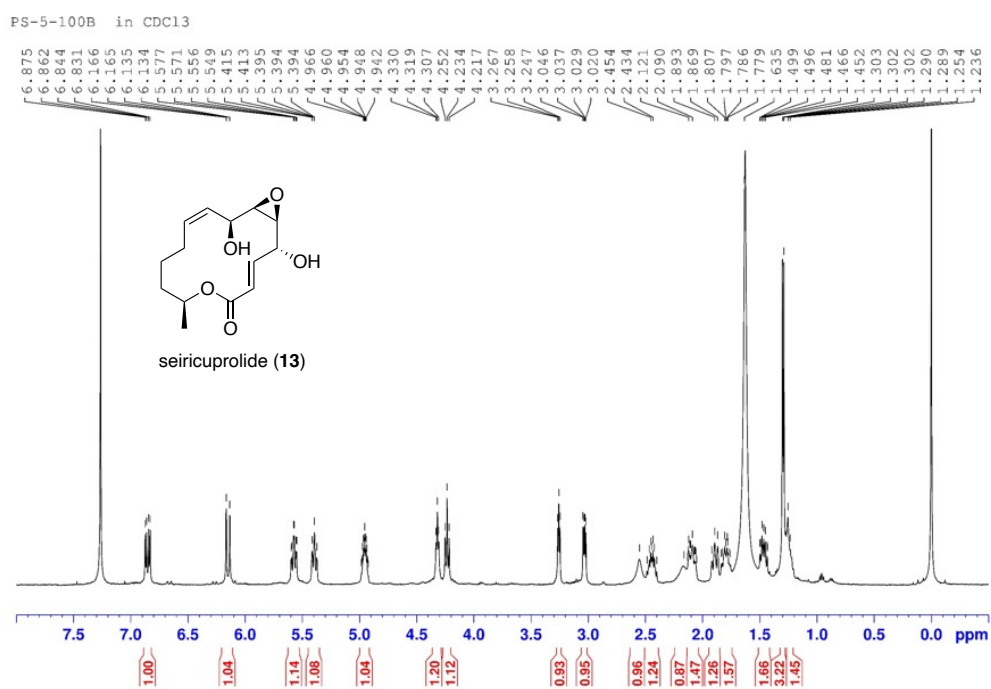
Figure 104 ^{13}C NMR (125 MHz, CDCl$_3$) spectrum of compound **13**
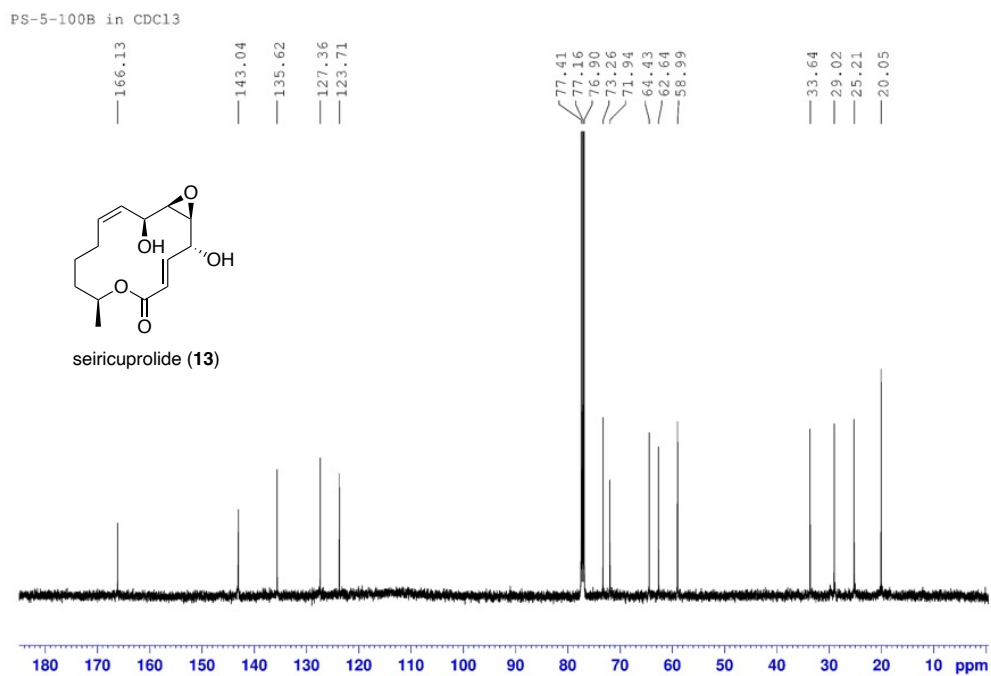
Figure 105 ^{1}H NMR (500 MHz, CDCl$_3$) spectrum of compound **150**
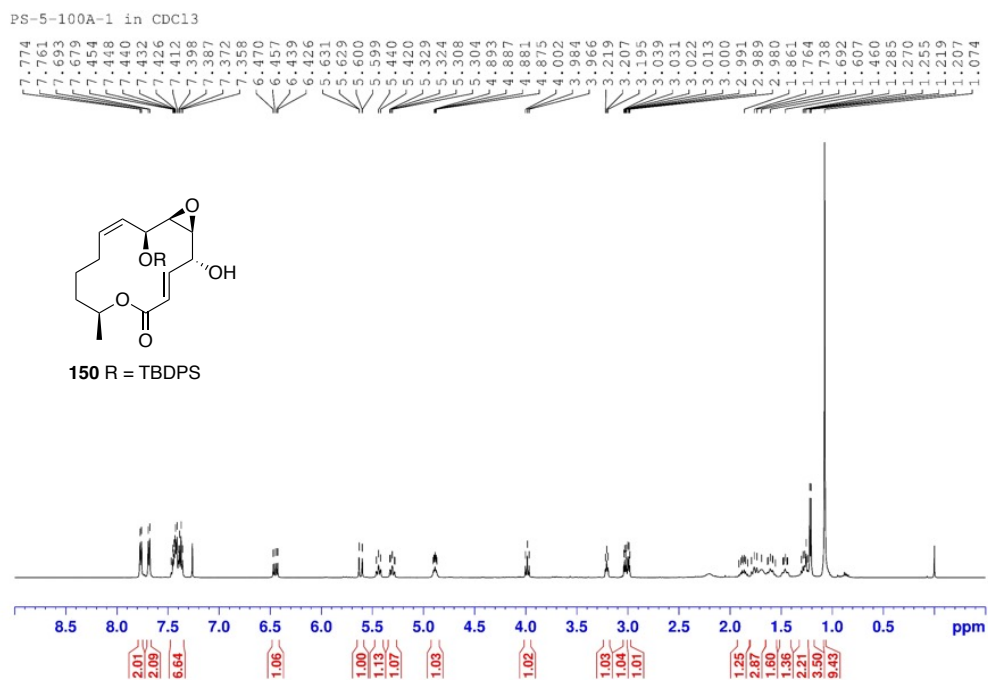
Figure 106 ^{13}C NMR (125 MHz, CDCl$_3$) spectrum of compound **150**
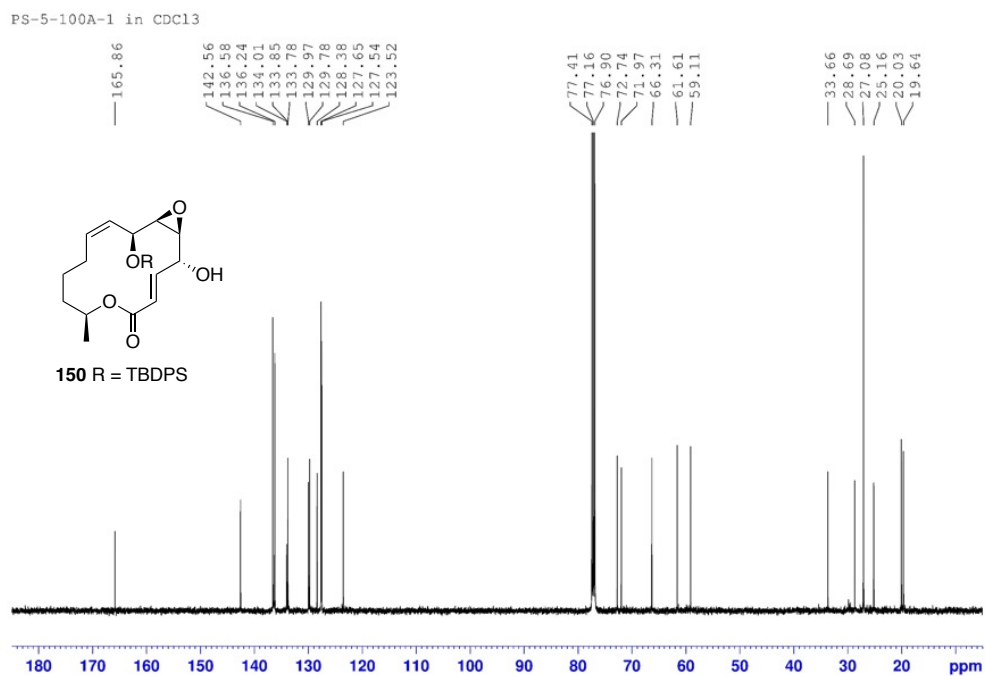
Figure 107 ^{1}H NMR (300 MHz, CDCl$_3$) spectrum of compound **156**
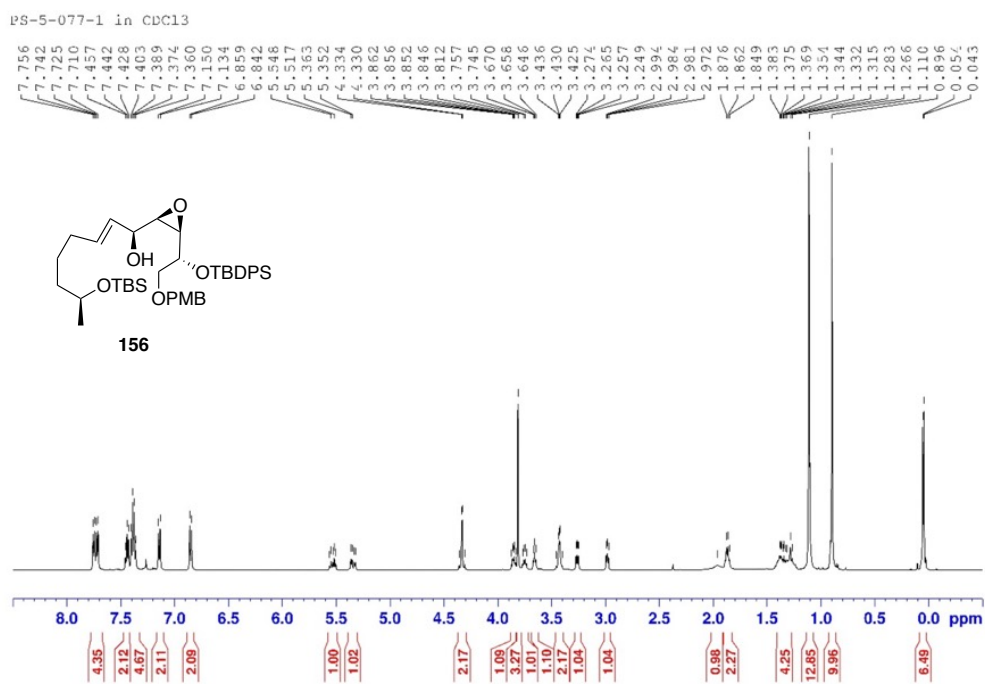
Figure 108 ^{13}C NMR (75 MHz, CDCl$_3$) spectrum of compound **156**
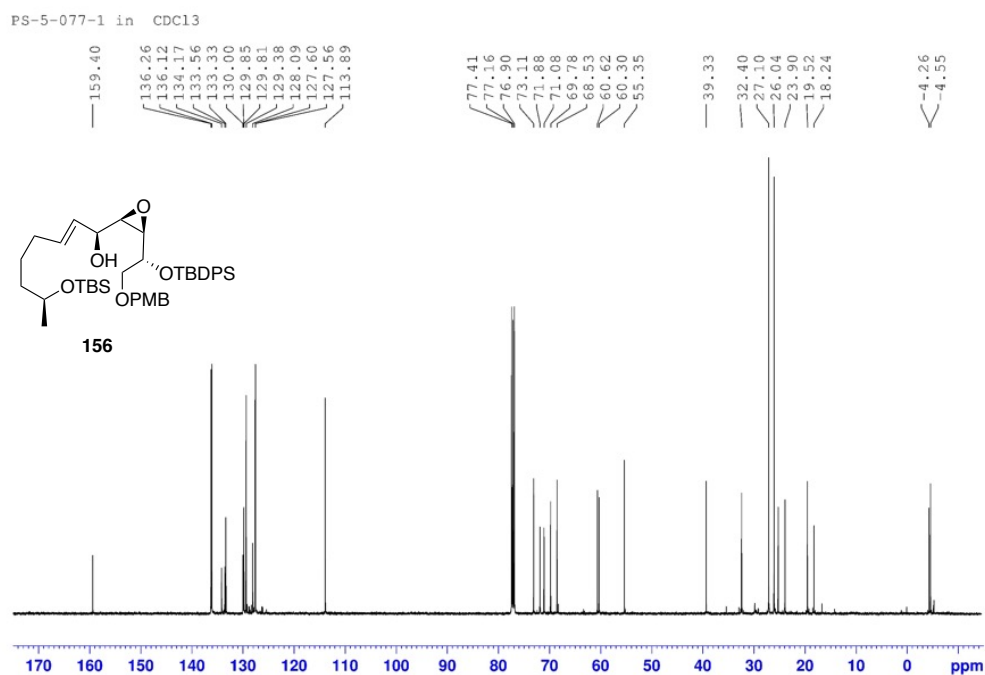
Figure 109 ^{1}H NMR (500 MHz, CDCl$_3$) spectrum of compound **166**
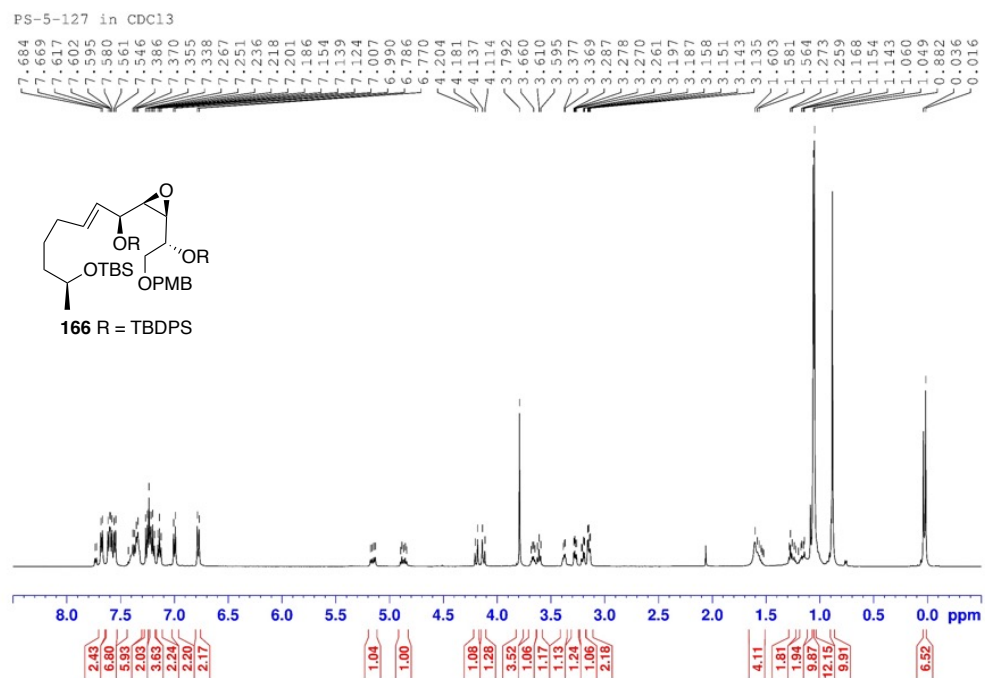
Figure 110 ^{13}C NMR (125 MHz, CDCl$_3$) spectrum of compound **166**
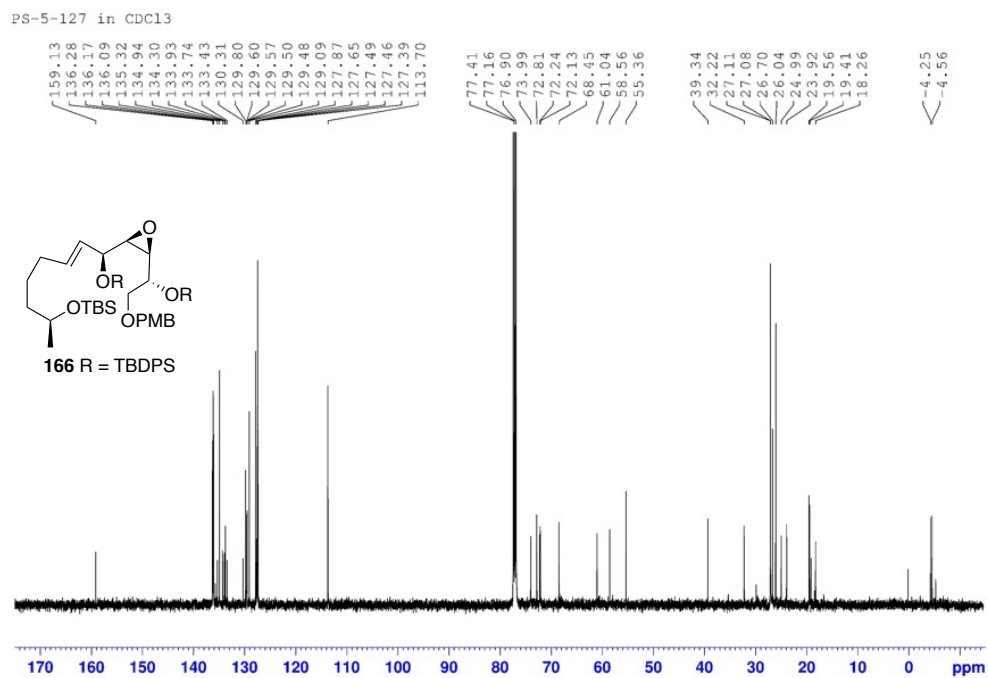
Figure 111 ^{1}H NMR (500 MHz, CDCl$_3$) spectrum of compound **158**
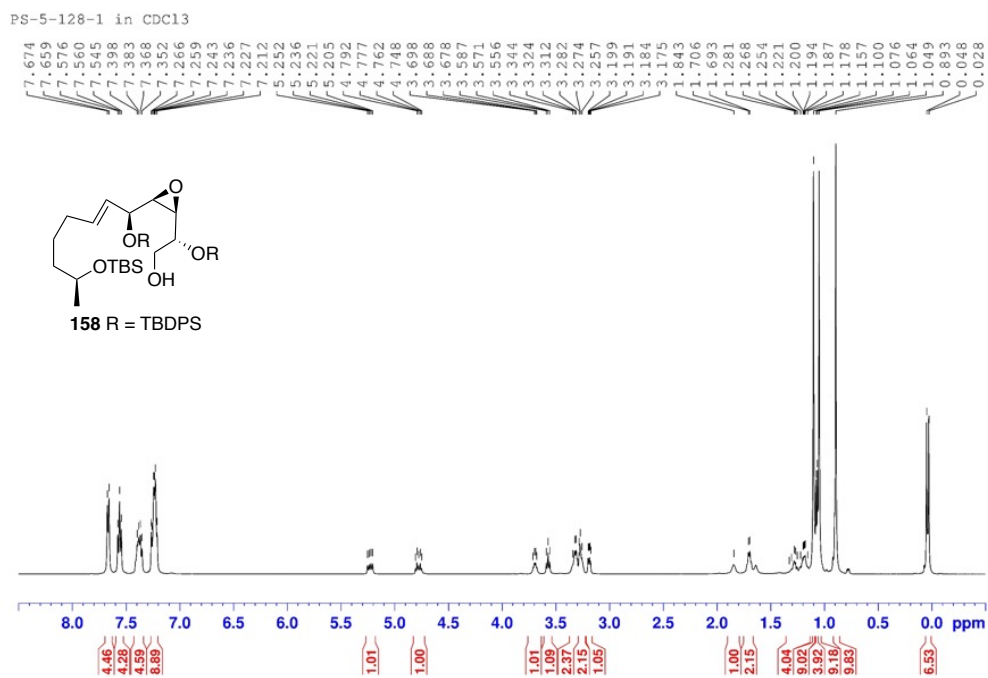
Figure 112 ^{13}C NMR (125 MHz, CDCl$_3$) spectrum of compound **158**
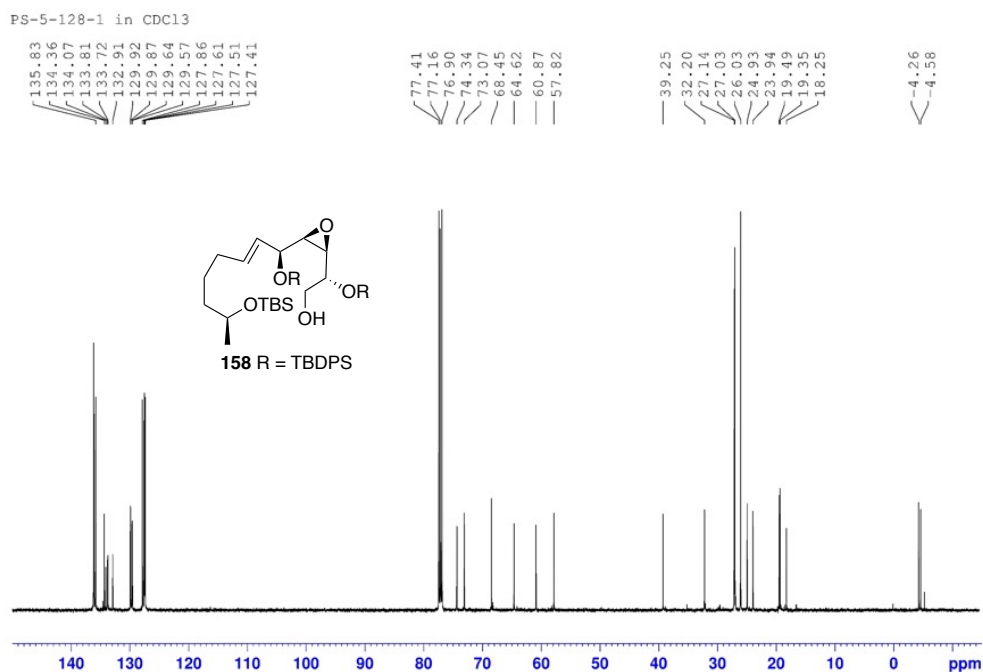
Figure 113 ^{1}H NMR (500 MHz, CDCl$_3$) spectrum of compound **159**
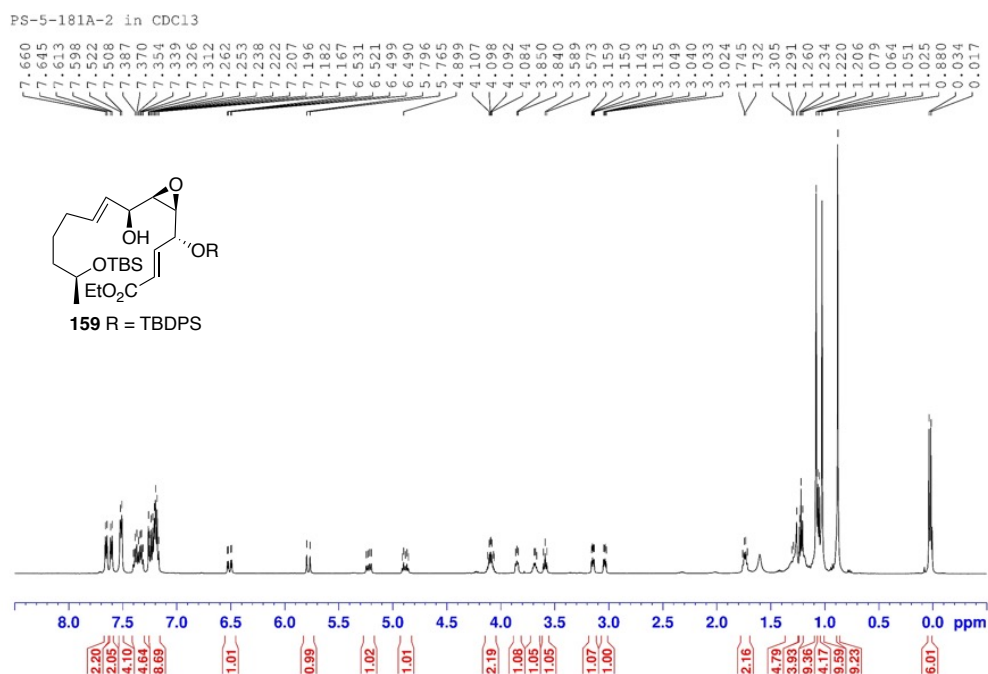
Figure 114 ^{13}C NMR (125 MHz, CDCl$_3$) spectrum of compound **159**
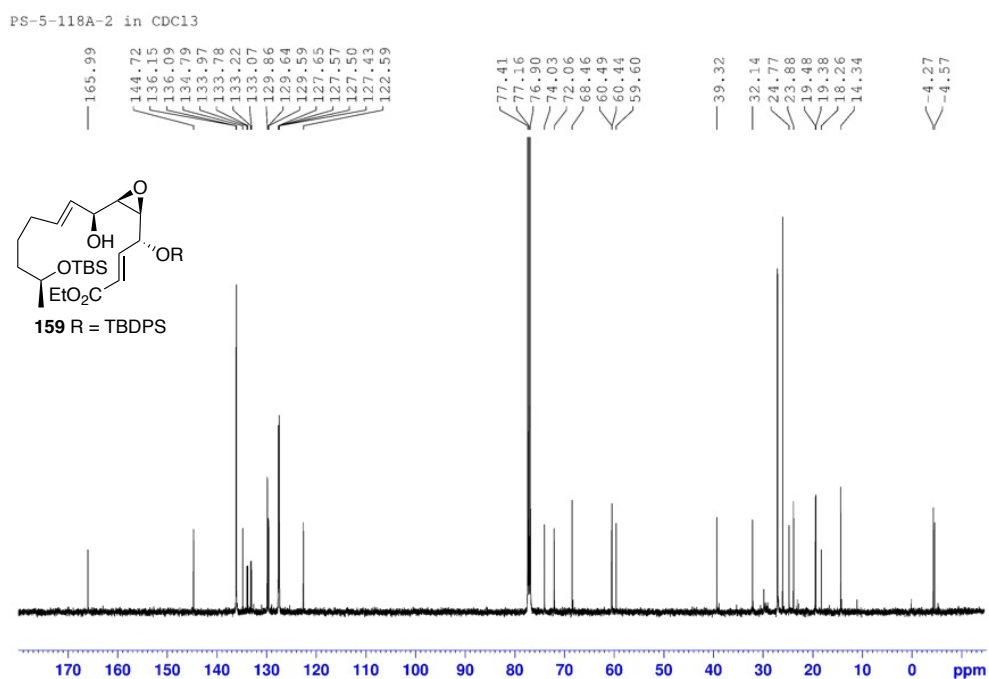
Figure 115 ^{1}H NMR (500 MHz, CDCl$_3$) spectrum of compound **160**
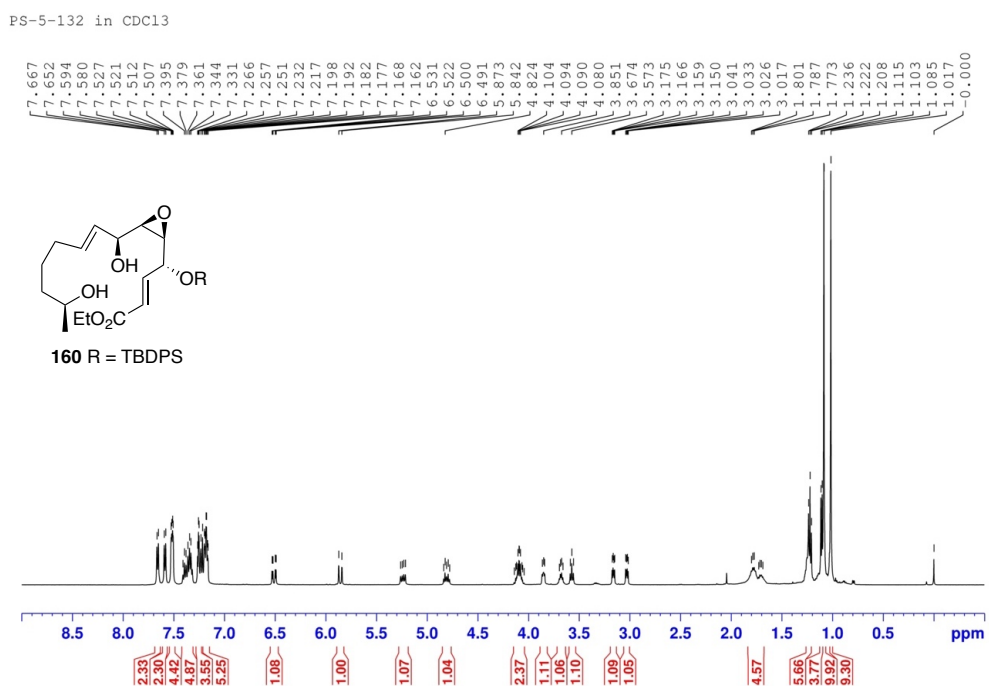
Figure 116 ^{13}C NMR (125 MHz, CDCl$_3$) spectrum of compound **160**
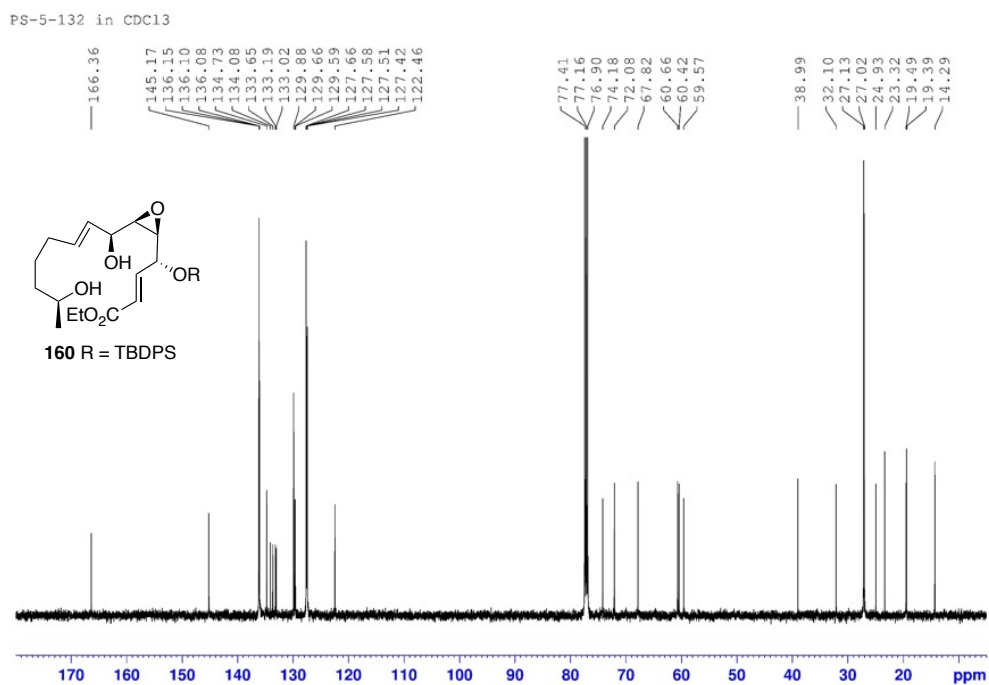
Figure 117 ^{1}H NMR (500 MHz, CDCl$_3$) spectrum of compound **129**

Figure 118 ¹³C NMR (125 MHz, CDCl₃) spectrum of compound **129**

Figure 119 ¹H NMR (500 MHz, CDCl₃) spectrum of compound **161**
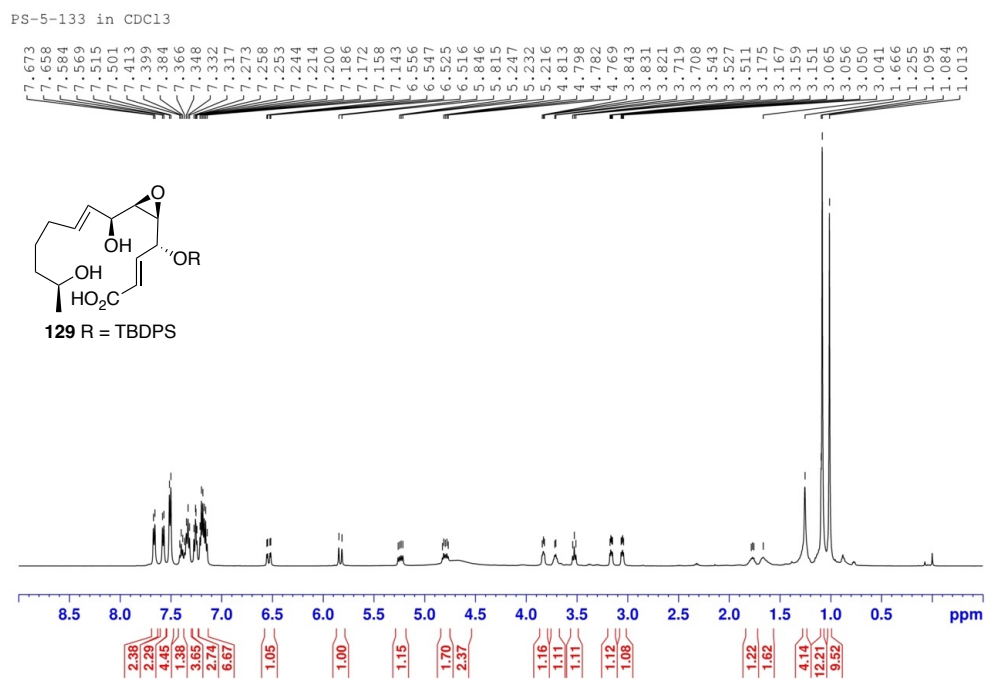
Figure 120 ^{13}C NMR (125 MHz, CDCl$_3$) spectrum of compound **161**
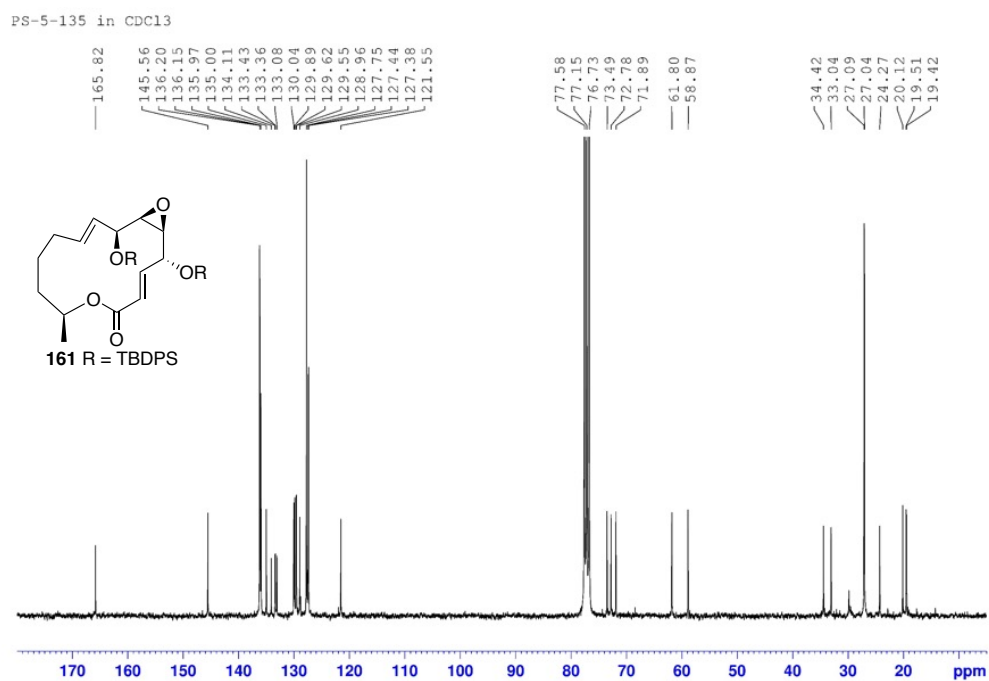
Figure 121 ^{1}H NMR (500 MHz, acetone-d_6) spectrum of compound **14**
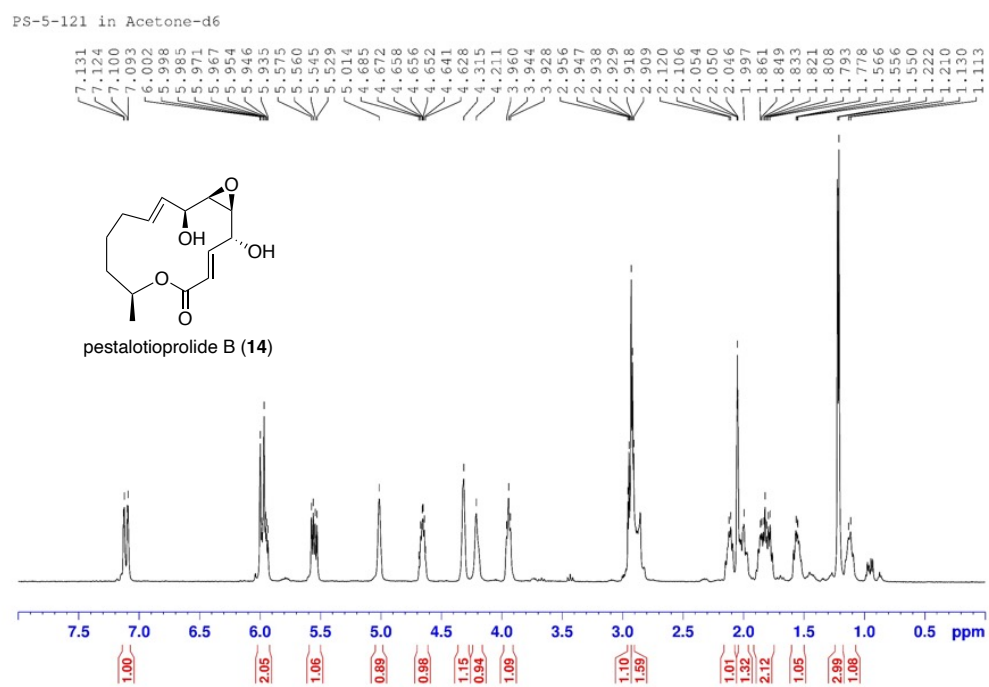
Figure 122 ^{13}C NMR (125 MHz, acetone-d_6) spectrum of compound **14**
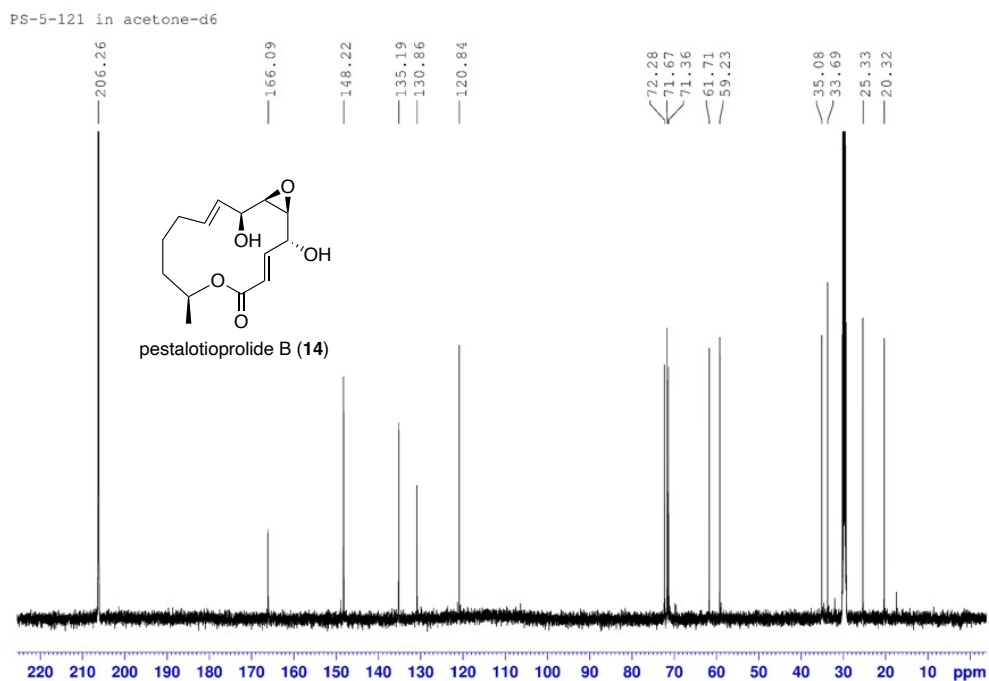
Figure 123 Comparison of ^{1}H NMR spectra of synthetic and natural seiricuprolide
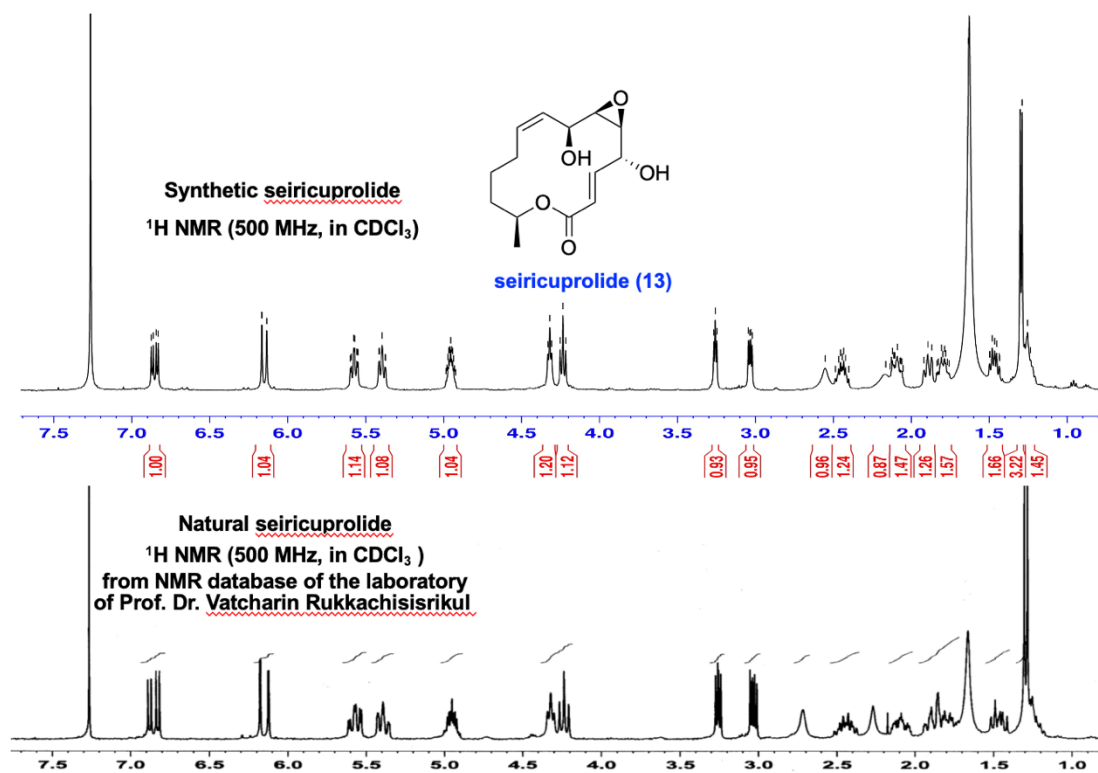
Figure 124 Comparison of ^{1}H NMR spectra of synthetic and natural
pestalotioprolide B
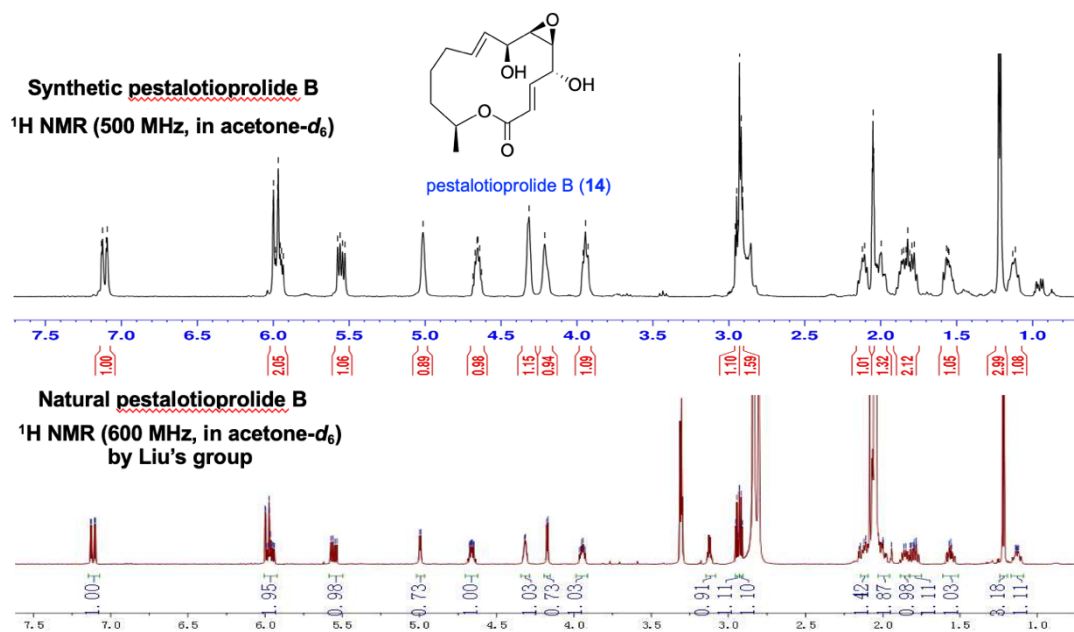
Figure 125 Comparison of ^{13}C NMR spectra of synthetic and natural
pestalotioprolide B
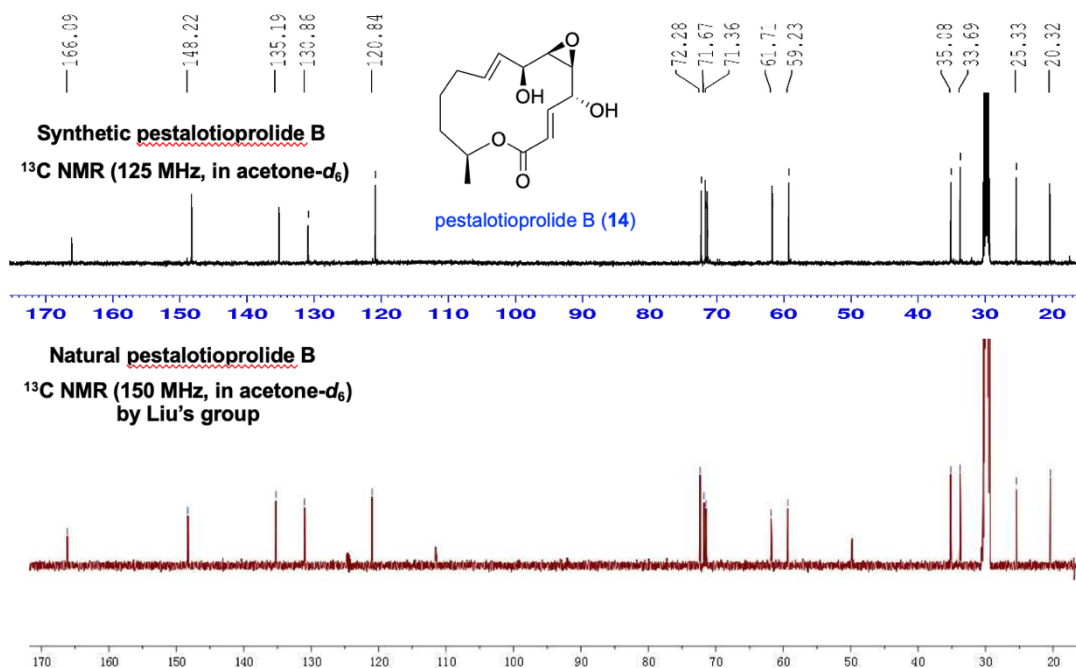
VITAE

Name   Mr. Pitipat   Sanphetchaloemchok
Student ID   6210220081

Educational Attanment

Degree	Name of Institution	Year of Graduation
Bachelor of Science (Chemistry)	Prince of Songkla University	2019

Scholarship Awards during Enrolment

Research Assistantship from Faculty of Science and Partial Scholarship from PERCH-CIC

List of Publication and Proceeding

Sanphetchaloemchok, P.; Aluwi, M. F. F. M.; Rullah, K; Wai, L. K. 2020. Synthesis, *In Silico* Molecular Docking Modeling and Pharmacophore Mapping of (*E*)-3-(4-Hydroxy-2,6-Dimethoxyphenyl)-1-Phenylprop-2-en-1-One as Potential New Inhibitor of Microsomal Prostaglandin E2 Synthase-1. Mater. Sci. Forum. 981, 247–252.

Sanphetchaloemchok, P.; Saikachain, N.; Khumliang, R.; Muanprasat, C.; Tadpetch, K. 2023. Total Synthesis and Biological Evaluation of Seiricuprolide and Pestalotioprolide B. Eur. J. Org. Chem. 26. e202300034.